DOCTORAL THESIS

Cellulose Dissolution and Transesterification in Superbase Ionic Liquid [mTBNH][OAc] with Green Co-solvents

Nutan Bharat Savale

Cellulose Dissolution and Transesterification in Superbase Ionic Liquid [mTBNH][OAc] with Green Co-solvents

NUTAN BHARAT SAVALE

TAL
TECH
PRESS

TALLINN UNIVERSITY OF TECHNOLOGY
School of Engineering
Department of Materials and Environmental Technology
This dissertation was accepted for the defence of the degree 12/02/2025

Supervisor: Professor Dr. Andres Krumme
                            School of Engineering
                            Tallinn University of Technology
                            Tallinn, Estonia

Co-supervisor: Senior Lecturer Dr. Elvira Tarasova
                            School of Engineering
                            Tallinn University of Technology
                            Tallinn, Estonia

Opponents: Senior University Lecturer Dr. Sami Heikki Olavi Hietala
                            Department of Chemistry
                            University of Helsinki
                            Helsinki, Finland

                            Professor Dr. Timo Kikas
                            Institute of Forestry and Engineering
                            Estonian University of Life Sciences
                            Tartu, Estonia

Defence of the thesis: 24/03/2025, Tallinn

Declaration:
Hereby, I declare that this doctoral thesis, my original investigation and achievement, submitted for the doctoral degree at Tallinn University of Technology has not been submitted for a doctoral or equivalent academic degree.

Nutan Bharat Savale

                            _____
                                             signature

Savale, N. (2025). *Cellulose Dissolution and Transesterification in Superbase Ionic Liquid [mTBNH][OAc] with Green Co-solvents* [TalTech Press]. https://doi.org/10.23658/taltech.13/2025

Tselluloosi lahustamine ja ümberesterdamine superaluselises ioonvedelikus [mTBNH][OAc] koos roheliste kaaslahustitega

NUTAN BHARAT SAVALE

TAL
TECH
KIRJASTUS

Contents

List of Publications

I   Tarasova, E., **Savale, N.**, Krasnou, I., Kudrjašova, M., Rjabovs, V., Reile, I., Vares, L., Kallakas, H., Kers, J. and Krumme, A. (2023). Preparation of thermoplastic cellulose esters in [mTBNH][OAC] ionic liquid by transesterification reaction. Polymers, 15(19), p. 3979.

II **Savale, N.**, Tarasova, E., Krasnou, I., Kudrjašova, M., Rjabovs, V., Reile, I., Heinmaa, I. and Krumme, A. (2024). Optimization and degradation studies of cellulose transesterification to palmitate esters in superbase ionic liquid. Carbohydrate Research, 537, p. 109047.

III Tarasova, E., **Savale, N.**, Ausmaa, P.M., Krasnou, I. and Krumme, A. (2024). Rheology and dissolution capacity of cellulose in novel [mTBNH][OAc] ionic liquid mixed with green co-solvents. Rheologica Acta, 63(2), pp. 167–178.

IV Tarasova, E., **Savale, N.**, Trifonova, L., Krasnou, I., Reile, I., Kudrjašova, M., Mere, A., Kaljuvee, T., Mikli, V., Sedrik, R. and Krumme, A. (2024). Effect of green co-solvents on properties and synthesis of cellulose esters in superbase ionic liquid. Cellulose, 31(8), pp. 4911–4927.

Author's Contribution to the Publications

Contribution to the papers in this thesis are:

I. The author synthesized cellulose esters (CEs), carried out 1D and 2D Nuclear Magnetic Resonance Spectroscopy (NMR) characterization, analyzed results, and wrote the major draft of the paper.

II. The author synthesized cellulose palmitates (CPs) and performed detailed optimization of reaction parameters, along with 1D and 2D NMR characterization and intrinsic viscosity measurements. The author also studied the stability of the solvent system and the compatibility between the reactants involved and the solvent system by employing methods like Fourier Transform infrared spectroscopy (FT-IR) and NMR, analyzed the results, and wrote the research article.

III. The author was involved in preparing cellulose/superbase ionic liquid/green co-solvent samples preparation and studied the dissolution behavior using rheology and optical microscopy. The author was involved in the data analysis and the writing of the major draft of a paper.

IV. The author synthesized CEs, carried out detailed NMR characterization of all the samples, analyzed the results, and wrote the major draft of the research paper.

Introduction

Non-renewable resources (NRRs), particularly crude oil utilized in polymer production, are being depleted at a rate that exceeds their natural replenishment. Thus, developing alternatives from renewable resources (RRs) is critically important. Cellulose, the most abundant natural polymer on Earth and a renewable resource derived from plants boasts remarkable properties such as biodegradability, non-toxicity, biocompatibility, mechanical strength, heat resistance, and solvent resilience (Feng, 2008). Cellulose has three hydroxy groups (-OH) per anhydroglucose unit (AGU) which undergo various chemical reactions typical of hydroxy groups, including acylation, etherification, oxidation, silylation, and polymer grafting. Despite these advantages, its semi-rigid chain structure poses significant challenges for dissolution in conventional organic and inorganic solvents, creating major barriers to its processing and practical applications (Qiu, 2013). Previous research has focused on developing innovative solvent systems for cellulose dissolution. However, many of these approaches are associated with high costs or require harsh operating conditions, leading to notable environmental and economic challenges.

Ionic liquids (ILs) present sustainable alternatives for cellulose dissolution and derivatization due to their superior properties like high polarity, low vapour pressure, non-volatility, and low toxicity (though this remains under investigation) (Pinkert, 2009; Han, 2009). Superbase ionic liquids (SB-IL), 5-methyl-1,5,7-triazabicyclo[4.3.0]non-6-enium acetate ([mTBNH][OAc]) has shown particular promise for cellulose dissolution and regeneration (Martins, 2022; Parviainen, 2015). The superbase 5-methyl-1,5,7-triazabicyclo[4.3.0]non-6-enium (mTBNH) shows excellent water stability and [mTBNH][OAc] remains liquid at room temperature, simplifying processing and reducing labour intensity, making it an ideal candidate for industrial applications.

Despite their remarkable properties, ILs also present some drawbacks, including a prolonged dissolution time for cellulose and the high viscosity of the resulting solution, which hinder subsequent cellulose modification. One approach to addressing these drawbacks is by adding low-viscosity co-solvents to ILs, creating binary solvent systems for cellulose dissolution. Polar aprotic solvents such as dimethyl sulfoxide (DMSO), *N,N*-Dimethylacetamide (DMAc), and *N,N*-Dimethylformamide (DMF) are commonly used with ILs for cellulose dissolution and modification. Adding low-cost co-solvents can reduce the reliance on expensive ILs, lowering processing costs. However, these co-solvents pose environmental and health risks due to toxicity and high energy demands, highlighting the need for alternatives in green chemistry. Greener solvents like γ-Valerolactone (GVL), dimethyl isosorbide (DMI), sulfolane (SLF), and *N,N*-Dimethylpropyleneurea (DMPU) are promising replacements for traditional polar aprotic co-solvents (Constable, 2007; Bryan, 2018).

To the best of our knowledge, there has been no research on using mixtures of green co-solvents with the novel [mTBNH][OAc] as dissolution and modification media for cellulose. This study aims to address this gap by investigating novel solvent systems composed of the SB-IL, [mTBNH][OAc] combined with green co-solvents such as GVL, DMI, SLF, and DMPU for cellulose dissolution and transesterification. The novelty of this research lies in the comprehensive examination of cellulose dissolution behavior in [mTBNH][OAc]/green co-solvent mixtures. The potential of these [mTBNH][OAc]/green co-solvent systems for synthesizing cellulose esters (CEs) through transesterification was

also assessed, with the resulting CEs analyzed for their chemical, structural, thermal, and mechanical properties.

The findings of this research could offer valuable insights into the impact of green co-solvents on the properties of CEs and contribute to the development of innovative solvent systems for cellulose-based functional materials.

Abbreviations and Symbols

AGU	Anhydroglucose unit
CAM	Contact angle measurement
CEs	Cellulose esters
CL	Cellulose laurate
CM	Cellulose myristate
CP	Cellulose palmitate
CS	Cellulose stearate
DMAc	*N,N*-Dimethylacetamide
DMF	*N,N*-Dimethylformamide
DMI	Dimethyl isosorbide
DMPU	*N,N*-Dimethylpropyleneurea
DMSO	Dimethyl sulfoxide
DP	Degree of polymerization
DS	Degree of substitution
DTG	Differential thermogravimetric analysis
GPC	Gel permeation chromatography
GVL	γ-Valerolactone
ILs	Ionic liquids
M_n	Number average molar mass
[mTBNH]	5-methyl-1,5,7-triazabicyclo[4.3.0]non-6-enium
[mTBNH][OAc]	5-methyl-1,5,7-triazabicyclo[4.3.0]non-6-enium acetate
M_w	Weight average molar mass
NMR	Nuclear magnetic resonance
NRRs	Non-renewable resources
RRs	Renewable resources
SB-IL	Superbase ionic liquid
SEC	Size exclusion chromatography
SEM	Scanning electron microscopy
SLF	Sulfolane
TGA	Thermogravimetric analysis
TMS	Tetramethylsilane
VEs	Vinyl esters
VL	Vinyl laurate
VM	Vinyl myristate
VP	Vinyl palmitate
VS	Vinyl stearate
XRD	X-ray diffraction
E_a	Activation energy
ω	Angular frequency

η^*	Complex viscosity
ω_c	Crossover point
Đ	Dispersity of molar mass
η	Intrinsic viscosity
G''	Loss modulus
τ	Relaxation time
$\dot{\gamma}$	Shear rate
G'	Storage modulus
λ	Wavelength
η_0	Zero-shear-rate viscosity

1 Literature Review

1.1 Background

Polymeric materials have become crucial across a wide range of applications, from packaging to high-performance uses such as lithium-ion batteries (Pham, 2022; Haag, 2006; Lopez-Rubio, 2004). These materials are widely valued for their versatility, attractive properties, and generally low cost. In 2021, global polymer production reached 390.7 million tons and is projected to continue growing (Plastics Europe). However, over 90% of these polymers were derived from non-renewable resources (NRRs), raising significant concerns due to the non-renewable and unsustainable nature of petroleum (Plastics Europe). NRRs, particularly crude oil used for producing polymeric materials, are being depleted rapidly, with current consumption rates outpacing natural replenishment by a factor of 100,000 (Pinkert, 2009). To tackle environmental challenges such as pollution and the depletion of NRRs, it is crucial to adopt more sustainable strategies that utilize renewable resources and improve production processes, ensuring a stable long-term supply and societal well-being.

1.2 Cellulose

Cellulose is the most abundant organic polymer in nature, was first isolated in 1837 by French chemist Anselm Payen (Klemm, 2005; Payen, 1838). He treated various plant tissues with acids and ammonia, followed by extraction with ether, water, and alcohol, leaving behind a fibrous solid. Using elemental analysis, Payen determined cellulose's molecular formula as $C_6H_{10}O_5$. In 1839, Dumas and colleagues confirmed its structure and named it "cellulose" because it is the primary component of wood cells (French: *cellules*) (Brongniart, 1839). Later, in 1920, Hermann Staudinger discovered that cellulose is not merely an aggregation of glucose units, but a polymer made of glucose molecules covalently bonded into long molecular chains (Staudinger, 1968). This insight came from his studies on cellulose acetylation and deacetylation.

The following sections of the literature review focus on the sources, structure, and isolation processes of cellulose and its dissolution in various solvents. Additionally, attention is given to the methods for modifying cellulose, with particular emphasis on cellulose transesterification.

1.2.1 Sources and isolation

Lignocellulose serves as the primary source of cellulose. It is present not only in wood but also in other biomass types like cotton and agricultural waste. The proportion of cellulose relative to hemicellulose, lignin, and extractives in different biomass sources is described in **Table 1**. Cellulose content varies both across different biomass types and within similar wood families. For example, hardwoods like poplar contain 51–53% cellulose, while eucalyptus has about 54% (Isikgor, 2015). In softwoods, pine ranges from 42–50%, and spruce is around 45% (Isikgor, 2015). Apart from plants, cellulose is also produced by bacteria like *Acetobacter xylinum* (now called *Gluconacetobacter xylinus*) and green algae (*Valonia species*) in a purer form, free from lignin (Cannon, 1991; Rainer 1998; Vandamme, 1998).

Table 1. Different biomass sources and their lignocellulose composition (adapted from Isikgor, 2015)

Biomass Source	Composition (%)		
	Cellulose	Hemicellulose	Lignin
Hardwood	40-54	18-36	16-24
Softwood	42-50	11-27	20-28
Grasses	25-40	25-50	10-30
Wheat Straw	35-39	23-30	12-16
Barley Hull	34	36	14-19
Barley Straw	36-43	24-33	6-10
Rice Straw	29-35	23-26	17-19
Rice Husk	29-36	12-29	15-20
Corn Cobs	34-41	32-36	6-16
Corn Stalks	35-40	17-35	7-18
Sugarcane Bagasse	25-45	28-32	15-25

The extraction of cellulose fibers from wood is known as pulping, which can be carried out using either mechanical or chemical methods. Mechanical pulping breaks down wood using mechanical energy, typically through grinding with a rotating stone or pressing between metal discs. This method yields over 90% and produces mechanical pulp (MP) or thermomechanical pulp (TMP) (Stevens, 2004). Chemothermomechanical pulping (CTMP), uses chemicals like sodium sulfite/sodium carbonate (Na_2SO_3/Na_2CO_3) or sodium hydroxide (NaOH) to lower the energy required for wood disintegration (Stevens, 2004). Chemical pulping, such as Kraft or sulfate pulping, is the primary method for producing paper-grade and textile-grade cellulose fibers. It uses "white liquor" (sodium sulfide Na_2S and NaOH), where OH^- and HS^- ions break the aryl linkages between lignin and cellulose, enabling lignin removal through washing (Stevens, 2004). In Pre-Hydrolysis Kraft (PHK), used for dissolving pulp, wood chips are pre-treated with steam or dilute acids reducing wood mass by about 20% by removing extractives, hemicellulose, and some lignin (Stevens, 2004). Sulphite pulping utilizes sulfurous acid (H_2SO_3) and hydrogen sulfite (HSO_3^-) ions for delignification (Ek, 2009). The newer organosolv method employs organic solvents like methanol or ethanol for lignin removal (Ek, 2009; Sjöström, 1993; Botello, 1999).

1.2.2 Structure
Cellulose is a homopolymer made of β-D-glucopyranose units or anhydroglucose units (AGU) linked together by 1,4-glycosidic bonds, forming a linear, unbranched chain. In crystalline cellulose, each AGU unit is rotated 180° relative to the next, giving the molecule a flat, ribbon-like shape. The smallest repeating unit in cellulose, known as cellobiose, consists of two AGU units. The molecular structure of cellulose polymer can be represented by **Figure 1**.
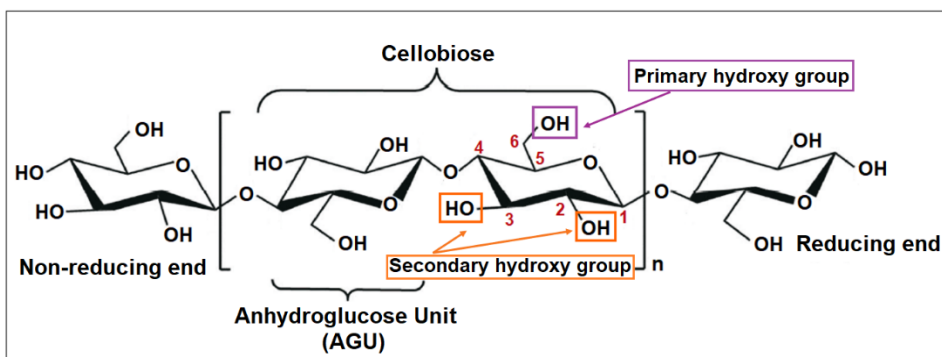
Figure 1. The molecular structure of cellulose (adapted from Pinkert, 2009).

Each AGU unit in cellulose has three hydroxy groups: one at C6 (primary) and two at C2 and C3 (secondary). These hydroxy groups form a strong hydrogen-bonding network, giving crystalline cellulose rigidity, strength, and reactivity. Intramolecular hydrogen bonds occur within the same chain, while intermolecular bonds link different chains. Van der Waals forces and hydrophobic interactions hold the planar structures together, forming microfibrils parallel to each other. The intra- and intermolecular hydrogen bonding in cellulose polymer can be represented in **Figure 2**.
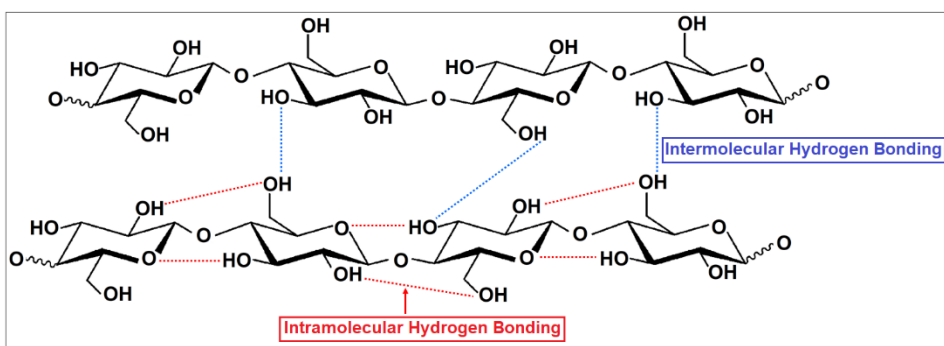

Figure 2. Intra- and intermolecular hydrogen bonding in cellulose (adapted from Pinkert, 2009).

The degree of polymerization (DP) refers to the number of AGUs in the cellulose chain and varies from 300 to 15,000, depending on the source (Klemm, 2005; Moon, 2011) and the raw biomass pretreatment conditions. Native cellulose typically has a higher DP than pulped or regenerated cellulose. DP affects the polymer's physical, mechanical, and solution properties. Cellulose is insoluble in water and most organic solvents, even at low DP, due to its hydrogen-bonding network. A high DP can further reduce reactivity due to hydroxy groups' inaccessibility to the reagents.

The properties of cellulose-based materials are significantly influenced by the degree DP of the starting cellulose. Additionally, the degree of crystallinity is crucial in determining their physical, mechanical, and chemical characteristics. For instance, crystallinity directly impacts the material's accessibility to chemical derivatization processes and its swelling behavior. The degree of crystallinity is a critical factor to consider when evaluating the applications of cellulose and cellulose-based materials (Schenzel, 2005; Agarwal, 2018). Cellulose chains aggregate into elementary fibrils composed of highly ordered crystalline

and less ordered amorphous regions. In the crystalline areas, strong interchain hydrogen bonds contribute to the fiber's high strength, superior axial stiffness, resistance to dissolution in most solvents, and the inability of cellulose to melt. The crystallinity index (CI) describes the proportion of crystalline material in cellulose. Its value typically falls between 40% and 70%, influenced by the source of the cellulose and the separation methods used. Reported CI values can also differ based on the measurement techniques employed (Park, 2010; Bernardinelli, 2015; Zhao, 2006; Thygesen, 2005; Engström, 2006).

1.3 Cellulose Dissolution

Why is the dissolution of cellulose so important? It allows for the development of regenerated materials, such as fibers for textile applications and films for packaging purposes. Additionally, it facilitates the production of valuable cellulose derivatives in a homogenous environment. Finally, efficient cellulose dissolution is crucial for depolymerization and controlled degradation, which is particularly important for biorefinery purposes.

   The dissolution of cellulose in different dissolution media facilitates its regeneration into various polymorphs (**Figure 3**). The process involves the complete dissolution of cellulose in a solvent system, followed by precipitation or regeneration, typically achieved by adding a non-solvent such as water or alcohol. The regenerated cellulose often exhibits altered structural, morphological, and thermal properties compared to its native form, depending on the specific solvent system, dissolution environment, and regeneration conditions used. The study by Hindi (2017) thoroughly discusses the formation of different cellulose polymorphs. Native untreated cellulose with a Cellulose I crystalline structure can be converted into Cellulose II by either chemical regeneration or mercerization. Cellulose III$_I$ and Cellulose III$_{II}$ can be produced from Cellulose I and Cellulose II respectively by exposure to gaseous or liquefied ammonia or certain amine reagents. The Cellulose IV$_I$ and Cellulose IV$_{II}$ polymorphs are formed irreversibly by heating Cellulose III$_I$ or III$_{II}$, respectively, up to 260 °C in a glycerol medium.
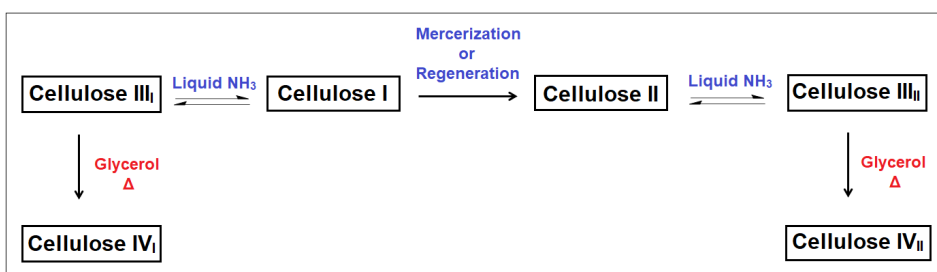

Figure 3. Various polymorphs in cellulose.

1.3.1 Solvents for cellulose dissolution and modifications

Cellulose dissolution methods are classified into derivatizing and non-derivatizing solvents. Historically, derivatizing approaches dominated, with one of the earliest examples being cellulose solubilization using "Schweizer's reagent" ($[Cu(NH_3)_4](OH)_2$) (Schweizer, 1857). Solubilized cellulose can be regenerated by adding an acid, enabling the extraction of cellulose from sources like wood pulp and cotton for producing regenerated fibers such as rayon. Another widely adopted derivatizing method is the viscose process, where cellulose reacts with carbon disulfide, CS_2 in an alkaline solution

to form xanthogenate moiety which disrupts hydrogen bonds and allows dissolution. Similar to "Schweizer's reagent," cellulose precipitates upon acid treatment, regenerating CS_2. However, the viscose process has significant drawbacks, including CS_2 toxicity and high waste production. To address these issues, the CarbaCell process, introduced in the year 2000, uses urea in alkaline conditions to form soluble cellulose carbamate, offering a less toxic alternative (Weißl, 2019; Fink, 2014).

Non-derivatizing solvents form the second category for cellulose solubilization. These solvents are typically polar enough to disrupt intra- and intermolecular hydrogen bonds between cellulose chains. Common examples include dimethyl sulfoxide-tetrabutylammonium fluoride (DMSO-TBAF) (Heinze, 2000; Ciacco, 2003), *N,N*-Dimethylacetamide-lithium chloride (DMAc-LiCl) (McCormick, 1987; Chrapava, 2003; Dawsey, 1990; Potthast, 2002), and N-methylmorpholine N-oxide (NMMO) (Fink, 2001). Among these, NMMO has gained significant attention for its use in the Lyocell process, developed in the 1980s and later scaled for industrial application. Similar to the viscose process, it produces regenerated cellulose fibers but is favored for its simplicity and near-complete solvent recovery, making it almost emission-free (Klemm, 2005).

Ionic liquids (ILs) and deep eutectic solvents (DESs) are relatively new classes of solvents, with ILs being highly effective for cellulose dissolution and modification, while DESs are comparatively less effective. The following section explores the role of ILs in cellulose dissolution.

1.3.2 Ionic liquids

Ionic liquids (ILs) are molten salts consisting of cations and anions with melting points below 100 °C (Wilkes, 2002; Marsh 2004). The first generation of ILs, such as the mixture of 1-butylpyridinium chloride ([BPy]Cl) and aluminum chloride ($AlCl_3$), faced significant limitations, including high sensitivity to moisture and susceptibility to hydrolysis and electrochemical reduction (Pinkert, 2009; Hapiot, 2008). These issues were resolved in the 1990s with the development of second-generation ILs that are stable in air and water (Plechkova, 2008; de María, 2011; Buzzeo, 2004).

Ionic liquids exhibit versatile physicochemical properties, making them suitable for a wide range of applications. Many ILs share common characteristics; for instance, those containing quaternary ammonium cations typically exhibit negligible vapor pressure and non-flammable behavior. Despite this, they can be distilled under reduced pressure and high temperatures without decomposing, enhancing their recyclability (Ostonen, 2016). This attribute contributes to their designation as "green chemicals" or "green solvents" (Anastas, 2010). Some common examples of cations and anions used in ILs are given in **Figure 4**.
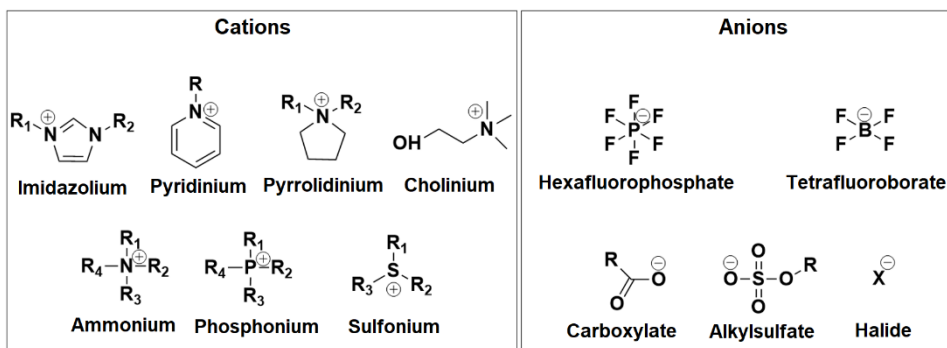
Figure 4. Typical ions of ionic liquids (ILs) (adapted from Silva, 2020).

1-Ethyl-3-methylimidazolium acetate ([EMIM][OAc]) has been recognized as one of the most effective ILs for cellulose dissolution and modifications (Köhler, 2007). However, first-generation imidazolium-based ILs pose challenges in recycling, with questionable stability (Xu, 2021; Kostag, 2019) and difficulty in distillation due to their very low vapor pressure. In contrast, superbases, particularly di- or triazabicyclo compounds derived from protonic ILs, are emerging as promising alternatives for cellulose dissolution, modification, and upscaling. These solvents can dissolve cellulose at high concentrations (up to 25 wt% for cellulose with a degree of polymerization around 200–300), exhibit low moisture sensitivity and toxicity, and can be repeatedly recycled without degradation (King, 2011; Hellsten, 2020; Ostonen, 2016). Recently, 5-methyl-1,5,7-triazabicyclo[4.3.0]non-6-enium acetate ([mTBNH][OAc]) has emerged as a promising candidate for cellulose dissolution and regeneration (Martins, 2022; Parviainen, 2015). The superbase 5-methyl-1,5,7-triazabicyclo[4.3.0]non-6-enium (mTBN) exhibits greater water stability compared to 7-methyl-1,5,7-triazabicyclo[4.4.0]dec-5-enium (mTBD) (Martins, 2022) and 1,5-diazabicyclo[4.3.0]-non-5-ene (DBN) (Ostonen, 2016). Unlike the highly crystalline 7-methyl-1,5,7-triazabicyclo[4.4.0]dec-5-enium acetate [mTBDH][OAc], [mTBNH][OAc] is liquid at room temperature (Hellsten, 2020), simplifying processing and reducing labour intensity. These features make this newly developed IL a strong candidate for industrial applications.

The effectiveness of cellulose dissolution in ILs depends on the nature and balance of cations and anions. Research shows that a slightly higher concentration of anion in the IL significantly improves carbohydrate dissolution (Wang, 2012; Badgujar, 2015; Freire, 2011). Ionic liquids with more electronegative anions exhibit greater dissolving power; for example, 1-butyl-3-methylimidazolium chloride, [BMIM][Cl] dissolves cellulose effectively, whereas 1-butyl-3-methylimidazolium bromide, [BMIM][Br] and 1-butyl-3-methylimidazolium, iodide, [BMIM][I] show limited solubility. Additionally, shorter alkyl chains on the cation significantly improve the solubility of imidazolium-based ionic liquids (Holm, 2011). Similarly, the introduction of an allyl group in the imidazolium cation further enhances their dissolving capability (Holm, 2011).

Cellulose dissolves in ionic liquids through strong interactions between the polar hydroxy (-OH) functional group and the ions (cations and anions) of the ionic liquids via hydrogen bonding. Holm and Lassi (2011) studied cellulose dissolution in ionic liquids with various cations and anions, demonstrating that the anion acts as a hydrogen acceptor, while the cation interacts with the electronegative oxygen of the hydroxy group.

These interactions disrupt the inter- and intramolecular hydrogen bonds in cellulose chains, leading to their dissolution. A proposed mechanism for this dissolution process has been illustrated in **Figure 5**.
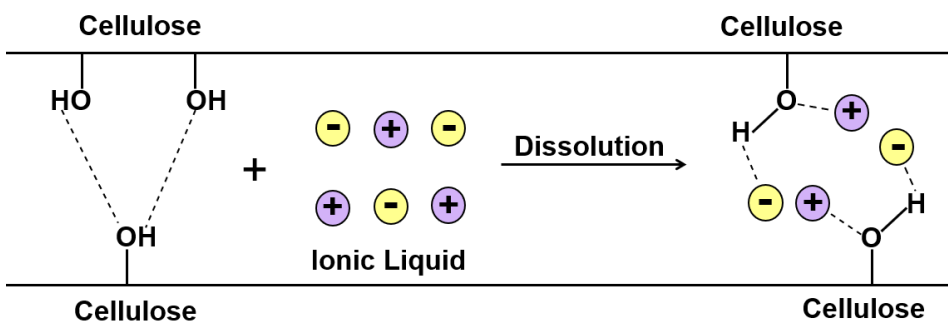

Figure 5. Cellulose dissolution mechanism in ionic liquid (IL) (adapted from VillaIta, 2022).

1.3.3 Role of co-solvents in cellulose dissolution

ILs are typically highly viscous, and adding polymers like cellulose further increases viscosity, posing challenges for practical use. High viscosity hinders mass transfer and requires significant energy for mixing cellulose into the solution. To address this, adding polar aprotic co-solvents has enhanced cellulose dissolution. As discussed in the previous section, the solubility of cellulose in ILs primarily depends on the hydrogen bond-accepting ability of IL anion. Co-solvents aid in cellulose dissolution by indirectly interacting with cellulose, facilitating the dissociation of cation-anion pairs in the IL. This process allows the IL cation to be solvated, freeing the anion to form hydrogen-bonded complexes with the cellulose (Lv, 2012; Li, 2016). The mechanism of cellulose in the IL/co-solvent system can be illustrated in **Figure 6**.

Co-solvents also improve mass transfer between cellulose and ILs and reduce the monomer friction coefficient by lowering solution viscosity (Lv, 2012; Andanson, 2014). Additionally, co-solvents reduce the reliance on costly ILs, lowering overall processing costs. The commonly used co-solvents for cellulose dissolution and modifications are dimethyl sulfoxide (DMSO), *N,N*-Dimethylacetamide (DMAc), and *N,N*-Dimethylformamide (DMF) (Phadagi, 2021; Mohan, 2016). IL/DMSO co-solvent solution was more effective in dissolving cellulose than pure ILs (Rinaldi, 2011).

However, the extensive use of stated co-solvents, which are mainly derived from fossil-based sources, raises environmental and health problems due to their toxicity and large energy inputs. Reducing reliance on these solvents and finding greener alternatives to them is vital in green chemistry research (Constable, 2007; Bryan, 2018). Greener alternatives should ideally come from renewable sources, be safer to handle, less toxic, and provide equal or superior solubilization compared to fossil-based options. Recently, green, bio-based solvents from biomass resources have shown the potential to curb the depletion of fossil fuels (Gu, 2013; Clark, 2015). Some examples of important green solvents are- γ-Valerolactone (GVL) (Horváth, 2008), dimethyl isosorbide (DMI) (Tundo, 2010), p-cymene (Clark, 2012), dihydrolevoglucosenone (Cyrene) (Sherwood, 2014; Camp, 2018), and diformylxylose (Komarova, 2021). GVL, a polar aprotic solvent derived from lignocellulosic biomass, is an excellent bio-based substitute for conventional polar aprotic solvents owing to its renewability, biodegradability, and non-toxicity (Strappaveccia, 2015; Duereh, 2015). Furthermore, its wide temperature range, with a

low melting point of -31 °C and a high boiling point of 207 °C, guarantees its safety for large-scale solvent usage. DMI, derived from glucose via sorbitol, distinguishes itself through its chiral structure and high polarity, making it a promising substitute for traditional polar aprotic solvents (Bryan, 2018; Wilson, 2018). Sulfolane (SLF) is a promising sustainable reaction medium (Tilstam, 2012; Henderson, 2011). Although it ranks lower on the sustainability scale, it proves invaluable in numerous applications, such as biomass valorization (Asakawa, 2019). *N,N*-Dimethylpropyleneurea (DMPU), a "green solvent" with a high boiling point, low melting point, and low toxicity, also offers an environmentally friendly option (Gören, 2016).
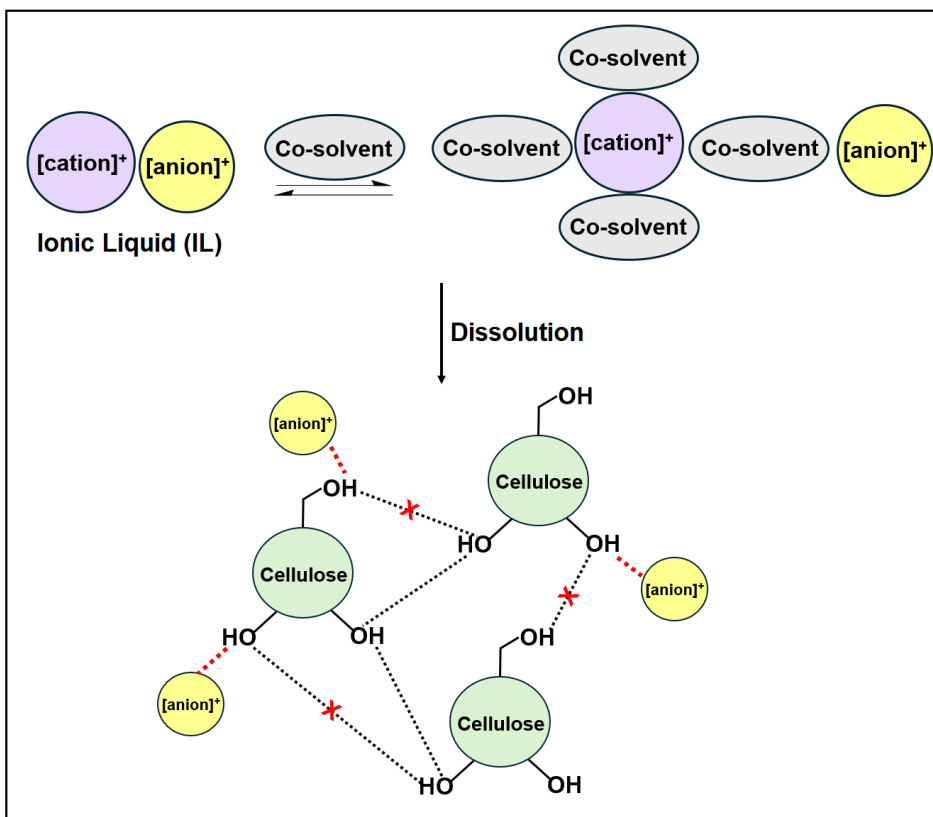

Figure 6. Cellulose dissolution mechanism in ionic liquid/co-solvent (adapted from Li, 2016; Seoud, 2019).

1.4 Chemical Modifications of Cellulose

Cellulose's three hydroxy (-OH) groups enable chemical transformations like esterification, etherification, silylation, polymer grafting, etc. Among various chemical modifications, the esterification of cellulose is one of the most versatile transformations, offering easy access to a wide range of functional cellulose-based materials. This modification transforms the hydroxy group of cellulose to the ester functional group, making the material thermoplastic. Key thermoplastic cellulose derivatives, commonly used in plastics, films, fibers, membranes, and coatings, include cellulose acetate, cellulose acetate butyrate, and cellulose acetate propionate (Rubin, 1990).

Cellulose esterification can be performed using two methods: heterogeneous and homogeneous. The heterogeneous method is favored at the industrial scale because it does not require complete dissolution of cellulose in the solvent system. However, since cellulose is not fully dissolved, its hydroxy groups are not entirely accessible to the chemical reagents, resulting in non-uniform esterification. In contrast, the homogeneous method involves the complete dissolution of cellulose in the solvent, allowing all hydroxy groups to be fully exposed to the chemical reagents, leading to uniform esterification along the entire cellulose polymer chain.

The degree of substitution (DS) refers to the number of hydroxy groups in a cellulose monomer that are replaced by ester groups during esterification. The maximum DS value is 3, while the minimum is 0. DS plays a crucial role in determining the properties of the final cellulose ester product. It can be controlled by optimizing reaction parameters such as temperature, time, and the molar ratios of reactants, which is feasible in the homogeneous method but not in the heterogeneous method. Considering the above reasons, homogeneous esterification is considered more effective for synthesizing cellulose esters than heterogeneous esterification.

1.4.1 Esterification vs Transesterification

Cellulose esterification typically involves the reaction between the hydroxy (-OH) group of cellulose with carboxylic acids with acid catalysts or activated derivatives like anhydrides or acid chlorides. Fatty acids are preferred for cellulose esterification over other carboxylic acids as their long hydrocarbon chains enhance the hydrophobicity of cellulose esters (CEs), improving water resistance and compatibility with nonpolar solvents. Their tunable chain length allows tailoring the properties of CEs, such as solubility, mechanical strength, and flexibility. CEs obtained from fatty acids offer enhanced thermal stability for heat-resistant applications. Moreover, fatty acid-based cellulose esters are biodegradable and environmentally friendly, aligning with sustainable and green chemistry goals. However, fatty acids are non-degradative to cellulose but have low reactivity due to the carboxylic acid group. To improve the reactivity, they are converted into more reactive forms like fatty acid anhydrides. When used with catalysts, they are more effective esterification agents for cellulose ester synthesis. However, reactivity decreases with longer carbon chains, making esterification with long-chain anhydrides challenging. Fatty acid chlorides are also important esterification agents for producing long-chain cellulose esters, but the reaction generates corrosive HCl as a by-product (**Figure 7**). HCl is neutralized using bases like pyridine, trimethylamine, or *N,N*-Dimethyl-4-aminopyridine (DMAP) to minimize cellulose degradation.

Synthesizing cellulose esters via transesterification with vinyl esters (VEs) is a greener alternative to traditional esterification methods. Using vinyl esters as acylating agents offers advantages over acid anhydrides and acid chlorides: the byproduct, vinyl alcohol, rapidly tautomerizes to low boiling point acetaldehyde (b.p. 20°C), which can be easily removed from the reaction system driving the reaction equilibrium toward the product (**Figure 7**). Additionally, this method operates under mild conditions without requiring hazardous substances and external catalysts.
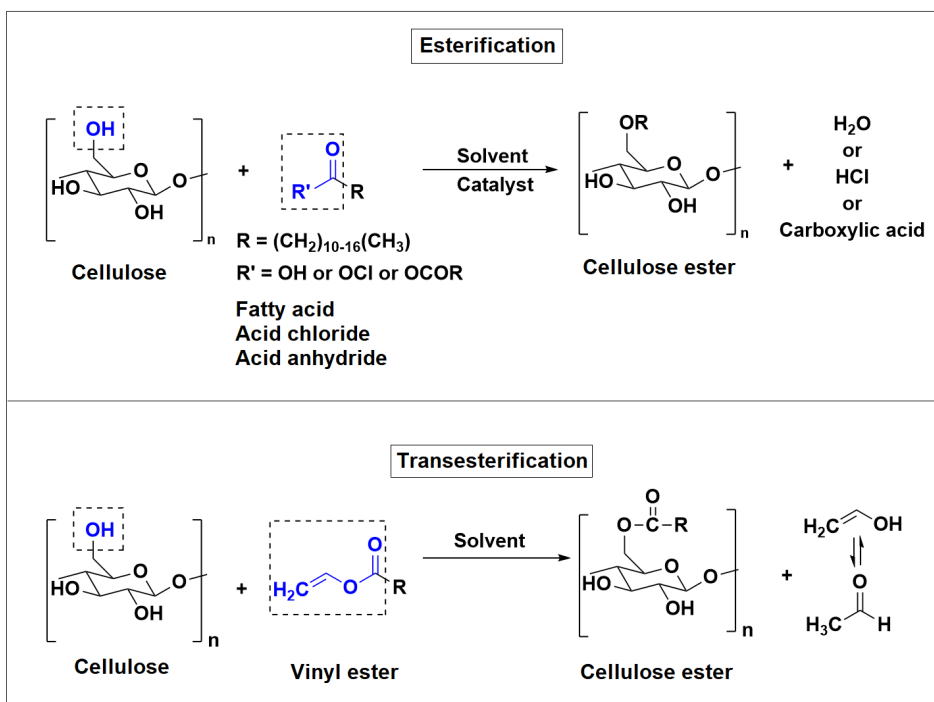
Figure 7. Synthesis of cellulose ester via esterification and transesterification routes.

1.4.2 Homogeneous transesterification of cellulose in ionic liquid

Over the past decade, various ionic liquids (ILs) have been successfully utilized for the homogeneous transesterification of cellulose.

Schenzel et al. (2014) reported a catalytic transesterification of cellulose was investigated under homogeneous conditions using IL, 1-butyl-3-methylimidazolium chloride ([BMIM][Cl]) as the solvent. This method effectively converted cellulose into cellulose esters using various methyl esters and 10 mol% of 1,5,7-triazabicyclo[4.4.0]dec-5-ene (TBD) as the catalyst. Through the optimization of reaction conditions, the degree of substitution (DS) of the resulting cellulose esters could be selectively controlled, yielding a maximum DS of 0.69 which was determined by the ^{1}H NMR method.

Cellulose fatty esters with various fatty acids, including lauric, myristic, palmitic, stearic, and oleic acid, all having the same degree of substitution (DS ≈ 2.0), were synthesized via homogeneous transesterification using ([BMIM][Cl]) were reported by (Singh, 2014). Tribological studies revealed promising antifriction properties for all the synthesized cellulose esters, highlighting their potential as bio-based lubricants.

Chen et al. (2017) successfully reported the homogeneous transesterification of sugarcane bagasse (SCB) using 1-ethyl-3-methylimidazolium chloride ([EMIM][Cl]) as the solvent using vinyl esters. The SCB ester films exhibited performance similar to that of cellulose derivatives obtained from commercial cellulose. This study introduced an alternative method for converting lignocellulosic biomass into bioplastics without the need for lignocellulose pretreatment.

The synthesis of cellulose laurate was studied through transesterification in a 1-allyl-3-methylimidazolium chloride [AMIM][Cl]/DMSO co-solvent system, using vinyl laurate as the acylation reagent and 1,8-diazabicyclo[5.4.0]undec-7-ene (DBU) as a catalyst by

Wen et al. (2017). DS varied from 1.47 to 2.74 by adjusting the reaction time, temperature, and the molar ratio of AGU to vinyl laurate. The chemical structure of the synthesized cellulose laurate was analyzed using FT-IR, ^{1}H NMR, ^{13}C NMR, HSQC, and XRD to confirm successful transesterification. The attachment of long aliphatic side chains enhanced the thermal stability of cellulose. The films demonstrated ductile mechanical properties and contact angle measurements confirmed their hydrophobic nature. With their combination of ductility and hydrophobicity, cellulose laurate films hold significant promise for applications in sustainable packaging.

Hanabusa et al. (2018) reported the synthesis of cellulose acetates using a range of protic ionic liquids (PILs), including 1,8-diazabicyclo[5.4.0]undec-7-enium acetate ([DBUH][OAc]) and 1,5-diazabicyclo[4.3.0]non-5-enium acetate ([DBNH][OAc]) with vinyl acetate as an acetylation agent.

Hirose et al. (2019) investigated the role of EMIM carboxylate-type ILs as both the solvent and organocatalyst in the transesterification reaction of cellulose. The study found that using [EMIM][OAc] and vinyl ester led to an undesired side reaction, where the acetate anion from [EMIM][OAc] was incorporated into the cellulose ester. The newly synthesized [EMIM][p-anisate] successfully facilitated the transesterification of cellulose, achieving a high DS value (> 2.9) from the vinyl esters and minimal side reactions (selectivity > 99%).

Yuan et al. (2019) studied the dissolution behavior of cellulose and its transesterification in a system combining [EMIM][OAc] with GVL as a co-solvent. The cellulose solubility in [EMIM][OAc]/GVL surpassed that in pure [EMIM][OAc], as evidenced by its relatively lower dissolution activation energy. The enhanced performance was further confirmed through rheological studies. The solution's potential for homogeneous derivatization was explored through the transesterification of α-cellulose with vinyl esters at 80 °C for 4 hours, using a low vinyl ester-to-anhydroglucose unit (AGU) molar ratio of 3. This process yielded cellulose laurate and cellulose pivalate esters with a DS of 3.0, as well as cellulose chloroacetate ester with a DS of 1.43.

Gao et al. (2023) reported the synthesis of a novel IL derived from 1,8-diazabicyclo[5.4.0]undec-7-enium (DBU), namely [DBUC$_8$][Cl]. This IL offers several advantages, including ease of synthesis, availability of raw materials, and good solubility for cellulose. Notably, the excellent cellulose solubility and the inherent catalytic activity of [DBUC$_8$][Cl] enable efficient homogeneous esterification of cellulose into cellulose acetate (CA) without the need for additional catalysts.

Todorov et al. (2023) reported the development of a sustainable homogeneous transesterification method using the superbase ionic liquid (SB-IL), 5-methyl-1,5,7-triaza-bicyclo-[4.3.0]non-6-enium acetate, [mTBNH][OAc] and unactivated methyl esters. This protocol enables the preparation of cellulose esters with a controllable DS.

1.4.3 Applications of cellulose esters

Cellulose esters (CEs) have long been used in coatings as additives, binders, lubricants, and film formers. They offer benefits like viscosity control, enhanced UV stability, improved sprayability, and reduced drying time in coating applications (Edgar, 2001; Amim, 2008). Over the last few decades, research has increasingly focused on developing cellulose ester-based packaging films as sustainable alternatives to non-renewable materials. These films are transparent, and rigid, and offer excellent barrier and antimicrobial properties, making them potential materials for packaging applications (Bras, 2007; Gouvêa, 2015; Gemili, 2009; Quintero, 2013). CEs exhibit thermoplastic

properties and can be processed using conventional methods like film extrusion and injection molding (Hooshmand, 2014; Wang, 2018; Law 2004; Krasnou, 2015). CEs are suitable for industrial-scale fiber production through melt spinning (Franko, 2001; Glasser, 1999). CEs are also effective as membranes for ultrafiltration applications, known for their good salt rejection and film-forming properties (Arthanareeswaran, 2010). Additionally, they are emerging as promising materials for 3D printing, providing a sustainable option for creating structures (Tenhunen, 2018; Dai, 2019; Pattinson, 2017). CEs are widely used in pharmaceutical controlled-release formulations, including osmotic and enteric-coated drug delivery systems, due to their low toxicity. Thin films of CEs have proven effective for selective adsorption of proteins and biomolecules (Wu, 2010; Shokri, 2013; Kosaka, 2007).

1.5 Summary of the Literature Review and Aim of the Study

Traditional polymeric materials derived from non-renewable resources (NRRs) contribute significantly to severe environmental challenges, including soil, water, and air pollution, as well as the depletion of fossil fuel reserves. Hence, identifying sustainable and eco-friendly alternatives to conventional polymers has become a critical priority. Cellulose, a natural polymer, is the most abundant renewable resource on Earth. As a primary constituent of biomass, it consists of numerous monomeric units, referred to as anhydroglucose units (AGU), interconnected through β-glycosidic bonds. The three hydroxyl (-OH) groups in AGU enable its modification into various derivatives with potential applications as bio-based functional polymeric materials.

Homogeneous transesterification offers a sustainable approach to synthesizing cellulose esters (CEs) by reacting cellulose with fatty acid esters, thereby imparting thermoplastic properties to native cellulose. Cellulose must first be dissolved in an appropriate solvent to enable homogeneous modification. Ionic liquids (ILs) have proven to be effective for cellulose dissolution and modification, offering advantages such as low toxicity, superior solubility compared to traditional solvents, low vapor pressure, and recyclability.

ILs are typically highly viscous, and adding cellulose further increases viscosity, complicating practical use. This high viscosity restricts mass transfer and demands considerable energy for mixing. Adding polar aprotic co-solvents like dimethyl sulfoxide (DMSO), *N,N*-Dimethylacetamide (DMAc), and *N,N*-Dimethylformamide (DMF) has improved cellulose dissolution – being significantly lower in viscosity compared to ILs, these co-solvents reduce the overall viscosity of the cellulose/IL mixtures, enhancing the mass transfer ratio and thereby improving cellulose dissolution in IL. Co-solvents, being more cost-effective than ILs, also reduce the overall processing cost.

The aim of this study was to develop novel, sustainable solvent systems for cellulose dissolution and transesterification and examine the properties of the resulting CEs.

The following objectives were set to achieve this aim:

- To evaluate the dissolution behavior of cellulose in superbase ionic liquid (SB-IL) combined with various green co-solvents, identifying the most effective SB-IL/ co-solvent combination and their optimal ratios for cellulose dissolution.
- To examine the structural and morphological changes in cellulose during dissolution and transesterification in various SB-IL/co-solvent combinations.
- To investigate the influence of green co-solvents on cellulose transesterification and the chemical, physical, and mechanical properties of the synthesized CEs.

The following activities were performed to achieve these objectives:

- Rheological analysis of cellulose/SB-IL solutions with various green co-solvents at different ratios was conducted to investigate cellulose dissolution behavior.
- Optimization experiments were first conducted via homogeneous transesterification of cellulose with vinyl esters (VEs) in SB-IL/DMSO to determine the reaction parameters for achieving the highest degree of substitution (DS) in the resulting CEs.
- Using these optimized reaction conditions, the influence of green co-solvents on the DS of CEs was further investigated by conducting homogeneous transesterification of cellulose with VEs in solvent systems containing SB-IL combined with various green co-solvents.
- Structural, thermal, rheological, mechanical (tensile testing), and surface properties of CEs were studied.

2 Experimental

Fibrous cellulose was selected as the starting material for the synthesis of cellulose esters (CEs). Superbase ionic liquid (SB-IL), [mTBNH][OAc] was chosen as the solvent for cellulose dissolution and transesterification. Different polar aprotic solvents like dimethyl sulfoxide (DMSO), γ-Valerolactone (GVL), dimethyl isosorbide (DMI), sulfolane (SLF), and *N,N*-Dimethylpropyleneurea (DMPU) were mixed with SB-IL in different ratios to make the binary solvent systems. Vinyl esters (VEs) namely vinyl laurate (VL), vinyl myristate (VM), vinyl palmitate (VP), and vinyl stearate (VS) were selected as acylating agents. A more detailed explanation of the materials and techniques used in this PhD thesis is given in the following chapter.

2.1 Materials

The cellulose used in this work has a fiber length of 0.02–0.1 mm and was purchased from Carl Roth GmbH (Karlsruhe, Germany). SB-IL, 5-methyl-1,5,7 triazabicyclo[4.3.0]non-6-enium acetate, [mTBNH][OAc] is not commercially available and was synthesized at the University of Helsinki by a stoichiometric mixture (1:1) of acetic acid and superbase, 5-methyl-1,5,7-triazabicyclo[4.3.0]non-6-enium (mTBNH) at room temperature with purity > 97% [Martins, 2022; Sosa, 2023] and supplied by Liuotin Group Oy (Porvoo, Finland). The melting point of SB-IL is 15 °C; density is 1.16 g/ml; viscosity is 205 mPa·s (25 °C); flash point more than 220 °C. DMSO with purity > 99% was purchased from Fisher Chemical (Pittsburgh, PA, USA). GVL, DMI, and SLF with purity > 99% were purchased from Sigma Aldrich (St. Louis, MO, USA). DMPU with purity > 99% was purchased from Acros Organics (Geel, Belgium). Vinyl esters (VEs)- VL, VM, VP, and VS with purity > 98% were purchased from Tokyo Chemical Industry Co (Tokyo, Japan). Chloroform-d (purity = 99.8 atom % D. contains 1 v/v% tetramethylsilane, TMS) for nuclear magnetic resonance (NMR) analysis was purchased from Acros Organics (Geel, Belgium). All other chemicals and solvents were used without further purification: Ethanol 98%; Acetone 95% (Keemiakaubandus AS, Maardu, Harju County, Estonia); and n-hexane ≥ 95% (Sigma Aldrich, St. Louis, MO, USA).

   Figure 8 illustrates the chemical structures of the SB-IL [mTBNH][OAc] and the green co-solvents used to prepare the binary solvent systems for cellulose dissolution and modification, whereas **Figure 9** depicts the chemical structures of all the acylating agents utilized in this study.
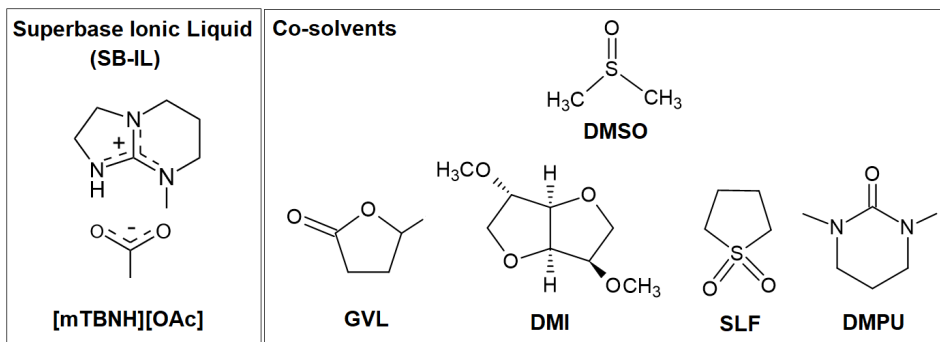

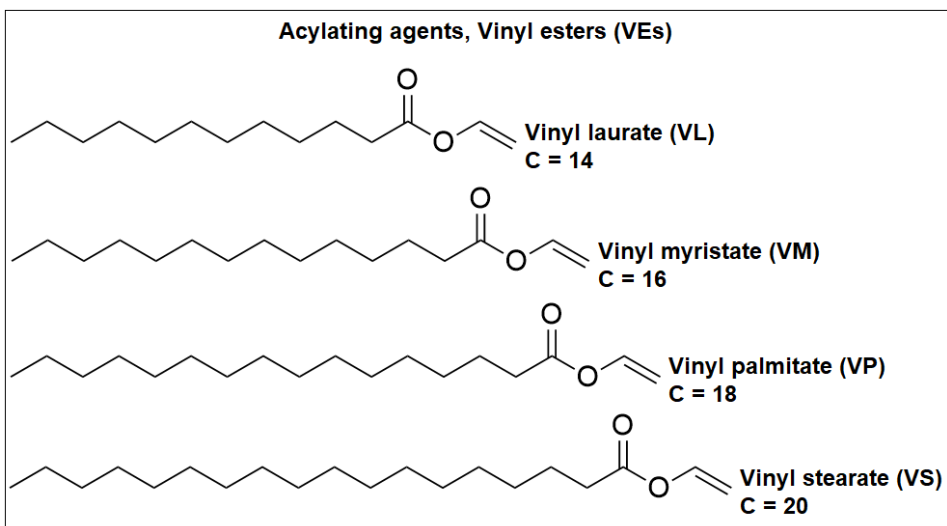*Figure 8. Chemical structures of SB-IL, [mTBNH][OAc], and co-solvents used in this study.*

Figure 9. Chemical structures of acylating agents (vinyl esters) used in this study.

2.2 Methods

2.2.1 Cellulose dissolution in [mTBNH][OAc]/co-solvent solutions

Cellulose was dried under vacuum at 105°C for 24 hours before use. The concentration of cellulose in all studied solutions was 2 wt%. Cellulose was dissolved in mixtures of SB-IL, [mTBNH][OAc] with co-solvents (DMSO, GVL, DMI, SLF, DMPU) with 2:1, 1:1, and 1:2 SB-IL:co-solvent weight ratios at 60°C until the clear, transparent solution was obtained.

2.2.2 Homogeneous transesterification of cellulose in [mTBNH][OAc]/ co-solvent with vinyl esters

To determine the optimized reaction conditions (temperature, time, and molar ratios), cellulose transesterification with vinyl esters (VEs) was performed in a 1:1 [mTBNH][OAc]/DMSO binary solvent system, without the use of an external catalyst. After the complete dissolution of 2 wt% of pre-dried cellulose in the solvent system, the chosen VE acylating agent (3–12 eq./anhydroglucose unit, AGU) was carefully added to the cellulose solution at the desired reaction temperature (60–120 °C) and duration (1–5 hours) under a nitrogen atmosphere. After the reaction was completed, the mixture was added to 250 mL of warm distilled water and vacuum filtered. The solid product was thoroughly washed with ethanol, acetone, and n-hexane to remove residual solvents and unreacted VE. The product was dried under a vacuum at 55 °C overnight.

To study the effect of the green co-solvents on the properties of cellulose esters, the cellulose transesterification with VEs was performed in a 2:1 [mTBNH][OAc]/green co-solvent binary system. The green co-solvents were mainly GVL, DMI, SLF, and DMPU. A calculated amount of VE (5 eq./AGU) was added to a 2 wt% cellulose solution in a 2:1 SB-IL: green co-solvent mixture within a chemical reactor equipped with a mechanical stirrer and nitrogen flow. The reaction proceeded at 70 °C for 2 hours under a nitrogen atmosphere with vigorous stirring. These reaction conditions were selected because temperatures exceeding 80 °C or reaction times longer than 3 hours led to the degradation of the reaction components and/or the final cellulose esters (CEs) (Savale, 2024). Upon

completion, the resulting cellulose ester was precipitated into 500 mL of warm distilled water. To eliminate solvents, the product was washed several times with 100–200 mL of ethanol, acetone, and hexane to remove any unreacted VE. The final product was dried overnight under vacuum at 55 °C.

2.2.3 Characterization

Molar mass determination

The molar mass of pure cellulose was determined at 25 °C using the intrinsic viscosity [η] (= 5 dL/g) of a cellulose solution in cupriethylenediamine hydroxide (Cuene), following the standard procedure ASTM D1795 – 13. The molar mass was then calculated using the Mark-Houwink equation with parameters K = 1.01×10^{-4} dL/g and a = 0.9 (Brandrup, 1999). The resulting molar mass was 163,000 g/mol (DP = 1000).

The size exclusion chromatography (SEC) profiles of CEs were obtained using gel permeation chromatography (GPC) on a Shimadzu Prominence system, equipped with a Shodex KF-804 column and a refractive index detector (RID-20A). The GPC system was calibrated with three polystyrene standards (74,800 Da, 230,900 Da, and 473,600 Da). CE samples (10 mg) were dissolved in 1–2 mL of pyridine, and the GPC analysis was conducted at 60 °C, using pyridine as the mobile phase with a flow rate of 0.5 mL/min. The molecular weights (number-average M_n, weight-average Mw, and dispersity Đ = Mw/M_n) of the CEs were calculated. Multiple samples were tested 2–3 times, and the molecular weight measurements' standard deviation was 3–8%.

Rheology

The rheological properties of cellulose/[mTBNH][OAc]/co-solvent solutions as well as cellulose ester (CE) films were analyzed using an Anton Paar Physica MCR501 rheometer with a cone-plate geometry (25 mm plate diameter, 2° cone angle). The CE films were prepared via solvent casting on a glass petri dish. CEs were dissolved in pyridine at a concentration of 5 wt% and stirred for 16 hours at 40–60 °C until fully dissolved. Once dissolved, the solution was poured into a glass petri dish, and the solvent was allowed to evaporate at room temperature for 24 hours. For rheological measurements, ~ 100 µm thick films were cut into 25 mm Ø discs.

Flow curves were measured over a shear rate (γ˙) range of 0.01 to 100–500 s^{-1}. Complex viscosity (η*) was determined across angular frequencies (ω) ranging from 0.01 to 500 rad/s (for cellulose/[mTBNH][OAc]/co-solvent solutions) and 0.1 to 100–500 rad/s (for CE films). A constant strain of 1% (for CE films) and 5% (for cellulose/[mTBNH][OAc]/co-solvent solutions) was applied to define the linear viscoelastic region (LVR), which was confirmed using an amplitude sweep test at 1 Hz.

For the rheological studies of cellulose/[mTBNH][OAc]/co-solvent solutions, measurements were conducted at 25°C, except for temperature-dependent zero-shear viscosity, which was evaluated over a 25–100°C range. While for the studies of CE films, all measurements were performed at 190°C. Standard equations were used to calculate rheological parameters (Malkin, 1994), and each curve was obtained 2–4 times to ensure reproducibility and accuracy of the results.

Nuclear magnetic resonance spectroscopy (NMR)

Since most CEs synthesized via the homogeneous transesterification process are soluble in organic solvents such as chloroform, DMSO, and pyridine, their structures can be analyzed using solution NMR. The CEs were examined with NMR techniques, including

^{1}H NMR and ^{13}C NMR, performed on an Agilent Technologies DD2 500 MHz spectrometer equipped with 5 mm broadband inverse (^{1}H) or broadband observe (^{13}C) probes.

Before acquiring the NMR spectra, a 15-minute temperature equilibration period was observed after sample insertion, with the sample temperature set at 20 °C below the boiling point of the chosen NMR solvent. For ^{1}H spectra, 64 scans were performed with a 25-second relaxation delay, while ^{13}C spectra required 20,000–45,000 scans with a 2.5-second recycle delay to achieve the desired signal-to-noise ratio.

NMR samples were prepared by dissolving 15–20 mg of the CE in 0.8–1.0 mL of deuterated solvent and heating the mixture at 40–45 °C for 30 minutes until a clear solution formed. The solution was prepared in a small, pre-dried glass bottle sealed with parafilm. Ultrasonic treatment was applied to ensure transparency. Tetramethylsilane (TMS) was used as an internal standard for the NMR experiments.

The degree of substitution (DS) represents the number of hydroxyl groups in AGU of the cellulose monomer that is replaced by the ester group. The DS of CEs was calculated from the ^{1}H NMR spectrum by analyzing the intensity of the corresponding resonances, as outlined in the method described by (Lowman, 1998):

$$DS = \frac{10 \times I_{CH_3} / 3}{I_{AGU} + I_{CH_3}/3} \qquad\qquad Eq.\ 1$$

where I_{CH_3} is the integral of terminal methyl protons of the aliphatic fatty acid chain region and I_{AGU} is the integral of all protons of AGU.

Dual or triple DS measurements were performed for each sample, and the average DS value was calculated. Deviations in DS between two or three measurements were within ±0.1.

X-ray diffraction (XRD) analysis
XRD analysis of the native cellulose and powdered samples of CE was performed using a Rigaku Ultima IV diffractometer equipped with a silicon detector and a Cu Kα radiation source (λ=0.1540 nm). Measurements were conducted over a 2θ range of 5° to 40°, with an anode voltage of 40 kV, an anode current of 40 mA, and a θ-θ scan mode at a step size of 0.02°.

Scanning electron microscopy (SEM)
The morphology of the CE films was examined using a Gemini Zeiss Ultra 55 scanning electron microscope (SEM) (Carl Zeiss, Germany). All specimens were then carbon-glued to the stud and vacuum-coated with Au/Pt before observation.

Thermogravimetric analysis (TGA)
The thermal stability and degradation behavior of CEs samples were investigated using a Setaram Labsys Evo 1600 thermoanalyzer. The experiments were conducted under non-isothermal conditions up to 600 °C at a heating rate of 10 °C/min in an argon atmosphere. Standard 100 μL alumina crucibles were employed, with sample masses of 6 ±1.0 mg, and a gas flow rate of 20 mL/min. The peak degradation temperatures were determined from the derivative thermograms (DTG).

Mechanical properties of cellulose ester films
Tensile tests were conducted using an Instron 5866 machine at 22 °C and 45% relative humidity for all samples. The cast films of CEs were cut into ribbons measuring 20 × 10 × ~ 0.1 mm. For each sample, 7–10 ribbon specimens were tested, and the average values of elastic modulus, strain at break, and stress at break were recorded. A pulling rate of 20 mm/min was applied during the measurements.

Contact angle measurements (CAM)

The hydrophobicity of the prepared CE film surfaces was assessed by measuring the equilibrium contact angle using a DataPhysics OCA 20 device and SCA 20 software (Riverside, CA, USA). Experiments were conducted on both sides of the films, and average values were calculated. Distilled water was used as the liquid agent to form a drop on the surface. A total of five measurements were taken for each variable and averaged. All contact angle measurements were performed at room temperature and 40% relative humidity.

3 Results and Discussion

3.1 Dissolution of Cellulose in [mTBNH][OAc]/green co-solvents (Publication III)

Superbase Ionic Liquids (SB-ILs) are effective for cellulose dissolution and modification, their high viscosity and cost can be mitigated by using lower-viscosity, inexpensive co-solvents like dimethyl sulfoxide (DMSO) (Tarasova, 2023). However, greener alternatives such as γ-Valerolactone (GVL), dimethyl isosorbide (DMI), and *N,N*-Dimethylpropyleneurea (DMPU) should be investigated for sustainable cellulose processing. It is still unclear how much these green co-solvents can reduce the viscosity of SB-IL/cellulose solutions and the optimal amount to add without negatively impacting cellulose solubility in SB-IL, which is necessary for their effective use as DMSO replacements, leaving room for further investigation in this area.

In this study, the effect of green co-solvent content on the rheological properties of cellulose/SB-IL/co-solvent solutions was investigated. SB-IL, [mTBNH][OAc] was combined with selected green co-solvent (GVL, DMI, or DMPU) in ratios of 2:1, 1:1, and 1:2 (by weight). As a reference, the impact of DMSO content on the rheological properties of cellulose/SB-IL/DMSO solutions was also assessed. To investigate the quality of the cellulose solutions, the dependences of the complex viscosity (η^*), and the storage (G') and loss (G'') moduli of the cellulose/SB-IL/co-solvent solutions on angular frequency (ω) were evaluated. The rheological tests were conducted at a temperature of 25 °C and all rheological plots are presented on double logarithmic scales. These measurements provided insights into gel formation caused by the reduced polymer solubility in the selected solvent system (Heinze, 2000). The dissolution behavior of cellulose in the chosen weight ratios of SB-IL/co-solvent was compared to its dissolution behavior in pure SB-IL.

Figure 10a shows the angular frequency dependence of complex viscosity of 2 wt% cellulose (DP = 1000) in pure SB-IL and SB-IL/DMSO binary mixtures with varying ratios of DMSO. All solutions exhibit non-Newtonian, shear-thinning behavior, indicating that all the solutions are located in the entanglement region. The viscosity of the cellulose solution in SB-IL decreases with the addition of DMSO while maintaining a constant cellulose concentration. This decrease in viscosity may be attributed to the lower viscosity of DMSO (2.0 mPa·s) compared to the [mTBNH][OAc] (200 mPa·s). Lv et al. (2012) reported a similar decrease in the viscosity of the cellulose solutions in imidazolium-based ILs when DMSO was used as a co-solvent. Additionally, the critical angular frequency, which is associated with the transition from Newtonian to shear-thinning behavior of the solutions shifts to a higher value as the DMSO content in the binary solvent system increases. However, when a 1:2 SB-IL/DMSO binary solvent system is used, the cellulose solution shows more pronounced shear-thinning behavior compared to 2:1 and 1:1 SB-IL/DMSO mixtures. This can be attributed to the solution entering a weakly structured pre-gel state. A similar gelation process was reported by Ilyin et al. (2023) in cellulose/[EMIM][OAc]/DMSO when higher DMSO content (75%) was used in a binary system.

The viscoelastic behaviour of cellulose/SB-IL/DMSO mixtures with different DMSO concentrations can be explained by **Figure 10b** via frequency sweep measurements. All the cellulose/SB-IL mixtures with DMSO as a co-solvent have their G' smaller than the G'' at low frequencies while at higher frequencies, the G' becomes larger than G''. At this

stage, two key parameters should be considered: the crossover frequency (ω_C), where $G' = G''$, which describes the material's viscoelastic behavior and indicates the transition from viscous to elastic behavior, and the relaxation time, which is the reciprocal of the crossover frequency and is denoted by $\tau = 1/\omega_C$. Compared to the cellulose solution in pure SB-IL, the crossover points shift to higher frequencies as the DMSO content increases. This suggests that the relaxation time of the cellulose chains decreases with higher DMSO content, due to fewer entanglements from neighbouring polymer chains.
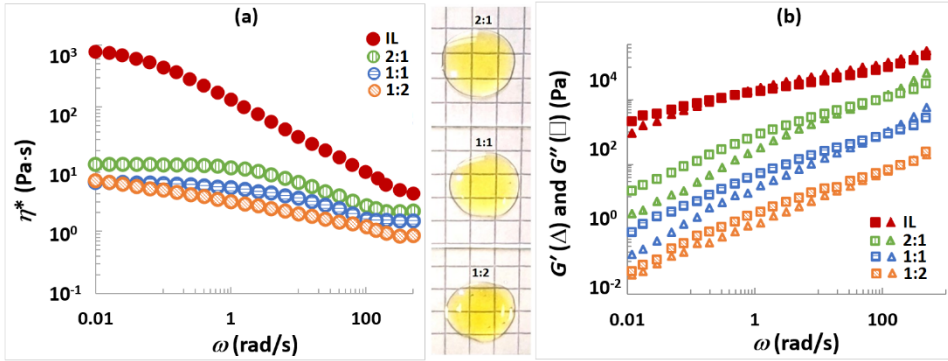
Figure 10. Dependences of a) complex viscosity η* and b) storage G' (triangle) and loss G" (square) moduli on angular frequency ω for cellulose solutions in pure [mTBNH][OAc] and in [mTBNH][OAc]/DMSO binary solvent. The ratio of [mTBNH][OAc]/DMSO is given in the legend. The central part demonstrates the appearance of cellulose solutions in [mTBNH][OAc]/DMSO mixtures.

It can be concluded that although DMSO is not a solvent for cellulose, unlike SB-IL [mTBNH][OAc], the cellulose's miscibility remains high across all studied compositions. This is evident from the photographs in **Figure 10**, which show that the cellulose solutions are transparent in all SB-IL/DMSO mixtures, with no visible phase separation.

The behavior of the cellulose/SB-IL/GVL solutions is almost identical to that of the DMSO-based solutions. **Figure 11** shows the angular frequency dependence of a) η*, and b) G' and G" of 2 wt% cellulose in pure SB-IL and SB-IL/GVL binary mixtures with varying ratios of GVL. Similar to DMSO, the studied cellulose/SB-IL/GVL solutions are non-Newtonian and show shear-thinning behaviour at higher shear rates when SB-IL:GVL ratios were 2:1 and 1:1. The viscosity of the cellulose solution in SB-IL decreases with the addition of GVL while maintaining a constant cellulose concentration at SB-IL:GVL ratios 2:1 and 1:1. Additionally, the 1:1 SB-IL/GVL solution exhibits a lower viscosity than the 2:1 solution. This can be explained similarly to DMSO, where the cellulose solution is diluted with a solvent of lower viscosity (GVL has a viscosity of 1.9 mPa·s) compared to the [mTBNH][OAc]. A similar behavior was previously reported by Yuan et al. (2019) for cellulose (18%) in [EMIM][OAc]/GVL mixtures with different ratios.
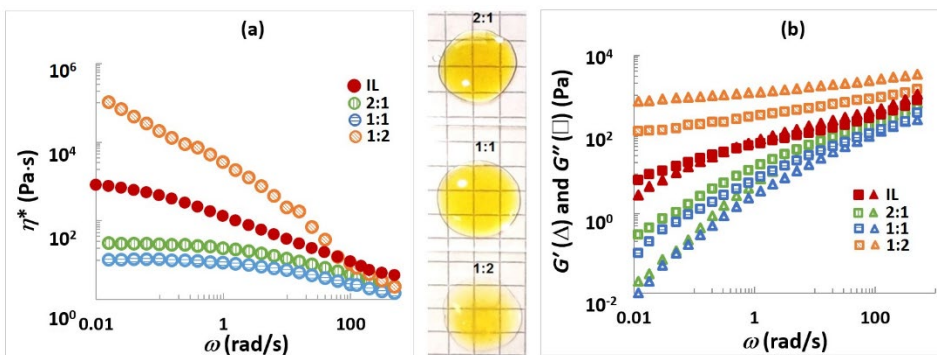
Figure 11. Dependences of a) complex viscosity η* and b) storage G' (triangle) and loss G" (square) moduli on angular frequency ω for cellulose solutions in pure [mTBNH][OAc] and in [mTBNH][OAc]/GVL binary solvent. The ratio of [mTBNH][OAc]/GVL is given in the legend. The central part demonstrates the appearance of cellulose solutions in [mTBNH][OAc]/GVL mixtures.

However, at an SB-IL/GVL solvent composition of 1:2, the cellulose solution's viscosity increases significantly. It begins to display pronounced shear-thinning behavior as shown in **Figure 11a**. Both the *G'* and *G"* show minimal dependence on frequency, with *G'* remaining greater than *G"* across the entire measurable frequency range. as shown in **Figure 11b**. This behavior is characteristic of a gel, where elastic or solid-like properties primarily govern the material's rheological response. According to data from the literature by Gandhi and Williams (1972), thermodynamically poor solvents, when added to a solution, result in significantly higher viscosities at high concentrations than good solvents. However, poor solvents reduce viscosity at lower concentrations due to coil shrinkage. A high GVL content appears to degrade the thermodynamic quality of the solution, leading to the formation of macromolecular aggregates. In contrast, systems with lower GVL content (2:1 and 1:1) behave as typical polymer solutions: at low frequencies, the loss modulus exceeds the storage modulus, and the crossover frequency of cellulose/SB-IL/GVL solutions shifts to lower ω as the GVL content decreases.

GVL is not a solvent for cellulose dissolution and induces gelation by promoting stronger macromolecular aggregate formation in the solution, which can eventually result in phase separation, as seen in the photos of the cellulose solutions in the middle section of **Figure 11**. Therefore, diluting [mTBNH][OAc] with GVL at compositions exceeding 1:1 does not effectively reduce the viscosity of the cellulose solution, unlike DMSO.
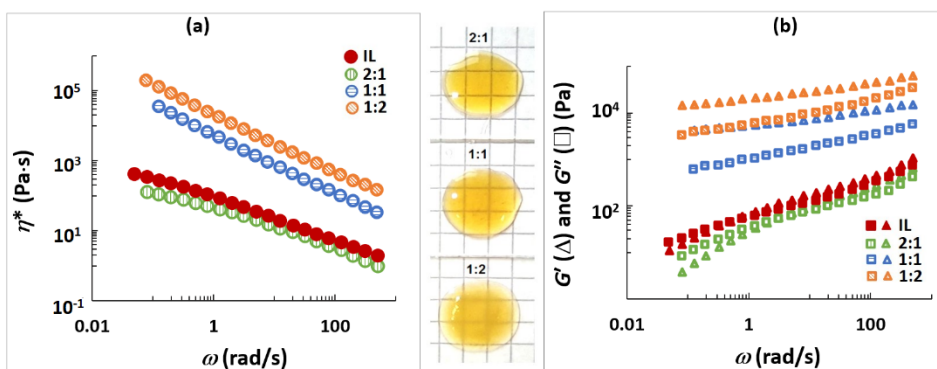
Figure 12. Dependences of a) complex viscosity η* and b) storage G' (triangle) and loss G" (square) moduli on angular frequency ω for cellulose solutions in pure [mTBNH][OAc] and in [mTBNH][OAc]/DMI binary solvent. The ratio of [mTBNH][OAc]/DMI is given in the legend. The central part demonstrates the appearance of cellulose solutions in [mTBNH][OAc]/DMI mixtures.

The viscoelastic behavior of cellulose solutions in SB-IL with DMI and DMPU is nearly identical. Hence, only the angular frequency dependencies of η*, G', and G" for cellulose solutions in SB-IL/DMI binary solvents with different ratios are shown in **Figure 12**. When cellulose is dissolved in 2:1 SB-IL/DMI and 2:1 SB-IL/DMPU mixtures, the viscosity of the resulting solutions is lower than that of cellulose in pure SB-IL due to the dilution effect. The absence of gelation can be seen from the frequency dependencies of the G' and G" moduli in **Figure 12b**, which exhibit typical concentrated polymer solution behavior: the G' is lower than the G" at low frequencies but becomes dominant at higher frequencies.

However, as the content of these green co-solvents in the binary mixtures increases to a 1:1 SB-IL/co-solvent ratio, the viscosity of the cellulose solutions increases as shown in Figure 3a. Further addition of DMI or DMPU, up to a 1:2 ratio, leads to an even greater increase in cellulose viscosity. This increase suggests higher possibilities of strong macromolecular aggregation. The solution's appearance also changes from transparent to opaque, as seen in the photos of cellulose solutions in the middle of **Figure 12**. Both G' and G" show only slight dependence on angular frequency, with G' > G" throughout the entire measurable range, which is characteristic of a gel or a viscoelastic solid. Additionally, the values of G' and G" for cellulose in 1:1 and 1:2 SB-IL/DMI (and SB-IL/DMPU) are 1 and 2 orders of magnitude higher, respectively, compared to the values for cellulose in pure SB-IL.

The further viscoelastic behavior of the cellulose/SB-IL/co-solvent mixtures and the gel formation at higher co-solvent concentrations can also be explained by considering interdependencies of storage (G') and loss (G") moduli using Cole-Cole plots. The experimental data for all cellulose/SB-IL/DMSO-based solutions closely follow the same straight line as shown in **Figure 13a** and overlap with the data for the cellulose solution in pure SB-IL. The consistent Cole-Cole plots indicate that DMSO does not alter the microstructure of the cellulose solution. The pre-gel state of the cellulose solution in 1:2 SB-IL/DMSO can be observed as a low-frequency deviation in the Cole-Cole plots. In **Figure 13b**, the Cole-Cole plots for cellulose solutions in SB-IL/GVL solvents are shown. The data for the cellulose solutions in 2:1 and 1:1 SB-IL/GVL mixtures align along the same straight line. However, in the 1:2 SB-IL/GVL system, the microstructure of the system changes, and the Cole-Cole plots no longer overlap with others.
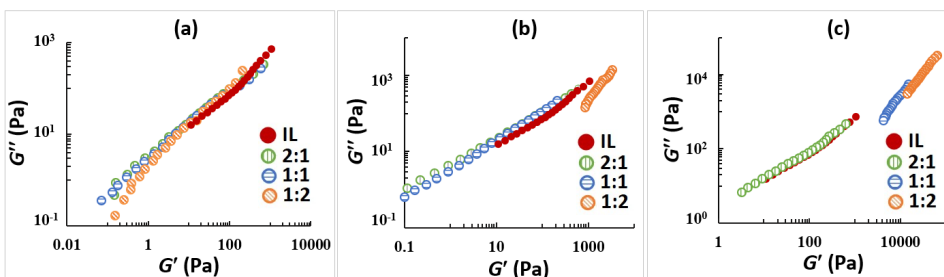
Figure 13. Cole-Cole plots for cellulose solution in (a) [mTBNH][OAc]/DMSO, (b) [mTBNH][OAc]/GVL, and (c) [mTBNH][OAc]/DMI binary solvents. The ratio of SB-IL/co-solvent is given in the legend.

It has been observed that the addition of DMI does not lead to new interactions between the cellulose macromolecules until they lose their solubility, resulting in gel formation. The experimental data for the cellulose solution in pure SB-IL and the SB-IL/DMI 2:1 solution overlap, suggesting that the microstructure remains unchanged. However, when a higher concentration of DMI is added, gel formation is initiated through microphase separation, as indicated by the shift in the Cole-Cole dependencies in **Figure 13c**.

The 2:1 SB-IL/co-solvent composition was selected for comparative analysis among the co-solvents because it is the only common composition that forms typical polymer solutions for all the co-solvents studied.

Figure 14 illustrates that the cellulose solution in 2:1 SB-IL/DMSO shows the lowest viscosity among all the other cellulose solutions. DMSO exhibits the highest dilution capacity, likely due to the comparatively low viscosity of the 2:1 SB-IL/DMSO solvent (30 mPa·s) among all binary solvents tested. The viscosity of the cellulose solution with DMI added to SB-IL is almost identical to those of DMPU, being five and 10 times higher than those for GVL and DMSO, respectively. However, the viscosity of DMPU- and DMI-based cellulose solutions is five times lower than that in pure SB-IL. It should be noted that the viscosities of 2:1 SB-IL/ DMI and SB-IL/DMPU binary solvents are also rather close to each other (58 and 60 mPa s, respectively) and higher than SB-IL/DMSO (30 mPa s) and SB-IL/GVL (50 mPa s).
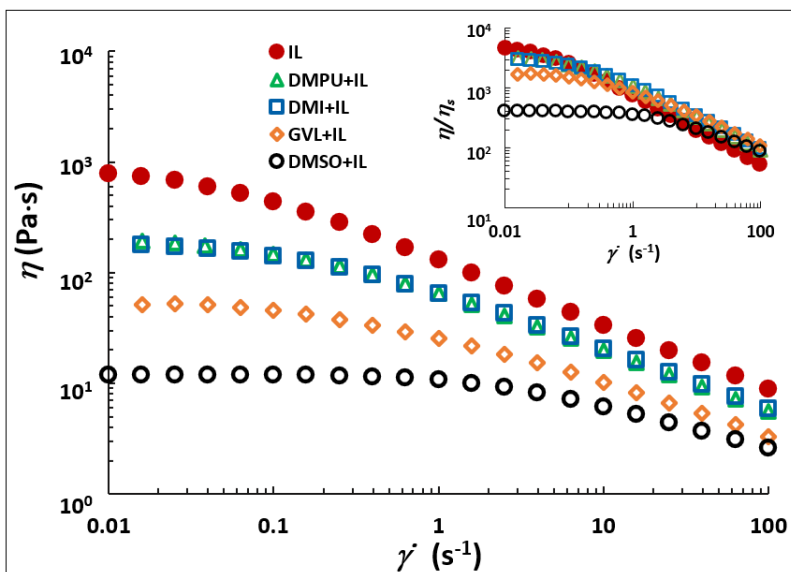
Figure 14. Shear rate dependence of shear viscosity for cellulose solutions in 2:1 [mTBNH][OAc]/ co-solvent. Inset demonstrates the shear rate dependence of the relative viscosity of cellulose solutions. Used co-solvents are listed in the legend.

The relative viscosity is used to account for the impact of binary solvent viscosity (SB-IL/co-solvent) on cellulose/SB-IL/co-solvent solutions. Defined as the ratio of the solution's viscosity (η for the cellulose/SB-IL/co-solvent solution) to the viscosity of the pure solvent (η_s for the SB-IL/co-solvent), the relative viscosity reflects the extent to which the solution's viscosity increases compared to the solvent.

The inset of **Figure 14** depicts the relative viscosity of all the 2:1 cellulose/SB-IL/ co-solvent solutions examined. The curves for cellulose in SB-IL/DMPU and SB-IL/DMI are nearly identical to those for pure IL, indicating that DMPU and DMI primarily act as diluents, reducing the viscosity of the cellulose solution. Conversely, the relative viscosity at zero shear for GVL- and DMSO-based solutions is approximately two and five times lower, respectively, than that of pure SB-IL solutions. This suggests that GVL, like DMSO, enhances the solvation of SB-IL cation by promoting the dissociation of SB-IL anion and cation. A similar solvation effect of [BMIM][OAc] by DMSO has been reported by Zhao et al. (2013) and (Xu et al. (2013).

The relaxation time, (τ) exhibited a clear variation with changes in the co-solvent. **Table 2** represents the relaxation times determined from the crossing points for all 2:1 cellulose solutions. The cellulose solution in pure IL showed the highest τ, which decreased in the order of SB-IL/DMPU > SB-IL/DMI > SB-IL/GVL > SB-IL/DMSO.

The concentrated polymer solutions consist of partially disrupted structures of the polymers themselves. In concentrated solutions, cellulose can form such structures due to its strong potential for intra- and intermolecular hydrogen bonding and a high degree of entanglement. The ability to break these structures depends on the balance between the structural energy and the energy of polymer-solvent interactions. Poor solvents are unable to disrupt these robust structures, while a good solvent can penetrate and break them down. As a result, the structures tend to be looser in good solvents, while in poor solvents, they remain larger and less mobile. As a result, the relaxation time τ of a polymer solution in a poor solvent is longer than that in a good solvent (Tager, 1975;

Cravotto, 2008). Based on the τ values for the systems studied, it can be concluded that SB-IL/DMPU and SB-IL/DMI act as "poorer" solvent systems for cellulose dissolution compared to SB-IL/GVL and SB-IL/DMSO. A similar effect was reported for tetraalkylphosphonium IL combined with DMPU and DMI by Xia et al. (2021).

Table 2. Relaxation time τ and activation energy E_a for cellulose solutions in 2:1 [mTBNH][OAc]/ Co-solvent mixtures.

Cellulose in…	τ, s	E_a, kJ/mol
SB-IL Pure	3.17	45.3
2:1 SB-IL: DMPU	0.53	41.3
2:1 SB-IL: DMI	0.50	40.7
2:1 SB-IL: GVL	0.020	36.9
2:1 SB-IL: DMSO	0.017	33.7

The thermodynamic quality of a solvent can be efficiently analyzed through the viscosity-temperature dependence of fluids. Accordingly, the influence of temperature (*T*) on the viscosity properties of 2:1 cellulose/SB-IL/co-solvent solutions was examined. As reported previously by Lefroy et al. (2021) and Yuan et al. (2019), a widely used approach for analyzing viscosity-temperature dependence is the Arrhenius equation **(Eq. 2)**.

$$\eta_0 = Ae^{Ea/RT}$$ *Eq. 2*

Here, E_a represents the activation energy, η_0 denotes the zero-shear-rate viscosity measured at low shear rates, *A* is a constant, *R* is the universal gas constant, and *T* is the absolute temperature.

The activation energy (E_a) values can be determined from the slope of *ln η_0* versus *1/T* in **Figure 15** and are provided in **Table 2**.

In polymer solutions, E_a reflects the challenge of transitioning a polymer chain from one position or state to another as presented in the literature by Budtova and Navard (2015), and is influenced by the strength of interactions between polymer chains of identical molar mass, chemical composition, and microstructure. **Table 2** shows that the E_a for cellulose solution in pure [mTBNH][OAc] is 45.3 kJ/mol, which is similar to the reported E_a values of 46 kJ/mol and 49 kJ/mol for MCC (DP 300) and spruce sulfite pulp (DP 1000) in [EMIM][OAc], respectively (Gericke, 2009). The E_a obtained for 2:1 [mTBNH][OAc]/GVL (36.9 kJ/mol) aligns closely with E_a = 35.1 kJ/mol for 3:2 [EMIM][OAc]/GVL, as reported by Yuan et al. (2019). To our knowledge, activation energy data are unavailable for cellulose solutions in IL/DMPU and IL/DMI, making direct comparisons impossible. The activation energy of cellulose/SB-IL/co-solvent systems decreases progressively based on the type of co-solvent in the order of DMPU > DMI > GVL > DMSO. Differences in activation energies suggest that the co-solvent affects the energy barrier for flow, with slightly more energy required for flow in DMPU- and DMI-based solutions than in GVL and DMSO. The lower E_a values align with

the observation that dissolution rates for SB-IL/co-solvent mixtures are faster than those of pure IL. This further indicates that co-solvents may enhance the efficiency of cellulose chemical modifications, such as transesterification.
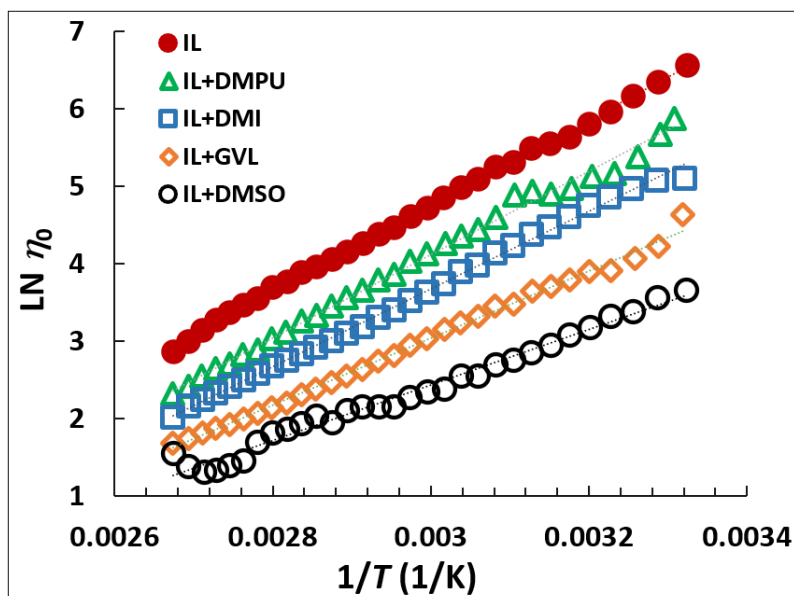

Figure 15. Arrhenius equation plots for cellulose in 2:1 [mTBNH][OAc]/Co-solvent. Used co-solvents are listed in the legend.

It can be concluded that DMSO is effective as a co-solvent with [mTBNH][OAc] for cellulose dissolution up to a 1:2 SB-IL/co-solvent ratio. GVL works at a 1:1 ratio, while DMI and DMPU require 2:1 for homogeneity. Although [mTBNH][OAc]/green co-solvent mixtures exhibit lower viscosity than pure [mTBNH][OAc], the co-solvent concentrations for forming homogeneous solutions are limited. These green co-solvents offer alternatives to DMSO but should be used moderately, keeping co-solvent content below 50% by weight.

3.2 Homogeneous Transesterification of Cellulose in [mTBNH][OAc]/DMSO with Vinyl Esters (Publications I and II)

After exploring the application of SB-IL/co-solvent-based solvent systems for cellulose dissolution and regeneration, this research aims to broaden the understanding of SB-IL's applications in cellulose modification. This work focuses on the catalyst-free synthesis of cellulose esters (CEs) via homogeneous transesterification of cellulose with vinyl esters (VEs) in the 1:1 [mTBNH][OAc]/DMSO under mild reaction conditions via sustainable and environmentally friendly process. The 1:1 [mTBNH][OAc]/DMSO ratio was chosen for this research due to its optimal balance between cellulose dissolution and reaction efficiency, providing better accessibility for acylating agents and improved reaction control. Additionally, this ratio uses a lower amount of SB-IL, which helps reduce the cost, as SB-IL is more expensive than DMSO, making it more cost-effective for extensive optimization experiments.

As shown in **Table 3**, cellulose transesterification in [mTBNH][OAc] with long-chain VEs achieved a DS of up to 1.8. The DS of the CEs is calculated by ^{1}H NMR according to *Eq. 1*. Comparable DS values were reported by Kakko et al. (2017) for cellulose acetate and propionate in [DBNH][OAc] and long-chain CEs in DMAc/LiCl by Samaranayake and Glasser (1993), though the latter is less favourable for sustainable applications.

Table 3. Synthesis of cellulose esters via transesterification with vinyl esters in a 1:1 [mTBNH][OAc]/DMSO solvent system.

Sample	Reaction conditions			DS	M_n, kDa	Đ
	Time, h	Temperature, °C	Molar ratio VE:AGU			
CL-a	3	70	3:1	1.55	532.7	1.14
CM-a	3	70	3:1	1.31	393.6	1.74
CP-a	3	70	3:1	1.08	370.2	1.50
CP-b	3	70	5:1	1.30	404.3	1.55
CP-c	3	80	3:1	1.80	222.1	1.77
CS-a	3	70	3:1	0.67	insoluble	
CS-b	3	70	6:1	1.40	471.2	1.41

The DS and M_n of CEs decrease with increasing fatty acid chain length due to higher steric hindrance. While cellulose laurate (CL), myristate (CM), and palmitates (CP) (DS > 1) are soluble in many organic solvents, cellulose stearate (CS-a) exhibits much lower DS and is insoluble.

DS is crucial for the thermoplastic behavior of CEs, ideally needing a value of ≥ 1.5. While CL and CM reached DS ~ 1.3, higher DS for palmitate and stearate requires modified reaction conditions. For example, increasing the reaction temperature to 80 °C improved DS for cellulose palmitate to 1.8, though M_n decreased due to cellulose backbone cleavage. Degradation of cellulose backbone during transesterification at ≥ 80 °C is evident from intrinsic viscosity [η] measurements, which directly correlate with molar mass. The higher the [η], the higher the MOLAR MASS. While CP-a and CP-b show [η] of 2.5 and 2.8 dL/g, respectively, CP-c has a significantly lower value of 1.1 dL/g, confirming cellulose backbone cleavage.

According to Le Chatelier's Principle, using excess vinyl esters (AGU:VE = 1:5 and 1:6) drives the reaction toward higher cellulose ester yield. As seen in **Table 3**, increasing the molar ratio improved the DS of CS-b to 1.4 and CP-b to 1.3, though further increases may complicate purification and SB-IL recycling due to unreacted VEs.

3.2.1 Optimization of reaction conditions via synthesis of cellulose palmitates

After successful cellulose transesterification in SB-IL/DMSO, this chapter focuses on the detailed optimization of reaction conditions for cellulose transesterification. Given the better performance of the cellulose palmitates (CPs) in the previous study, the synthesis of CPs in a 1:1 [mTBNH][OAc]/DMSO using vinyl palmitate (VP) as the acylating agent was selected for the optimization study. It provides details on how various reaction parameters like reaction temperature, reaction time, and the molar ratio (VP:AGU) affect the DS of CPs (**Table 4**).

To investigate the effect of reaction temperature on DS, CPs were synthesized between 60 °C and 120 °C, with a constant molar ratio (3 eq. VP/AGU) and a 2-hour reaction time. As shown in **Table 4**, DS initially increased with temperature which became the highest at 2.3 (CP-5) before dropping to 0.5 (CP-8). A significant increase in DS from 0.7 (CP-1) to 1.5 (CP-3) occurred as the temperature rose from 60 °C to 70 °C. However, after reaching 80 °C, DS decreased sharply to 1.0 (CP-6) and declined gradually across the studied temperature range. CP yield followed a similar trend, rising gradually from 60 °C to 75 °C before declining rapidly until 90 °C. Beyond 75 °C, the reaction mixture's color changed from orange to dark brown, suggesting potential degradation of the solvent system, reactants, or CPs. Similar trends were reported by Hinner et al. (2016) for cellulose laurate and by Zhou et al. (2014) for cellulose octanoate, which showed decreased DS and yield at elevated temperatures respectively.

Table 4. DS of CPs synthesized by transesterification of cellulose with VP in a 1:1 [mTBNH][OAc]/DMSO.

Sample	Reaction parameters			DS (±0.1)	Yield (%)
	Temperature (°C)	Time (h)	Molar ratio (VP:AGU) (mol/mol)		
CP-1	60	2	3:1	0.7	42
CP-2	65	2	3:1	1.2	60
CP-3	70	2	3:1	1.5	79
CP-4	75	2	3:1	1.8	85
CP-5	80	2	3:1	2.3	71
CP-6	90	2	3:1	1.0	36
CP-7	100	2	3:1	0.9	33
CP-8	120	2	3:1	0.5	31
CP-9	70	1	3:1	0.7	38
CP-10	70	1.5	3:1	1.3	60
CP-11	70	2.5	3:1	1.2	80
CP-12	70	3	3:1	1.1	52
CP-13	70	4	3:1	1.0	38
CP-14	70	5	3:1	1.0	35
CP-15	70	2	4:1	1.6	81
CP-16	70	2	5:1	1.6	82
CP-17	70	2	6:1	1.6	83
CP-18	70	2	7:1	1.6	83
CP-19	70	2	9:1	1.6	83
CP-20	70	2	12:1	1.6	83

To examine the effect of reaction time on the DS of CPs, we periodically sampled the reaction mixture at intervals between 1 and 5 hours, keeping the temperature constant at 70 °C and using a molar ratio of 3 eq. VP/AGU. **Table 4** shows the relationship between DS and percent yield OF CPs over time. In the initial one hour, transesterification progressed rapidly, increasing DS from 0.7 (CP-9) to 1.5 (CP-3), a 2.1-fold rise. However,

after 2 hours, DS began to decline along with the discoloration of reaction mixtures which suggests possible degradation. The percent yield of CPs increased gradually until 2.5 hours, then decreased, further indicating degradation of the reaction components. The drop in yield over extended reaction times likely results from cellulose degradation, similar to findings by Huang et al. (2011) during prolonged cellulose esterification. The decline in DS over time may be due to competition between transesterification and partial hydrolysis of ester groups by moisture in the reaction medium (Freire, 2006).

To explore how the molar ratio affects the DS, we varied the VP/AGU ratio from 3:1 to 12:1, keeping the temperature at 70 °C and the reaction time at 2 hours. The DS increased steadily with the molar ratio, stabilizing at ratios above 5:1 (**Table 4**). The absence of discoloration of the reaction mixtures indicated no degradation. However, the large aliphatic chain of VP caused steric hindrance, leading to the stabilization of DS and yield beyond the 5:1 ratio, a trend also observed by Hinner et al. (2016) and Zhou et al. (2014). While a higher VP amount enhances DS, excess unreacted VP can complicate post-reaction work-up and hinder the recycling of the SB-IL.

3.2.2 Structural determination of cellulose esters with ^{1}H and ^{13}C NMR

In the ^{1}H NMR spectra of all CPs, peaks between 5.30–3.00 ppm correspond to H-1 to H-6' of the AGU in cellulose. Signals at 2.393–2.223, 1.695–1.460, and 1.424–1.125 ppm are attributed to methylene protons (H-8 to H-21), while signals at 0.955–0.794 ppm correspond to the terminal methyl protons (H-22). The ^{1}H NMR of CP-5 (DS = 2.3) is shown in **Figure 16**.
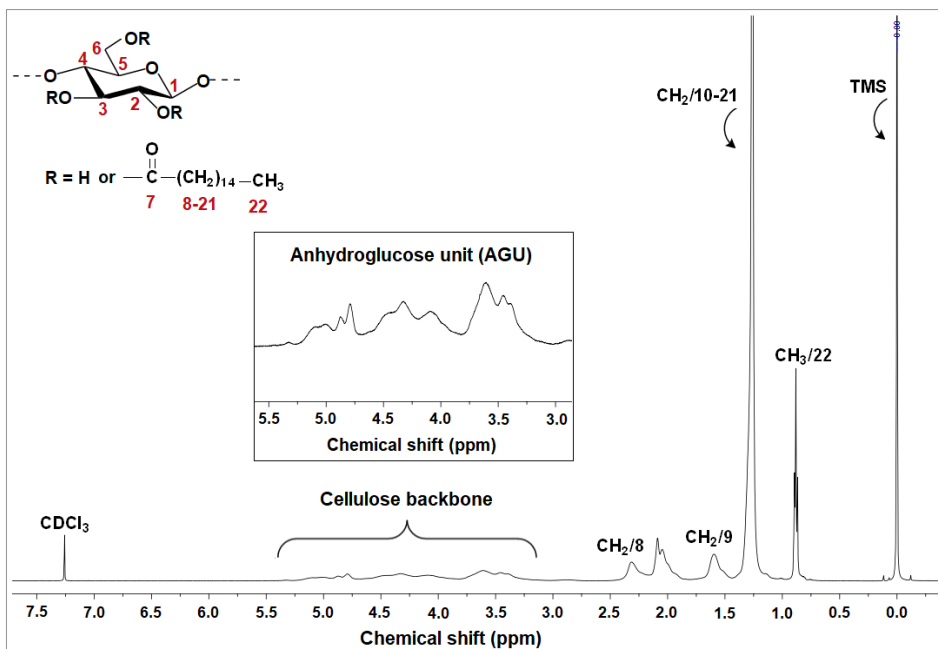
Figure 16. ^{1}H NMR spectrum of CP-5 (DS = 2.3) in Chloroform-d at 40 °C.

41

In the ^{13}C NMR spectrum of CP (**Figure 17**), signals at 34.08, 31.96, 24.90, 22.71, and 14.09 ppm correspond to C-8, C-20, C-9, C-21, and C-22 in the aliphatic side chain. Carbons C(10–19) appear between 30.85–28.77 ppm, while AGU carbons C-1, C-1', C-4, C-2,3,5, and C-6 are observed at 104.29, 101.58, 82.20, 74.68–72.24, and 62.52 ppm, respectively. Carbonyl carbons at 173.09–170.16 ppm confirm the attachment of the fatty acid chain, with three peaks indicating substitution at OH groups on positions 2, 3, and 6, following the order C6–OH > C2–OH > C3–OH.
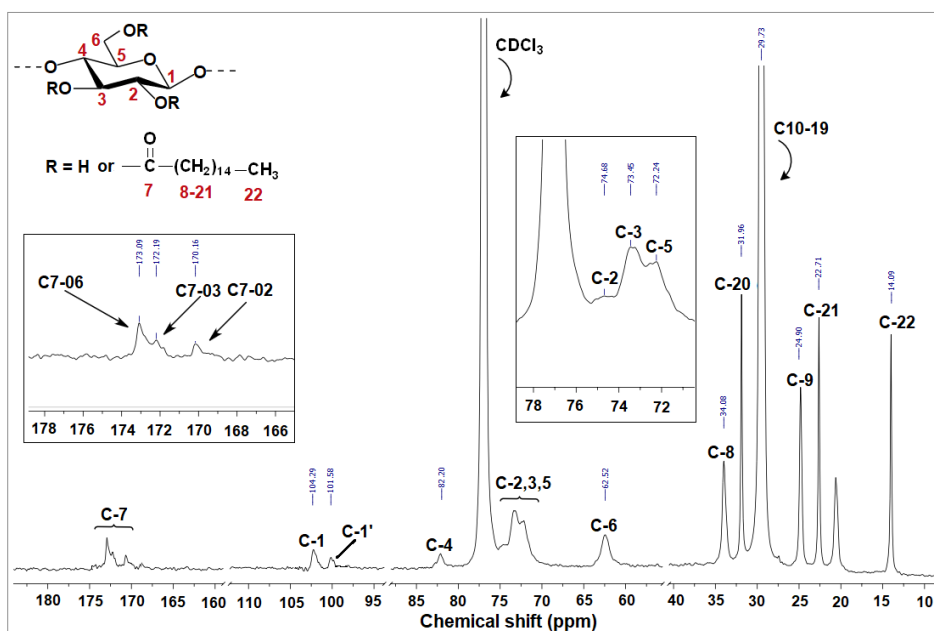
Figure 17. ^{13}C NMR spectrum of CP-5 (DS = 2.3) in Chloroform-d at 40 °C.

It can be concluded that CPs degrade at a reaction temperature of 75 °C and a reaction time of 2.5 hours. Beyond a molar ratio (VP:AGU) of 5:1, the DS of the CPs remains constant. Considering all the above observations, the reaction temperature of 70 °C; reaction time of 2 hours, and molar ratio of 5 equivalents of vinyl ester to an anhydroglucose unit will be used for the transesterification of cellulose in the solvent systems containing SB-IL, [mTBNH][OAc]. Although these optimized reaction parameters are obtained for CPs, these conditions were generally applicable to all cellulose esters and were used for further experiments.

3.3 Homogeneous Transesterification of Cellulose in [mTBNH][OAc]/green co-solvents with Vinyl Esters (Publication IV)

To investigate the impact of green co-solvents on the transesterification of cellulose and the properties of the resulting cellulose esters (CEs), a detailed synthesis of CEs was conducted via homogeneous transesterification. A 2 wt% cellulose solution in a 2:1 [mTBNH][OAc]/green co-solvent with vinyl esters (VEs) was used, under conditions of 70 °C reaction temperature, 2 hours reaction time, and a molar ratio (VE:AGU) of 5:1. The weight ratios of SB-IL and co-solvents, cellulose concentration, and the dissolution and reaction parameters were selected based on previous studies outlined in Sections

3.1 and 3.2. The green co-solvents employed included GVL, DMI, SLF, and DMPU, while the acylating agents were predominantly vinyl laurate (VL), myristate (VM), and palmitate (VP).

Although cellulose laurates (CLs), cellulose myristates (CMs), and cellulose palmitates (CPs) were synthesized, the analysis of the structural, thermal, rheological, mechanical, and surface properties primarily focuses on the cellulose myristates (CMs) in the following chapters, due to their similar overall behavior.

The DS of cellulose myristates (CMs) was calculated using ^{1}H NMR spectroscopy with *Eq. 1* and described in **Table 5**. The DS increases in the order of CM-GVL > CM-DMI > CM-SLF > CM-DMPU.

Table 5. Reaction parameters in 2:1 [mTBNH][OAc]/green co-solvent mixtures, and the DS of the synthesized CEs.

Sample	Reaction conditions			Green co-solvent	DS
	Time, h	Temperature, °C	Molar ratio VE:AGU		
CM-DMPU	2	70	5:1	DMPU	1.23
CM-SLF	2	70	5:1	SLF	1.32
CM-DMI	2	70	5:1	DMI	1.42
CM-GVL-1	2	70	5:1	GVL	1.51
CM-GVL-2	2.5	70	3:1	GVL	1.41
CM-GVL-3	1.5	70	3:1	GVL	1.27
CL-DMPU	2	70	5:1	DMPU	1.37
CL-GVL	2	70	5:1	GVL	1.55
CP-DMPU	2	70	5:1	DMPU	1.16

3.3.1 Structural and physical properties of CEs

The XRD patterns of CMs confirm a highly amorphous structure, indicating the loss of native cellulose I crystallinity after transesterification. The peak intensity at $2\theta = 20°$ decreases in the order: CM-DMPU > CM-SLF > CM-DMI > CM-GVL (**Figure 18**). This trend in amorphization may correspond to the DS of the samples: the higher the DS, the greater the amorphization.
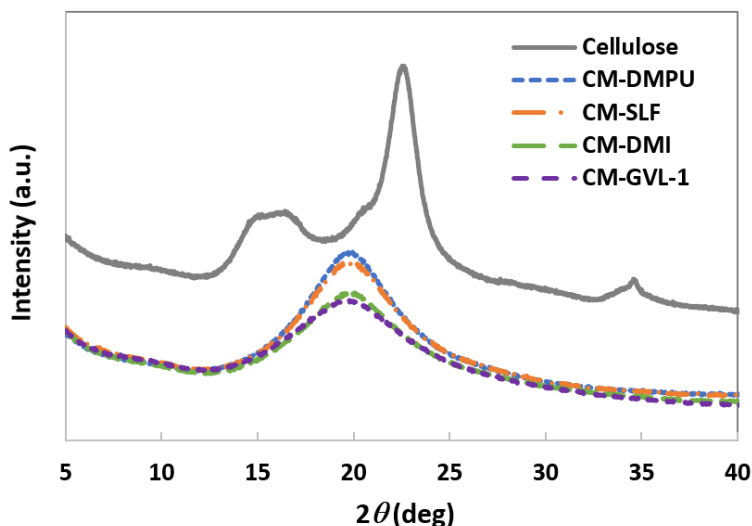
Figure 18. XRD patterns of native cellulose and CMs synthesized in different [mTBNH][OAc]/green co-solvent mixtures.

The thermal stability of CMs in powder form was analyzed using TGA/DTG from 30 °C to 600 °C. As shown in **Figure 19**, all samples exhibited high thermal stability and started to decompose around 320 °C. At 50% weight loss, the decomposition temperatures were approximately 355 °C for CM-GVL and CM-DMI, 361 °C for CM-SLF, and 367 °C for CM-DMPU. These temperatures are comparable to those of cellulose laurates reported by Wen et al. (2017). Above 400 °C, samples undergo pyrolysis.
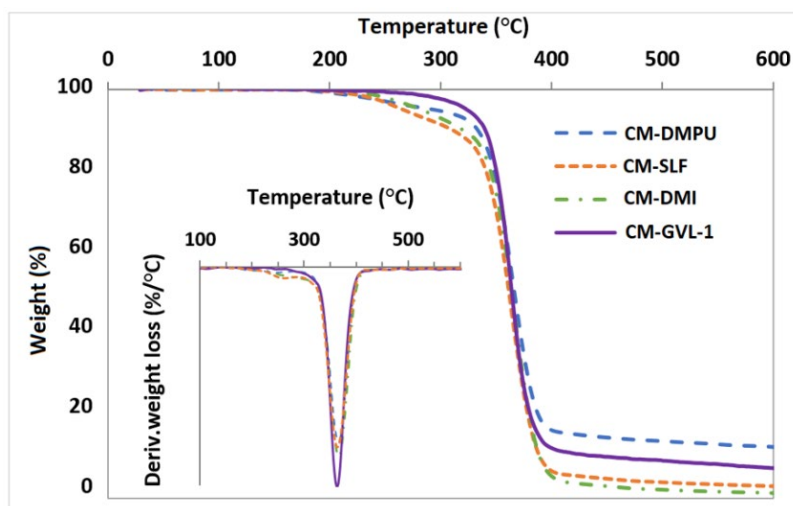
Figure 19. TGA/DTG curves of CMs prepared in different [mTBNH][OAc]/green co-solvents. Samples are tested in powder form.

The DTG curves (**see Figure 19 inset**) showed the maximum degradation rate at around 353 °C for CM-GVL and CM-SLF, and 355 °C for CM-DMI and CM-DMPU, indicating nearly identical decomposition temperatures.

The melt flow behavior of CMs was analyzed to assess the thermoplastic properties of the materials. **Figure 20** illustrates the angular frequency dependence of the complex viscosity (η^*) and storage (G') and loss (G'') moduli of CMs in various green co-solvents, using double-logarithmic scales. As shown in **Figure 20a**, all CMs exhibit shear-thinning behavior across the angular frequency range, with no linear viscosity observed. Among them, CM-DMPU has the highest viscosity, while CM-GVL shows the lowest. The viscosity reduction in CM samples from various co-solvents cannot be explained by their molar mass alone. CM-DMPU, CM-SLF, CM-DMI, and CM-GVL have weight-average molar masses of 202 kg/mol, 302 kg/mol, 311 kg/mol, and 591 kg/mol, respectively. Despite CM-GVL having the highest molar mass, it shows the lowest viscosity. **Figure 20b** indicates that both storage (G') and loss (G'') moduli have minimal frequency dependence, with G' consistently exceeding G''. This indicates that the rheological behavior of CMs is primarily governed by an elastic or solid-like response. The dominance of the elastic response can be attributed to the deformation and movement of the cellulose backbone in the CM macromolecule. Interestingly, the magnitude of the complex moduli of CMs follows the order DMPU > SLF > DMI > GVL, aligning with the viscosity data but is in the reverse order of the DS values for the samples. Melt elasticity is the key factor that dictates the behavior of a molten material. This elasticity leads to effects like die swell during processing. A higher G' value results in greater die swell and thicker products.
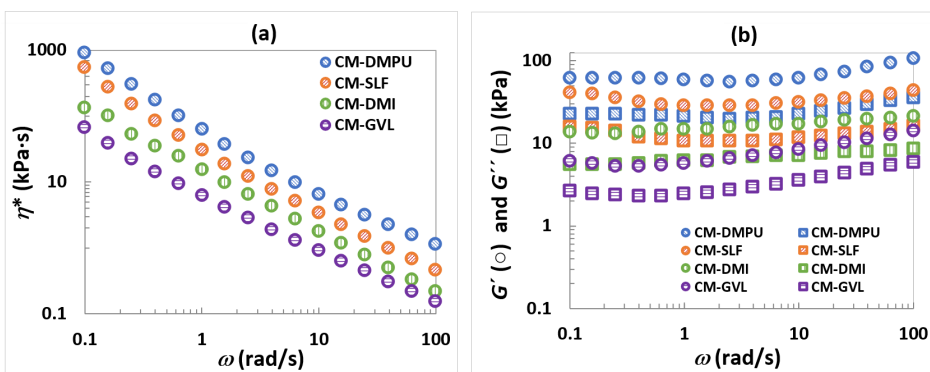
Figure 20. Dependences of (a) complex viscosity η* and (b) storage G' (circle) and loss G" (square) moduli on angular frequency ω for CM films prepared in various green co-solvents, taken at 190 °C.

Similar angular dependencies of complex viscosity and moduli were observed for cellulose laurates (CL-DMPU, CL-GVL) and cellulose palmitate (CP-DMPU) samples, as shown in **Figure 21**. Variations in viscosity and moduli can be attributed to the type of green co-solvent used, and its indirect influence on the properties of the cellulose esters, or to the DS of the synthesized CEs.
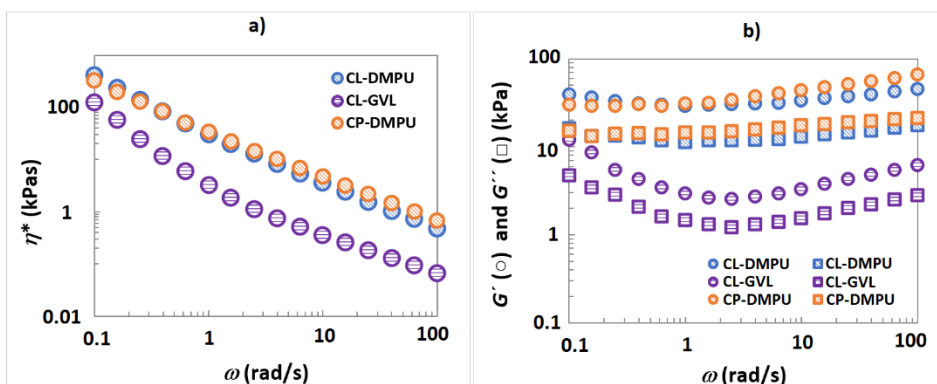
Figure 21. Dependences of (a) complex viscosity η* and (b) storage G' (circle) and loss G" (square) moduli on angular frequency ω for CL and CP films prepared in various green co-solvents, taken at 190 °C.

The Cole-Cole plots in **Figure 22** show that the G' and G'' values for all CMs, regardless of co-solvent type, follow the same straight line, indicating consistent microstructure (Ilyin, 2020). Interestingly, the experimental points for CL and CP samples align with the same CM line, suggesting that the behavior of these materials is primarily influenced by the DS of the cellulose esters.
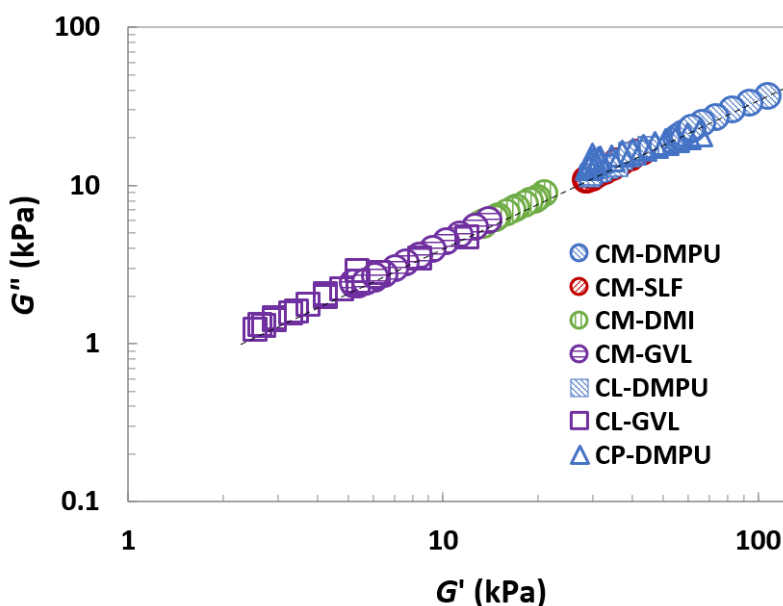
Figure 22. Cole-Cole plots for CMs, CLs, and CP films obtained in [mTBNH][OAc]/green co-solvent systems.

To examine the impact of DS on the complex moduli and complex viscosities of CMs, two additional CMs with lower DS, CM-GVL-2, and CM-GVL-3, were synthesized as detailed in **Table 5**. These CMs were prepared using the same SB-IL/GVL systems to eliminate any influence from the co-solvent nature. As shown in **Figure 23a**, the complex modulus data for CM-GVL-1, -2, and -3 all lie on the same straight line. However, there is

a translational shift based on DS: higher DS results in lower complex modulus values. Additionally, complex viscosity decreases with increasing DS, as seen in **Figure 23b**. Therefore, it can be concluded that the degree of substitution significantly affects both the viscosities and complex moduli of CMs.
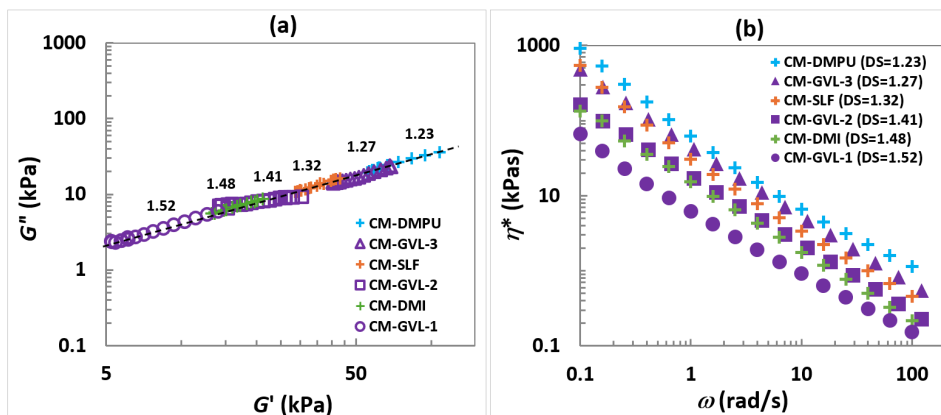

Figure 23. (a) Cole-Cole plots for CMs with different DS obtained in [mTBNH][OAc]/green co-solvent systems. The values of DS are listed over the line; (b) Dependence of complex viscosities η* on angular frequency ω for CMs with various DS.

The G-moduli reflect sample stiffness which further affects polymer chain structure and interchain interactions. (Mead, 2011) found through stress-optical analysis that esterification does not affect cellulose backbone stiffness, but fatty acid side chains act as plasticizers, reducing contour length concentration. This explains the decrease in G-moduli for CM films with increasing DS: higher DS enhances thermoplasticity. This aligns with XRD data, indicating that higher DS results in more amorphous, and therefore less rigid, CMs.

The rigidity of the samples can be influenced by the dissolution of CMs in pyridine, which is affected by their DS. The low solubility capacity of SB-IL/DMPU, for example, results in lower DS of CM-DMPU and may cause crystalline regions in cellulose that add rigidity to the samples. In contrast, more homogeneous dissolution in solvents like SB-IL/GVL leads to higher DS in the synthesized CMs, reducing rigidity further.

The mechanical properties of CMs were evaluated by tensile testing, with DS playing a key role in all characteristics. Three CM samples with varying DS namely CM-GVL-1, CM-GVL-2, and CM-GVL-3, prepared in the same SB-IL/GVL solvent at different reaction times as explained in **Table 5**, were tested using tensile tests. Stress-strain curves for these CMs at room temperature are shown in **Figure 24a**.
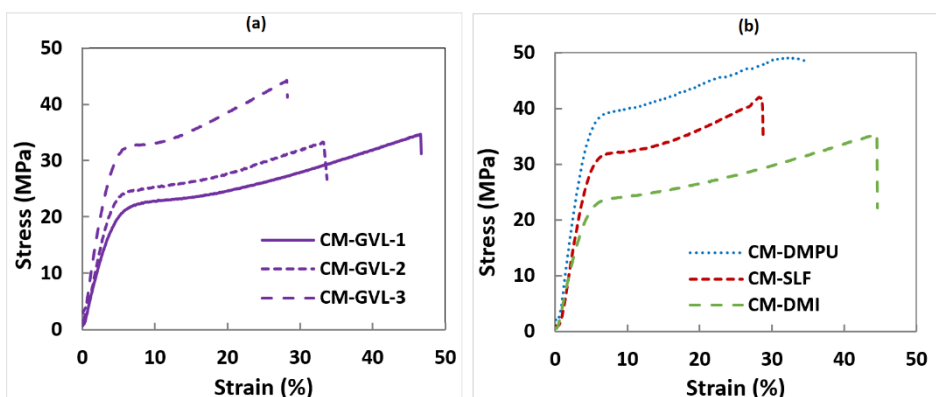
Figure 24. Stress-stain curves of CM films with different DS prepared in (a) 2:1 [mTBNH][OAc]/GVL and (b) 2:1 [mTBNH][OAc]/green co-solvents. DS for the samples are listed in Table 5.

As DS increases, the samples exhibit more thermoplastic behavior, leading to higher strain at break. Meanwhile, Young's modulus (initial slope of the stress-strain curve) and the yield point decrease. This is likely due to the increased plasticizing effect of the myristate chains at higher DS, as seen in the rheological behavior section. Young's modulus correlates with storage modulus: higher DS reduces sample rigidity. Similar trends were observed in cellulose laurates by Duchatel-Crépy et al. (2020) and other cellulose esters by Katsuhara et al. (2023) and Crépy et al. (2009).

Hydrophobicity is a key characteristic of films, making them ideal for food packaging by providing resistance to liquids and extending shelf life (Asim, 2022). A higher DS is expected to increase the contact angle (Willberg-Keyrilainen, 2017; Crépy, 2009). Contact angle measurements (CAM) assessed CM films for surface wettability. **Figure 25a** shows the average contact angles of different CMs, which decrease from 104.8° to 84.9° in the order CM-DMPU > CM-SLF > CM-DMI > CM-GVL, even though the DS increases.
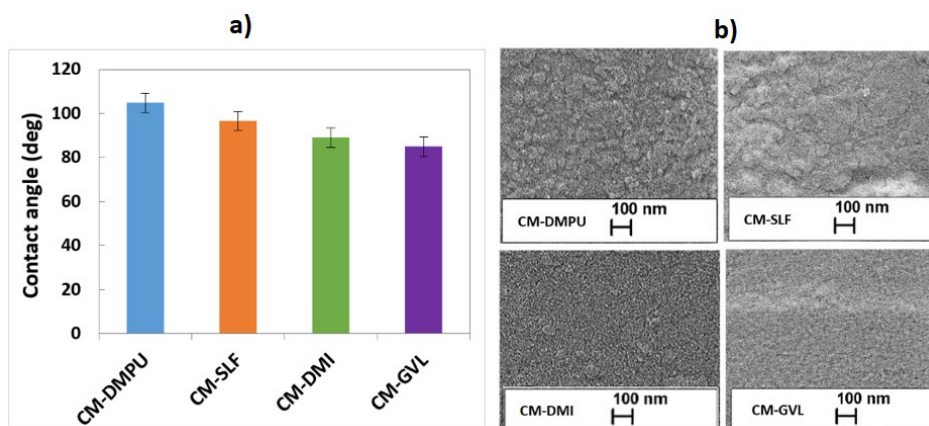

Figure 25. (a) Average contact angles of CMs (in film form), and (b) SEM images of CMs (in film form) synthesized different [mTBNH][OAc]/green co-solvents.

This unexpected trend contrasts with that reported by Wen et al. (2017), who suggest that esterifying cellulose with a hydrophobic aliphatic chain reduces its hydrophilic properties, especially when all OH groups are substituted.

SEM was used to analyze surface properties to investigate the unusual wettability behavior of CM films. The unexpected decrease in contact angles may be linked to the films' surface roughness. SEM images (**Figure 25b**) suggest that crystallites (aggregates) on the film surface contribute to this roughness. CM-DMPU has the roughest surface, followed by CM-SLF and CM-DMI, with CM-GVL being the smoothest. According to Wenzel (1936), increased surface roughness enhances contact angle and thus hydrophobicity. Thus, the higher contact angles in CM-DMPU and CM-SLF, both above 90°, are likely due to their rougher surfaces.

All the above results demonstrate the following order - CM-DMPU, CM-SLF, CM-DMI, and CM-GVL - results in a) an increase in DS; b) the amorphization of cellulose esters; and c) improved mechanical properties and processing performance due to enhanced internal plasticization. The degradation temperatures of CMs prepared using different green co-solvents were observed to remain consistent. Moreover, contact angle measurements confirmed the hydrophobic nature of the films. Surface roughness plays a critical role in determining the hydrophobicity of the CM films. Greater surface roughness was noted in CM-DMPU and CM-SLF, attributed to the presence of aggregates, which increased the contact angle of the cellulose myristate films despite their lower DS compared to others.

Conclusions

This study aimed to develop novel and sustainable solvent systems for cellulose dissolution and transesterification while exploring the properties of the resulting CEs. To achieve this, cellulose dissolution behavior in SB-IL combined with various green co-solvents was assessed using rheology, identifying the most effective SB-IL/co-solvent combinations and their optimal ratios. Transesterification processes were optimized to get optimal reaction conditions and to achieve the highest DS in CEs, with a focus on the influence of green co-solvents on DS and the chemical, physical, and mechanical properties of the synthesized CEs using XRD, TGA, rheology, tensile strength testing, CAM, and SEM. Based on the study the following conclusions can be drawn:

- This study concludes that DMSO is an effective co-solvent with [mTBNH][OAc] for cellulose dissolution at ratios 2:1, 1:1, and 1:2, while GVL works well at 1:1, and DMI and DMPU at 2:1. Co-solvent content should not exceed 50% for effective cellulose dissolution. GVL and DMSO enhance solvation by aiding SB-IL dissociation by solvating the ions, and the activation energies of flow for cellulose in SB-IL/co-solvent decreases in the order of DMPU > DMI > GVL > DMSO. This suggests that co-solvents not only facilitate cellulose dissolution but also enhance the efficiency of chemical modifications such as transesterification.

- Optimal reaction conditions for CE synthesis were determined to be a temperature of 70°C, a reaction time of 2 hours, and a molar ratio of 5:1 (VE:AGU) in SB-IL/[mTBNH][OAc] solvent systems. While initially optimized for cellulose palmitates, these conditions were found to be broadly applicable to all cellulose esters and were adopted for subsequent experiments.

- It was revealed that the order DMPU → SLF → DMI → GVL reflects increasing DS, amorphization, and improved mechanical and processing performance due to enhanced plasticization. Degradation temperatures remained consistent, while contact angle measurements confirmed film hydrophobicity, influenced by surface roughness. Aggregates in CM-DMPU and CM-SLF, caused by lower solubility and incomplete substitution, contributed to higher rigidity, viscosities, G-moduli, stress levels, and Young's modulus.

The investigated solvent systems have the potential for future use in the sustainable synthesis of CEs through reactive extrusion, supporting eco-friendly manufacturing practices. However, further investigation is warranted to elucidate the complex interactions between SB-IL, co-solvents, and the cellulose polymer. A critical area of focus lies in understanding the specific roles and interactions of the cation and anion components of the SB-IL with co-solvents and cellulose. Additionally, exploring the potential interactions between vinyl esters and the SB-IL/co-solvent-based systems could yield insights into enhancing system efficacy.

References

Agarwal, U. P., Ralph, S. A., Reiner, R. S., & Baez, C. (2018). New cellulose crystallinity estimation method that differentiates between organized and crystalline phases. *Carbohydrate polymers*, *190*, 262-270.

Anastas, P., & Eghbali, N. (2010). Green chemistry: principles and practice. *Chemical Society Reviews*, *39*(1), 301-312.

Andanson, J. M., Bordes, E., Devémy, J., Leroux, F., Pádua, A. A., & Gomes, M. F. C. (2014). Understanding the role of co-solvents in the dissolution of cellulose in ionic liquids. *Green Chemistry*, *16*(5), 2528-2538.

Amim, J., Kosaka, P. M., & Petri, D. F. S. (2008). Characteristics of thin cellulose ester films spin-coated from acetone and ethyl acetate solutions. *Cellulose*, *15*, 527-535.

Arthanareeswaran, G., & Thanikaivelan, P. (2010). Fabrication of cellulose acetate–zirconia hybrid membranes for ultrafiltration applications: Performance, structure and fouling analysis. *Separation and Purification Technology*, *74*(2), 230-235.

Asakawa, M., Shrotri, A., Kobayashi, H., & Fukuoka, A. (2019). Solvent basicity controlled deformylation for the formation of furfural from glucose and fructose. *Green Chemistry.*

Asim, N., Badiei, M., & Mohammad, M. (2021). Recent advances in cellulose-based hydrophobic food packaging. *Emergent Materials*, 1-16.

Badgujar, K. C., & Bhanage, B. M. (2015). Factors governing dissolution process of lignocellulosic biomass in ionic liquid: current status, overview and challenges. *Bioresource technology*, *178*, 2-18.

Bernardinelli, O. D., Lima, M. A., Rezende, C. A., Polikarpov, I., & deAzevedo, E. R. (2015). Quantitative 13 C MultiCP solid-state NMR as a tool for evaluation of cellulose crystallinity index measured directly inside sugarcane biomass. *Biotechnology for biofuels*, *8*, 1-11.

Botello, J. I., Gilarranz, M. A., Rodriguez, F., & Oliet, M. (1999). Preliminary study on products distribution in alcohol pulping of Eucalyptus globulus. *Journal of Chemical Technology & Biotechnology: International Research in Process, Environmental & Clean Technology*, *74*(2), 141-148.

Brandrup, J., Immergut, E. H., Grulke, E. A., Abe, A., & Bloch, D. R. (Eds.). (1999). *Polymer handbook* (Vol. 89, pp. V87-V90). New York: Wiley.

Bras, J., Vaca-Garcia, C., Borredon, M. E., & Glasser, W. (2007). Oxygen and water vapor permeability of fully substituted long chain cellulose esters (LCCE). *Cellulose*, *14*, 367-374.

Brongniart, A., Pelouze, T. J., & Dumas, A. B. (1839). Rapport sur un mémoire de M. Payen, relatif à la composition de la matière ligneuse. *CR Hebd Seances Acad Sci*, *8*, 51-53.

Bryan, M. C., Dunn, P. J., Entwistle, D., Gallou, F., Koenig, S. G., Hayler, J. D., ... & Weiberth, F. J. (2018). Key Green Chemistry research areas from a pharmaceutical manufacturers' perspective revisited. *Green Chemistry*, *20*(22), 5082-5103.

Budtova, T., & Navard, P. (2015). Viscosity-temperature dependence and activation energy of cellulose solutions. *Nordic Pulp & Paper Research Journal*, *30*(1), 99-104.

Buzzeo, M. C., Evans, R. G., & Compton, R. G. (2004). Non-haloaluminate room-temperature ionic liquids in electrochemistry—A review. *ChemPhysChem*, *5*(8), 1106-1120.

Camp, J. E. (2018). Bio-available solvent Cyrene: synthesis, derivatization, and applications. *ChemSusChem*, *11*(18), 3048-3055.

Cannon, R. E., & Anderson, S. M. (1991). Biogenesis of bacterial cellulose. *Critical reviews in microbiology*, *17*(6), 435-447.

Chrapava, S., Touraud, D., Rosenau, T., Potthast, A., & Kunz, W. (2003). The investigation of the influence of water and temperature on the LiCl/DMAc/cellulose system. *Physical Chemistry Chemical Physics*, *5*(9), 1842-1847.

Chen, M. J., Li, R. M., Zhang, X. Q., Feng, J., Feng, J., Liu, C. F., & Shi, Q. S. (2017). Homogeneous transesterification of sugar cane bagasse toward sustainable plastics. *ACS Sustainable Chemistry & Engineering*, *5*(1), 360-366.

Ciacco, G. T., Liebert, T. F., Frollini, E., & Heinze, T. J. (2003). Application of the solvent dimethyl sulfoxide/tetrabutyl-ammonium fluoride trihydrate as reaction medium for the homogeneous acylation of Sisal cellulose. *Cellulose*, *10*, 125-132.

Clark, J. H., Farmer, T. J., Hunt, A. J., & Sherwood, J. (2015). Opportunities for bio-based solvents created as petrochemical and fuel products transition towards renewable resources. *International Journal of Molecular Sciences*, *16*(8), 17101-17159.

Clark, J. H., Macquarrie, D. J., & Sherwood, J. (2012). A quantitative comparison between conventional and bio-derived solvents from citrus waste in esterification and amidation kinetic studies. *Green chemistry*, *14*(1), 90-93.

Constable, D. J., Dunn, P. J., Hayler, J. D., Humphrey, G. R., Leazer Jr, J. L., Linderman, R. J., ... & Zhang, T. Y. (2007). Key green chemistry research areas—a perspective from pharmaceutical manufacturers. *Green Chemistry*, *9*(5), 411-420.

Cravotto, G., Gaudino, E. C., Boffa, L., Lévêque, J. M., Estager, J., & Bonrath, W. (2008). Preparation of second generation ionic liquids by efficient solvent-free alkylation of N-heterocycles with chloroalkanes. *Molecules*, *13*(1), 149-156.

Crépy, L., Chaveriat, L., Banoub, J., Martin, P., & Joly, N. (2009). Synthesis of cellulose fatty esters as plastics—influence of the degree of substitution and the fatty chain length on mechanical properties. *ChemSusChem: Chemistry & Sustainability Energy & Materials*, *2*(2), 165-170.

Dai, L., Cheng, T., Duan, C., Zhao, W., Zhang, W., Zou, X., ... & Ni, Y. (2019). 3D printing using plant-derived cellulose and its derivatives: A review. *Carbohydrate polymers*, *203*, 71-86.

Dawsey, T. R., & McCormick, C. L. (1990). The lithium chloride/dimethylacetamide solvent for cellulose: a literature review. *Journal of Macromolecular Science—Reviews in Macromolecular Chemistry and Physics*, *30*(3-4), 405-440.

de María, P. D., & Maugeri, Z. (2011). Ionic liquids in biotransformations: from proof-of-concept to emerging deep-eutectic-solvents. *Current opinion in chemical biology*, *15*(2), 220-225.

Duereh, A., Sato, Y., Smith Jr, R. L., & Inomata, H. (2015). Replacement of hazardous chemicals used in engineering plastics with safe and renewable hydrogen-bond donor and acceptor solvent-pair mixtures. *ACS Sustainable Chemistry & Engineering*, *3*(8), 1881-1889.

Duchatel-Crépy, L., Joly, N., Martin, P., Marin, A., Tahon, J. F., Lefebvre, J. M., & Gaucher, V. (2020). Substitution degree and fatty chain length influence on structure and properties of fatty acid cellulose esters. *Carbohydrate polymers*, *234*, 115912.

Edgar, K. J., Buchanan, C. M., Debenham, J. S., Rundquist, P. A., Seiler, B. D., Shelton, M. C., & Tindall, D. (2001). Advances in cellulose ester performance and application. *Progress in polymer science*, *26*(9), 1605-1688.

Ek, M., Gellerstedt, G., & Henriksson, G. (Eds.). (2009). *Paper chemistry and technology*. Walter de Gruyter.

El Seoud, O. A., Kostag, M., Jedvert, K., & Malek, N. I. (2019). Cellulose in ionic liquids and alkaline solutions: Advances in the mechanisms of biopolymer dissolution and regeneration. *Polymers*, *11*(12), 1917.

Engström, A. C., Ek, M., & Henriksson, G. (2006). Improved accessibility and reactivity of dissolving pulp for the viscose process: pretreatment with monocomponent endoglucanase. *Biomacromolecules*, *7*(6), 2027-2031.

Feng, L., & Chen, Z. L. (2008). Research progress on dissolution and functional modification of cellulose in ionic liquids. *Journal of Molecular Liquids*, *142*(1-3), 1-5.

Fink, H. P., Ganster, J., & Lehmann, A. (2014). Progress in cellulose shaping: 20 years industrial case studies at Fraunhofer IAP. *Cellulose*, *21*, 31-51.

Fink, H. P., Weigel, P., Purz, H. J., & Ganster, J. (2001). Structure formation of regenerated cellulose materials from NMMO-solutions. *Progress in Polymer Science*, *26*(9), 1473-1524.

Franko, A., Seavey, K. C., Gumaer, J., & Glasser, W. G. (2001). Continuous cellulose fiber-reinforced cellulose ester composites III. Commercial matrix and fiber options. *Cellulose*, *8*, 171-179.

Freire, C. S. R., Silvestre, A. J. D., Neto, C. P., Belgacem, M. N., & Gandini, A. (2006). Controlled heterogeneous modification of cellulose fibers with fatty acids: effect of reaction conditions on the extent of esterification and fiber properties. *Journal of Applied Polymer Science*, *100*(2), 1093-1102.

Freire, M. G., Teles, A. R. R., Rocha, M. A., Schröder, B., Neves, C. M., Carvalho, P. J., ... & Coutinho, J. A. (2011). Thermophysical characterization of ionic liquids able to dissolve biomass. *Journal of Chemical & Engineering Data*, *56*(12), 4813-4822.

Gandhi, K. S., & Williams, M. C. (1972). Effect of solvent character on polymer entanglements. *Journal of Applied Polymer Science*, *16*(10), 2721-2725.

Gao, X., Liu, H., Shuai, J., Zhao, J., Zhou, G., Huang, Q., ... & Wang, X. (2023). Rapid transesterification of cellulose in a novel DBU-derived ionic liquid: Efficient synthesis of highly substituted cellulose acetate. *International Journal of Biological Macromolecules*, *242*, 125133.

Gemili, S., Yemenicioğlu, A., & Altınkaya, S. A. (2009). Development of cellulose acetate based antimicrobial food packaging materials for controlled release of lysozyme. *Journal of Food Engineering*, *90*(4), 453-462.

Gericke, M., Schlufter, K., Liebert, T., Heinze, T., & Budtova, T. (2009). Rheological properties of cellulose/ionic liquid solutions: from dilute to concentrated states. *Biomacromolecules*, *10*(5), 1188-1194.

Glasser, W. G., Taib, R., Jain, R. K., & Kander, R. (1999). Fiber-reinforced cellulosic thermoplastic composites. *Journal of Applied Polymer Science*, *73*(7), 1329-1340.

Gören, A., Mendes, J., Rodrigues, H. M., Sousa, R. E., Oliveira, J., Hilliou, L., ... & Lanceros-Méndez, S. (2016). High performance screen-printed electrodes prepared by a green solvent approach for lithium-ion batteries. *Journal of Power Sources*, *334*, 65-77.

Gouvêa, D. M., Mendonça, R. C. S., Soto, M. L., & Cruz, R. S. (2015). Acetate cellulose film with bacteriophages for potential antimicrobial use in food packaging. *LWT-Food Science and Technology*, *63*(1), 85-91.

Gu, Y., & Jérôme, F. (2013). Bio-based solvents: an emerging generation of fluids for the design of eco-efficient processes in catalysis and organic chemistry. *Chemical Society Reviews*, *42*(24), 9550-9570.

Haag, R., & Kratz, F. (2006). Polymer therapeutics: concepts and applications. *Angewandte Chemie International Edition*, *45*(8), 1198-1215.

Han, S., Li, J., Zhu, S., Chen, R., Wu, Y., Zhang, X., & Yu, Z. (2009). POTENTIAL APPLICATIONS OF IONIC LIQUIDS IN WOOD RELATED INDUSTRIES. *BioResources*, *4*(2).

Hanabusa, H., Izgorodina, E. I., Suzuki, S., Takeoka, Y., Rikukawa, M., & Yoshizawa-Fujita, M. (2018). Cellulose-dissolving protic ionic liquids as low cost catalysts for direct transesterification reactions of cellulose. *Green Chemistry*, *20*(6), 1412-1422.

Hapiot, P., & Lagrost, C. (2008). Electrochemical reactivity in room-temperature ionic liquids. *Chemical reviews*, *108*(7), 2238-2264.

Heinze, T., Dicke, R., Koschella, A., Kull, A. H., Klohr, E. A., & Koch, W. (2000). Effective preparation of cellulose derivatives in a new simple cellulose solvent. *Macromolecular Chemistry and Physics*, *201*(6), 627-631.

Hellsten, S. (2020). Recycling of Superbase-Based Ionic Liquid Solvents for the Production of Textile-Grade Regenerated Cellulose Fibers in the Lyocell Process.

Henderson, R. K., Jiménez-González, C., Constable, D. J., Alston, S. R., Inglis, G. G., Fisher, G., ... & Curzons, A. D. (2011). Expanding GSK's solvent selection guide–embedding sustainability into solvent selection starting at medicinal chemistry. *Green Chemistry*, *13*(4), 854-862.

Hindi, S. (2017). The interconvertiblity of cellulose's allomorphs. *Int. J. Innov. Res. Sci. Eng. Technol*, *6*, 715-722.

Hinner, L. P., Wissner, J. L., Beurer, A., Nebel, B. A., & Hauer, B. (2016). Homogeneous vinyl ester-based synthesis of different cellulose derivatives in 1-ethyl-3-methyl-imidazolium acetate. *Green Chemistry*, *18*(22), 6099-6107.

Hirose, D., Kusuma, S. B. W., Nomura, S., Yamaguchi, M., Yasaka, Y., Kakuchi, R., & Takahashi, K. (2019). Effect of anion in carboxylate-based ionic liquids on catalytic activity of transesterification with vinyl esters and the solubility of cellulose. *RSC advances*, *9*(7), 4048-4053.

Holm, J., & Lassi, U. (2011). *Ionic liquids in the pretreatment of lignocellulosic biomass*. Rijeka, Croatia: INTECH Open Access Publisher.

Hooshmand, S., Aitomäki, Y., Skrifvars, M., Mathew, A. P., & Oksman, K. (2014). All-cellulose nanocomposite fibers produced by melt spinning cellulose acetate butyrate and cellulose nanocrystals. *Cellulose*, *21*, 2665-2678.

Horváth, I. T., Mehdi, H., Fábos, V., Boda, L., & Mika, L. T. (2008). γ-Valerolactone—a sustainable liquid for energy and carbon-based chemicals. *Green Chemistry*, *10*(2), 238-242.

Huang, K., Xia, J., Li, M., Lian, J., Yang, X., & Lin, G. (2011). Homogeneous synthesis of cellulose stearates with different degrees of substitution in ionic liquid 1-butyl-3-methylimidazolium chloride. *Carbohydrate polymers*, *83*(4), 1631-1635.

Ilyin, S. O., Kostyuk, A. V., Anokhina, T. S., Melekhina, V. Y., Bakhtin, D. S., Antonov, S. V., & Volkov, A. V. (2023). The effect of non-solvent nature on the rheological properties of cellulose solution in diluted ionic liquid and performance of nanofiltration membranes. *International Journal of Molecular Sciences*, *24*(9), 8057.

Ilyin, S. O., Makarova, V. V., Polyakova, M. Y., & Kulichikhin, V. G. (2020). Phase behavior and rheology of miscible and immiscible blends of linear and hyperbranched siloxane macromolecules. *Materials Today Communications*, *22*, 100833.

Isikgor, F. H., & Becer, C. R. (2015). Lignocellulosic biomass: a sustainable platform for the production of bio-based chemicals and polymers. *Polymer chemistry*, *6*(25), 4497-4559.

Jonas, R., & Farah, L. F. (1998). Production and application of microbial cellulose. *Polymer degradation and stability*, *59*(1-3), 101-106.

Kakko, T., King, A. W., & Kilpeläinen, I. (2017). Homogenous esterification of cellulose pulp in [DBNH][OAc]. *Cellulose*, *24*, 5341-5354.

Katsuhara, S., Sunagawa, N., Igarashi, K., Takeuchi, Y., Takahashi, K., Yamamoto, T., ... & Satoh, T. (2023). Effect of degree of substitution on the microphase separation and mechanical properties of cellooligosaccharide acetate-based elastomers. *Carbohydrate Polymers*, *316*, 120976.

King, A. W., Asikkala, J., Mutikainen, I., Järvi, P., & Kilpeläinen, I. (2011). Distillable acid–base conjugate ionic liquids for cellulose dissolution and processing. *Angewandte Chemie-International Edition*, *50*(28), 6301.

Klemm, D., Heublein, B., Fink, H. P., & Bohn, A. (2005). Cellulose: fascinating biopolymer and sustainable raw material. *Angewandte chemie international edition*, *44*(22), 3358-3393.

Köhler, S., Liebert, T., Schöbitz, M., Schaller, J., Meister, F., Günther, W., & Heinze, T. (2007). Interactions of Ionic Liquids with Polysaccharides 1. Unexpected Acetylation of Cellulose with 1-Ethyl-3-methylimidazolium Acetate. *Macromolecular Rapid Communications*, *28*(24), 2311-2317.

Komarova, A. O., Dick, G. R., & Luterbacher, J. S. (2021). Diformylxylose as a new polar aprotic solvent produced from renewable biomass. *Green Chemistry*, *23*(13), 4790-4799.

Kosaka, P. M., Kawano, Y., & Petri, D. F. S. (2007). Dewetting and surface properties of ultrathin films of cellulose esters. *Journal of colloid and interface science*, *316*(2), 671-677.

Kostag, M., Gericke, M., Heinze, T., & El Seoud, O. A. (2019). Twenty-five years of cellulose chemistry: Innovations in the dissolution of the biopolymer and its transformation into esters and ethers. *Cellulose*, *26*, 139-184.

Krasnou, I., Tarasova, E., Märtson, T., & Krumme, A. (2015). Thermoplastic cellulose stearate and cellulose laurate: melt rheology, processing and application potential. *International Polymer Processing*, *30*(2), 210-216.

Law, R. C. (2004, March). 5. Applications of cellulose acetate 5.1 Cellulose acetate in textile application. In *Macromolecular Symposia* (Vol. 208, No. 1, pp. 255-266). Weinheim: WILEY-VCH Verlag.

Lefroy, K. S., Murray, B. S., & Ries, M. E. (2021). Rheological and NMR studies of cellulose dissolution in the ionic liquid BmimAc. *The Journal of Physical Chemistry B*, *125*(29), 8205-8218.

Li, J., Dai, Z., Usman, M., Qi, Z., & Deng, L. (2016). CO2/H2 separation by amino-acid ionic liquids with polyethylene glycol as co-solvent. *International Journal of Greenhouse Gas Control*, *45*, 207-215.

Lopez-Rubio, A., Almenar, E., Hernandez-Muñoz, P., Lagarón, J. M., Catalá, R., & Gavara, R. (2004). Overview of active polymer-based packaging technologies for food applications. *Food Reviews International*, *20*(4), 357-387.

Lowman, D. W. (1998). Characterization of cellulose esters by solution-state and solid-state NMR spectroscopy.

Lv, Y., Wu, J., Zhang, J., Niu, Y., Liu, C. Y., He, J., & Zhang, J. (2012). Rheological properties of cellulose/ionic liquid/dimethylsulfoxide (DMSO) solutions. *Polymer*, *53*(12), 2524-2531.

Malkin, Y. A. (1994). Rheology Fundamentals, ChemTec. *Publishing, Ontario*.

Marsh, K. N., Boxall, J. A., & Lichtenthaler, R. (2004). Room temperature ionic liquids and their mixtures—a review. *Fluid phase equilibria*, *219*(1), 93-98.

Martins, M. A., Sosa, F. H., Kilpeläinen, I., & Coutinho, J. A. (2022). Physico-chemical characterization of aqueous solutions of superbase ionic liquids with cellulose dissolution capability. *Fluid Phase Equilibria*, *556*, 113414.

McCormick, C. L., & Callais, P. A. (1987). Derivatization of cellulose in lithium chloride and NN-dimethylacetamide solutions. *Polymer*, *28*(13), 2317-2323.

Mead, D. W. (2011). Analytic derivation of the Cox–Merz rule using the MLD "toy" model for polydisperse linear polymers. *Rheologica acta*, *50*(9), 837-866.

Mohan, M., Banerjee, T., & Goud, V. V. (2016). Effect of protic and aprotic solvents on the mechanism of cellulose dissolution in Ionic liquids: A combined molecular dynamics and experimental insight. *ChemistrySelect*, *1*(15), 4823-4832.

Moon, R. J., Martini, A., Nairn, J., Simonsen, J., & Youngblood, J. (2011). Cellulose nanomaterials review: structure, properties and nanocomposites. *Chemical Society Reviews*, *40*(7), 3941-3994.

Ostonen, A., Bervas, J., Uusi-Kyyny, P., Alopaeus, V., Zaitsau, D. H., Emel'yanenko, V. N., ... & Verevkin, S. P. (2016). Experimental and theoretical thermodynamic study of distillable ionic liquid 1, 5-diazabicyclo [4.3. 0] non-5-enium acetate. *Industrial & Engineering Chemistry Research*, *55*(39), 10445-10454.

Park, S., Baker, J. O., Himmel, M. E., Parilla, P. A., & Johnson, D. K. (2010). Cellulose crystallinity index: measurement techniques and their impact on interpreting cellulase performance. *Biotechnology for biofuels*, *3*, 1-10.

Parviainen, A., Wahlström, R., Liimatainen, U., Liitiä, T., Rovio, S., Helminen, J. K. J., ... & Kilpeläinen, I. (2015). Sustainability of cellulose dissolution and regeneration in 1, 5-diazabicyclo [4.3. 0] non-5-enium acetate: a batch simulation of the IONCELL-F process. *RSC advances*, *5*(85), 69728-69737.

Pattinson, S. W., & Hart, A. J. (2017). Additive manufacturing of cellulosic materials with robust mechanics and antimicrobial functionality. *Advanced Materials Technologies*, *2*(4), 1600084.

Payen, A. (1838). Sur un moyen d'isoler le tissue élémentaire des bois. *CR Hebd. Seances Acad. Sci*, *7*(1125), 26.

Phadagi, R., Singh, S., Hashemi, H., Kaya, S., Venkatesu, P., Ramjugernath, D., ... & Bahadur, I. (2021). Understanding the role of dimethylformamide as co-solvents in the dissolution of cellulose in ionic liquids: Experimental and theoretical approach. *Journal of Molecular Liquids*, *328*, 115392.

Pham, Q. T., & Chern, C. S. (2022). Applications of polymers in lithium-ion batteries with enhanced safety and cycle life. *Journal of Polymer Research*, *29*(4), 124.

Pinkert, A., Marsh, K. N., Pang, S., & Staiger, M. P. (2009). Ionic liquids and their interaction with cellulose. *Chemical reviews*, *109*(12), 6712-6728.

Plechkova, N. V., & Seddon, K. R. (2008). Applications of ionic liquids in the chemical industry. *Chemical Society Reviews*, *37*(1), 123-150.

Potthast, A., Rosenau, T., Buchner, R., Röder, T., Ebner, G., Bruglachner, H., ... & Kosma, P. (2002). The cellulose solvent system N, N-dimethylacetamide/lithium chloride revisited: the effect of water on physicochemical properties and chemical stability. *Cellulose*, *9*, 41-53.

Qiu, X., & Hu, S. (2013). "Smart" materials based on cellulose: a review of the preparations, properties, and applications. *Materials*, *6*(3), 738-781.

Quintero, R. I., Rodriguez, F., Bruna, J., Guarda, A., & Galotto, M. J. (2013). Cellulose acetate butyrate nanocomposites with antimicrobial properties for food packaging. *Packaging Technology and Science*, *26*(5), 249-265.

Rinaldi, R. (2011). Instantaneous dissolution of cellulose in organic electrolyte solutions. *Chemical Communications*, *47*(1), 511-513.

Rubin, I. I. (1990). Handbook of plastic materials and technology. *(No Title)*.

Samaranayake, G., & Glasser, W. G. (1993). Cellulose derivatives with low DS. I. A novel acylation system. *Carbohydrate polymers*, *22*(1), 1-7.

Savale, N., Tarasova, E., Krasnou, I., Kudrjašova, M., Rjabovs, V., Reile, I., ... & Krumme, A. (2024). Optimization and degradation studies of cellulose transesterification to palmitate esters in superbase ionic liquid. *Carbohydrate Research*, *537*, 109047.

Schenzel, K., Fischer, S., & Brendler, E. (2005). New method for determining the degree of cellulose I crystallinity by means of FT Raman spectroscopy. *Cellulose*, *12*(3), 223-231.

Schenzel, A., Hufendiek, A., Barner-Kowollik, C., & Meier, M. A. (2014). Catalytic transesterification of cellulose in ionic liquids: sustainable access to cellulose esters. *Green Chemistry*, *16*(6), 3266-3271.

Schweizer, E. (1857). *Das Kupferoxyd-Amrnoniak, ein Auflosungs-mittel fur die Pflanzenfaser*.

Shokri, J., & Adibkia, K. (2013). Application of cellulose and cellulose derivatives in pharmaceutical industries. In *Cellulose-medical, pharmaceutical and electronic applications*. IntechOpen.

Silva, W., Zanatta, M., Ferreira, A. S., Corvo, M. C., & Cabrita, E. J. (2020). Revisiting ionic liquid structure-property relationship: A critical analysis. *International journal of molecular sciences*, *21*(20), 7745.

Singh, R. K., Sharma, O. P., & Singh, A. K. (2014). Evaluation of cellulose laurate esters for application as green biolubricant additives. *Industrial & Engineering Chemistry Research*, *53*(25), 10276-10284.

Sherwood, J., Constantinou, A., Moity, L., McElroy, C. R., Farmer, T. J., Duncan, T., ... & Clark, J. H. (2014). Dihydrolevoglucosenone (Cyrene) as a bio-based alternative for dipolar aprotic solvents. *Chemical communications*, *50*(68), 9650-9652.

Sosa, F. H., Kilpeläinen, I., Rocha, J., & Coutinho, J. A. (2023). Recovery of superbase ionic liquid using aqueous two-phase systems. *Fluid Phase Equilibria*, *573*, 113857.

Staudinger, H. (1968). On polymerization. In *Source Book in Chemistry, 1900–1950* (pp. 259-264). Harvard University Press.

Stevens, C. V., & Verhé, R. (Eds.). (2004). *Renewable bioresources: scope and modification for non-food applications*. John Wiley & Sons.

Strappaveccia, G., Luciani, L., Bartollini, E., Marrocchi, A., Pizzo, F., & Vaccaro, L. (2015). γ-Valerolactone as an alternative biomass-derived medium for the Sonogashira reaction. *Green Chemistry*, *17*(2), 1071-1076.

Tager, A. A. (1975). Effect of solvent quality on the viscosity of flexible-chain and rigid-chain polymers in a wide range of concentrations. *Rheological Theories· Measuring Techniques in Rheology Test Methods in Rheology· Fractures Rheological Properties of Materials· Rheo-Optics· Biorheology*, 831-840.

Tarasova, E., Savale, N., Ausmaa, P. M., Krasnou, I., & Krumme, A. (2024). Rheology and dissolution capacity of cellulose in novel [mTBNH][OAc] ionic liquid mixed with green co-solvents. *Rheologica Acta*, *63*(2), 167-178.

Tarasova, E., Savale, N., Krasnou, I., Kudrjašova, M., Rjabovs, V., Reile, I., ... & Krumme, A. (2023). Preparation of thermoplastic cellulose esters in [mTBNH][OAC] ionic liquid by transesterification reaction. *Polymers*, *15*(19), 3979.

Tenhunen, T. M., Moslemian, O., Kammiovirta, K., Harlin, A., Kääriäinen, P., Österberg, M., ... & Orelma, H. (2018). Surface tailoring and design-driven prototyping of fabrics with 3D-printing: An all-cellulose approach. *Materials & Design*, *140*, 409-419.

Thygesen, A., Oddershede, J., Lilholt, H., Thomsen, A. B., & Ståhl, K. (2005). On the determination of crystallinity and cellulose content in plant fibres. *Cellulose*, *12*, 563-576.

Tilstam, U. (2012). Sulfolane: A versatile dipolar aprotic solvent. *Organic Process Research & Development*, *16*(7), 1273-1278.

Todorov, A. R., King, A. W., & Kilpeläinen, I. (2023). Transesterification of cellulose with unactivated esters in superbase–acid conjugate ionic liquids. *RSC advances*, *13*(9), 5983-5992.

Tundo, P., Aricò, F., Gauthier, G., Rossi, L. I., Rosamilia, A. E., Bevinakatti, H. S., ... & Newman, C. P. (2010). Green synthesis of dimethyl isosorbide.

Vandamme, E. J., De Baets, S., Vanbaelen, A., Joris, K., & De Wulf, P. (1998). Improved production of bacterial cellulose and its application potential. *Polymer degradation and stability*, *59*(1-3), 93-99.

Villalta, E., Riba Moliner, M., & Lis Arias, M. J. (2022). Recovery of cellulose from polyester/cotton fabrics making use of ionic liquids. *Polymer Science: Peer Review Journal*, *4*(3, article 000590).

Wang, H., Gurau, G., & Rogers, R. D. (2012). Ionic liquid processing of cellulose. *Chemical Society Reviews*, *41*(4), 1519-1537.

Wang, X., Wang, Y., Xia, Y., Huang, S., Wang, Y., & Qiu, Y. (2018). Preparation, structure, and properties of melt spun cellulose acetate butyrate fibers. *Textile Research Journal*, *88*(13), 1491-1504.

Wen, X., Wang, H., Wei, Y., Wang, X., & Liu, C. (2017). Preparation and characterization of cellulose laurate ester by catalyzed transesterification. *Carbohydrate Polymers*, *168*, 247-254.

Wenzel, R. N. (1936). Resistance of solid surfaces to wetting by water. *Industrial & engineering chemistry*, *28*(8), 988-994.

Weißl, M., Hobisch, M. A., Johansson, L. S., Hettrich, K., Kontturi, E., Volkert, B., & Spirk, S. (2019). Cellulose carbamate derived cellulose thin films: preparation, characterization and blending with cellulose xanthate. *Cellulose*, *26*, 7399-7410.

Wilkes, J. S. (2002). A short history of ionic liquids—from molten salts to neoteric solvents. *Green Chemistry*, *4*(2), 73-80.

Willberg-Keyriläinen, P., Vartiainen, J., Harlin, A., & Ropponen, J. (2017). The effect of side-chain length of cellulose fatty acid esters on their thermal, barrier and mechanical properties. *Cellulose*, *24*, 505-517.

Wilson, K. L., Murray, J., Sneddon, H. F., Jamieson, C., & Watson, A. J. (2018). Dimethylisosorbide (DMI) as a bio-derived solvent for Pd-catalyzed cross-coupling reactions. *Synlett*, *29*(17), 2293-2297.

Wu, X. M., Branford-White, C. J., Zhu, L. M., Chatterton, N. P., & Yu, D. G. (2010). Ester prodrug-loaded electrospun cellulose acetate fiber mats as transdermal drug delivery systems. *Journal of Materials Science: Materials in Medicine*, *21*, 2403-2411.

Xu, A., Zhang, Y., Zhao, Y., & Wang, J. (2013). Cellulose dissolution at ambient temperature: Role of preferential solvation of cations of ionic liquids by a cosolvent. *Carbohydrate polymers*, *92*(1), 540-544.

Xu, C., & Cheng, Z. (2021). Thermal stability of ionic liquids: Current status and prospects for future development. *Processes*, *9*(2), 337.

Xia, J., King, A. W., Kilpeläinen, I., & Aseyev, V. (2021). Phase-separation of cellulose from ionic liquid upon cooling: preparation of microsized particles. *Cellulose*, *28*, 10921-10938.

Yuan, C., Shi, W., Chen, P., Chen, H., Zhang, L., Hu, G., ... & Lu, S. (2019). Dissolution and transesterification of cellulose in γ-valerolactone promoted by ionic liquids. *New Journal of Chemistry*, *43*(1), 330-337.

Zhao, H., Kwak, J. H., Wang, Y., Franz, J. A., White, J. M., & Holladay, J. E. (2006). Effects of crystallinity on dilute acid hydrolysis of cellulose by cellulose ball-milling study. *Energy & fuels*, *20*(2), 807-811.

Zhao, Y., Liu, X., Wang, J., & Zhang, S. (2013). Insight into the cosolvent effect of cellulose dissolution in imidazolium-based ionic liquid systems. *The journal of physical Chemistry B*, *117*(30), 9042-9049.

Zhou, Y., Min, D. Y., Wang, Z., Yang, Y., & Kuga, S. (2014). Cellulose esterification with octanoyl chloride and its application to films and aerogels. *BioResources*, *9*(3), 3901-3908.

https://www.plasticseurope.org/application/files/9715/7129/9584/FINAL_web_version _Plastics_the_facts2019_14102019.pdf

Acknowledgments

Abstract

Cellulose Dissolution and Transesterification in Superbase Ionic Liquid [mTBNH][OAc] with Green Co-solvents

The thesis explores the potential of various green co-solvents such as γ-Valerolactone (GVL), dimethyl isosorbide (DMI), sulfolane (SLF), and *N,N*-Dimethylpropyleneurea (DMPU) when mixed with distillable superbase ionic liquid (SB-IL), 5-methyl-1,5,7-triaza-bicyclo-[4.3.0]non-6-enium acetate ([mTBNH][OAc]) to improve cellulose dissolution and transesterification efficiency. This SB-IL demonstrates high dissolving power for cellulose and chemical durability for recycling. However, its high viscosity limits the cellulose concentration in the solution, and its cost poses a barrier to commercialization. To address these challenges, bio-based, low-cost, and low-viscosity co-solvents were introduced to reduce the cost and viscosity of the SB-IL.

Several studies have been carried out to study cellulose dissolution and transesterification using different ILs in combination with different polar aprotic co-solvents. Limited studies explore cellulose's dissolution behavior in ionic liquids (ILs) combined with green co-solvents. [mTBNH][OAc] mixed with green co-solvents mentioned above as a dissolution or modification medium for cellulose has not been studied. Therefore, this study evaluates the dissolution of cellulose in a mixture of [mTBNH][OAc] with green co-solvents, focusing on their impacts on the structure and properties of cellulose esters (CEs) produced in these solvent systems.

The rheological behavior of cellulose/SB-IL/co-solvent solutions was studied as a foundation for cellulose transesterification in these SB-IL/co-solvents. The impact of green co-solvent type and content on rheological properties was assessed under steady and oscillatory shear conditions. Cellulose dissolution and activation energies in the SB-IL with co-solvents GVL, DMPU, and DMI, were compared to those using dimethyl sulfoxide (DMSO) as a co-solvent. Rheology revealed that low co-solvent concentrations (≤ 50 wt%) reduce viscosity, while high concentrations (≥ 50 wt%) induce gelation or phase separation. Flow activation energy in SB-IL/co-solvent systems is lower than in pure SB-IL, decreasing in the order of DMPU > DMI > GVL > DMSO. GVL and DMSO enhance solvation by promoting SB-IL dissociation through ion solvation. Overall, lower activation energies in co-solvent mixtures lead to higher dissolution rates, indicating that co-solvents aid cellulose dissolution and boost the efficiency of chemical modifications like transesterification.

Following successful cellulose dissolution in SB-IL [mTBNH][OAc], its role as a medium for cellulose transesterification was with DMSO as a co-solvent. The effects of reaction temperature, time, and vinyl ester to anhydroglucose unit (VE:AGU) molar ratio on the degree of substitution (DS) were evaluated by nuclear magnetic resonance spectroscopy (NMR). CEs with varying DS (0.5–2.3) were synthesized. Higher temperatures (≥ 75 °C) and longer reaction times (≥ 2.5 hours) reduced the DS of CEs, likely due to cellulose degradation. A reaction temperature of 70 °C, a reaction time of 2 hours, and a 5:1 molar ratio were identified as optimal for cellulose transesterification in the SB-IL/DMSO solvent system.

Finally, the study investigated the impact of green co-solvents on the chemical and physical properties of CEs. CEs with DS up to 1.6 were synthesized via transesterification under optimal reaction conditions using a solvent system containing SB-IL and various green co-solvents. The choice of co-solvent influences the DS in the CEs in the following

order: DMPU < SLF < DMI < GVL. Rheological study showed that the internal plasticization efficiency of the esters increased with higher DS. Thermogravimetric analysis (TGA) revealed that all cellulose esters exhibited nearly identical degradation temperatures, Strain at break of CEs increase as DS increases, while

Young's modulus and yield point decrease due to the plasticizing effect of ester chains, reducing overall rigidity. Additionally, the contact angle measurements revealed the hydrophobic character of CE films.

The findings of this study pave the way for significant advancements in the development of sustainable solvent systems tailored for cellulose dissolution and transesterification. These advancements promise to improve the functional properties of CEs, especially in their utilization for eco-friendly packaging applications.

Lühikokkuvõte

Tselluloosi lahustamine ja ümberesterdamine superaluselises ioonvedelikus [mTBNH][OAc] koos roheliste kaaslahustitega

Doktoritöös uuritakse erinevate roheliste kaaslahustite, nagu γ-valerolaktooni (GVL), dimetüülisosorbiidi (DMI), sulfolaani (SLF) ja N,N-dimetüülpropüleenuureai (DMPU) potentsiaali, kui need on segatud destilleeritava superaluselise ioonse vedelikuga (SB-IL), 5-metüül-1,5,7-triasabitsüklo-[4.3.0]non-6-eeniumatsetaadiga ([mTBNH][OAc]), et parandada tselluloosi lahustumist ja ümberesterdamise efektiivsust. Sellel SB-IL-il on kõrge tselluloosi lahustumisvõime ja keemiline vastupidavus taaskasutusel. Selle kõrge viskoossus piirab aga tselluloosi kontsentratsiooni lahuses ja selle kõrge maksumus takistab kommertsialiseerimist. Nende probleemide lahendamiseks võeti kasutusele biopõhised, odavad ja madala viskoossusega kaaslahustid, et vähendada SB-IL hinda ja viskoossust.

Tselluloosi lahustumise ja ümberesterdamise uurimiseks on läbi viidud mitmeid uuringuid, kasutades erinevaid IL-sid koos erinevate polaarsete aprotoonsete kaaslahustitega. Mõningad uuringud on käsitlenud ka tselluloosi lahustumiskäitumist ioonsetes vedelikes (IL) kombineerituna roheliste kaaslahustitega. [mTBNH][OAc]-i segatuna ülalnimetatud roheliste kaaslahustitega ei ole tselluloosi lahustamis- või modifikatsioonikeskkonnana uuritud. Seetõttu hinnatakse käesolevas uuringus tselluloosi lahustumist [mTBNH][OAc] segus roheliste kaaslahustitega, keskendudes nende mõjule antud lahustisüsteemides sünteesitud tselluloosi estrite (CE-de) struktuurile ja omadustele.

Tselluloosi/SB-IL/kaaslahusti lahuste reoloogilist käitumist uuriti tselluloosi ümberesterdamise alusena nendes SB-IL/kaaslahustites. Rohelise kaaslahusti tüübi ja sisalduse mõju reoloogilistele omadustele hinnati püsiva ja võnkuva nihkekiiruse korral. Tselluloosi lahustumis- ja aktiveerimisenergiat SB-IL-is koos kaaslahustitega GVL-s, DMPU-s ja DMI-s, võrreldi tulemustega, mis saadi dimetüülsulfoksiidi (DMSO) kasutamisel kaaslahustina. Reoloogia uuring näitas, et madal kaaslahusti kontsentratsioon (≤ 50 massiprotsenti) vähendas viskoossust, samas kui kõrge kontsentratsioon (≥ 50 massiprotsenti) kutsus esile geelistumise või faaside eraldumise. Voolamise aktivatsioonienergia oli SB-IL/kaaslahusti süsteemides madalam kui puhta SB-IL korral, vähenedes kaaslahusti liikide järjekorras DMPU > DMI > GVL > DMSO. GVL ja DMSO suurendavad solvatatsiooni, soodustades SB-IL dissotsiatsiooni ioonide solvatatsiooni kaudu. Üldiselt põhjustavad kaaslahusti segude madalamad aktivatsioonienergiad kiirema lahustumise, mis näitab, et kaaslahustid soodustavad tselluloosi lahustumist ja suurendavad keemiliste modifikatsioonide, näiteks ümberesterdamise, tõhusust.

Pärast tselluloosi edukat lahustumist SB-IL-s [mTBNH][OAc] uuriti selle rolli tselluloosi ümberesterdamise keskkonnana, kasutades kaaslahustina DMSO-d. Reaktsiooni temperatuuri, aja ja vinüülestri ning anhüdroglükoosiühiku molaarsuhte (VE:AGU) mõju asendusastmele (DS) hinnati tuumamagnetresonantsspektroskoopia (NMR) abil. Sünteesiti erinevate asendusastmetega (0,5–2,3) CE-d. Kõrgemad temperatuurid (≥ 75 °C) ja pikemad reaktsiooniajad (≥ 2,5 tundi) vähendasid CE-de DS-i, tõenäoliselt tselluloosi lagunemise tõttu. Reaktsioonitemperatuur 70 °C, reaktsiooniaeg 2 tundi ja molaarsuhe 5:1 leiti olevat optimaalsed tselluloosi ümberesterdamiseks SB-IL/DMSO lahustisüsteemis.

Viimaks uuriti roheliste kaaslahustite mõju CE-de keemilistele ja füüsikalistele omadustele. Ümberesterdamise teel sünteesiti optimaalsetes reaktsioonitingimustes CE-d, mille DS oli kuni 1,6, kasutades SB-IL-i ja erinevaid rohelisi kaaslahusteid sisaldavat lahustisüsteemi. Kaaslahusti valik mõjutas DS-i CE-des järgmises järjekorras: DMPU < SLF < DMI < GVL. Reoloogiline uuring näitas, et estrite sisemise plastifitseerimise efektiivsus suurenes DS-i kasvades. Termogravimeetriline analüüs (TGA) näitas, et kõigi tselluloosi estrite lagunemistemperatuurid olid peaaegu identsed. DS-i kasvuga kasvas CE-de deformatsioon purunemisel, samal ajal kui Youngi moodul ja voolavuspunkt vähenesid estri ahelate plastifitseeriva toime tõttu, vähendades üldist jäikust. Lisaks näitasid kontaktnurga mõõtmised CE kilede hüdrofoobset iseloomu.

Selle uuringu tulemused sillutavad teed olulistele edusammudele jätkusuutlike lahustisüsteemide väljatöötamisel, mis on kohandatud tselluloosi lahustamiseks ja ümberesterdamiseks. Need edusammud lubavad parandada CE-de funktsionaalseid omadusi, eriti nende kasutamisel keskkonnasõbralike pakkematerjalidena.

Appendix

Publication I

Tarasova, E., Savale, N., Krasnou, I., Kudrjašova, M., Rjabovs, V., Reile, I., Vares, L., Kallakas, H., Kers, J., Krumme, A. (2023). Preparation of thermoplastic cellulose esters in [mTBNH][OAC] ionic liquid by transesterification reaction. Polymers, 15(19), 3979.

Article

Preparation of Thermoplastic Cellulose Esters in [mTBNH][OAC] Ionic Liquid by Transesterification Reaction

Elvira Tarasova [1], Nutan Savale [1], Illia Krasnou [1,*], Marina Kudrjašova [2], Vitalijs Rjabovs [3], Indrek Reile [3], Lauri Vares [4], Heikko Kallakas [1], Jaan Kers [1] and Andres Krumme [1]

1   School of Engineering, Department of Materials and Environmental Technology, Tallinn University of Technology, Ehitajate tee 5, 19086 Tallinn, Estonia; elvira.tarasova@taltech.ee (E.T.); nutan.savale@taltech.ee (N.S.); jaan.kers@taltech.ee (J.K.); andres.krumme@taltech.ee (A.K.)
2   School of Science, Department of Chemistry and Biotechnology, Tallinn University of Technology, Akadeemia tee 15, 12618 Tallinn, Estonia
3   National Institute of Chemical Physics and Biophysics, Akadeemia tee 23, 12618 Tallinn, Estonia
4   Faculty of Science and Technology, Institute of Technology, Tartu University, Nooruse 1, 50090 Tartu, Estonia
*   Correspondence: illia.krasnou@taltech.ee

Abstract: The transesterification of cellulose with vinyl esters in ionic liquid media is suggested as a prospective environmentally friendly alternative to conventional esterification. In this study, various long-chain cellulose esters (laurate, myristate, palmitate, and stearate) with a degree of substitution (DS) up to 1.8 have been synthesized in novel distillable ionic liquid, [mTBNH][OAC]. This IL has high dissolving power towards cellulose, which can improve homogeneous transesterification. Additionally, [mTBNH][OAC] has durability towards recycling and can be regenerated and re-used again for the next cycles of esterification. DMSO is used as a co-solvent because of its ability to speed up mass transport due to lower solvent viscosity. The optimization of the reaction parameters, such as co-solvent content, temperature (20–80 °C), reaction time (1–5 h), and a molar ratio of reactants (1–5 eq. AGU) is reported. It was found that within studied reaction conditions, DS increases with increasing reaction time, temperature, and added vinyl esters. Structure analysis using FTIR, ^{1}H, and ^{13}C NMR after acylation revealed the introduction of the alkyl chains into cellulose for all studied samples. The results also suggested that the substitution order of the OH group is C7-O6 > C7-O2 > C7-O3. Unique, complex thermal and rheological investigation of the cellulose esters shows the growth of an amorphous phase upon the degree of substitution. At the same time, the homogeneous substitution of cellulose with acyl chains increases the melt viscosity of a material. Internal plasticization in cellulose esters was found to be the mechanism for the melt processing of the material. Long-chain cellulose esters show the potential to replace commonly used externally plasticized cellulose derivatives.

Keywords: transesterification; cellulose esters; mTBN superbase; ionic liquids; rheology; FACE

1. Introduction

Cellulose is the most important biopolymer from renewable resources to produce polymeric materials and composites. Cellulose has several beneficial properties, such as biodegradability, nontoxicity, and biocompatibility, as well as great mechanical strength, heat stability, and resistance to many solvents [1]. Some of these benefits are also drawbacks for processing: it is hard to dissolve cellulose and cellulose is not thermoplastic in its natural state [2].

Acylation of the cellulose macromolecules and substitution of hydroxyl groups of the anhydroglucose repeating units (AGU) by ester groups allows for solving the issue of material thermoplasticity. Such derivatives lose hydrogen bonding between macromolecules and obtain thermoplastic behavior [3,4]. The most important thermoplastic derivative of cellulose, widely used in plastics, films, fibers, membranes, and coatings, is cellulose

acetate [5]. However, the melt viscosity of conventional thermoplastic derivatives of cellulose is still high (10^4–10^6 Pa·s compared to 10^2–10^3 Pa·s for polyolefin thermoplastics) and decomposition during melt processing may be a problem.

The cellulose esters (CEs) substituted with long chains (laurate, myristate, palmitate, and stearate) have lower melting temperatures (require less energy in processing) and better solubility in common solvents of lower polarity [6]. Such CEs exhibit plasticized polymer behavior [3]. Long-chain ester branches also have an internal plasticizing effect, which reduces or eliminates the need for added plasticizers, which are common for cellulose acetate, propionate, butyrate, or their mixed esters [7]. Thus, long-chain esters show potential as packaging and coating material with effective barrier properties.

CEs are usually prepared by esterification or transesterification procedures with different acyl donors, such as: (a) acid anhydrides; (b) acid chlorides; and (c) carboxylic acids. Long-chain fatty acids are among the most promising types of acyl donors; however, it is difficult to obtain long-chain fatty acid cellulose esters (FACEs), because of poor solubility of fatty acid compounds in polar solvent systems [8]. Strong acids as catalysts are needed as well [9].

The obstacle to acylation with acid anhydrides or acid chlorides is the formation of strongly acidic by-products, which are corrosive [10] and can reduce the degree of polymerization of cellulose. To overcome these problems, it has been recommended to use a tertiary base, such as harmful pyridine and trimethylamine [11].

In transesterification reactions, either (a) carboxylic esters [12] or (b) vinyl esters are used as acyl donors [13,14]; in this case, a large excess of the reagents and high temperature are required, and usually a low degree of substitution (DS) is obtained. The by-products of transesterification using vinyl esters as acylating agents are relatively simple compounds like alcohols, aldehydes, and ketones, which can be easily separated and recycled. Transesterification reactions have mostly been performed under heterogeneous conditions, which usually need a long reaction time (from hours to days). Furthermore, in transesterification, a catalyst is necessary to initiate the reaction [4,15], for example, sulfuric acid. In these reactions, the cellulose is not fully solubilized. Therefore, such technologies can be used mostly for the synthesis of short-chain fatty acids (with acyl chains C2–C4) [15].

Homogeneous esterification fully solubilizes cellulose and could synthesize cellulose esters of a high degree of substitution (DS) with even longer acyl chains [16]. During past decades, a large number of solvent systems were developed to dissolve and transesterify cellulose, for example, *N*-methylmorpholine *N*-oxide (NMO) [17], *N*,*N*-dimethylacetamide–lithium chloride (DMAc–LiCl) [18], dimethylsulfoxide–tetrabutylammonium fluoride (DMSO–TBAF) [19], and DMSO/KOH [15]. However, long pretreatment, long reaction times (more than 40 h), or high temperatures (>100 °C) were required, leading to relatively low DS (<2).

Those commercialized solvent systems have environmental problems; they are toxic or have low stability. Fortunately, a relatively "green" group of solvents for cellulose, ionic liquids, have been recently introduced and are under continuous development [20].

Ionic liquids (ILs) are polar substances and, therefore, can break the hydrogen bonds between macromolecules of cellulose. In addition, ILs are not volatile, they do not enter the atmosphere, harming humans and animals, and do not cause ozone depletion or climate change [2,21]. From this point of view, ILs can be considered green solvents, unlike DMAc–LiCl and NMO, whose broad industrial utilization is limited by instability. The number of different ILs is also nearly unlimited due to the high number of anions and cations that can be combined. Cellulose can be efficiently dissolved in many ILs and turned into a thermoplastic material by acylation in homogeneous conditions [22].

Processing in homogeneous conditions is one of the prospective solutions, considering commercial production of long-chain FACEs. The recent developments in IL synthesis address the durability of ILs in repeated recycling [23], combined with high dissolving power towards cellulose. Up to now, 1-ethyl-3-metyl-imidazolium acetate ([Emim][OAc]) ionic liquid was considered good for laboratory research—it has a sufficient cellulose

dissolution power and can act as an in situ catalyst for the transesterification of cellulose with vinyl esters [24]. Several different CEs were prepared in [Emim][OAc] under relatively mild conditions, but an unwanted side reaction between the acetate anion of IL and the cellulose backbone has been found [25,26]. Furthermore, it is difficult to recycle the first-generation imidazolium-based ILs due to their questionable stability [27,28]. Therefore, the imidazolium-based ILs have not been used for industrial upscaling, and intensive research is going on to develop a new generation of ILs for cellulose dissolution.

Superbases (mostly di- or triazabicyclo compounds) originating from protonic ILs are the most novel and promising solvents for cellulose dissolution and modification, for several reasons. They can dissolve cellulose to a high extent (up to 25%), have low moisture sensitivity, low toxicity, and can be recycled without degradation [29,30]. Additionally, they behave as ionic compounds with a low vapor pressure at temperatures typical for acylation reactions but can be dissociated to their superbase and acid at higher temperatures. This allows for the purification of the components by distillation [23].

More recently, 7-methyl-1,5,7-triazabicyclo[4.4.0]dec-5-enium acetate ([mTBDH][OAc]), and 5-methyl-1,5,7-triaza-bicyclo[4.3.0]non-6-enium acetate ([mTBNH][OAC]), were proposed to be good candidates for cellulose dissolution and regeneration [31]. The superbase mTBD demonstrates lower hydrolysis compared to DBN and the superbase mTBN shows better stability in the presence of water [23]. [mTBNH][OAC] can be recycled to either pure IL or to its starting compounds [32]. Moreover, [mTBNH][OAC] is a liquid at room temperature [33] which makes processing with this IL less labor intensive.

In this study, we focus on one of these newly developed ILs, namely [mTBNH][OAC]. We use dimethyl sulfoxide (DMSO) as a co-solvent to improve the solubility, reduce the viscosity of the reaction media, and decrease the total cost of the solvents used in synthesis. DMSO was used because it is widely available, relatively sustainable regarding production methods, recyclable, and has low toxicity [2,20].

Working with ILs as functionalization media allows precise control over DS by adjusting the reaction time, temperature, and molar ratio of reagents [12]. Control over DS also provides control over the viscoelastic properties of the produced thermoplastic materials. The degree of polymerization (DP) of cellulose, DS of the derivative, and the type of acylating agent determines the melt viscosity of the thermoplastic material and also affects elasticity, glass transition temperature [34], and thermal stability.

CEs with aliphatic moieties C8–C18 appear thermoplastic in the DS range from 0.56 to 3. According to the literature, there is no need to produce fully substituted CEs. A DS $\geq$ 1.5 is high enough since CEs with a DS between 1.5 and 3 show similar mechanical and thermoplastic properties [35,36].

The plasticizing effect of aliphatic chains was found to be dependent more on the DS than on the fatty chain length, but no clear influence of the DS on thermal transitions was observed [36]. No glass transition T_g in cellulose palmitate is reported in the paper [37]. Jinlei Li in his work discovered a correlation between T_g increase and the formation of materials with solid-like behavior in a molten state. At the same time, in contradiction to previous research, it is stated that T_g is influenced more by acyl side chain length than the DS [38]. Additionally, CEs with short alkyl chains were found to exhibit a narrow thermoplastic window between melt flow and thermal degradation [39]. Recent developments show that long-chain FACEs are promising but underdeveloped thermoplastic materials with complex relationships between properties and structure.

In this work, we investigate the optimization of the homogenous transesterification of cellulose with long-chain fatty vinyl esters (VEs) in distillable IL, [mTBNH][OAC], without any additional catalysts and under mild conditions, to produce thermoplastic FACEs by a sustainable and green procedure. This will complete the picture of [mTBNH][OAC] application for cellulose modification, as far as it has mostly been studied for cellulose regeneration [29], and for preparation of cellulose acetate [40].

Another goal of this study is to disclose the melt flow behavior and the rheology of long-chain FACEs, which are not widely presented in the literature. Melt properties

and behavior are important for understanding the proper processing conditions for blow molding, injection molding, sheet forming, extrusion, fiber spinning, etc. Herein, we further develop the main concepts of our previous rheological studies discussed [41,42].

2. Experimental Section

2.1. Materials

Microcrystalline cellulose (MCC) by Carl Roth GMBH (Karlsruhe, Germany). Vinyl laurate, vinyl myristate, vinyl palmitate, and vinyl stearate with purity > 98% were purchased from Tokyo Chemical Industry Co. (Tokyo, Japan). Ionic liquid 5-Methyl-1,5,7-triaza-bicyclo-[4.3.0]non-6-enium acetate, [mTBNH][OAC], was not commercially available and was synthesized by Liuotin Group Oy (Porvoo, Finland). The melting point of IL is 15 °C; the flash point is more than 220 °C. DMSO with a purity of 99.9% was purchased from Fisher Chemical (Pittsburgh, PA, USA). Low-density polyethylene (LDPE), Petrothene NA960000 supplied by LyondellBasell (Rotterdam, Netherlands). Diethyl phthalate plasticized (24% DEP) cellulose acetate (Mazzucchelli PCA) supplied via S. e P. Mazzucchelli (Castiglione Olona, Italy). Pyridine-d_5 (purity = 99.5 atom % D. contains 0.03 v/v% TMS) and Chloroform-d (purity = 99.8 atom % D. contains 1 v/v% TMS) for NMR were purchased from Acros Organics (Geel, Belgium).

2.2. Cellulose Dissolution and Esterification Procedure

MCC was dried under a vacuum at 105 °C for 24 h before use. Cellulose concentration in solutions was 2–5%. 2–5 g of MCC (12.3–30.7 mmol for the AGU) was dissolved in 100 g [mTBNH][OAC] (505 mmol) and stirred at 60 °C for 24 h until the cellulose was completely dissolved to yield 2–5 wt%-solution. To decrease the viscosity, a co-solvent DMSO was added. In the case of the use of co-solvent, IL and DMSO have been first mixed and then cellulose has been added to this binary solvent. Different ratios of DMSO/IL have been prepared and studied. The designed amount of the respective vinyl ester (from 1 up to 6 equivalents to cellulose anhydroglucose unit (eq./AGU)) without any external catalyst was added to the cellulose solution in a chemical reactor equipped with a mechanical stirrer and nitrogen flow, and then the reaction was performed at designed conditions under nitrogen atmosphere and intensive stirring. When the reaction was completed, the obtained cellulose esters were precipitated into 500 mL of water (for laurate and myristate) or ethanol (for palmitate and stearate). To remove solvent and vinyl ester residuals, the product was washed several times in 100–200 mL of ethanol, then acetone, and with hexane. Finally, the product was dried under a vacuum at 55 °C overnight.

For the prepared products, transesterification of CEs was repeated 2–3 times to verify the reproducibility of the reaction. It was found that DS deviates within 5–10% for the batches.

2.3. Characterization

The FT-IR spectra of MCC and cellulose derivatives were recorded on Interspec 200-X using the Quest ATR accessory purchased from Specac Ltd (Orpington, UK) in the range of 500–4000 cm^{-1} with a resolution of 4 cm^{-1}. All samples were dried at 80 °C in a vacuum oven overnight before the FTIR measurement to remove the moisture.

The ^{1}H NMR, ^{13}C NMR, COSY, and HSQC NMR spectra of cellulose derivatives were acquired on an Agilent Technologies DD2 500 MHz spectrometer equipped with 5 mm broadband inverse (^{1}H, HH-COSY, HC-HSQC spectra) or broadband observe (^{13}C spectra) probes. A 15 min temperature equilibration delay was allowed between sample insertion and NMR acquisition at 40 °C (cellulose palmitate and stearate in CDCl$_3$) or 80 °C (cellulose laurate in DMSO-d_6 and cellulose myristate and laurate in Py-d_5) sample temperature. Typically, for ^{1}H spectra, 32 scans with 25 s relaxation delay were acquired and for [13]C 20,000–45,000 scans with 2.5 s recycle delay were acquired to achieve the desired signal-to-noise ratio. An HMBC spectrum for sample CP-3 was acquired in 16 h on an 800 MHz Bruker Avance III spectrometer equipped with a He-cooled cryoprobe.

The NMR samples were prepared in a small glass bottle where 20–25 mg of the sample was dissolved in 0.8 mL of deuterated NMR solvent for 90 min at 40–65 °C until a clear solution was obtained. The glass bottle containing the mixture was dried and carefully sealed with parafilm. The samples were then subjected to ultrasonic treatment to obtain a transparent solution.

The DS of cellulose laurate, -myristate, -palmitate, and -stearate was calculated from the ^{1}H NMR spectrum by taking an integral of the area of terminal methyl groups ($I_{(CH3)}$) and AGU signals (I_{AGU}) based on the reported method [43]:

$$DS = 10 \cdot \frac{I_{(CH_3)}}{\left(3 \cdot I_{AGU} + I_{(CH_3)}\right)} \tag{1}$$

Additionally, the DS of obtained samples was also verified by the standard saponification ASTM D871-96 method. The DS was calculated according to [34]:

$$DS = \frac{162\,E}{100M - E \cdot (M-1)} \tag{2}$$

where E is the ester content obtained by the saponification method, and M is the molecular weight of the grafted acyl residue.

To study the rheological properties of samples, an Anton Paar Physica MCR501 rheometer, with cone-plate measuring geometry was used. To prevent oxidation, the experiments were carried out in a nitrogen atmosphere and did not last longer than 10 min at a temperature of 190 °C. Flow curves were obtained at a shear rate $\dot{\gamma}$ range from 0.01 to 100 s^{-1}. Complex viscosity was determined in the range of angular frequencies ω = 0.01 to 500 rad/s. A constant strain of γ = 5% was determined from the linear viscoelastic region (LVR). An amplitude sweep test to determine the LVR was conducted at a frequency of 1 Hz. Samples for rheology were prepared from 100 μm thick films cast from solution in chloroform or pyridine at room temperature overnight by cutting 2.5 mm Ø discs. Non-soluble materials were compressed by a hydraulic press into 100 μm thick and 2.5 mm Ø discs in a stainless-steel mold at a pressure of 70 bar at room temperature.

A differential scanning calorimeter (Perkin Elmer DSC-7) was used for the thermal analysis of materials at scanning rates of 30 °C/min. Nitrogen was used to purge the furnace. To avoid differences in melting and crystallization temperatures caused by variations in sample weight, a sample mass of 5.00 ± 0.02 mg was used in all DSC experiments. Film samples were packed into aluminum foil to maximize thermal contact between the sample and the calorimetric furnace. DSC samples were prepared from solvent-cast 100 μm thick films. Non-soluble materials were compressed by the hydraulic press into 100 μm thick flakes in a stainless-steel mold at a pressure of 70 bars at room temperature.

The size exclusion chromatography (SEC) curves of cellulose esters were determined using gel permeation chromatography (GPC) on the Shimadzu Prominence system equipped with a Shodex KF-804 column and a refractive index detector (RID-20A). Calibration of the GPC system was performed using 3 separate polystyrene standards (74,800 Da, 230,900 Da, and 473,600 Da). CE samples (10 mg) were dissolved in pyridine (1–2 mL) and the GPC analysis was conducted at 60 °C using pyridine as the mobile phase with a flow rate of 0.5 mL/min. Molecular weights (number-average M_n and weight-average M_w, polydispersity index PDI = M_w/M_n) of cellulose esters have been calculated. Several samples were tested 2–3 times and the obtained standard deviation of MM measurements was 3–8%.

Molar mass (MM) of pure MCC was determined at 25 °C from the intrinsic viscosity [η] of cellulose solution in cupriethylenediamine hydroxide solution, Cuene, according to a standard procedure [44]. The MM was then calculated by the Mark–Houwink equation with parameters K = 1.01 × 10^{-4} dL/g and a = 0.9 [45]. The obtained MM was 163,000 g/mol.

3. Results and Discussion

3.1. Preparation of Cellulose Esters

Scheme 1 shows the pathway for cellulose transesterification with vinyl esters. Cellulose esters were synthesized in one step and low-vapor-point ethanol (in situ tautomerization to acetaldehyde) as the byproduct can be easily evaporated from the reaction system at elevated temperatures.
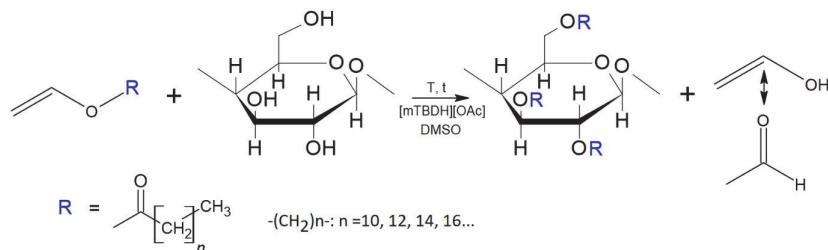
Scheme 1. Transesterification of cellulose with vinyl esters.

It is well known that ILs are efficient solvents for the dissolution and modification of cellulose; however, there are also some drawbacks, such as high cost and high viscosity. For example, in the current work, it was possible to dissolve cellulose in pure IL only at 2 wt% concentration—higher concentrated solutions were not possible to stir effectively due to high viscosity. To scale up the entire production process, the cellulose content should be raised. This drawback can be overcome by using the mixtures of IL with cheaper and less viscous co-solvents. A dipolar aprotic solvent such as DMSO is an effective co-solvent for cellulose dissolution. The addition of DMSO to IL can enhance its solvating ability because DMSO can speed up mass transport due to lower solvent viscosity. Indeed, if the content of DMSO is increased, the viscosity of cellulose solution in binary IL:DMSO solvent drops significantly (see Table 1 and Supporting Information Figure S1) at all studied temperatures (including temperatures at which the transesterification reactions were conducted) while the concentration of cellulose in all tested solutions was fixed at 2 wt%. As is seen in Table 1, the viscosity of cellulose solution in 1:3 IL:DMSO binary solvent is approximately seven times lower than in pure IL. Surprisingly, even 25% of IL in binary solvent (i.e., 1:3 IL:DMSO ratio) is sufficient to dissolve cellulose, and optically transparent solutions of cellulose are observed. This indirectly confirms the high efficiency of novel IL to dissolve cellulose. Taking into account such low viscosity of cellulose in a binary solvent, it is possible to increase the cellulose solution concentration from 2 wt% up to 5 wt% and even more, keeping the same mixing level. Hence, the consumption of IL can be decreased while the level of CE production can be increased 2–3 times.

Table 1. DS of cellulose laurate prepared by transesterification in different IL:DMSO mixtures.

Sample	IL:DMSO	DS	The Viscosity of Cellulose Solution at 60 °C, Pas
CL-1	no DMSO	0.70	2.56
CL-2	3:1	0.60	1.10
CL-3	1:1	0.60	0.75
CL-4	1:2	0.38	0.47
CL-5	1:3	0.35	0.40

Several reactions have been conducted at different IL:DMSO ratios, while the reaction conditions were kept constant, (T = 60 °C, t = 2 h, 3 eq./AGU). Vinyl laurate (VL) was chosen as an acylation agent. The results of this study are presented in Table 1. DMSO is not a solvent for cellulose; an increase in DMSO content could limit the ability of cellulose

toward homogeneous transesterification. This could explain the DS and viscosity drop for CL-4 and CL-5 when the IL:DMSO ratio exceeds 1:1.

Structure analysis utilizing FTIR after acylation revealed the introduction of the alkyl chains into cellulose for all studied samples. FTIR spectra of native cellulose and its laurate derivatives were obtained in solvents with different IL:DMSO ratios (see Supporting Information Figure S2). The strongest evidence of successful acylation is the appearance of an absorption band at 1746 cm^{-1} that corresponds to the stretching of the ester carbonyl (>C=O) group. Compared to unmodified MCC, there were several new peaks in the FTIR spectra of modified samples. New peaks at 2950 cm^{-1} and 2847 cm^{-1} correspond, respectively, to asymmetric and symmetric stretching of the methylene group present in cellulose laurate (CL). The presence of these peaks indicates that the methylene and carbonyl groups were attached to cellulose, and hence, successful transesterification of cellulose in the novel [mTBNH][OAC] IL mixed with DMSO, without external catalyst, has been conducted.

All produced CLs are soluble in several organic solvents, mostly DMSO, THF, and pyridine, which enables direct measurements of NMR spectra in the form of solution and, thus, provides a tool for the calculation of DS. The chemical structure of the cellulose laurate (CL) was confirmed by ^{1}H NMR and ^{13}C NMR. In the ^{1}H NMR spectrum of the CLs (See Supporting Information, Figure S3), the proton signals from approximately 6.00 to 3.50 ppm are assigned to H-1, H-2, H-3, H-4, H-5, H-6, and H-6′ of AGU in cellulose. The signals at 2.32–1.93, 1.88–1.45, and 1.27 ppm are associated with the methylene protons at H-8, H-9, and H-10–17, respectively. The signals at 0.98–0.79 ppm are attributed to the methyl protons at H-18.

In the ^{13}C NMR spectrum of cellulose laurate, presented in Figure 1, the signals at 34.78, 32.61, 25.80, 23.34, and 14.60 ppm are assigned to carbons of C-8, C-16, C-9, C-17 and C-18 of the aliphatic side chain, respectively. The carbons at C(10-15) give signals starting from 30.44 to 30.04 ppm. The AGU carbons C-1, C-1′, C-4, C-2,3,5, C-6, and C-6′ give signals at 104.98, 102.33, 81.50, 76.91–74.35, 64.32 and 62.68 ppm, respectively. The signals from 173.89 to 170.98 ppm correspond to the carbonyl carbon at C-7, which provides the direct confirmation of the successful attachment of the long-chain fatty acid chain to the cellulose backbone. Three peaks for the carbonyl group indicate that all OH groups at positions 2, 3, and 6 were acylated [19]. According to the ref. [46], by peak integration of carbonyl carbons (C7-O2, C7-O3, and C7-O6), it can be suggested that the partial DSs of C7-O6, C7-O2, and C7-O3 are 0.41, 0.11, and 0.08, and, consequently, the substitution order of the OH group is C7-O6 > C7-O2 > C7-O3.

The data of DS obtained from NMR spectra are presented in Table 1. Although the cellulose solution viscosity decreases with increasing DMSO content in a binary solvent, the DSs of samples are not much changed until the ratio 1:1 IL:DMSO. The further increase in DMSO content decreases the DS of CLs 1.5 times. Therefore, it can be concluded that DMSO content exceeding the amount of IL in a mixture, causes obstacles in the transesterification process of cellulose with vinyl esters. Therefore, for further experiments, the optimum 1:1 IL:DMSO ratio was chosen for cellulose dissolution and modification. This helps to decrease the cost of production, due to the lower IL content used and the higher yield of the cellulose derivatives.

As is seen in Table 1, CLs synthesized in the above-mentioned reaction conditions have rather a low DS. However, it should be noted that in our study DS = 0.6 was obtained during 2 h of reaction at a moderate temperature of 60 °C, whereas similar DS values have been reported by Wu et al. [47] but the reaction time was 24 h. No external catalyst or activation was required to achieve this reactivity in [mTBNH][OAC]. Partial decomposition of such ILs during the acylation process liberates the superbase [48], which can act as a basic catalyst to promote the transesterification reaction analogically to 1,8-diazabicyclo[5.4.0]undec-7-ene (DBU) [47], 1,5,7-triazabicyclododecene (TBD) and 1,5-diazabicyclo(4.3.0)non-5-ene DBN [49]. TBD and DBU are also known as superbases, which give protonic ILs in

combination with an acid component. The organocatalytic effect of DBU and TBD during transesterification was demonstrated by several authors [47,49,50].
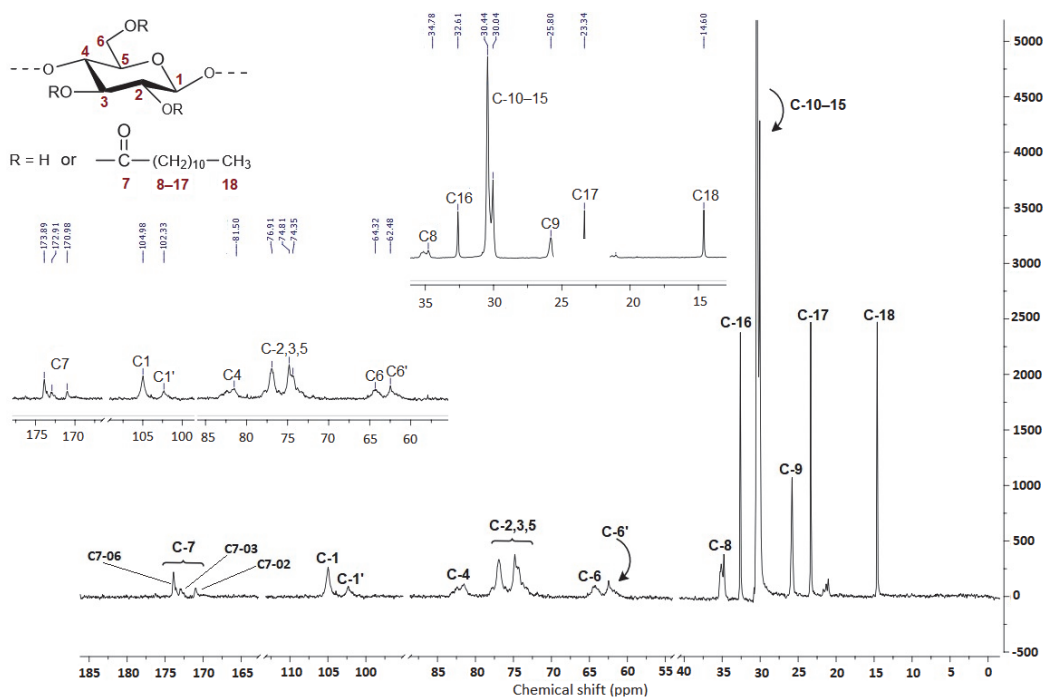
Figure 1. ^{13}C NMR spectrum of Cellulose Laurate (CL-3) in Pyridine-d$_5$ (125 MHz, 80 °C. Empty and solvent regions are left out for clarity. Full spectrum is available in Supporting Information).

Several attempts to improve the degree of substitution have been made. The results are presented in Table 2.

Table 2. Tunable synthesis of cellulose laurates by transesterification reaction of cellulose with vinyl laurate (VL) in 1:1 IL:DMSO solvent system.

Sample	Reaction Conditions			DS	M$_n$, kDa	PDI
	Time, h	Temperature, °C	AGU:VL			
CL-6	2	20	1:3	0	insoluble	
CL-3	2	60	1:3	0.6	237.7	1.64
CL-7	2	80	1:3	1.2	221.0	2.01
CL-8	4	60	1:3	1.6	358.0	1.28
CL-9	5	60	1:3	2.0	304.0	1.50
CL-10	3	70	1:3	1.55	532.7	1.14
CL-11	3	80	1:3	1.58	317.5	1.40

Additionally, SEC measurements of the different CLs were performed, as the cellulose esters were all soluble in pyridine, except CL-6. SEC curves of studied CLs are presented in Supporting Information Figure S7.

To investigate the effect of the reaction time on the transesterification, the reactions were carried out at 2 (CL-3), 4 (CL-8), and 5 (CL-9) hours at the same temperature of 60 °C

and AGU:VL = 1:3. Analysis of the reaction products reveals that the DS can be increased by employing longer times of reaction. For example, the DS obtained at 4 h of reaction (CL-8) is approximately 2.6 times higher than the DS obtained at 2 h of reaction (CL-3, see Table 2). At 5 h of reaction, the DS is even higher, achieving values of 2.0 (CL-9). However, starting at 4 h the color of the reaction medium started changing from dark yellow (at 4 h) and even brown (at 5 h). The color change can be a sign of either IL or cellulose degradation. To clarify, IL has been held for 3 h at different temperatures: room temperature, 60 °C, 70 °C, 80 °C, 100 °C, and even 110 °C. No signs of IL degradation have been detected. FTIR spectra of all ILs treated at different temperatures were identical; color has not been changed. It can be concluded that IL is stable at the studied temperatures.

However, SEC data (see Table 2) of cellulose laurates show that samples undergo some degradation with prolonged reaction times. Taking into account the viscosity-average MM of cellulose (163 kDa), MM of vinyl laurate (226 Da), and definite degree of substitution, it is possible to estimate the molar mass of cellulose laurate at certain DSs (note that viscosity-average MM is always a little bit higher than M_n). The estimated molar mass of CL-3 is close to the experimentally obtained one. However, the estimated MM of CL-8 should be around 500 kDa, while the M_n of CL-8 is only 358 kDa. Experimentally obtained M_n of CL-9 decreases down to 304 kDa, which is twice lower than the estimated MM (around 600 kDa) and 1.2 times lower than CL-8.

The effect of reaction temperature on DS was investigated by using three temperatures for the transesterification, while the time of reaction (2 h) and molar ratio AGU:VL (1:3) were kept the same. In the first reaction, 20 °C was used for the transesterification, yielding degrees of substitution equal to zero—no transesterification at room temperature was possible. Further reactions were carried out at 60 °C, revealing that an elevation of the temperature leads to successful transesterification of cellulose with a DS = 0.6. The increase in the DS can be explained by the higher flexibility of the cellulose chain, and easier removal of acetaldehyde as a by-product of the reaction. The last reaction was conducted at 80 °C, giving cellulose laurate with a DS = 1.2. A similar effect of temperature was detected for cellulose palmitates. However, at 80 °C and higher temperatures, the reactive solutions turned dark brown, indicating the hydrolysis process of IL and/or cellulose esters. SEC data (see Table 2) showed that compared to the unmodified MCC, the molecular weights M_n of the acylated samples increased with increasing DS. However, samples undergo degradation, both with prolonged reaction times and at high reaction temperatures ≥80 °C. The MM of CL-7 obtained at 80 °C is smaller than that of CL-3 synthesized at 60 °C. The same is true for samples prepared at 3 h of reaction and different temperatures; MM of CL-11 is approximately 1.7 times smaller than that of CL-10 (see Table 2). Right away, we have no suitable explanation for this chain degradation. Somewhat analogically to [DBNH][OAc] ionic liquid [49], it can be suggested that degradation of the cellulose backbone starts with the generation of acetic acid, which initially was entrapped by the excess of mTBN.

Therefore, for the transesterification process in [mTBNH][OAC] temperatures of reaction lower than 80 °C should be employed. The optimum conditions were chosen as 70 °C and 3 h, which give the highest DS without degradation. However, it should be stressed here that in our case the degradation of cellulose esters is not a big issue. Taking into account very high molar masses of final products, some decrease in MM of cellulose esters can even be an advantage for processing and thermoplastic properties of products.

The chosen optimum reaction conditions were applied to the synthesis of longer (than laurate) FACEs, namely cellulose myristate (CM), cellulose palmitate (CP), and cellulose stearate (CS). The parameters of synthesis are listed in Table 3. Structure analysis of all samples using NMR and FTIR after acylation discovered the attachment of the alkyl chains onto cellulose. ^{1}H/^{13}C NMR spectra of CM, CP, and CS samples are presented in Supporting Information.

Table 3. Tunable synthesis of different cellulose esters produced by transesterification reaction of cellulose with vinyl esters (VE) in 1:1 IL:DMSO solvent system.

Sample	Reaction Conditions			DS	M_n, kDa	PDI
	Time, h	Temperature, °C	AGU:VE			
CL-10	3	70	1:3	1.55	532.7	1.14
CM	3	70	1:3	1.31	393.6	1.74
CP-1	3	70	1:3	1.08	370.2	1.50
CP-2	3	70	1:5	1.30	404.3	1.55
CP-3	3	80	1:3	1.80	222.1	1.77
CS-1	3	70	1:3	0.67	insoluble	
CS-2	3	70	1:6	1.40	471.2	1.41

To confirm further the assignment of the signals of cellulose esters, the HSQC spectrum was collected. The example of ^{1}H-^{13}C HSQC for cellulose palmitate is presented in Figure 2, where the cellulose region (Figure 2a) and aliphatic side chain region (Figure 2b) are shown. As can be seen, in the aliphatic side chain region, the correlation of C-21/H-21, C-20/H-20, C-22/H-22, and C-10–19/H-10–19 were located at δH/δC at 1.29/22.54, 1.27/31.76, 0.89/13.90 and 1.26/29.46, respectively. In the cellulose region, the strong correlations were distinguished at δH/δC 5.14/72.17, 4.82/71.93, 4.42/101.59, 4.19/62.34, 3.52/73.06, and 3.36/82.31 for C-3/H-3, C-2/H-2, C-1/H-1, C-6/H-6, C-5/H-5, and C-4/H-4, respectively. The two decentralized signals of C-8/H-8 and C-9/H-9 are represented by δH/δC at 2.32/33.80 and 1.59/24.78, respectively.

(a)   (b)
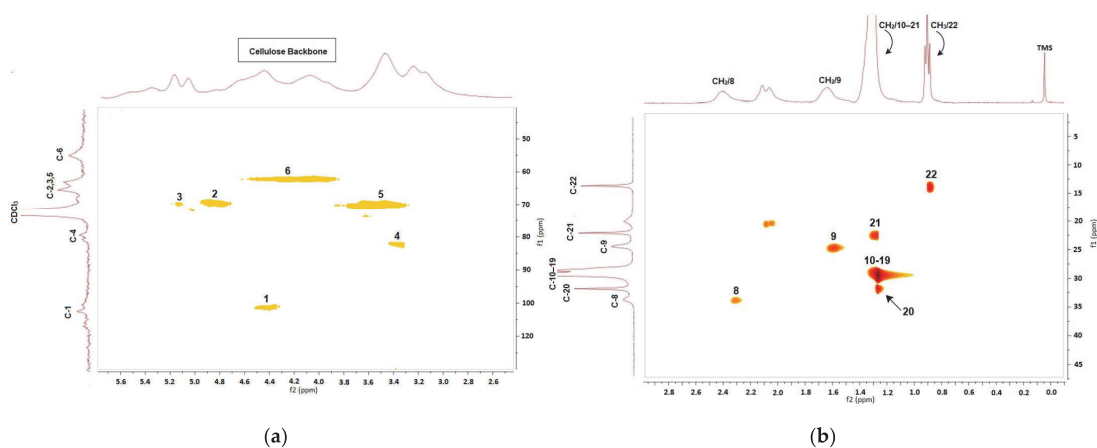
Figure 2. Cellulose (**a**) and aliphatic side chain (**b**) region of HSQC spectrum of cellulose palmitate, CP-3, in Chloroform-d (500 MHz, 25 °C).

Figure 2 reveals that under optimized reaction conditions, complete acylation of C6-O is achieved as only a single resonance of the corresponding group in ^{13}C. Additionally, the intensity of the characteristic cross-peak of C2-OAcyl (4.8–4.9/72 ppm) is greater than that of C3-OAcyl (5.1/72 ppm), thus indicating a preferential acylation.

An estimation of acylation efficiency at different positions in the CP was performed by comparing respective signal integrals from HSQC spectra. Integration of the corresponding signals in the HSQC spectra showed that a total degree of substitution (DS = 1.80, see Table 3) has, within a reasonable error margin, ratios of 1.00: 0.47: 0.33 for C7-O6: C7-O2: C7-O3 positions, respectively. Consequently, similarly to CL, the substitution order of the OH group in CP is C7-O6 > C7-O2 > C7-O3.

The ^{1}H-^{1}H COSY spectra, presented in Figure 3, revealed the correlation of proton-proton signals. Figure 3b indicates the coupling between hydrogens of the aliphatic side chain region. Cross peaks at frequencies 1.26/0.87 and 0.87/1.29 show coupling between $CH_3/22$ and $CH_2/10-19$. Cross peaks at frequencies 1.57/1.32 and 1.27/1.60 show coupling between the peaks $CH_2/10-19$ and $CH_2/9$. Similarly, cross peaks at frequencies 2.31/1.60 and 1.62/2.31 show the coupling between $CH_2/9$ and $CH_2/8$.
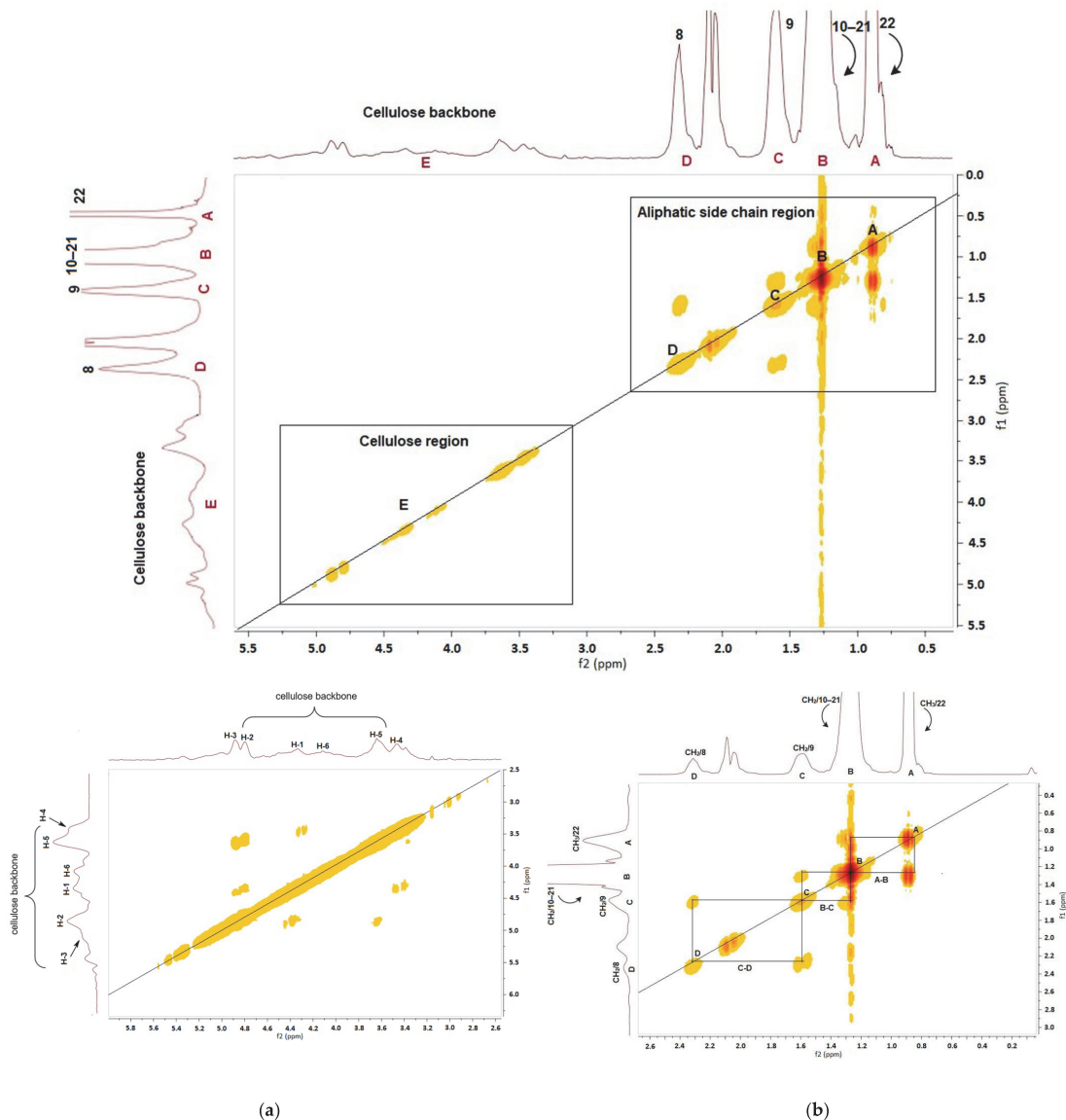
Figure 3. Cellulose (**a**) and aliphatic side chain (**b**) region of the COSY spectrum of Cellulose palmitate, CP-3, in Chloroform-d (500 MHz, 25 °C).

In the AGU region (Figure 3a), the spectrum is more crowded, as many correlations for various combinations of non/acylated components are present. Thus, two correlations of the glycosidic H-1 and acylated H-2 are visible at 4.4/4.8 and 4.4/4.9 ppm, depending

on the substituent at O-3. The correlations of the H-2 with acylated and unsubstituted H-3 are observed at 4.9/5.1 and 4.8/3.6 ppm, respectively. Correlations of H-3 and H-4 are at 5.1/3.8 and 3.6/3.7 ppm, those of H-4 and H-5 are observed at ~3.7/3.4, and those of H-5 and acylated H6 and H6′ are at 3.4/4.3 and 3.4/4.0 ppm, respectively.

Heteronuclear multibond correlation spectroscopy (HMBC) was also conducted to analyze the hydroxy (-OH) substitution at the cellulose backbone. The HMBC spectrum (see Supporting information, Figure S8) showed the correlations between the acyl carbon (C-7) signal at 170.95 ppm and H-3 proton signal at 4.84 ppm and H-2 proton signal at 4.77 ppm, additionally proving the esterification of positions C7-O3 and C7-O2, respectively. Unfortunately, the correlation between C-7 and H-6 protons of AGU was not detected. However, according to the literature, this correlation peak is much weaker and usually not detected by HMBC for cellulose esters [51].

As can be seen in Table 3, transesterification of cellulose in [mTBNH][OAC] with longer vinyl esters was successfully conducted and a DS up to 1.8 has been achieved. A similar DS was obtained by T. Kakko et al. [49], but for cellulose acetate and propionate in another distillable IL, namely [DBNH][OAc]. For long-chain CEs, it was possible to obtain similar values of DS but in DMAc/LiCl [52], which is an undesirable solvent for a future greener life.

By comparing the DS for the different cellulose esters, it can be said that under the same reaction conditions, the DS and, as a consequence, M_n of the cellulose esters decrease with increasing fatty acid chain length. Such a result is expected due to the higher steric hindrance of long ester chains and it has been demonstrated in the literature [12]. Cellulose laurate, myristate, and palmitate show DS > 1, which makes them soluble in many organic solvents. However, cellulose stearate CS-1 shows approximately twice the lower values of DS and as a result, CS-1 is insoluble in any tested solvents.

DS is the most important property determining the thermoplastic behavior of CEs, and, as it was explained before, the DS value should be close to or above 1.5 to expect similar processing behavior as commodity polymers have. For cellulose laurate and myristate, it was possible to obtain a DS ≥ 1.3; however, for cellulose palmitate and stearate the reaction conditions should be modified to achieve a higher DS. DS can further be increased by increasing the temperature of the reaction. Indeed, for cellulose palmitate CP-3 prepared at 80 °C, the DS has been improved up to 1.8. However, instead of an expected increase in M_n, CP-3 demonstrates a drop in molecular weight, which can be attributed to the cleavage of the cellulose backbone.

Degradation of cellulose backbone during transesterification reaction at temperatures ≥80 °C can be revealed also by measuring intrinsic viscosity [η]. As it is well known, the intrinsic viscosity of the polymer directly depends on its molar mass; the higher the [η] the higher the MM. The intrinsic viscosity of CP-1 in pyridine at 20 °C was 2.5 dL/g, CP-2 has an intrinsic viscosity of 2.8 dL/g, whereas CP-3 has [η] = 1.1 dL/g, which is more than two times lower and confirms the cellulose degradation.

It is well known by Le Chatelier's Principle that an excess of one reactant will drive the reaction to the right, increasing the production of ester, and finally increasing the yield of ester. Therefore, in subsequent steps for preparation of CP and CS of higher DS without degradation, the reactions were carried out using excess vinyl esters, namely molar ratios AGU:VE = 1:5 and 1:6 were employed. As can be seen in Table 3, the degree of substitution of CS (CS-2) was improved more than two times, and DS = 1.4 was achieved when 6 eq/AGU were taken. For CP the DS = 1.30 was already obtained at 5 eq/AGU. Further, an increase in the ratio of the vinyl esters probably will allow for achieving a higher DS, but an unreacted vinyl ester and its by-product stay in a supernatant phase and make purification of end-product and IL recycling difficult.

Generally, the cellulose esters with DS varying from 0.6 (and probably lower) up to 2.0, depending on the reaction parameters and the vinyl ester used, can be produced. It should be noted that the reaction conditions used in the current work are much milder than those which are used usually in transesterification reactions in other ILs, where higher

temperature, longer reaction time, and the presence of a catalyst are required to achieve an appropriate DS [4,15]. The developed method demonstrates the first successful homogeneous, catalyst-free transesterification reaction on cellulose in [mTBNH][OAC]. Moreover, [mTBNH][OAC]+DMSO mixtures can be recycled via precipitation of by-products with volatile solvents and consequent removal of solvents and used again for the reaction.

Ionic Liquid Recycling

The usage of ionic liquid for cellulose dissolution is beneficial regarding green chemistry concepts, but also, ILs could be regenerated and recycled to make it applicable under circular economy requirements. In the current study, the first trial to recover [mTBNH][OAC]+DMSO for further transesterification has been conducted. This is the first experimental attempt to recycle [mTBNH][OAC] after a transesterification reaction.

For the regeneration of [mTBNH][OAC]+DMSO binary solvent from the waste solution, the following procedure was established:

1. Evaporation of water and ethanol through thin film or rotary distillation–waste pre-concentrate.
2. Waste pre-concentrate mixed with acetone in a 1:8 ratio–hydrophilic by-products precipitate.
3. Filtration of mixture and evaporation of acetone–waste concentrate obtained.
4. Waste concentrate mixed with distilled water in 1:10–hydrophobic by-products precipitate.
5. Filtration of mixture and evaporation of acetone–regenerated IL:DMSO binary solvent (recyclate) obtained.

FTIR and solubility tests were used to analyze precipitated by-product: hydrophobic precipitant is insoluble in water and common polar solvents (alcohols) and has a strong methylene group absorption peak in the FTIR spectrum; hydrophilic precipitant is insoluble in acetone and common non-polar solvents (toluene, hexane), showing strong absorption in the hydroxyl group band.

The regenerated binary solvent has been used for the dissolution of cellulose with subsequent transesterification with vinyl laurate. Cellulose was successfully dissolved and its viscosity was identical to that of cellulose in fresh [mTBNH][OAC]:DMSO mix. Next, transesterification has been conducted under reaction conditions similar to CL-3. It was confirmed by NMR that the obtained product is CL with DS = 0.58, which is close to the value of DS = 0.6 obtained for CL-3. This trial confirms the efficiency of regenerated [mTBNH][OAC] usage for transesterification.

3.2. Physical Properties of Cellulose Esters

3.2.1. DSC

All studied cellulose esters show similar thermal behavior in general. DSC curves for CL-10, CM, CP-3, and CS-2 in the range 1 < DS < 2 are shown in Figure 4.

As could be seen in the plot, only CS-2 shows a strong peak at 53 °C, which corresponds to the melting of fatty acid chain crystals. All samples have glass transitions in the range 170–177 °C, which is comparable to the values reported in the literature [50].

The best DSC curves were obtained for the cellulose palmitate series (see Figure 5), where DS varied from 1 to 1.8. The specimen with DS ≈ 1 represents only fatty acid melting at 96 °C; the specimen with DS = 1.30 shows transient behavior; melting of ester chains at 108 °C coexists with a glass transition of cellulose ester chain above 160 °C. The sample with high DS = 1.80 shows a well-distinguishable glass transition temperature at 170 °C.
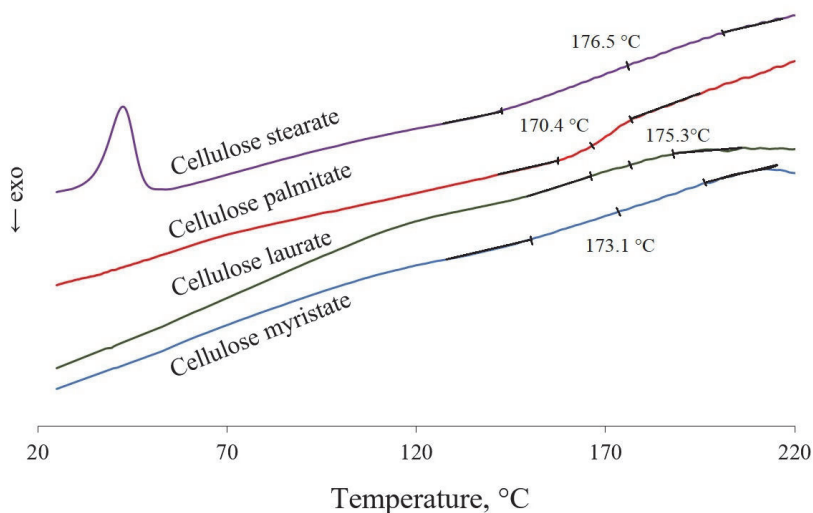
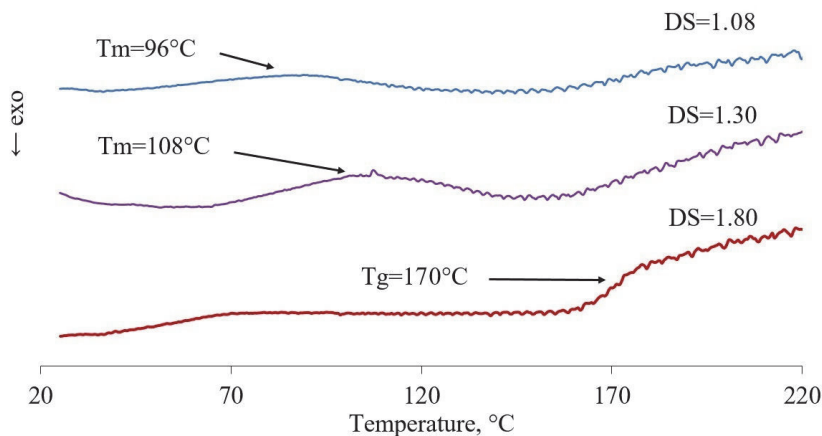**Figure 4.** DSC curves for cellulose derivatives with DS in the range of 1.3 to 1.8.

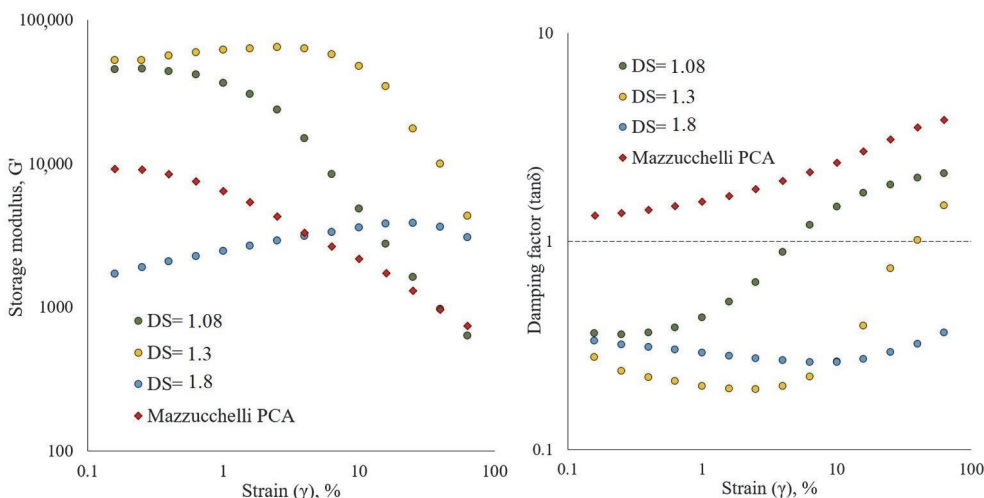**Figure 5.** DSC curves for cellulose palmitate with different DS.

This kind of behavior evidences a significant change in the chain structure of cellulose esters with an increase of DS; at low DS, probably transesterification is not uniform, and the material contains a highly substituted phase and regenerated cellulose phase. The ester-rich crystalline phase has a melting point of around 100 °C. The melting peak is very broad, which could be evidence of strong variation in these crystalline phase structures.

An increase in DS leads to uniform ester chain distribution along the cellulose backbone. An amorphous phase on esterified cellulose is formed and can be observed when glass transitions near 180 °C at the DSC curve. In addition, films made of low substituted cellulose esters shrink significantly upon heating above 150 °C, which makes DSC curves noisy. Strong variation in crystalline and amorphous phase structure hinders the observation of phase transitions. Unfortunately, it was not possible to trace phase transitions regarding DS for all types of materials, only for cellulose palmitate.

3.2.2. Rheology

To understand the thermoplastic properties of materials, the melt flow behavior was examined. The behavior of melt flow at low strains has a direct correlation to the macromolecular structure, molecular mass, and mass distribution of the polymer. The strain dependence of storage and loss moduli is used to evaluate thermoplastic material processability and future performance.

The dependences of storage modulus $G´$ and damping factor $\tan\delta$ on strain are depicted in Figure 6. As can be seen in the plots, the damping factor for highly substituted material is below one in the whole measured range, while materials with DS ≤ 1.3 pass a crossover point from the rubbery region (where elastic deformations of the material dominate) at low strains to the transition region (where plastic deformations become dominant) at higher strains. The storage modulus for low-substituted CP materials drops significantly at low strains, and for the high-substituted one $G´$ drops above 10%. The cellulose backbone plays the main role in the viscoelastic properties of the studied materials. One could conclude that in low DS materials, flexible fatty acid branches form a separate phase with a low melting point, and this phase works as an internal plasticizer for cellulose esters. For comparison, commercially available injection-molding grade plasticized cellulose acetate by Mazzucchelli was studied. As can be seen, the shape of curves for low DS materials is similar to those for Mazzucchelli PCA, which strengthens the hypothesis of internal plasticizing by fatty acid branches.

Figure 6. Storage modulus (**left**) and damping factor (**right**) dependence on strain amplitude for cellulose palmitate with different degrees of substitution.

The material with high DS appears as a homogeneous amorphous phase where fatty acid chains are evenly distributed over the cellulose backbone. The plasticizing effect of branches became less pronounced, and the material underwent only elastic deformations in all studied strain ranges.

To summarize the strain-dependent flow, the elastic deformations of the cellulose backbone, a fluctuation of physical crosslinking points, or junctions, are dominating at low strains, while the entanglement density remains constant. Fatty acid chains bonded to cellulose macromolecules are involved in the local orientation motion. A higher strain induces the inelastic motion of chains which increases the orientation of macromolecules and leads to energy dissipation due to friction. Friction significantly increases the damping factor for low-substituted materials. High-substituted materials are prone to decreasing the

entanglement density only (junction points move away from each other) in the analogy with extended interconnected springs.

The viscoelastic properties of thermoplastics strongly depend on deformation (dynamic oscillations) frequency. In the frequency range between 0.1 and 100 s^{-1}, studied samples of CP curves represent a rubbery plateau (see Figure 7 left), where storage prevails over loss modulus. The crossover point from the rubbery plateau to the transition region for material with the lowest DS is marked with the red arrow on the plot. At the same time conventional thermoplastic materials, like LDPE and plasticized cellulose acetate (see Figure 7 right), in this frequency range have crossover from transition region to glassy region (crossover point labeled with red arrows). As could be seen, flexible chains of LDPE and externally plasticized rigid chains of cellulose acetate at high frequencies show perfect elastic behavior and turn viscoelastic upon frequency decrease (transition zone). Cellulose palmitates in the whole frequency range show rubbery behavior due to the strong entanglement of macromolecules, which is similar to cross-linked materials. It is worth noting that CP with DS = 1.08 has crossover from rubbery to transition zone at a relatively high frequency—around 10 s^{-1}; these short-range motions could be attributed to plastic deformations of fatty ester branches.
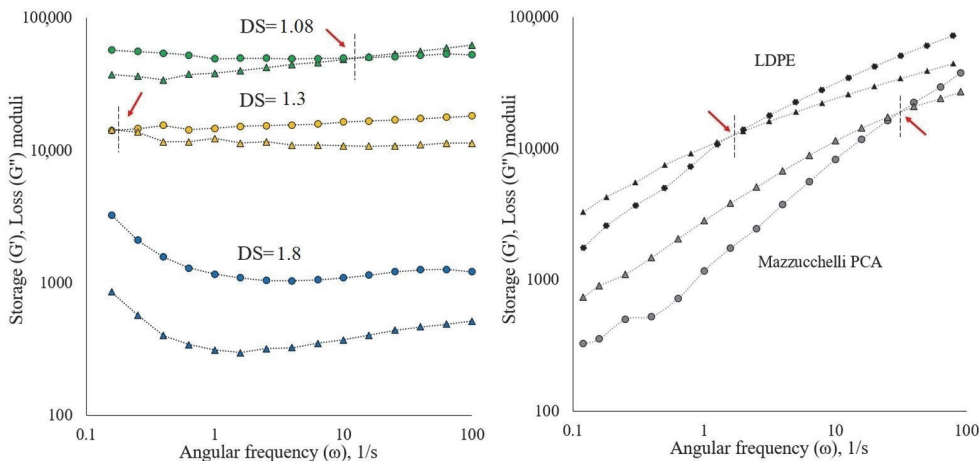
Figure 7. Storage modulus G' (○) and loss modulus G'' (△) dependence on angular frequency for cellulose palmitate with different degrees of substitution.

One could conclude that the melt flow of CP materials is stipulated by a rigid backbone of the cellulose chain that creates many junctions. Furthermore, material could contain solid phases of regenerated cellulose. In addition, the structural mobility could be attributed to the ester chain phase, which works as a self-lubricant for CP macromolecules in the melt. From the applied point of view, rubbery behavior makes the processing of thermoplastic material complicated. Therefore, to bring cellulose ester materials into the lower storage modulus, according to the time–temperature superposition theory, longer times for deformation, or equivalent higher temperatures, should be used. Time–temperature superposition is valid for linear homopolymers, but it highlights the approaches for materials development. A higher degree of substitution and shorter macromolecular chains should decrease entanglement density. In addition, an increase of free space within the material could cause it to soften, which could be achieved by the addition of plasticizers.

Dynamic viscosities vs. shear rate dependencies are shown in Figure 8. All samples show non-Newtonian behavior in the whole range of shear rates—no linear viscosity range could be observed. We assume that the combination of a rigid cellulose backbone with flexible fatty acid branches creates dynamic structures in the melt that are very sensitive to

applied shear. The rise of the shear elastic response of the backbone, overlapped by plastic deformation of branches, leads to a continuous decrease in viscosity. Externally plasticized cellulose acetate (Mazzucchelli PCA) shows a very similar flow curve.
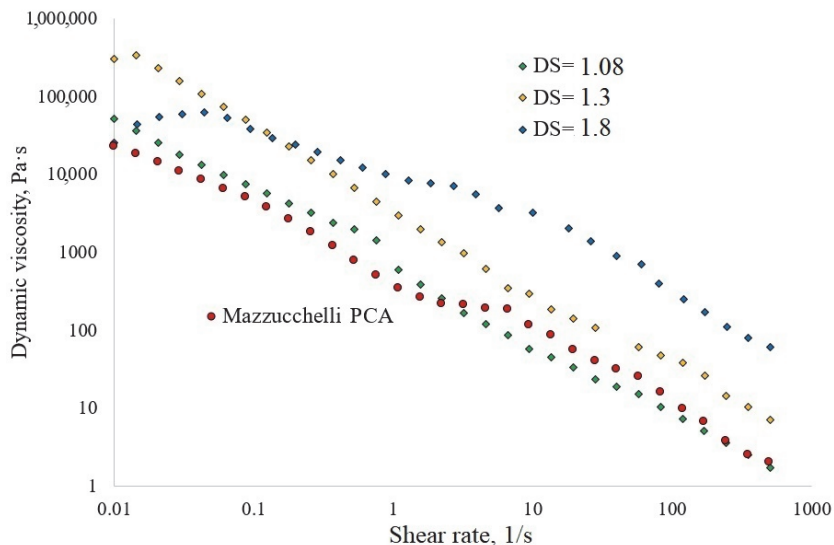
Figure 8. Dynamic viscosity dependence on shear rate for cellulose palmitate with different degrees of substitution.

To summarize the rheological properties of the materials, we could conclude that two phases are present in the material formed by rigid cellulose backbone and flexible ester chains. Low-substituted material contains two distinguishable phases (probably regenerated cellulose and blocks of fatty acid chains), and high-substituted material consists of a single phase (uniformly substituted cellulose). A significant increase in relaxation times upon an increase in the degree of substitution could be caused by flexible ester chain phase elimination.

4. Conclusions

The present study presents an optimized FACE production method by cellulose transesterification in a novel ionic liquid, [mTBNH][OAC]. One of the important contributions of the current study is a proposed eco-friendly, catalyst-free procedure, which is a prospective alternative to commercial esterification. IL can be recycled and reused, no harmful catalyst is required, and reactants are consumed in a better stoichiometric balance. The use of a co-solvent was found to be efficient in decreasing the amount of expensive IL.

The reported approach allows the production of FACEs with selectively tuned DS from 0 up to 1.8 by controlling the following reaction conditions: the IL:DMSO ratio, temperature, and time. Moreover, the reported path allows solubility and thermoplastic properties of the end-product tuning by DS control.

It was found that DS can be increased by increasing time, temperature, and molar ratio. However, the temperature of the reaction should not exceed 80 °C and the time of reaction should be less than 5 h to avoid degradation processes. It was proved that the OH group in cellulose AGU is substituted in the order of C7-O6 > C7-O2 > C7-O3.

A second important contribution of the work is that it provides a novel, previously unreported correlation between the melt flow behavior, structure, and the degree of substitution of FACEs. At low DS, FACEs have a two-phase structure that consists of fatty ester crystalline blocks and regenerated cellulose. This type of material has a semi-solid

structure and shows thermoplasticity due to the internal plasticization and self-lubricating effect of ester chains.

At high DS, CEs form a single amorphous phase that consists of uniformly esterified cellulose macromolecules. Furthermore, high-substituted materials show strong elastic response due to high junction-point density, which makes material melt flow behavior elastomer-like.

The synthesized FACEs are promising for packaging applications and could be used to substitute commercially available cellulose acetate plasticized with diethyl phthalate.

References

1. Qiu, X.; Hu, S. "Smart" Materials Based on Cellulose: A Review of the Preparations, Properties, and Applications. *Materials* **2013**, *6*, 738–781. [CrossRef] [PubMed]
2. Han, S.; Li, J.; Zhu, S.; Chen, R.; Wu, Y.; Zhang, X.; Yu, Z. Potential applications of ionic liquids in wood related industries. *Bioresources* **2009**, *4*, 825–834. [CrossRef]
3. Crépy, L.; Miri, V.; Joly, N.; Martin, P.; Lefebvre, J.-M. Effect of side chain length on structure and thermomechanical properties of fully substituted cellulose fatty esters. *Carbohydr. Polym.* **2011**, *83*, 1812–1820. [CrossRef]
4. Heinze, T.; Dicke, R.; Koschella, A.; Kull, A.H.; Klohr, E.-A.; Koch, W. Effective preparation of cellulose derivatives in a new simple cellulose solvent. *Macromol. Chem. Phys.* **2000**, *201*, 627–631. [CrossRef]
5. Young, R.J. Handbook of plastic materials and technology. In *Polymer International*; Rubin, I.I., Ed.; John Wiley & Sons Inc.: New York, NY, USA, 1991; Volume 25, p. 1745. ISBN 0-47-1-09634-2.
6. Nawaz, H.; Zhang, J.; Tian, W.; Wu, J.; Zhang, J. Chemical Modification of Cellulose in Solvents for Functional Materials. In *Green Chemistry and Chemical Engineering*; Han, B., Wu, T., Eds.; Springer: New York, NY, USA, 2019; pp. 427–460.
7. Zugenmaier, P. Materials of cellulose derivatives and fiber-reinforced cellulose-polypropylene composites: Characterization and application. *Pure Appl. Chem.* **2006**, *78*, 1843–1855. [CrossRef]

8. Cumpstey, I. Chemical Modification of Polysaccharides. *ISRN Org. Chem.* **2013**, *2013*, 417672. [CrossRef] [PubMed]
9. Freire, C.S.R.; Silvestre, A.J.D.; Neto, C.P.; Belgacem, M.N.; Gandini, A. Controlled heterogeneous modification of cellulose fibers with fatty acids: Effect of reaction conditions on the extent of esterification and fiber properties. *J. Appl. Polym. Sci.* **2006**, *100*, 1093–1102. [CrossRef]
10. Onwukamike, K.N.; Grelier, S.; Grau, E.; Cramail, H.; Meier, M.A.R. Sustainable Transesterification of Cellulose with High Oleic Sunflower Oil in a DBU-CO2 Switchable Solvent. *ACS Sustain. Chem. Eng.* **2018**, *6*, 8826–8835. [CrossRef]
11. Barthel, S.; Heinze, T. Acylation and carbanilation of cellulose in ionic liquids. *Green Chem.* **2006**, *8*, 301–306. [CrossRef]
12. Schenzel, A.; Hufendiek, A.; Barner-Kowollik, C.; Meier, M.A. Catalytic transesterification of cellulose in ionic liquids: Sustainable access to cellulose esters. *Green Chem.* **2014**, *16*, 3266–3271. [CrossRef]
13. Antova, G.; Vasvasova, P.; Zlatanov, M. Studies upon the synthesis of cellulose stearate under microwave heating. *Carbohydr. Polym.* **2004**, *57*, 131–134. [CrossRef]
14. Vicente, G.; Martínez, M.; Aracil, J. Integrated biodiesel production: A comparison of different homogeneous catalysts systems. *Bioresour. Technol.* **2004**, *92*, 297–305. [CrossRef]
15. Cao, X.; Sun, S.; Peng, X.; Zhong, L.; Sun, R.; Jiang, D. Rapid Synthesis of Cellulose Esters by Transesterification of Cellulose with Vinyl Esters under the Catalysis of NaOH or KOH in DMSO. *J. Agric. Food Chem.* **2013**, *61*, 2489–2495. [CrossRef] [PubMed]
16. Gericke, M.; Fardim, P.; Heinze, T. Ionic Liquids—Promising but Challenging Solvents for Homogeneous Derivatization of Cellulose. *Molecules* **2012**, *17*, 7458–7502. [CrossRef] [PubMed]
17. Fink, H.P.; Weigel, P.; Purz, H.J.; Ganster, J. Structure formation of regenerated cellulose materials from NMMO-solutions. *Prog. Polym. Sci.* **2001**, *26*, 1473–1524. [CrossRef]
18. McCormick, C.L.; Dawsey, T.R. Preparation of Cellulose Derivatives via Ring-Opening Reactions with Cyclic Reagents in Lithium Chloride/N, N-Dimethylacetamide. *Macromolecules* **1990**, *23*, 3606–3610. [CrossRef]
19. Heinze, T.; Liebert, T.; Koschella, A. *Esterification of Polysaccharides*, 1st ed.; Springer: Berlin/Heidelberg, Germany, 2006.
20. Mäki-Arvela, P.; Anugwom, I.; Virtanen, P.; Sjöholm, R.; Mikkola, J.P. Dissolution of lignocellulosic materials and its constituents using ionic liquids—A review. *Ind. Crops Prod.* **2010**, *32*, 175–201. [CrossRef]
21. Flieger, J.; Flieger, M. Ionic Liquids Toxicity-Benefits and Threats. *Int. J. Mol. Sci.* **2020**, *21*, 6267. [CrossRef] [PubMed]
22. Isik, M.; Sardon, H.; Mecerreyes, D. Ionic Liquids and Cellulose: Dissolution, Chemical Modification and Preparation of New Cellulosic Materials. *Int. J. Mol. Sci.* **2014**, *15*, 11922–11940. [CrossRef]
23. Ostonen, A.; Bervas, J.; Uusi-Kyyny, P.; Alopaeus, V.; Zaitsau, D.H.; Emel'yanenko, V.N.; Schick, C.; King, A.W.; Helminen, J.; Kilpelainen, I.; et al. Experimental and Theoretical Thermodynamic Study of Distillable Ionic Liquid 1,5-Diazabicyclo[4.3.0]non-5-enium Acetate. *Ind. Eng. Chem. Res.* **2016**, *55*, 10445–10454. [CrossRef]
24. Köhler, S.; Liebert, T.; Schöbitz, M.; Schaller, J.; Meister, F.; Günther, W.; Heinze, T. Interactions of Ionic Liquids with Polysaccharides 1. Unexpected Acetylation of Cellulose with 1-Ethyl-3-ethylimidazolium Acetate. *Macromol. Rapid Commun.* **2007**, *28*, 2311–2317. [CrossRef]
25. Hinner, L.P.; Wissner, J.L.; Beurer, A.; Nebel, B.A.; Hauer, B. Homogeneous vinyl ester-based synthesis of different cellulose derivatives in 1-ethyl-3-methyl-imidazolium acetate. *Green Chem.* **2016**, *18*, 6099–6107. [CrossRef]
26. Szabó, L.; Milotskyi, R.; Sharma, G.; Takahashi, K. Cellulose processing in ionic liquids from a materials science perspective: Turning a versatile biopolymer into the cornerstone of our sustainable future. *Green Chem.* **2023**, *25*, 5338–5389. [CrossRef]
27. Kostag, M.; Gericke, M.; Heinze, T.; El Seoud, O.A. Twenty-five years of cellulose chemistry: Innovations in the dissolution of the biopolymer and its transformation into esters and ethers. *Cellulose* **2019**, *26*, 139–184. [CrossRef]
28. Xu, C.; Cheng, Z. Thermal Stability of Ionic Liquids: Current Status and Prospects for Future Development. *Processes* **2021**, *9*, 337. [CrossRef]
29. Elsayed, S.; Hellsten, S.; Guizani, C.; Witos, J.; Rissanen, M.; Rantamäki, A.H.; Varis, P.; Wiedmer, S.K.; Sixta, H. Recycling of Superbase-Based Ionic Liquid Solvents for the Production of Textile-Grade Regenerated Cellulose Fibers in the Lyocell Process. *ACS Sustain. Chem. Eng.* **2020**, *8*, 14217–14227. [CrossRef]
30. King, A.W.T.; Asikkala, J.; Mutikainen, I.; Järvi, P.; Kilpeläinen, I. Distillable Acid–Base Conjugate Ionic Liquids for Cellulose Dissolution and Processing. *Angew. Chem. Int. Ed.* **2011**, *50*, 6301–6305. [CrossRef]
31. Martins, M.A.R.; Sosa, F.H.B.; Kilpeläinen, I.; Coutinho, J.A.P. Physico-chemical characterization of aqueous solutions of superbase ionic liquids with cellulose dissolution capability. *Fluid Phase Equilibria* **2022**, *556*, 113414. [CrossRef]
32. Parviainen, A.; Wahlström, R.; Liimatainen, U.; Liitiä, T.; Rovio, S.; Helminen, J.K.J.; Hyväkkö, U.; King, A.W.T.; Suurnäkki, A.; Kilpeläinen, I. Sustainability of cellulose dissolution and regeneration in 1,5-diazabicyclo[4.3.0]non-5-enium acetate: A batch simulation of the IONCELL-F process. *RSC Adv.* **2015**, *5*, 69728–69737. [CrossRef]
33. Elsayed, S.; Viard, B.; Guizani, C.; Hellstén, S.; Witos, J.; Sixta, H. Limitations of Cellulose Dissolution and Fiber Spinning in the Lyocell Process Using [mTBDH][OAc] and [DBNH][OAc] Solvents. *Ind. Eng. Chem. Res.* **2020**, *59*, 20211–20220. [CrossRef]
34. Huang, F.Y. Synthesis and Properties of Cellulose Stearate. *Adv. Mater. Res.* **2011**, *228–229*, 919–924. [CrossRef]
35. Crépy, L.; Chaveriat, L.; Banoub, J.; Martin, P.; Joly, N. Synthesis of Cellulose Fatty Esters as Plastics—Influence of the Degree of Substitution and the Fatty Chain Length on Mechanical Properties. *ChemSusChem* **2009**, *2*, 165–170. [CrossRef]
36. Duchatel-Crépy, L.; Joly, N.; Martin, P.; Marin, A.; Tahon, J.-F.; Lefebvre, J.-M.; Gaucher, V. Substitution degree and fatty chain length influence on structure and properties of fatty acid cellulose esters. *Carbohydr. Polym.* **2020**, *234*, 115912. [CrossRef]

37. Willberg-Keyriläinen, P.; Talja, R.; Asikainen, S.; Harlin, A.; Ropponen, J. The effect of cellulose molar mass on the properties of palmitate esters. *Carbohydr. Polym.* **2016**, *151*, 988–995. [CrossRef] [PubMed]
38. Li, J.; Baker, T.; Sacripante, G.G.; Lawton, D.J.W.; Marway, H.S.; Zhang, H.; Thompson, M.R. Solvent-free production of thermoplastic lignocellulose from wood pulp by reactive extrusion. *Carbohydr. Polym.* **2021**, *270*, 118361. [CrossRef]
39. Virtanen, S.; Talja, R.; Vuoti, S. Synthesis and melt processing of cellulose esters for preparation of thermoforming materials and extended drug release tablets. *Carbohydr. Polym.* **2017**, *177*, 105–115. [CrossRef] [PubMed]
40. Todorov, A.R.; King, A.W.T.; Kilpeläinen, I. Transesterification of cellulose with unactivated esters in superbase–acid conjugate ionic liquids. *RSC Adv.* **2023**, *13*, 5983–5992. [CrossRef]
41. Krasnou, I.; Gårdebjer, S.; Tarasova, E.; Larsson, A.; Westman, G.; Krumme, A. Permeability of water and oleic acid in composite films of phase separated polypropylene and cellulose stearate blends. *Carbohydr. Polym.* **2016**, *152*, 450–458. [CrossRef]
42. Krasnou, I.; Tarasova, E.; Märtson, T.; Krumme, A. Thermoplastic Cellulose Stearate and Cellulose Laurate: Melt Rheology, Processing and Application Potential. *Int. Polym. Process.* **2015**, *30*, 210–216. [CrossRef]
43. Lowman, D.W. Characterization of Cellulose Esters by Solution-State and Solid-State NMR Spectroscopy. In *Cellulose Derivatives*; American Chemical Society: Washington, DC, USA, 1998; Volume 688, pp. 131–162.
44. *ASTM D1795−13*; Standard Test Method for Intrinsic Viscosity of Cellulose. ASTM International: West Conshohocken, PA, USA, 2013.
45. Brandrup, J.; Immergut, E.H.; Grulke, E.A.; Abe, A.; Bloch, D.R. *Polymer Handbook*, 4th ed.; John Wiley & Sons: Hoboken, NJ, USA, 2005.
46. Wen, X.; Wang, H.; Wei, Y.; Wang, X.; Liu, C. Preparation and characterization of cellulose laurate ester by catalyzed transesterification. *Carbohydr. Polym.* **2017**, *168*, 247–254. [CrossRef]
47. Wu, J.; Zhang, J.; Zhang, H.; He, J.; Ren, Q.; Guo, M. Homogeneous Acetylation of Cellulose in a New Ionic Liquid. *Biomacromolecules* **2004**, *5*, 266–268. [CrossRef] [PubMed]
48. Yang, Y.; Xie, H.; Liu, E. Acylation of cellulose in reversible ionic liquids. *Green Chem.* **2014**, *16*, 3018–3023. [CrossRef]
49. Kakko, T.; King, A.W.T.; Kilpeläinen, I. Homogenous esterification of cellulose pulp in [DBNH][OAc]. *Cellulose* **2017**, *24*, 5341–5354. [CrossRef]
50. Chen, H.; Yang, F.; Du, J.; Xie, H.; Zhang, L.; Guo, Y.; Xu, Q.; Zheng, Q.; Li, N.; Liu, Y. Efficient transesterification reaction of cellulose with vinyl esters in DBU/DMSO/CO2 solvent system at low temperature. *Cellulose* **2018**, *25*, 6935–6945. [CrossRef]
51. Xu, D.; Voiges, K.; Elder, T.; Mischnick, P.; Edgar, K.J. Regioselective Synthesis of Cellulose Ester Homopolymers. *Biomacromolecules* **2012**, *13*, 2195–2201. [CrossRef] [PubMed]
52. Samaranayake, G.; Glasser, W.G. Cellulose derivatives with low DS. I. A novel acylation system. *Carbohydr. Polym.* **1993**, *22*, 1–7. [CrossRef]
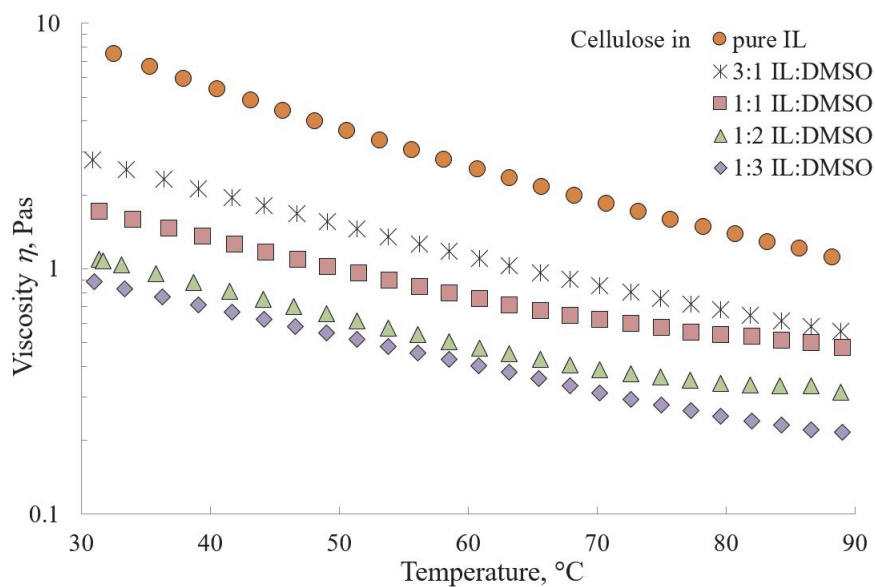
Figure S1. Temperature dependence of viscosity of cellulose solution in IL:DMSO binary solvent at various IL:DMSO ratios. The concentration of all solutions is 2 wt%.
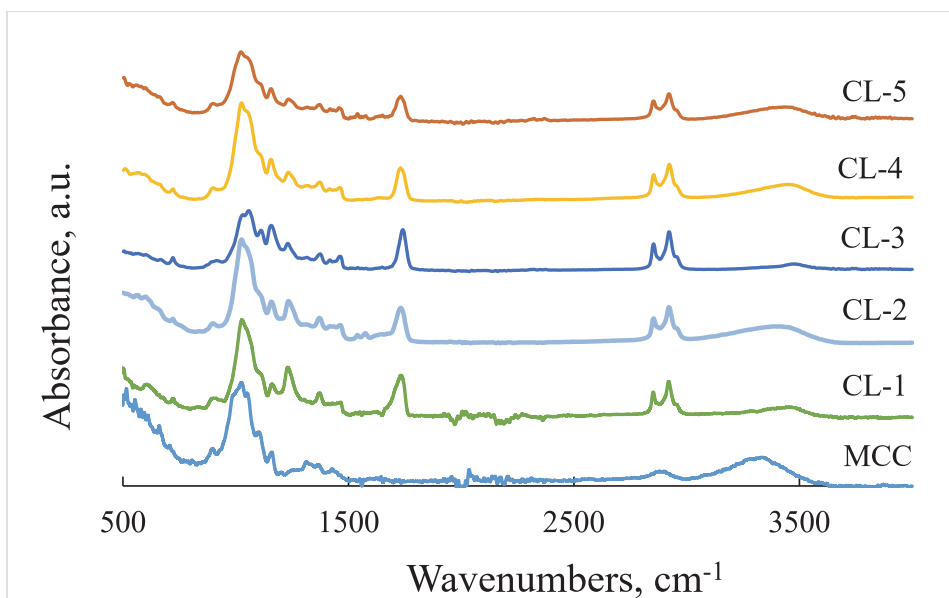
Figure S2. FTIR spectra of MCC and cellulose laurates obtained in IL:DMSO mixture of various ratios.
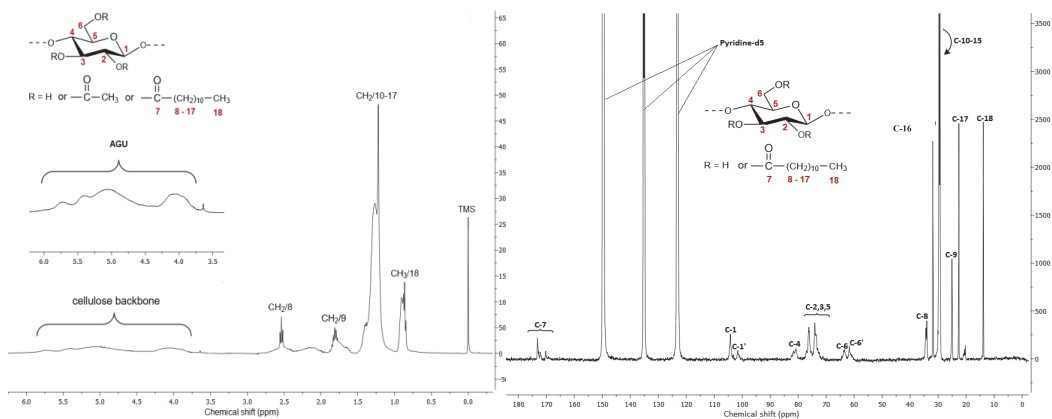
(a)

(b)

Figure S3. (a) ¹H NMR spectrum of Cellulose Laurate CL-3 in Pyridine-d₅ (500 MHz, 25°C); (b) Full ¹³C NMR spectrum of Cellulose Laurate CL-3 in Pyridine-d₅ (125 MHz, 80 °C).
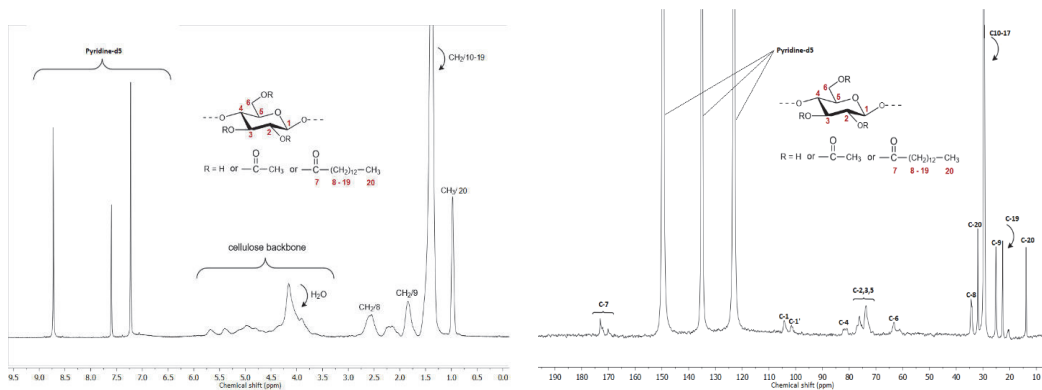
(a)

(b)

Figure S4. (a) ¹H NMR spectrum of Cellulose Myristate in Pyridine-d₅ (500 MHz, 80°C); (b) ¹³C NMR spectrum of Cellulose Myristate in Pyridine-d₅ (125 MHz, 80 °C).
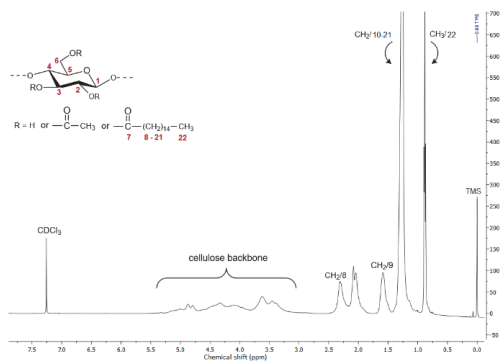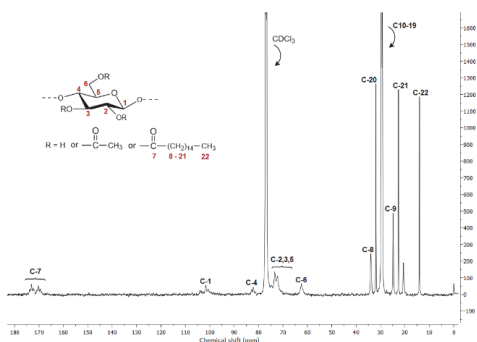
Figure S5. (a) ¹H NMR spectrum of Cellulose Palmitate CP-3 in Chloroform-d (500 MHz, 25°C); (b) ¹³C NMR spectrum of Cellulose Palmitate CP-3 in Chloroform-d (125 MHz, 40 °C).
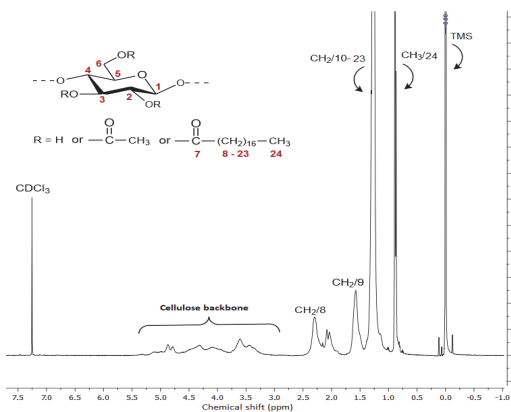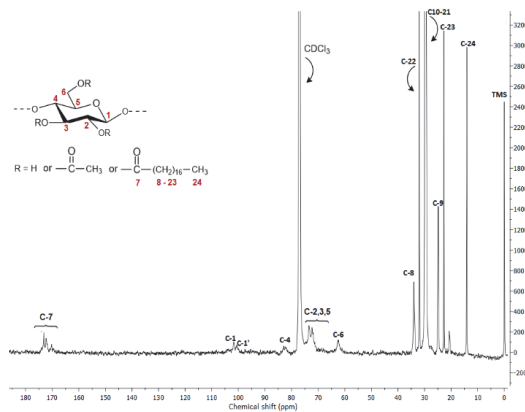
Figure S6. (a) ¹H NMR spectrum of Cellulose Stearate CS-2 in Chloroform-d (500MHz, 40°C); (b) ¹³C NMR spectrum of Cellulose Stearate CS-2 in Chloroform-d (125 MHz, 40 °C).
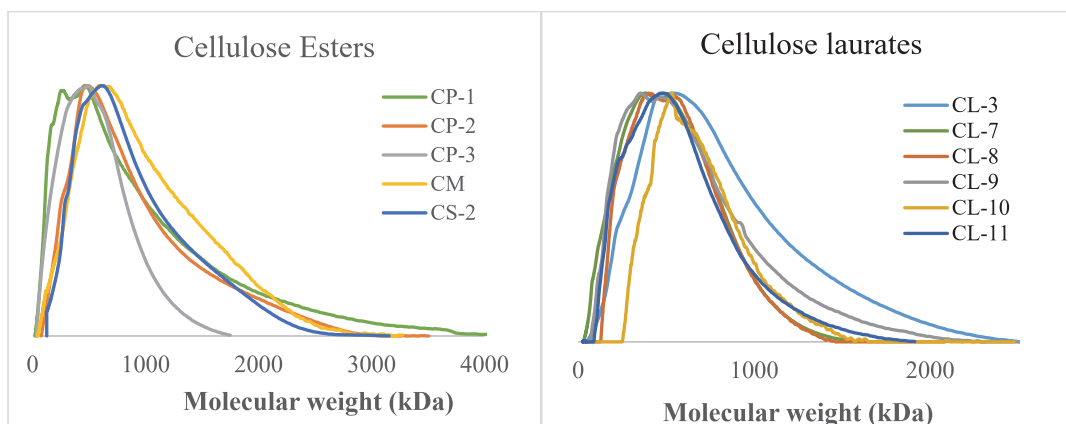
Figure S7. Molar mass distribution of cellulose esters.
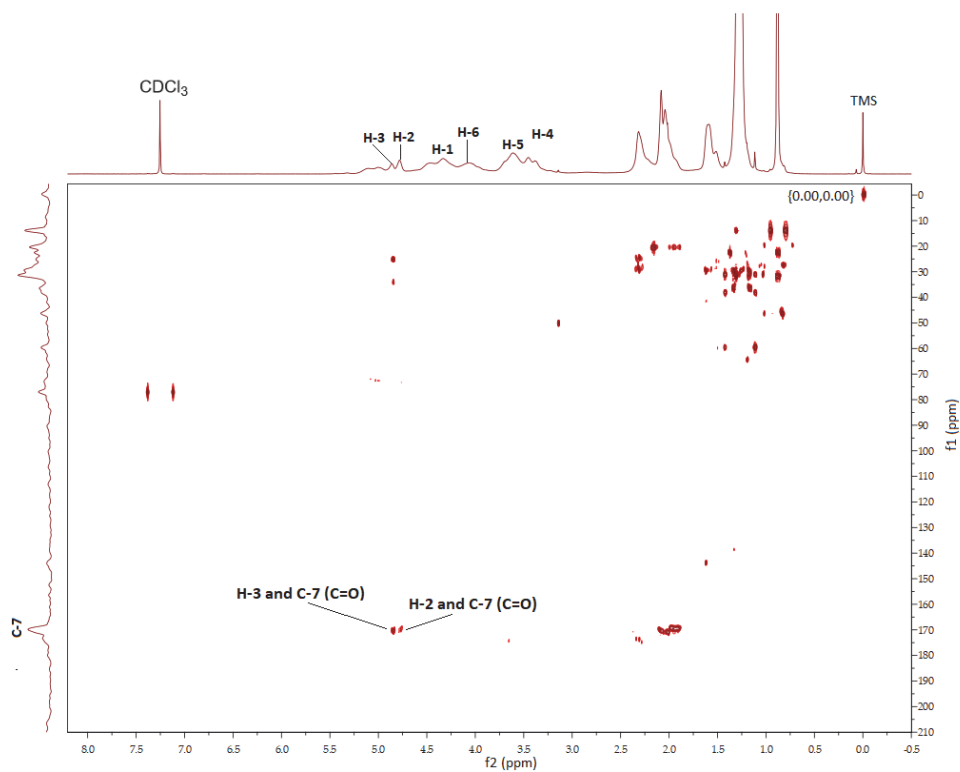
Figure S8. HMBC spectrum of Cellulose Palmitate (CP-3) in Chloroform-d (800 MHz Cryoprobe, 256 scans, 128 increments, 16 h acquisition time, 323 K).

Publication II

Savale, N., Tarasova, E., Krasnou, I., Kudrjašova, M., Rjabovs, V., Reile, I., Heinmaa, I., Krumme, A. (2024). Optimization and degradation studies of cellulose transesterification to palmitate esters in superbase ionic liquid. Carbohydrate Research, 537, 109047.

Optimization and degradation studies of cellulose transesterification to palmitate esters in superbase ionic liquid

N. Savale [a,*], E. Tarasova [a], I. Krasnou [a], M. Kudrjašova [b], V. Rjabovs [c], I. Reile [c], I. Heinmaa [c], A. Krumme [a]

[a] School of Engineering, Department of Materials and Environmental Technology, Tallinn University of Technology, Ehitajate tee 5, 19086, Tallinn, Estonia
[b] School of Science, Department of Chemistry and Biotechnology, Tallinn University of Technology, Akadeemia tee 15, 12618, Tallinn, Estonia
[c] National Institute of Chemical Physics and Biophysics, Akadeemia tee 23, 12618, Tallinn, Estonia

ABSTRACT

Cellulose palmitates (CPs) were synthesized with varying degrees of substitution (DS) via a catalyst-free, homogeneous transesterification of cellulose in a novel superbase ionic liquid (SB-IL) system, specifically 5-methyl-1,5,7-triaza-bicyclo[4.3.0]non-6-enium acetate [mTBNH][OAc], combined with dimethyl sulfoxide (DMSO) as a co-solvent, using vinyl palmitate as the acylating agent. We examined the influence of reaction temperature, reaction time, and the molar ratio of vinyl palmitate to anhydroglucose unit (AGU) on the DS, which ranged from 0.5 to 2.3 under the given conditions. Notably, the reaction order of the three hydroxy groups was C6–OH > C2–OH > C3–OH. To elucidate the chemical structure of CPs and confirm the transesterification process, various spectroscopic techniques including ^{1}H nuclear magnetic resonance (NMR), ^{13}C NMR, heteronuclear single quantum correlation (HSQC), and solid-state NMR were employed. Higher reaction temperatures and extended reaction times led to a decrease in the DS of CPs, potentially due to the degradation of some of the involved chemicals during the transesterification process. We also investigated the stability of the pure ionic liquid (IL) and the IL + DMSO solvent system at elevated temperatures by heating them at 100 °C for 5 h, confirming their chemical integrity through ^{1}H NMR analysis. Additionally, we assessed the compatibility between the solvent system and cellulose by subjecting a mixture of cellulose and the solvent system to 100 °C for 5 h. To compare the structures of untreated cellulose and regenerated cellulose, Fourier transform infrared (FT-IR) spectroscopy was employed. Furthermore, we determined the molar mass of both untreated cellulose and regenerated cellulose, as well as CPs synthesized at higher reaction temperatures and longer durations, using intrinsic viscosity measurements. Lastly, we examined the solubility properties of CPs.

1. Introduction

Cellulose, a prominent renewable resource (RR) with an annual global production of about 90 gigatons, offers a multifaceted value proposition [1]. Derived from agricultural or forestry residues, it avoids competition with food resources and exhibits a spectrum of advantageous attributes, including biodegradability, non-toxicity, biocompatibility, robust mechanical strength, heat resistance, and solvent resilience [2,3]. With three hydroxy groups per anhydroglucose unit (AGU), cellulose readily engages in diverse hydroxy-group reactions, such as acylation (esterification), etherification, oxidation, silylation, and polymer grafting. Although cellulose is non-thermoplastic in its natural state, acylation is widely used to synthesize various cellulose-based

functional materials with thermoplastic properties. Prominent thermoplastic cellulose derivatives like cellulose acetate, cellulose acetate butyrate, and cellulose acetate propionate find extensive utility in plastics, films, fibres, membranes, and coatings [4].

The synthesis of cellulose esters primarily involves acylation conducted in either heterogeneous or homogeneous systems. Homogeneous solutions are preferred for their superior ability to regulate the degree of substitution (DS), resulting in a more consistent product pattern [5]. Nevertheless, the dissolution of cellulose in water or commonly used organic solvents poses a formidable challenge, due to the robust inter- and intra-molecular hydrogen bonding. In recent decades, extensive efforts have been dedicated to pioneering novel cellulose solvent systems, such as dimethyl sulfoxide/tetrabutylammonium fluoride

(DMSO/TBAF) [6], N.N-dimethylacetamide/lithium chloride (DMA-C/LiCl) [7], N-methylmorpholine (NMMO) [8], and NaOH/urea [9]. Regrettably, these solvents are either cost-prohibitive or necessitate severe operating conditions. Their widespread application not only raises environmental concerns but also jeopardizes economic feasibility.

Ionic Liquids (ILs), eco-friendly cellulose solvents, have emerged recently and continue to undergo refinement [10]. ILs possess high polarity, enabling the disruption of hydrogen bonds among cellulose macromolecules. Furthermore, they exhibit non-volatility, recyclability, and, for the most part, non-toxicity [the last is under ongoing investigation [1,11]]. The vast array of ILs derives from the numerous anion-cation combinations [12]. Many ILs efficiently dissolve cellulose, converting it into thermoplastic materials through acylation [13]. 1-Ethyl-3-methyl-imidazolium acetate ([Emim][OAc]) ionic liquid has been a prominent choice in laboratory research due to its adequate cellulose solubility and catalytic potential for in situ cellulose transesterification with vinyl esters [14]. However, faces setbacks due to undesired side reactions between the acetate anion in the IL and the cellulose backbone [15]. Furthermore, first-generation imidazolium-based ILs present complications in terms of recycling, displaying questionable stability [16,17] and impractical distillation owing to their extremely low vapor pressure. These challenges impede the removal of side products from the solvent. Superbase ionic liquids (SB-ILs), notably di- and triazabicyclo compounds, present a groundbreaking and highly promising class of solvents for cellulose dissolution. Their standout features include the ability to dissolve cellulose at high concentrations, low sensitivity to moisture, minimal toxicity, and recyclability without degradation [18–24]. During acylation, these ILs partially decompose, releasing superbases that catalyze the reaction [25,26]. Moreover, they function as ionic compounds with a low vapor pressure at cellulose acylation temperatures but can be dissociated into superbases and acids at higher temperatures, enabling component purification through distillation, earning the label "distillable ILs" [27]. Noteworthy candidates like 7-methyl-1,5,7-triazabicyclo[4.4.0]dec-5-enium acetate [mTBDH] [OAc] and 5-methyl-1,5,7-triaza-bicyclo[4.3.0]non-6-enium acetate [mTBNH][OAc] have recently emerged for cellulose dissolution and regeneration [28]. In this study, our focus is on [mTBNH][OAc], a newly developed ionic liquid (IL). Some IL-based solvents use co-solvents to adjust solubility and viscosity. Dimethyl sulfoxide (DMSO), a common choice, stands out for its recyclability, sustainable production, and low toxicity. Co-solvent systems prove more effective for cellulose dissolution than pure ILs [29], enhancing viscosity reduction, mass transfer rates, and steric hindrance mitigation [30], and being inexpensive thereby lowering the overall cost of the synthesis. Thus, we also employed DMSO as a co-solvent in this investigation.

Sustainability assessment encompasses the origin of acylating agents, acylation efficiency/control, and the nature of by-products. Acid anhydrides or chlorides are not only moisture sensitive [31] but utilizing them as acylating agents generates highly acidic and corrosive by-products [32] which can diminish the degree of polymerization (DP) of cellulose and eventually affect DS of the final products adversely. Thus, the more sustainable preference is the transesterification route, yielding less harsh by-products like alcohols, aldehydes, and ketones, readily separable and recyclable to meet sustainability goals.

Investigation of fatty acid cellulose esters (FACEs) within the aliphatic C8–C18 range, with DS values ranging from 0.56 to 3, has revealed that FACEs with a DS of 1.5 exhibit thermoplastic characteristics. FACEs within the DS spectrum of 1.5–3 manifest analogous mechanical and thermoplastic characteristics [33,34]. Moreover, it was determined that the plasticizing effect of aliphatic chains primarily hinges on DS rather than the length of the fatty chain. Thus, long-chain FACEs show promise as materials, and ascertaining their DS represents a pivotal step toward the effective utilization of FACEs as "thermoplastic materials." Establishing direct correlations between acylation conditions in specific ILs and the DS of FACEs can further yield insights into their rheological and thermal properties. It is possible to modulate DS by altering parameters like reaction temperature, reaction time, and re-agent ratios.

This study delves into the meticulous optimization of reaction conditions for the homogeneous transesterification of cellulose with vinyl palmitate (VP) using the novel distillable ionic liquid, [mTBNH][OAc], aiming to produce cellulose palmitates (CPs) with a DS spanning the range of 0.5–2.3. Our work represents a pioneering experimental endeavor in utilizing [mTBNH][OAc] as a functionalization medium for cellulose, yielding CPs across a broad DS spectrum. Previously, [mTBNH][OAc] had found application in cellulose regeneration [22] and served as a solvent for transesterification, primarily with unactivated to moderately activated esters and cyclic esters such as lactones, generating DS values within the range of 0.07–1.29 [35]. Recently, [mTBNH][OAc]/DMSO solvent system was successfully utilized for the synthesis of FACEs (DS = 0.6 to 2.0) via homogeneous transesterification of cellulose [36]. Notably, our current investigation enables the synthesis of CPs in this medium via transesterification without the need for additional catalysts, operating under mild conditions. An additional merit of this study lies in the provision of valuable insights, often lacking in existing literature, regarding the stability of the solvent system (SB-IL + DMSO) at elevated temperatures and extended durations, along with insights into the compatibility of the solvent system with the reactants employed in transesterification. Such information holds significance for the future utilization of this solvent system, particularly in the synthesis of cellulose palmitates and other long-chain FACEs through homogeneous transesterification while considering vital factors such as cost, availability, and the limited understanding of SB-IL recycling processes.

2. Experimental section

2.1. Materials

Fibrous cellulose with a fiber length of 0.02 mm was purchased from Carl Roth GmbH + Co. KG (Karlsruhe, Germany). The superbase-based ionic liquid (SB-IL), 5-methyl-1,5,7 triaza-bicyclo- [4.3.0] non-6-enium acetate [mTBNH][OAc] was not commercially available and was synthesized at the University of Helsinki by a stoichiometric mixture (1:1) of acetic acid and mTBNH at room temperature with purity >97% [28,37] and supplied by Liuotin Group Oy (Porvoo, Finland). Dimethyl sulfoxide (DMSO) and pyridine with purity >99% were purchased from Fisher Chemical (Pittsburgh, PA, USA). Vinyl palmitate (VP) with a purity of >98% was purchased from Tokyo Chemical Industry Co., Ltd (Tokyo, Japan). Pyridine-d5 (purity = 99.5 atom % D. contains 0.03 v/v % TMS) and chloroform-d (purity = 99.8 atom % D. contains 1 v/v% TMS) for NMR were purchased from Acros Organics (Geel, Belgium). All other chemicals and solvents were used without further purification: chloroform ≥99.8% (Honeywell/Riedel-de Haën, Muskegon, MI, USA); N,N-Dimethylformamide (DMF) 99.8% (Sigma Aldrich, St. Louis, MO, USA); tetrahydrofuran (THF) ≥99.9% (Sigma Aldrich, St. Louis, MO, USA).

2.2. Cellulose dissolution in the solvent system

The cellulose was dried at 105°C for 12 h under vacuum. IL and DMSO were stored under the nitrogen atmosphere before use. 0.4 g of cellulose was suspended in the 1:1 mixture of 10.0 g of IL and 10.0 g of DMSO (the volume of the total solvent system is 20.0 g) in a 100 ml conical flask equipped with a magnetic stirrer. The addition of reagents was conducted under a nitrogen atmosphere. The entire assembly was set up in an oil bath. The dissolution of cellulose was carried out at 60°C for 6–8 h with constant stirring until the clear, transparent solution was obtained.

2.3. Experimental procedure: Synthesis of cellulose palmitate derivatives via homogeneous transesterification

The transesterification of cellulose with vinyl palmitate was carried out in a novel [mTBNH][OAc]/DMSO binary solvent system without employing an external catalyst. Following the complete dissolution of cellulose in the solvent system, the esterification agent, vinyl palmitate was cautiously added to the cellulose solution (3–12 eq./anhydroglucose unit, AGU) at the preferred reaction temperature (60–120°C) and duration (1–5 h) under nitrogen atmosphere.

After completing the reaction, the mixture was added to 250 mL of warm distilled water and filtered under vacuum. The solid product underwent thorough washing with ethanol, acetone, and n-hexane to eliminate the residual solvent system and impurities. Subsequently, the product was dried at 70 °C for 12 h, milled into a fine powder, and subjected to a second wash with ethanol, acetone, and n-hexane. The product was then dried again, first at 80 °C for 4–5 h and subsequently at 100 °C for 1 h. Upon cooling to room temperature, the product yield was determined as an average of three experiments. The resulting solid products were off-white to light brown in color and stored under a nitrogen atmosphere for further characterization.

2.4. Chemical characterization of cellulose palmitate derivatives by nuclear magnetic resonance (NMR) spectroscopy

The cellulose palmitate derivatives were subjected to NMR analysis, including ^{1}H NMR, ^{13}C NMR, and HSQC NMR, using an Agilent Technologies DD2 500 MHz spectrometer equipped with 5 mm broadband inverse (^{1}H, HC-HSQC) or broadband observe (^{13}C spectra) probes. A 15-min temperature equilibration delay was allowed between sample insertion and NMR acquisition at 40 °C (CPs in chloroform-d) and 80 °C (CPs in pyridine-d$_5$) sample temperature. In the case of ^{1}H spectra, 64 scans were conducted with a 25-s relaxation delay, while for ^{13}C spectra, 20000–45000 scans were performed with a 2.5-s recycle delay to achieve the desired signal-to-noise ratio. NMR samples were prepared by dissolving 15–20 mg of the sample in 0.7 ml of deuterated NMR solvent and heating the mixture for 30 min at 40–45 °C until a clear solution was obtained in a small pre-dried glass bottle. The glass bottle containing the mixture was carefully sealed with parafilm. Ultrasonic treatment was applied to the samples to obtain a transparent solution. Dual or triple DS measurements were conducted for each sample, and the average DS value was calculated. It was noted that the DS obtained from two (or three) measurements exhibited a deviation of ±0.1. Tetramethylsilane (TMS) was used as an internal standard for the NMR experiments.

In the case of long-chain cellulose esters, the liquids ^{13}C NMR suffered from poor intensity and resolution of AGU peaks. The ^{13}C MAS experiment can produce high-resolution spectra. Therefore, ^{13}C MAS NMR spectra were recorded on Bruker AVANCE-II spectrometer at 14.1 T magnetic field (150.9 MHz) using a home-built MAS probe for 25 × 4 mm Si3N4 rotors. In all experiments, the sample spinning was 12.5 kHz. The spectrum was recorded in parameters: 4000 scans, 30 s relaxation delay.

2.5. Determination of DS of cellulose palmitates

The degree of substitution, DS, is the number of substituted hydroxy groups of AGU with palmitate molecules. The DS of cellulose palmitate was determined from the ^{1}H NMR spectrum by assessing the intensity of the relevant resonances, following the procedure described in Ref. [38]:

$$DS = \frac{10 \times I_{CH_3} \div 3}{I_{AGU} + I_{CH_3} \div 3} \qquad \text{Eq. 1}$$

where I_{CH_3} is the integral of terminal methyl protons of the aliphatic fatty acid chain region and I_{AGU} is the integral of all protons of anhydroglucose unit (AGU).

2.6. Interaction between solvent system and reactants

0.4 g of pre-dried cellulose (at 100 °C for 12 h) dissolved in 20.0 g of a solvent mixture (1:1 of IL:DMSO) at 60 °C for 8 h, followed by heating at 100 °C for 5 h, all under a nitrogen atmosphere. Afterward, cellulose was recovered by pouring the hot mixture into warm distilled water, followed by multiple washes with ethanol, acetone, and n-hexane. The regenerated cellulose was dried at 70 °C for 5 h, milled into a fine powder, and then further dried at 100 °C for 8 h before cooling and storage under nitrogen.

Fourier transform infrared (FT-IR) spectra of both pure and regenerated cellulose were obtained using an Interspec 200-X spectrometer with the Quest ATR accessory from Specac (Orpington, UK), spanning the range of 500–4000 cm^{-1} with a 4 cm^{-1} resolution. Before the FTIR analysis, all samples were vacuum-dried overnight at 80 °C to eliminate moisture.

Nine samples (S1–S9) were prepared by combining a solvent system (2.0 g) and VP (0.5 g) under a nitrogen atmosphere. To examine temperature influence, five were heated from 60 °C to 100 °C by a margin of 10 °C for a consistent duration of 2 h. Simultaneously, the remaining four were heated at 70 °C for varying durations from 1 to 5 h by a margin of 1 h. The physical appearance of each sample was scrutinized for potential degradation indicators, such as discoloration.

2.7. Intrinsic viscosity measurements

The molecular weight (MW) of untreated cellulose and regenerated cellulose was determined at 25 °C from the intrinsic viscosity [η] of cellulose solution in cupriethylenediamine hydroxide solution, Cuene, according to a standard procedure ASTM D1795−13.

The MW was then calculated by the Mark-Kuhn-Houwink-Sakurada equation:

$$[\eta] = K \times MW^a \qquad \text{Eq. 2}$$

where K = 1.01 × 10-4 dL/g and a = 0.9 [39]. The degree of polymerization (DP) of the cellulose polymer can be calculated by dividing the molecular weight of the cellulose by the molecular weight of the cellulose monomer (162 g/mol).

Degradation of cellulose backbone during transesterification reaction at temperatures ≥80 °C and times ≥2 h can be revealed by measuring the intrinsic viscosity of the CPs. Unfortunately, constants K and a are not available anywhere in the literature for fatty acid cellulose derivatives with side chains longer than acetyl. However, the changes in MW can be still recorded through the variation of the intrinsic viscosity of cellulose ester solutions that depends on their MW. Therefore, cellulose palmitate samples synthesized at different reaction temperatures and times, namely CP-3, CP-4, CP-5, CP-11, and CP-12 (see Table 1), were chosen to investigate the effect of reaction temperature and time on polymer degradation (decreasing of MM) and their intrinsic viscosities were calculated by using pyridine as solvent at 25 °C.

The intrinsic viscosity can be calculated as follows (Equation (3)) -

$$[\eta] = \lim_{C \to 0} \frac{\eta_{sp}}{C} \qquad \text{Eq. 3}$$

where

$$\eta_{sp} = \eta_r - 1 = \frac{\eta}{\eta_0} - 1 \qquad \text{Eq. 4}$$

η$_r$, η, and η$_0$ are the relative viscosity and viscosities of the solution and solvent respectively. C is the concentration of the CPs in pyridine.

3. Results and discussion

3.1. Synthesis of cellulose palmitate derivatives

Scheme 1 shows the chemical pathway of the transesterification of cellulose in the presence of vinyl palmitate without the addition of any external catalyst. The by-product, alcohol, or aldehyde, being volatile can be easily removed from the reaction system at elevated temperatures. In this work, cellulose palmitate derivatives (3) were synthesized by catalyst-free sustainable homogeneous transesterification of cellulose (1) with vinyl palmitate (2) in the presence of an ionic liquid/co-solvent-based system. [mTBNH][OAc] is a novel, distillable ionic liquid having high efficiency towards cellulose dissolution. DMSO was used as a co-solvent.

All synthesized CPs are soluble in several organic solvents like chloroform, pyridine, DMSO, DMAc, DMF, THF, and toluene which facilitates direct measurements of NMR spectra in the form of solution and thereby provides a way towards structural analysis and calculation of DS. Although several solvents were used to determine the solubility of the CPs, the NMR studies were mainly done with pyridine-d_5 and chloroform-d.

Fig. 1 represents the ^{1}H NMR spectrum of CP-5 (DS = 2.28, see Table 1).

In the ^{1}H NMR spectra of all examined CPs, the proton peaks in the range of 5.30 to 3.00 ppm correspond to H-1, H-2, H-3, H-4, H-5, H-6, and H-6' of the anhydroglucose units in cellulose. The signals in the ranges of 2.393–2.223, 1.695–1.460, and 1.424–1.125 ppm are associated with the methylene protons at H-8, H-9, and H-10–21, respectively. The signals at 0.955–0.794 ppm are assigned to the terminal methyl protons at H-22.

In the ^{13}C NMR spectrum of CP (Fig. 2), we observe signals at 34.08, 31.96, 24.90, 22.71, and 14.09 ppm, which correspond to the carbons of C-8, C-20, C-9, C-21, and C-22 in the aliphatic side chain respectively. The carbons within the range of C(10–19) exhibit signals ranging from 30.85 to 28.77 ppm. For the AGU carbons, C-1, C-1', C-4, C-2,3,5, and C-6, we observe signals at 104.29, 101.58, 82.20, 74.68–72.24, and 62.52 ppm, respectively. The signals spanning from 173.09 to 170.16 ppm are associated with the carbonyl carbon at C-7, providing direct confirmation of the successful attachment of the long-chain fatty acid chain to the cellulose backbone. The presence of three peaks for the carbonyl group suggests that OH groups at positions 2, 3, and 6 were substituted with palmitates [40]. It's important to note that not all OH groups in one AGU are substituted, but this indicates that any of these three positions can be acylated. As given in reference [41], by integrating the carbonyl carbons (C7–O2, C7–O3, and C7–O6), we can infer that the order of OH group substitution is C6–OH > C2–OH > C3–OH.

The small signals at approximately 2.00 ppm in ^{1}H NMR and 20.00 ppm in ^{13}C NMR represent the acetyl group from by-product cellulose acetate which might have formed during the transesterification process. The by-product cellulose acetate may have formed through three potential pathways: 1) the generation of acid anhydride via the reaction

between the acetate ion of the IL and vinyl palmitate, succeeded by a reaction with cellulose; 2) the formation of cellulose palmitate, followed by a subsequent nucleophilic displacement reaction with the acetate ion of the IL; 3) a combination of both mechanisms. The authors recommend conducting additional in-depth kinetic experiments, followed by spectroscopic analysis, before making definitive conclusions about the acetylation side reaction. Similar observations were reported by Köhler et al. in their investigation involving the interaction of cellulose with *p*-Toluenesulfonyl Chloride in the presence of carboxylate IL, [Emim] [OAc] [14].

In addition to conducting ^{1}H and ^{13}C NMR investigations, a comprehensive structural analysis of CP-5 was pursued through the application of solid-state NMR spectroscopy and with the advanced two-dimensional Heteronuclear Single Quantum Coherence (HSQC) experiment. In the ^{13}C MAS NMR spectrum of CP-5 (full spectrum is available in supporting information, Fig. S2), the signals at 34.10, 32.60, 25.30, 23.30, and 14.50 ppm are assigned to carbons of C-8, C-20, C-9, C-21, and C-22 of the aliphatic side chain, respectively. The carbons at C (10–19) give signals at 30.50 ppm. The AGU carbons C-1, C-4, C-2,3,5, and C-6 give signals at 102.00, 84.00, 73.00 and 64.00 ppm, respectively. The signal at 173.00 ppm corresponds to the carbonyl carbon at C-7.

To confirm further the assignment of the signals of CP, the ^{1}H–^{13}C HSQC spectrum was studied (Refer to supporting information, Fig. 3a and b), where the aliphatic side chain region (Fig. 3a) and cellulose region (Fig. 3b) are shown. In the aliphatic side chain region, notable correlations were observed for C-21/H-21, C-20/H-20, C-22/H-22, and C-10–19/H-10-19, with δ_H/δ_C values of 1.26/22.55, 1.25/31.80, 0.84/13.86, and 1.28/29.52, respectively. Within the cellulose region, strong correlations were evident at δ_H/δ_C 5.61/75.23, 5.35/73.77, 4.93/102.51, 4.58/63.90, 3.97/72.57, and 3.86/82.44, corresponding to C-3/H-3, C-2/H-2, C-1/H-1, C-6/H-6, C-5/H-5, and C-4/H-4, respectively. The decentralized signals for C-8/H-8 and C-9/H-9 were represented by δ_H/δ_C values of 2.32/33.91 and 1.59/24.95, respectively. The δ_H/δ_C signals observed at 2.09/19.98 further confirm the formation of by-product cellulose acetate.

In Fig. 3b, it's evident that with the reaction conditions optimized, full acylation of C6–O has been successfully attained, as only one resonance of the corresponding group is detected in the ^{13}C spectrum. Furthermore, the intensity of the distinct cross-peak of C2-OAcyl (5.4/74ppm) is higher compared to that of C3-OAcyl (5.6/75 ppm), indicating a preference for acylation at the former position. To assess acylation efficiency at various positions in the CP, we conducted a comparison of signal integrals from HSQC spectra. Integration of these signals in the HSQC spectrum revealed that the overall degree of substitution (DS = 2.28, refer to Table 1) has a ratio of approximately 1.00: 0.76: 0.52 for the C7–O6, C7–O2, and C7–O3 positions, respectively, within a reasonable margin of error.
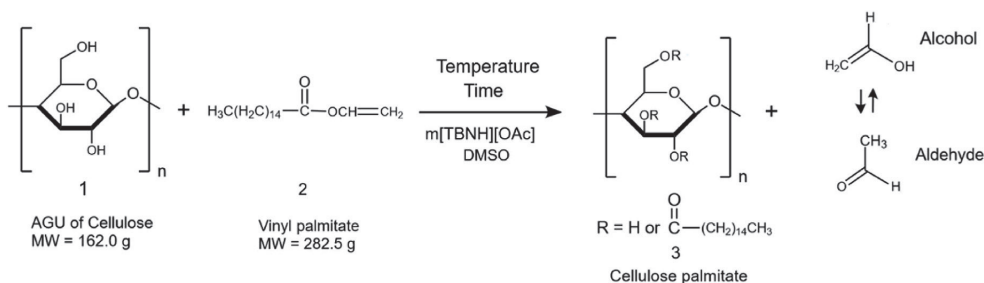
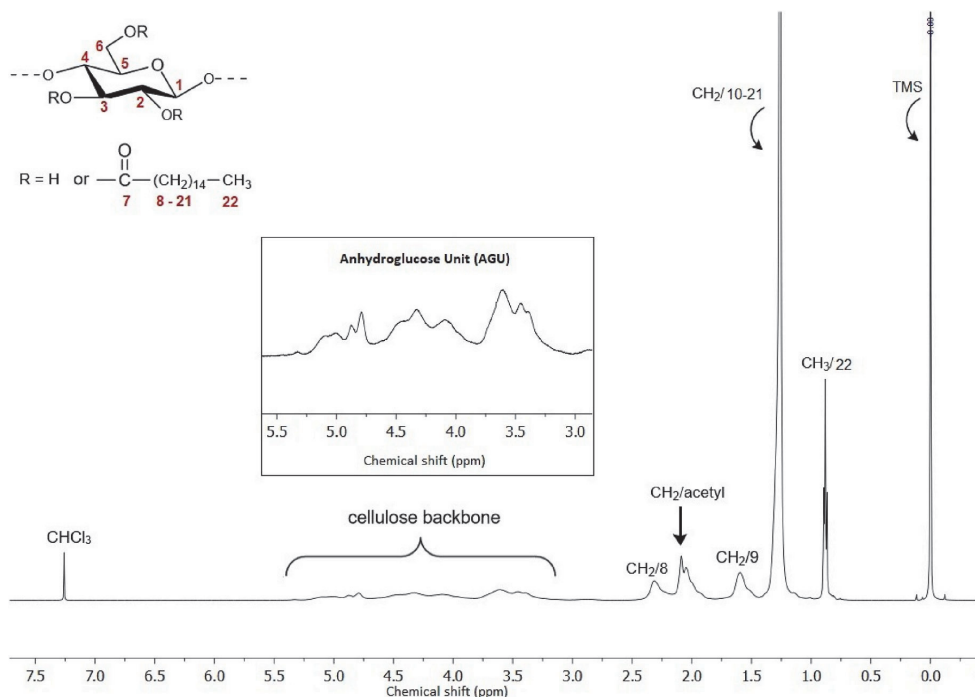**Scheme 1.** Transesterification of cellulose with vinyl palmitate.

Fig. 1. ^{1}H NMR spectrum of CP-5 (DS = 2.3) in chloroform-d (500 MHz, 40 °C).

Table 1
DS of cellulose palmitates (CPs) synthesized by transesterification of cellulose with vinyl palmitate (VP) in a 1:1 IL/DMSO solvent system.

Sample	Reaction parameters			DS (±0.1)	Yield (%)	Solubility[a]				
	T (°C)	Time (h)	Molar ratio (VP:AGU, mol/mol)			Chloroform	THF	Pyridine	DMF	DMSO
CP-1	60	2	3:1	0.7	42	–	++	++	++	++
CP-2	65	2	3:1	1.2	60	–	++	++	++	++
CP-3	70	2	3:1	1.5	79	+	++	++	+	+
CP-4	75	2	3:1	1.8	85	++	++	++	–	–
CP-5	80	2	3:1	2.3	71	++	++	++	–	–
CP-6	90	2	3:1	1.0	36	–	–	++	–	–
CP-7	100	2	3:1	0.9	33	–	–	++	–	–
CP-8	120	2	3:1	0.5	31	–	–	++	–	–
CP-9	70	1	3:1	0.7	38	–	++	++	++	++
CP-10	70	1.5	3:1	1.3	60	+	++	++	++	++
CP-11	70	2.5	3:1	1.2	80	–	++	++	+	+
CP-12	70	3	3:1	1.1	52	–	++	++	+	+
CP-13	70	4	3:1	1.0	38	–	–	++	–	–
CP-14	70	5	3:1	1.0	35	–	–	++	–	–
CP-15	70	2	4:1	1.6	81	+	++	++	+	+
CP-16	70	2	5:1	1.6	82	+	++	++	+	+
CP-17	70	2	6:1	1.6	83	+	++	++	+	+
CP-18	70	2	7:1	1.6	83	+	++	++	+	+
CP-19	70	2	9:1	1.6	83	+	++	++	+	+
CP-20	70	2	12:1	1.6	83	+	++	++	+	+

The concentration at which the solubility of CPs was determined was 5%.
[a] "++" Highly soluble; "+" Swellable; "–" Insoluble.

3.2. Optimizing reaction conditions of homogeneous transesterification of cellulose

Zhou et al. [42] have studied the effect of reaction temperature and reaction time on the DS of cellulose esters. It was observed that the DS of cellulose ester increased with increasing reaction temperature and time. We studied the optimization of reaction conditions for homogeneous transesterification of cellulose in more detail. The optimized reaction conditions were acquired by performing a series of CP syntheses by altering reaction parameters like reaction temperature, reaction time, and molar ratio (VP: AGU). As explained in section 2.3, a broad range of temperature, time, and molar ratio was selected, and the transesterification was carried out followed by post-reaction work-up in the identical way for the synthesized CPs. The DS of all the synthesized CPs were calculated by NMR spectroscopy as explained in section 2.4 (Table 1).
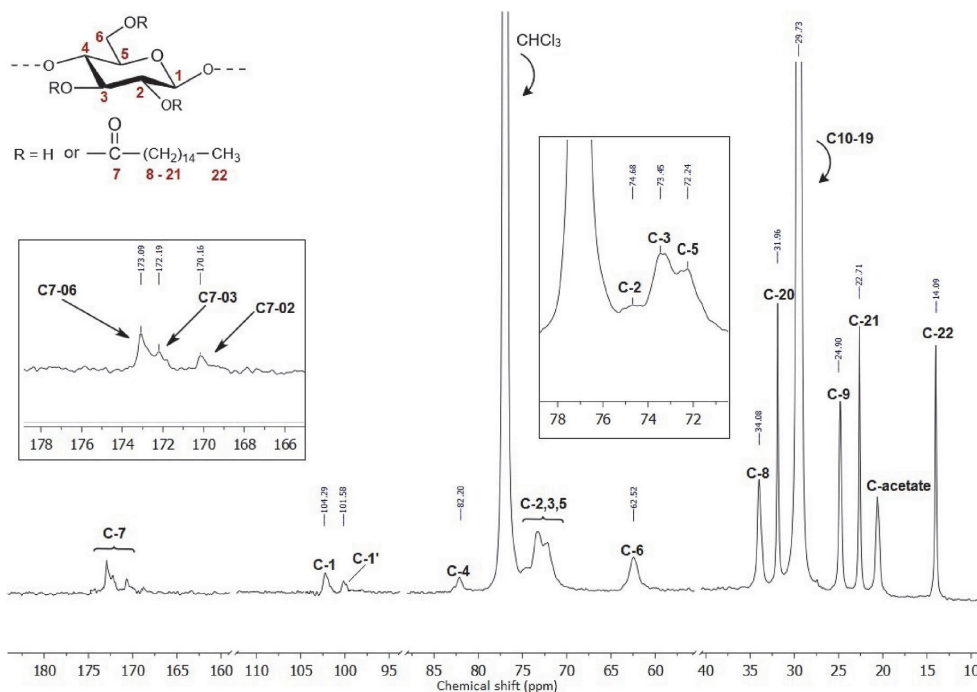
Fig. 2. ^{13}C NMR spectrum of CP-5 (DS = 2.3) in chloroform-d (125 MHz, 40 °C). Empty and solvent regions are left out for clarity. The full spectrum is available in supporting information (Fig. S1).

3.2.1. Effect of reaction temperature on DS and yield of CPs

To investigate the impact of reaction temperature on DS, CPs were synthesized within the temperature range of 60 °C–120 °C while maintaining a constant molar ratio of 3 eq./AGU and a reaction time of 2 h. Fig. 4 illustrates the relationship between DS and percent yield with reaction temperature. The results reveal that DS initially rises with increasing reaction temperature, reaching a peak value of 2.3 (CP-5), before declining to 0.5 (CP-8). Notably, there was a significant acceleration of transesterification as the temperature increased from 60 °C to 70 °C, leading to a DS increase from 0.7 (CP-1) to 1.5 (CP-3), representing a 2.1-fold enhancement. However, DS sharply decreased after reaching 80 °C, decreasing to 1.0 (CP-6), and continued to decline gradually across the studied temperature range.

Likewise, the yield of CPs displayed a gradual increase as the temperature rose from 60 °C to 75 °C, followed by a rapid decrease up to 90 °C before stabilizing. Beyond 75 °C, a noticeable color change in the reaction mixture from orange to dark brown was observed indicating potential degradation of either ionic liquid (IL) and/or cellulose, and/or CPs. The decline in both the degree of substitution (DS) and the percentage yield of cellulose palmitates (CPs) under excessive temperatures is likely attributed to CP degradation. A similar impact of reaction temperature on the DS was observed in the study conducted by Hinner et al., in 2016 [15]. In their investigation, the DS of cellulose ester, specifically laurate, exhibited a diminishing trend at elevated reaction temperatures of 90 °C and 110 °C. About the influence of reaction temperature on the final product yield, findings by Zhou et al., in 2014 [42] corroborated our observations. Their research highlighted a reduction in the cellulose ester, octanoate, yield as the reaction temperature escalated from 80 °C to 120 °C, aligning with our experimental results.

3.2.2. Effect of reaction time on DS and yield of CPs

To investigate the impact of time on the degree of substitution (DS), we periodically sampled small portions of the reaction mixture at intervals ranging from 1 to 5 h, while maintaining a constant reaction temperature of 70 °C and a molar ratio of 3 eq./AGU. Fig. 5 presents the relationship between DS and percent yield over time. During the initial hour, transesterification exhibited a notably faster, resulting in a substantial DS increase from 0.7 (CP-9) to 1.5 (CP-3), representing a 2.1-fold enhancement. However, as the reaction time extended beyond 2 h, DS began to decline, accompanied by a similar discoloration of the reaction mixture observed at elevated temperatures which indicates the possibility of degradation.

The percent yield of CPs displayed a gradual rise until the 2.5-h mark, after which it started to decrease, further supporting degradation. The reduction in CPs' percentage yield with extended reaction durations may be attributed to cellulose degradation during the protracted reaction process. A similar effect was observed by Huang et al. [13] during the homogeneous esterification of cellulose in 1-butyl-3-methylimidazolium chloride with stearyl chloride at prolonged reaction durations of 1.5–2 h and more. Furthermore, the decrease in DS of CPs with prolonged reaction times can be elucidated by the potential competition between transesterification reactions and the partial hydrolysis of ester groups generated by entrapped moisture within the reaction medium [43].

From the observations and obtained results from sections 3.3.1 and 3.3.2, we can say that there is a degradation of the either-or multiple involved chemicals has happened during the homogeneous transesterification process. A congruent pattern of discoloration in the reaction mixture, coupled with degradation of the final product, was observed at elevated temperatures and extended reaction durations during the synthesis of cellulose esters within the same solvent system, as previously reported by our group [36].
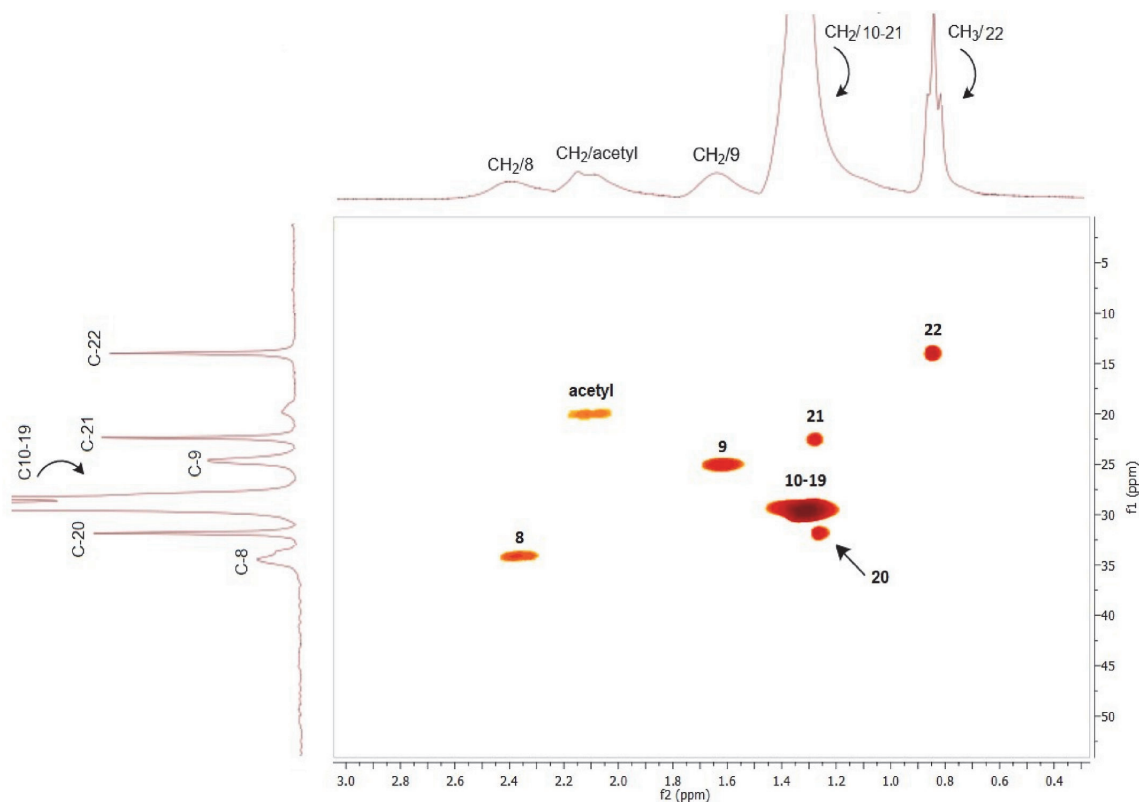
Fig. 3a. Aliphatic side chain region of HSQC spectrum of CP-5 (DS = 2.3) in chloroform-d (125 MHz, 25 °C).

3.2.3. Effect of molar ratio on DS and yield of CPs

Le Chatelier's Principle is a well-established concept indicating that an excess of one reactant can drive a reaction towards the right, leading to increased ester production and subsequently higher ester yields. To investigate the impact of the molar ratio on the degree of substitution (DS), we varied the molar ratio VP:AGU, ranging from 3:1 up to 12:1, while keeping the reaction temperature and time constant at 70 °C and 2 h, respectively. The DS exhibited a continuous increase across the chosen molar ratios, eventually stabilizing at ratios exceeding 5:1 (Fig. 6). Notably, there was no discernible discoloration in the reaction mixtures, ruling out degradation as a factor. However, due to the spatial steric effects of VP's lengthy aliphatic chain, the transesterification was impeded, resulting in the stabilization of both DS and yield beyond the 5:1 M ratio. A similar effect of the molar ratio of the esterification agent to AGU on DS and the yield of the final product was observed by Hinner et al. and Zhou et al. [15,42].

While a higher quantity of VP is desirable for achieving a higher DS in the final product, it's important to note that a substantial amount of unreacted vinyl palmitate would remain in the supernatant phase. This can pose challenges for post-reaction work-up and hinder the recycling of the ionic liquid (IL).

In comparison with the previously reported study of cellulose transesterification in (AmimCl)/DMSO solvent system in the presence of DBU catalyst which used a reaction temperature of 110 °C for the reaction time of 3 h with the molar ratio of 6:1 (vinyl ester:AGU) to get vinyl ester with DS 2.32 [41], the reported method achieved the same DS value at relatively milder reaction conditions without using any additional catalyst. In comparison with the data presented by Todorov

et al. [35], where the solvent [mTBNH][OAc] was used for the synthesis of cellulose esters at the reaction time of 20–72 h, the present method used significantly shorter reaction durations resulted in even higher DS values. Willberg-Keyriläinen et al. [44] studied the effect of the molar mass of the starting cellulose on the DS of the final cellulose palmitates. It has been found that as the molar mass of the starting cellulose increases, the DS of the final cellulose palmitates decreases. A similar reasoning can apply to our research. As the molar mass of the cellulose in the presented study is high i.e., 163.15 kg/mol, the DS of the final synthesized CPs is lower.

We further performed a series of experiments to get to know more about the stability of IL, compatibility between components of the solvent system and reactants as well as the possible degradation of the obtained final products.

3.3. Stability of solvent system at elevated temperature and time

2.0 g of pure IL (bottle 1) and a 1:1 mixture (1.0 g of each) of IL and DMSO (bottle 2) were heated at 100 °C for 5 h with continuous stirring under an inert nitrogen atmosphere in separate glass containers. After 5 h, their appearance was compared to pure IL (bottle 3) and the IL + DMSO solvent system (bottle 4), which were stored at room temperature under inert conditions.

Also, the structural analysis of all four samples was carried out by using ^{1}H NMR spectroscopy using chloroform-d as a solvent and TMS as an internal standard.

After 5 h of heating, no discoloration was observed in either the pure IL or the IL + DMSO solvent system, even at elevated temperatures and
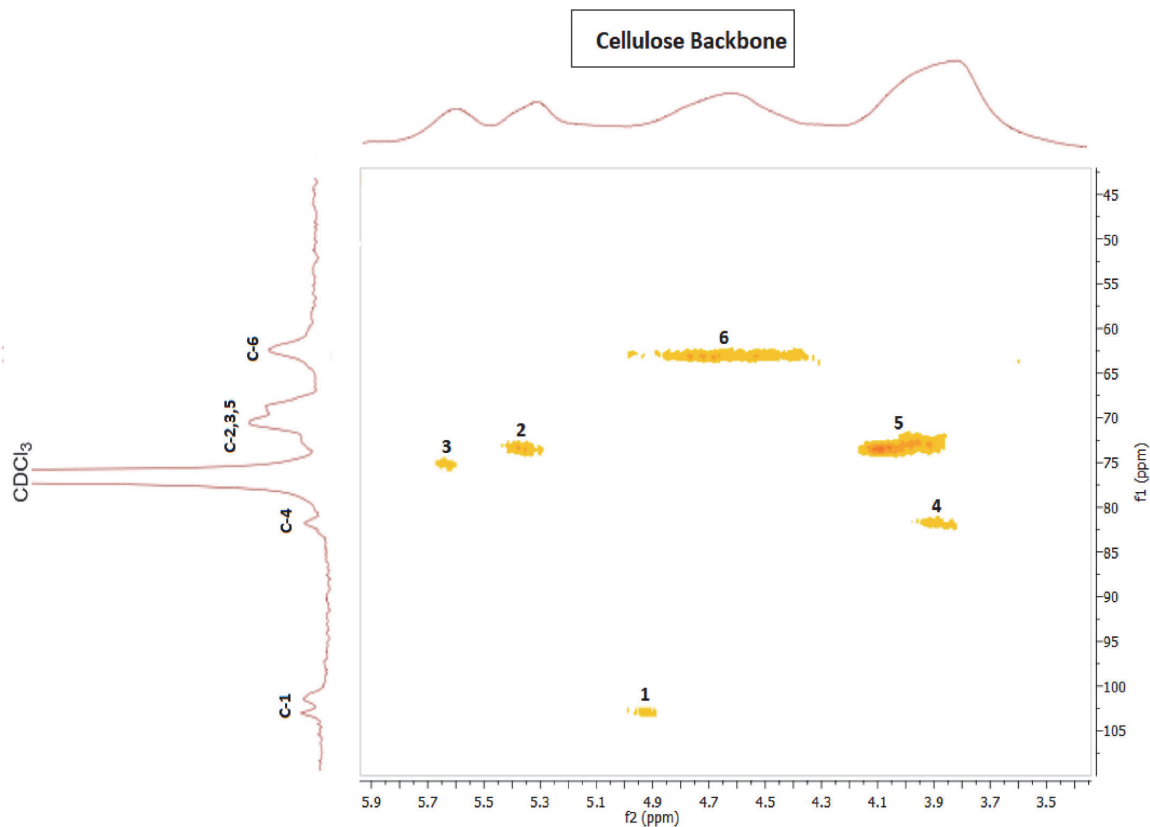
Fig. 3b. Cellulose region of HSQC spectrum of CP-5 (DS = 2.3) in chloroform-d (125 MHz, 25 °C).
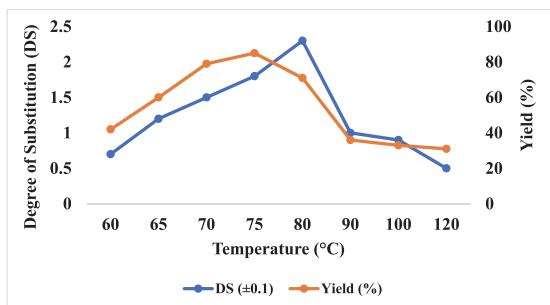

Fig. 4. Effect of reaction temperature on DS and percent yield of CPs (molar ratio of VP:AGU is 3:1; reaction time is 2 h).

Fig. 5. Effect of reaction time on DS and percent yield of CPs (molar ratio of VP:AGU is 3:1; reaction temperature is 70 °C).

extended heating durations. This observation confirms the exceptional stability of IL when exposed to high temperatures and prolonged heating. Images of all four solutions under comparison can be viewed in supporting information in Fig. S3.

We conducted a comparative analysis of the ^{1}H NMR spectra for all four solutions to substantiate our findings, as depicted in Fig. 7. The NMR investigation revealed no discernible evidence of degradation in either the pristine ionic liquid or the solvent system. These observations collectively lead us to the conclusion that the ionic liquid exhibits noteworthy stability under reaction conditions characterized by
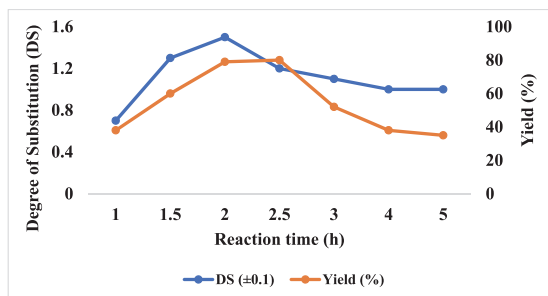
elevated temperatures and prolonged reaction durations, without undergoing any degradation, in line with the reference [Tarasova, 2023].

3.4. Compatibility of solvent system and reactants

The formation of a yellowish-orange, transparent solution consisting of the solvent system IL + DMSO and cellulose, following 5 h of heating at 100 °C under inert conditions, without any signs of discoloration or potential degradation, serves as a clear indicator of successful cellulose dissolution within the solvent system (see Fig. S4).
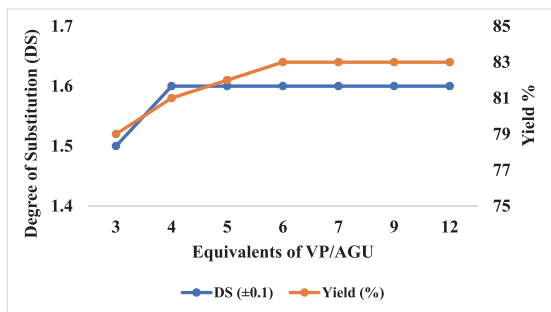
Fig. 6. Effect of molar ratio on DS and percent yield of CPs (reaction temperature is 70 °C; reaction time is 2 h).

To ascertain cellulose integrity, we determined the molecular weights of dried untreated cellulose and regenerated cellulose via intrinsic viscosity measurements (see Fig. 8). Cellulose solutions ranging from 0.2 to 1.0 g/dl in cuene as the solvent were prepared. Three measurements per sample yielded the relative viscosity, with a maximum error of 2%. The molecular weights of untreated cellulose and regenerated cellulose were 163.15 kg/mol and 162.82 kg/mol, respectively. These values allowed us to calculate the degree of polymerization (DP), which for untreated cellulose was 1007 and for regenerated cellulose was 1005, which are within experimental error.

Intrinsic viscosity measurements confirm that there was no significant cellulose degradation under elevated temperature and time in the IL + DMSO system. The DP of the regenerated cellulose closely matched that of the initial untreated cellulose, ruling out the possibility of cellulose depolymerization, in line with reference [35].

The results of Fourier-transform infrared spectroscopy (FT-IR) analysis indicated that the spectra of untreated cellulose and regenerated cellulose exhibited substantial similarity (Fig. 9). No discernible peaks corresponding to the solvent system, or the solvents utilized in the post-reaction purification process were detected. This observation suggests that the regenerated cellulose sample had undergone thorough washing and drying procedures before analysis, ensuring the removal of any residual contaminants. Carboxylate-based ionic liquids show the possibility of acetylation which is an unwanted side reaction and forms cellulose acetate as a side-product [15]. Moreover, there was no evidence of acetylation occurring during the cellulose dissolution process which is usually confirmed by the presence of carbonyl (C=O) stretch at 1750–1735 cm^{-1}. The observed absorbance peaks in the spectra of both untreated cellulose (at 3337 cm^{-1}) and regenerated cellulose (at 3392 cm^{-1}) within the range of 3310–3400 cm^{-1} were attributed to the stretching vibrations of the O–H group. Another notable peak at 2911 cm^{-1} was attributed to the stretching vibrations of the CH$_2$ group [45]. Distinctly, the peak at 1643 cm^{-1} was attributed to the C–O stretching vibration of the C–O–H group, becoming sharper in the case of regenerated cellulose [46]. Concurrently, the peak at 1428 cm^{-1} was linked to the bending motion of the CH$_2$ group, displaying a slight reduction in intensity in the regenerated cellulose spectra. This reduction indicated the potential disruption of intramolecular hydrogen bonds, specifically involving O6 in the glucose unit [47]. Furthermore, the absorbance at 1369 cm^{-1} was attributed to O–H bending, while the bands at 1215 cm^{-1} and 1157 cm^{-1} were associated with C–O stretching vibrations. The peak at 1020 cm^{-1} was attributed to the C–O bond stretching of the C–O–C group within the anhydroglucose unit (AGU) [48]. Notably, the
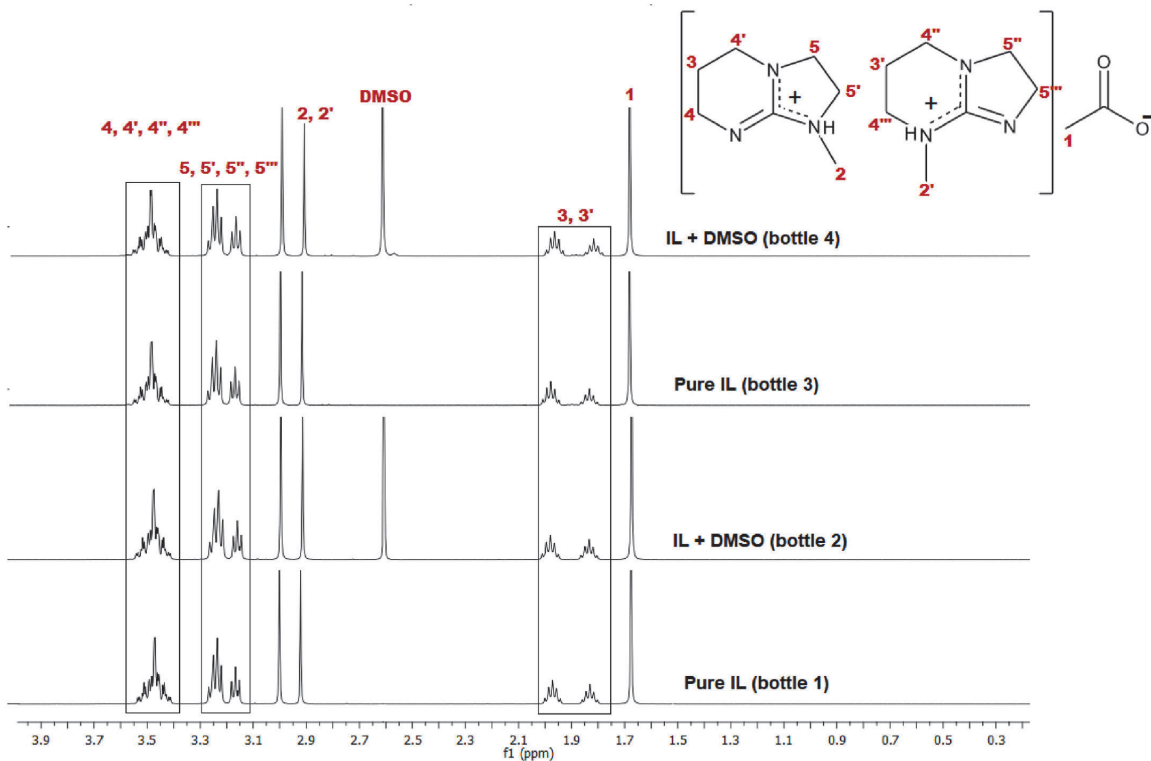

Fig. 7. ^{1}H NMR spectra of pure IL & IL + DMSO in chloroform-d (500 MHz, 25 °C).
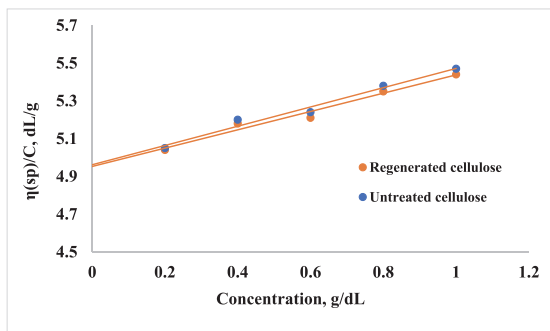
Fig. 8. Huggin's plot of specific viscosity divided by concentration (η_{sp}/C) as a function of cellulose concentration, was used to extrapolate values of intrinsic viscosity at 25 °C for regenerated and untreated cellulose dissolved in cuene.
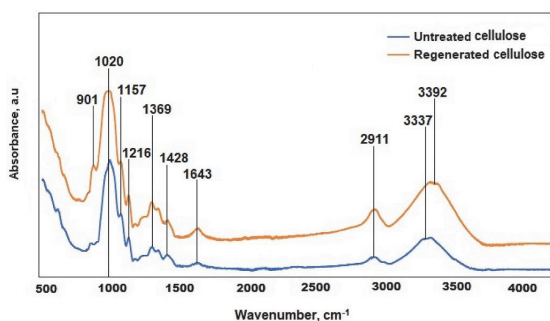

Fig. 9. FT-IT spectra of untreated cellulose and regenerated cellulose.

band at approximately 895 cm^{-1}, characteristic of β-anomers or β-linked glucose polymers, exhibited enhanced intensity in the regenerated sample, indicative of a more amorphous structural nature [47]. The O–H stretching band of the hydroxy groups at 3337 cm^{-1} in untreated cellulose shifted slightly to a higher wavenumber in regenerated cellulose i. e., 3392 cm^{-1} along with a slight sharpening of peak which further confirms weakening for intra- and intermolecular hydrogen bonding and eventually lowering crystallinity of cellulose [47]. In summary, based on the observations, it can be concluded that the cellulose structure remained largely unaffected by the presence of the solvent system

utilized in the study.

Compatibility between the solvent system [mTBNH][OAc] and the esterification agent, vinyl palmitate (VP) was assessed by preparing solvent mixtures of solvent system with a 1:4 ratio and by subjecting them to various temperatures (S1–S5, Fig. 10) and durations (S6–S9, Fig. 10). It was found that when solvent mixtures were heated at temperatures 60 °C and 70 °C for 2 h, they did not show any sign of possible degradation which can be confirmed by the orange color of both solvent mixtures. Similarly, after an hour of heating at 70 °C, the solvent mixture was quite stable which can be confirmed by the yellowish-orange color (S6). Notably, at temperatures exceeding 70 °C i.e., S3 (80 °C, 2 h), S4(90 °C, 2 h), S5 (100 °C, 2 h) and after a duration of 2 h i. e., S7 (3 h, 70 °C), S8 (4 h, 70 °C), S9 (5 h, 70 °C), the solvent mixtures exhibited a transition from initial coloration to progressively darker shades, ultimately reaching a dark brown to black hue, indicating the potential onset of degradation.

However, the precise components undergoing degradation, the underlying chemical interactions, the resulting degradation products, and whether this phenomenon is indeed degradation or something else, all remain unresolved questions at this juncture. Consequently, the author recommends further comprehensive investigations in this domain to provide definitive insights.

3.5. Degradation of CPs synthesized at elevated reaction temperature and time

The intrinsic viscosity [η] is directly correlated with the molar mass (MM) through Equation (2). By knowing the intrinsic viscosity [η] of cellulose palmitate (CP) solutions, it becomes feasible to estimate and compare the molar mass of different CP samples. Regrettably, this represents the sole reliable approach for conducting comparative analyses of CPs based on their molar mass. This is due to the challenges associated with determining molar mass through gel permeation chromatography (GPC) or static light scattering (SLS), primarily caused by the very low values of the specific refractive index increment (dn/dc), which are less than 0.1. These low values of dn/dc render the system "blind" in light scattering patterns, leading to inaccuracies in the determination of molar mass.

The degradation of CPs at elevated reaction temperatures and prolonged reaction times can be elucidated through the analysis of specific viscosity (η_{sp}) plotted against the concentration of the CP solution (Fig. 11a and b). To investigate CP degradation under elevated temperatures, CPs synthesized at 70 °C, 75 °C, and 80 °C were examined. Fig. 11a illustrates that samples prepared at 70 °C (CP-3, DS = 1.5) and 75 °C (CP-4, DS = 1.8) exhibit similar behavior. [η] value of CP-4 is slightly lower than CP-3. However, a noticeable decrease in [η] is
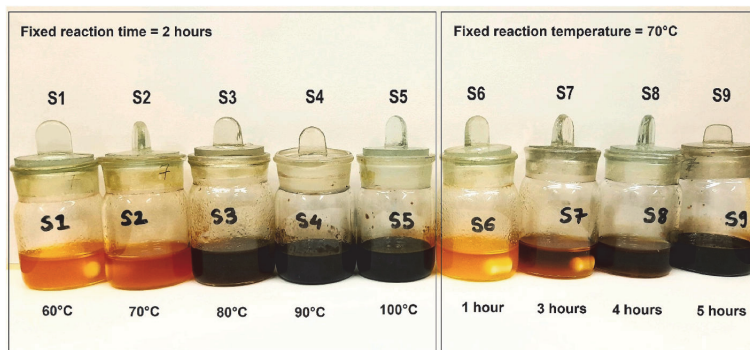

Fig. 10. A comparative study explaining compatibility between solvent system [mTBNH][OAc] and VP at different temperatures with solvent mixtures S1(60 °C, 2 h), S2(70 °C, 2 h), S3(80 °C, 2 h), S4(90 °C, 2 h), S5 (100 °C, 2 h) and times S6(70 °C, 1 h), S7(70 °C, 3 h), S8(70 °C, 4 h) & S9(70 °C, 5 h).
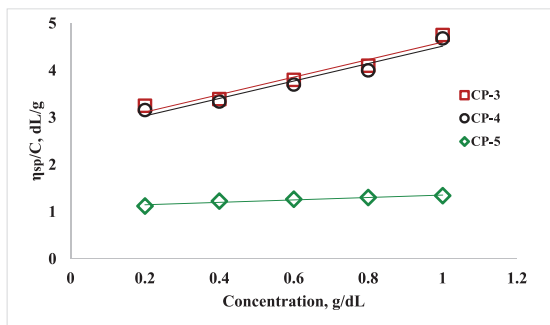
Fig. 11a. Huggin's plot of specific viscosity divided by concentration (η_{sp}/C) as a function of CP concentration was used to extrapolate values of intrinsic viscosity at 25 °C for CP-3, CP-4, and CP-5 dissolved in pyridine.
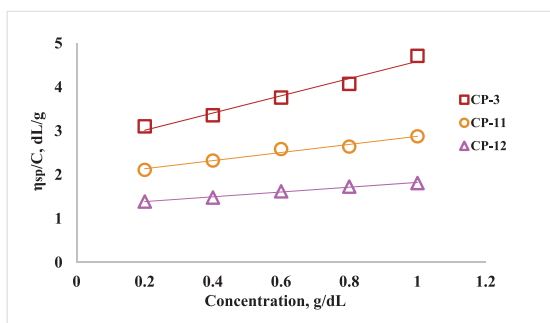

Fig. 11b. Huggin's plot of specific viscosity divided by concentration (η_{sp}/C) as a function of CP concentration, was used to extrapolate values of intrinsic viscosity at 25 °C for CP-3, CP-11, and CP-12 dissolved in pyridine.

evident as the reaction temperature increases to 80 °C, even though DS increases (CP-5, DS = 2.3). Given the viscosity-average MM of cellulose (163 kDa), the MM of vinyl palmitate (282 Da), and a specific degree of substitution (DS), it is feasible to make estimations regarding the molar mass of cellulose palmitate at distinct DS levels. It is important to note that the viscosity-average MM, typically slightly exceeds the actual number average molecular weight, M_n. The calculated molar masses for CP-3, CP-4, and CP-5 are approximately 520 kDa, 590 kDa, and 710 kDa, respectively. It means, that the expected intrinsic viscosity of CP-4 should be higher than for CP-3, and CP-5 should demonstrate the highest values of intrinsic viscosities among all samples. However, the viscosity of the samples exhibits a declining trend, with a pronounced decrease in viscosity observed for CP-5. This reduction in viscosity is indicative of the degradation of cellulose palmitates, commencing at a reaction temperature of 75 °C.

For CPs synthesized with extended reaction times, specifically CP-11 (2.5 h, DS = 1.2) and CP-12 (3 h, DS = 1.1), a gradual decline in intrinsic viscosity was observed (Fig. 11b). Due to the difference in DS, the expected MM values of CP-11 and CP-12 are 450 kDa and 420 kDa, respectively, which are lower than CP-3 (520 kDa). The observed (in Fig. 11b) decrease in viscosity can be attributed both to the decrease in DS and possible degradation of CP with prolonged reaction time.

It is known that changes in intrinsic viscosity can be assigned both by MM and thermodynamic properties of polymers. Fig. 12 depicts the Wolf plot for reduced viscosity of CP solutions in pyridine. The Wolf plot provides master curves using C[η], independent of molecular mass (MM), with the slope of the line reflecting the sample's structure and hydrodynamic properties. As can be seen, all CP data are superimposed,
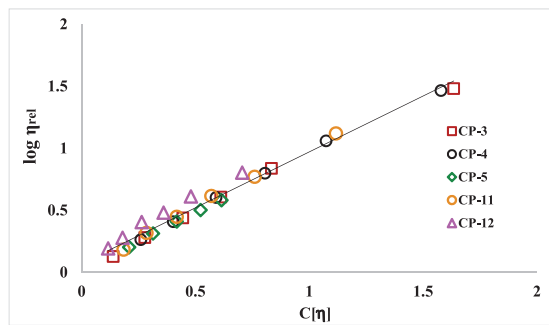

Fig. 12. Reduced Wolf plot (logarithm of relative viscosity as a function of reduced polymer concentration) for the solutions of CP-3, CP-4, CP-5, CP-11, and CP-12 at 25 °C dissolved in pyridine.

indicating identical hydrodynamic properties of the materials. Consequently, a decrease in [η] is caused by a reduction in MM and not by changes in thermodynamic properties.

Therefore, for the synthesis of cellulose palmitates in [mTBNH] [OAc]/DMSO solvent system using vinyl palmitate via transesterification, it is advisable to use reaction temperatures below 80 °C and reaction durations less than 3 h. Therefore, by considering all the information obtained by the above experiments, the optimum conditions were chosen as 70 °C and 2 h which give the highest DS without degradation. Since the synthesis of FACEs with higher DS needs a higher molar ratio but at the same time an excessive amount of unreacted esterification agent interferes with the final purification of the FACEs and recycling of solvent system, the ideal value of VP:AGU molar ratio should be 5:1.

3.6. Solubility test

We investigated the solubility of prepared CPs in five different solvents (Table 1). We selected chloroform, tetrahydrofuran (THF), pyridine, N,N-Dimethylformamide (DMF), and dimethyl sulfoxide (DMSO). Our investigation revealed that all CPs exhibited a notably high degree of solubility in pyridine. This remarkable solubility can likely be attributed to the presence of hydrophobic fatty acid long-chain ester moieties along the cellulose backbone [49,50]. Furthermore, we observed that CPs with higher degrees of substitution (DS), denoted as CP-4 (DS = 1.8) and CP-5 (DS = 2.3), displayed solubility in the non-polar solvent chloroform. This enhanced solubility in chloroform can be attributed to the increased non-polar characteristics conferred by the higher DS values. In contrast, CPs with DS values on the lower end of the spectrum, specifically CP-1 (DS = 0.7), CP-2 (DS = 1.2), CP-9 (DS = 0.7), and CP-10 (DS = 1.3), exhibited solubility in aprotic polar solvents such as DMF and DMSO. Interestingly, we noted that CPs that had undergone degradation under elevated reaction temperatures and prolonged reaction times (CP-6, CP-7, CP-8, CP-13, CP-14) displayed a lack of solubility in any of the solvents, except for pyridine. Pyridine is the strongest in terms of forming hydrogen bonds with cellulose esters. Its nitrogen atom can serve as a hydrogen bond acceptor, allowing it to interact with the hydroxy and ester groups in cellulose esters. Pyridine's ability to engage in both hydrogen bonding and dipole-dipole interactions makes it highly effective at dissolving cellulose esters. Tetrahydrofuran (THF), which falls into the category of moderately polar solvents, demonstrated the ability to dissolve CPs across a wide range of DS values. Cellulose palmitates have a combination of polar (ester group) and non-polar (cellulose backbone) regions. THF's moderate polarity strikes a balance, making it effective at dissolving CPs with different DS. THF can engage in dipole-dipole interactions with cellulose esters which make it a good solvent for cellulose ester

dissolution. Also, THF is a relatively small solvent molecule compared to DMSO and DMF which are larger and more polar. The smaller size of THF allows it to penetrate cellulose ester structure more easily, promoting better solvation.

4. Conclusions

This study introduces sustainable, catalyst-free homogeneous cellulose transesterification using novel superbase ionic liquid [mTBNH] [OAc]) with a co-solvent, DMSO to synthesize cellulose palmitates (CPs) which are long-chain fatty acid esters that have substantial potential for application as valuable functional materials. The CPs with various degree of substitution (DS) values (0.5–2.3) can be obtained by controlling the reaction temperature, reaction time, and the molar ratio of vinyl palmitate to AGU. Notably, our research highlights the stability of this previously unreported solvent system at high temperatures and long reaction times, its compatibility with the reactants involved, and the intrinsic viscosity analysis of CPs. This study also confirms the order of OH group substitution in cellulose units: C6–OH > C2–OH > C3–OH, aligning with our earlier research [36]. The DS of CPs initially rises, then drops notably at elevated reaction temperatures and times. This corresponds with decreased yield and visible discoloration of the reaction mixture, suggesting possible degradation. Interestingly, using higher ratios of VP:AGU (above 5:1 at 70 °C, 2 h) maintained stable DS and yield without discoloration. The solvent system remained stable at high temperatures and times, not harming cellulose, or inducing unwanted reactions during its dissolution. Yet, pieces of evidence indicate the formation of a by-product, cellulose acetate, during transesterification. The authors propose a comprehensive investigation to elucidate the mechanism underlying this undesired by-product formation. When mixed with the esterification agent, vinyl palmitate, discoloration occurred at temperatures above 70 °C and durations beyond 2 h, indicating potential degradation. At present, it is challenging to provide specific insights into the exact components undergoing degradation, the underlying chemical interactions, the resulting degradation products, or whether this observed phenomenon indeed constitutes degradation or another chemical process. We recommend that further comprehensive research in this domain is essential to elucidate these aspects. The intrinsic viscosity of cellulose palmitates (CPs) synthesized at elevated reaction conditions, was found to be lower than that of CP synthesized at 70 °C for 2 h. Despite this variation, their hydrodynamic properties remained similar, indicating that the intrinsic viscosities of CPs are attributed to a reduction in molar mass, thus confirming the occurrence of degradation. As a result, the authors recommend that the solvent system described in this work be used with relatively mild reaction parameters, such as a reaction temperature of 70 °C, a reaction time of 2 h, and a molar ratio of 5:1, particularly when synthesizing fatty acid cellulose esters (FACEs) through transesterification using vinyl esters in the presented solvent system [mTBNH][OAc]/DMSO.

CRediT authorship contribution statement

N. Savale: Writing – original draft, Visualization, Validation, Methodology, Investigation, Formal analysis, Data curation, Conceptualization. **E. Tarasova:** Writing – review & editing, Visualization, Validation, Supervision, Methodology, Investigation, Formal analysis, Data curation, Conceptualization. **I. Krasnou:** Writing – review & editing, Methodology, Investigation, Data curation. **M. Kudrjašova:** Visualization, Validation, Investigation. **V. Rjabovs:** Visualization, Validation, Investigation. **I. Reile:** Visualization, Validation, Investigation. **I. Heinmaa:** Visualization, Validation, Investigation. **A. Krumme:** Writing – review & editing, Supervision, Resources, Project administration, Funding acquisition, Conceptualization.

Declaration of competing interest

The authors declare that they have no known competing financial interests or personal relationships that could have appeared to influence the work reported in this paper.

Data availability

Data will be made available on request.

Appendix A. Supplementary data

Supplementary data to this article can be found online at https://doi.org/10.1016/j.carres.2024.109047.

References

[1] A. Pinkert, K.N. Marsh, S. Pang, M.P. Staiger, Ionic liquids and their interaction with cellulose, Chem. Rev. 109 (12) (2009) 6712–6728.
[2] L. Feng, Z.L. Chen, Research progress on dissolution and functional modification of cellulose in ionic liquids, J. Mol. Liq. 142 (1–3) (2008) 1–5.
[3] X. Qiu, S. Hu, "Smart" materials based on cellulose: a review of the preparations, properties, and applications, Materials 6 (3) (2013) 738–781.
[4] I.I. Rubin, Handbook of Plastic Materials and Technology, 1990. No Title.
[5] T. Heinze, T. Liebert, Unconventional methods in cellulose functionalization, Prog. Polym. Sci. 26 (9) (2001) 1689–1762.
[6] G.T. Ciacco, T.F. Liebert, E. Frollini, T.J. Heinze, Application of the solvent dimethyl sulfoxide/tetrabutyl-ammonium fluoride trihydrate as reaction medium for the homogeneous acylation of Sisal cellulose, Cellulose 10 (2003) 125–132.
[7] B.A. Ass, G.T. Ciacco, E. Frollini, Cellulose acetates from linters and sisal: correlation between synthesis conditions in DMAc/LiCl and product properties, Bioresour. Technol. 97 (14) (2006) 1696–1702.
[8] H.P. Fink, P. Weigel, H.J. Purz, J. Ganster, Structure formation of regenerated cellulose materials from NMMO-solutions, Prog. Polym. Sci. 26 (9) (2001) 1473–1524.
[9] J. Cai, L. Zhang, Rapid dissolution of cellulose in LiOH/urea and NaOH/urea aqueous solutions, Macromol. Biosci. 5 (6) (2005) 539–548.
[10] P. Mäki-Arvela, I. Anugwom, P. Virtanen, R. Sjöholm, J.P. Mikkola, Dissolution of lignocellulosic materials and its constituents using ionic liquids—a review, Ind. Crop. Prod. 32 (3) (2010) 175–201.
[11] S. Han, J. Li, S. Zhu, R. Chen, Y. Wu, X. Zhang, Z. Yu, Potential applications of ionic liquids in wood related industries, Bioresources 4 (2) (2009).
[12] J.D. Holbrey, K.R. Seddon, Ionic liquids, Clean Prod. Process. 1 (4) (1999) 223–236.
[13] K. Huang, J. Xia, M. Li, J. Lian, X. Yang, G. Lin, Homogeneous synthesis of cellulose stearates with different degrees of substitution in ionic liquid 1-butyl-3-methylimidazolium chloride, Carbohydr. Polym. 83 (4) (2011) 1631–1635.
[14] S. Köhler, T. Liebert, M. Schöbitz, J. Schaller, F. Meister, W. Günther, T. Heinze, Interactions of ionic liquids with polysaccharides 1. Unexpected acetylation of cellulose with 1-Ethyl-3-methylimidazolium acetate, Macromol. Rapid Commun. 28 (24) (2007) 2311–2317.
[15] L.P. Hinner, J.L. Wissner, A. Beurer, B.A. Nebel, B. Hauer, Homogeneous vinyl ester-based synthesis of different cellulose derivatives in 1-ethyl-3-methyl-imidazolium acetate, Green Chem. 18 (22) (2016) 6099–6107.
[16] C. Xu, Z. Cheng, Thermal stability of ionic liquids: current status and prospects for future development, Processes 9 (2) (2021) 337.
[17] M. Kostag, M. Gericke, T. Heinze, O.A. El Seoud, Twenty-five years of cellulose chemistry: Innovations in the dissolution of the biopolymer and its transformation into esters and ethers, Cellulose 26 (2019) 139–184.
[18] T. Kakko, A.W. King, I. Kilpeläinen, Homogenous esterification of cellulose pulp in [DBNH][OAc], Cellulose 24 (2017) 5341–5354.
[19] A. Parviainen, R. Wahlström, U. Liimatainen, T. Liitiä, S. Rovio, J.K.J. Helminen, I. Kilpeläinen, Sustainability of cellulose dissolution and regeneration in 1, 5-diazabicyclo [4.3. 0] non-5-enium acetate: a batch simulation of the IONCELL-F process, RSC Adv. 5 (85) (2015) 69728–69737.
[20] W. Ahmad, A. Ostonen, K. Jakobsson, P. Uusi-Kyyny, V. Alopaeus, U. Hyväkkö, A. W. King, Feasibility of thermal separation in recycling of the distillable ionic liquid [DBNH][OAc] in cellulose fiber production, Chem. Eng. Res. Des. 114 (2016) 287–298.

[21] A.W. King, J. Asikkala, I. Mutikainen, P. Järvi, I. Kilpeläinen, Distillable acid–base conjugate ionic liquids for cellulose dissolution and processing, Angew. Chem. Int. Ed. 50 (28) (2011) 6301–6305.

[22] S. Elsayed, J. Helminen, S. Hellsten, C. Guizani, J. Witos, M. Rissanen, H. Sixta, Correction to "recycling of superbase-based ionic liquid solvents for the production of textile-grade regenerated cellulose fibers in the lyocell process", ACS Sustain. Chem. Eng. 8 (49) (2020), 18345-18345.

[23] S.K. Mikkola, A. Robciuc, J. Lokajova, A.J. Holding, M. Lämmerhofer, I. Kilpelainen, S.K. Wiedmer, Impact of amphiphilic biomass-dissolving ionic liquids on biological cells and liposomes, Environ. Sci. Technol. 49 (3) (2015) 1870–1878.

[24] T. Heinze, S. Dorn, M. Schöbitz, T. Liebert, S. Köhler, F. Meister, Interactions of ionic liquids with polysaccharides–2: cellulose, Macromol. Symp. 262 (1) (2008, January) 8–22. Weinheim: WILEY-VCH Verlag.

[25] Y. Yang, H. Xie, E. Liu, Acylation of cellulose in reversible ionic liquids, Green Chem. 16 (6) (2014) 3018–3023.

[26] R. Kakuchi, M. Yamaguchi, T. Endo, Y. Shibata, K. Ninomiya, T. Ikai, K. Takahashi, Efficient and rapid direct transesterification reactions of cellulose with isopropenyl acetate in ionic liquids, RSC Adv. 5 (88) (2015) 72071–72074.

[27] A. Ostonen, J. Bervas, P. Uusi-Kyyny, V. Alopaeus, D.H. Zaitsau, V. N. Emel'yanenko, S.P. Verevkin, Experimental and theoretical thermodynamic study of distillable ionic liquid 1, 5-diazabicyclo [4.3. 0] non-5-enium acetate, Ind. Eng. Chem. Res. 55 (39) (2016) 10445–10454.

[28] M.A. Martins, F.H. Sosa, I. Kilpeläinen, J.A. Coutinho, Physico-chemical characterization of aqueous solutions of superbase ionic liquids with cellulose dissolution capability, Fluid Phase Equil. 556 (2022) 113414.

[29] R. Rinaldi, Instantaneous dissolution of cellulose in organic electrolyte solutions, Chem. Commun. 47 (1) (2011) 511–513.

[30] S.J. Lee, H.S. Lee, S.W. Jeong, H.C. Kim, S.G. Lee, T.H. Oh, Effect of dimethyl sulfoxide on synthesis of thermoplastic cellulose-Graft-poly (l-lactide) copolymer using ionic liquid as reaction media, J. Appl. Polym. Sci. 132 (4) (2015).

[31] D. Hirose, S.B.W. Kusuma, S. Nomura, M. Yamaguchi, Y. Yasaka, R. Kakuchi, K. Takahashi, Effect of anion in carboxylate-based ionic liquids on catalytic activity of transesterification with vinyl esters and the solubility of cellulose, RSC Adv. 9 (7) (2019) 4048–4053.

[32] K.N. Onwukamike, S. Grelier, E. Grau, H. Cramail, M.A. Meier, Sustainable transesterification of cellulose with high oleic sunflower oil in a DBU-CO2 switchable solvent, ACS Sustain. Chem. Eng. 6 (7) (2018) 8826–8835.

[33] L. Crépy, L. Chaveriat, J. Banoub, P. Martin, N. Joly, Synthesis of cellulose fatty esters as plastics—influence of the degree of substitution and the fatty chain length on mechanical properties, ChemSusChem: Chem. Sustain. Energy Mater. 2 (2) (2009) 165–170.

[34] L. Duchatel-Crépy, N. Joly, P. Martin, A. Marin, J.F. Tahon, J.M. Lefebvre, V. Gaucher, Substitution degree and fatty chain length influence on structure and properties of fatty acid cellulose esters, Carbohydr. Polym. 234 (2020) 115912.

[35] A.R. Todorov, A.W. King, I. Kilpeläinen, Transesterification of cellulose with unactivated esters in superbase–acid conjugate ionic liquids, RSC Adv. 13 (9) (2023) 5983–5992.

[36] E. Tarasova, N. Savale, I. Krasnou, M. Kudrjašova, V. Rjabovs, I. Reile, A. Krumme, Preparation of thermoplastic cellulose esters in [mTBNH][OAC] ionic liquid by transesterification reaction, Polymers 15 (19) (2023) 3979.

[37] F.H. Sosa, I. Kilpeläinen, J. Rocha, J.A. Coutinho, Recovery of Superbase Ionic Liquid Using Aqueous Two-phase Systems, Fluid Phase Equilibria, 2023 113857.

[38] D.W. Lowman, Characterization of Cellulose Esters by Solution-State and Solid-State NMR Spectroscopy, 1998.

[39] J. Brandrup, E.H. Immergut, E.A. Grulke, A. Abe, D.R. Bloch (Eds.), Polymer Handbook, vol. 89, Wiley, New York, 1999.

[40] T. Heinze, T. Liebert, B. Heublein, S. Hornig, Functional polymers based on dextran, Polysaccharides Ii (2006) 199–291.

[41] X. Wen, H. Wang, Y. Wei, X. Wang, C. Liu, Preparation and characterization of cellulose ester by catalyzed transesterification, Carbohydr. Polym. 168 (2017) 247–254.

[42] Y. Zhou, D.Y. Min, Z. Wang, Y. Yang, S. Kuga, Cellulose esterification with octanoyl chloride and its application to films and aerogels, Bioresources 9 (3) (2014) 3901–3908.

[43] C.S.R. Freire, A.J.D. Silvestre, C.P. Neto, M.N. Belgacem, A. Gandini, Controlled heterogeneous modification of cellulose fibers with fatty acids: effect of reaction conditions on the extent of esterification and fiber properties, J. Appl. Polym. Sci. 100 (2) (2006) 1093–1102.

[44] P. Willberg-Keyriläinen, R. Talja, S. Asikainen, A. Harlin, J. Ropponen, The effect of cellulose molar mass on the properties of palmitate esters, Carbohydr. Polym. 151 (2016) 988–995.

[45] H. Lateef, S. Grimes, P. Kewcharoenwong, B. Feinberg, Separation and recovery of cellulose and lignin using ionic liquids: a process for recovery from paper-based waste, J. Chem. Technol. Biotechnol. 84 (12) (2009) 1818–1827.

[46] Z. Liu, H. Wang, Z. Li, X. Lu, X. Zhang, S. Zhang, K. Zhou, Characterization of the regenerated cellulose films in ionic liquids and rheological properties of the solutions, Mater. Chem. Phys. 128 (1–2) (2011) 220–227.

[47] N.A. El-Wakil, M.L. Hassan, Structural changes of regenerated cellulose dissolved in FeTNa, NaOH/thiourea, and NMMO systems, J. Appl. Polym. Sci. 109 (5) (2008) 2862–2871.

[48] M.A. Murakami, Y. Kaneko, J.I. Kadokawa, Preparation of cellulose-polymerized ionic liquid composite by in-situ polymerization of polymerizable ionic liquid in cellulose-dissolving solution, Carbohydr. Polym. 69 (2) (2007) 378–381.

[49] Y. Guo, X. Wang, D. Li, H. Du, X. Wang, R. Sun, Synthesis and characterization of hydrophobic long-chain fatty acylated cellulose and its self-assembled nanoparticles, Polym. Bull. 69 (2012) 389–403.

[50] H. Nawaz, J. Zhang, W. Tian, J. Wu, J. Zhang, Chemical modification of cellulose in solvents for functional materials, in: Encyclopedia of Sustainability Science and Technology, Springer New York, New York, NY, 2018, pp. 1–34.

Supporting information
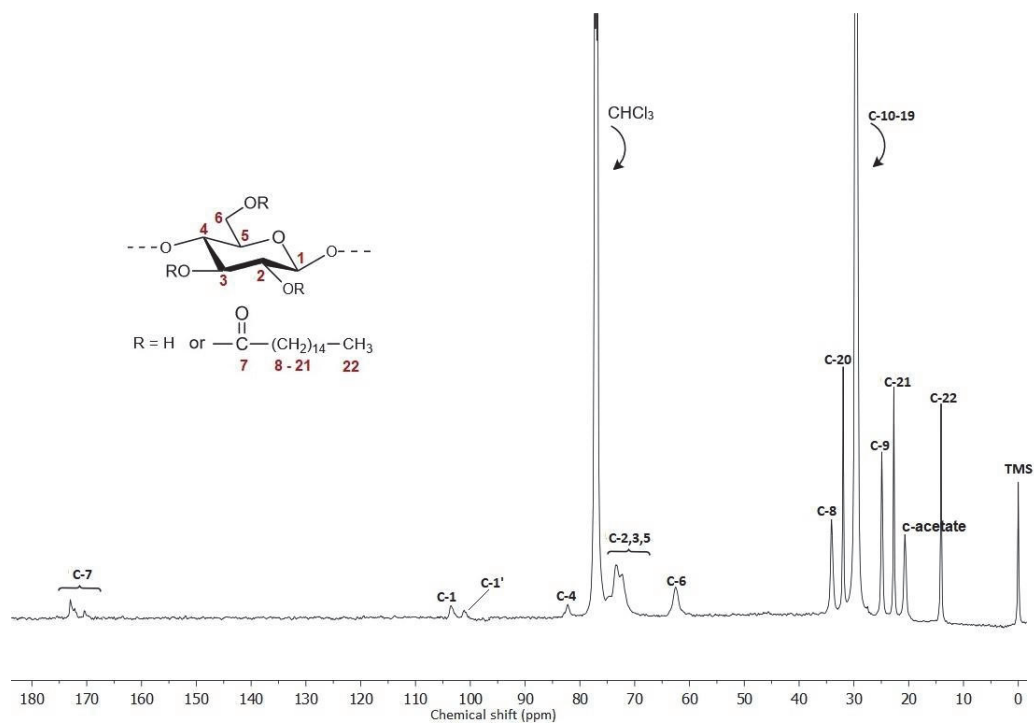
Figure S1. Full ^{13}C NMR spectrum of CP-5 (DS= 2.3) in chloroform-d (125 MHz, 40°C).
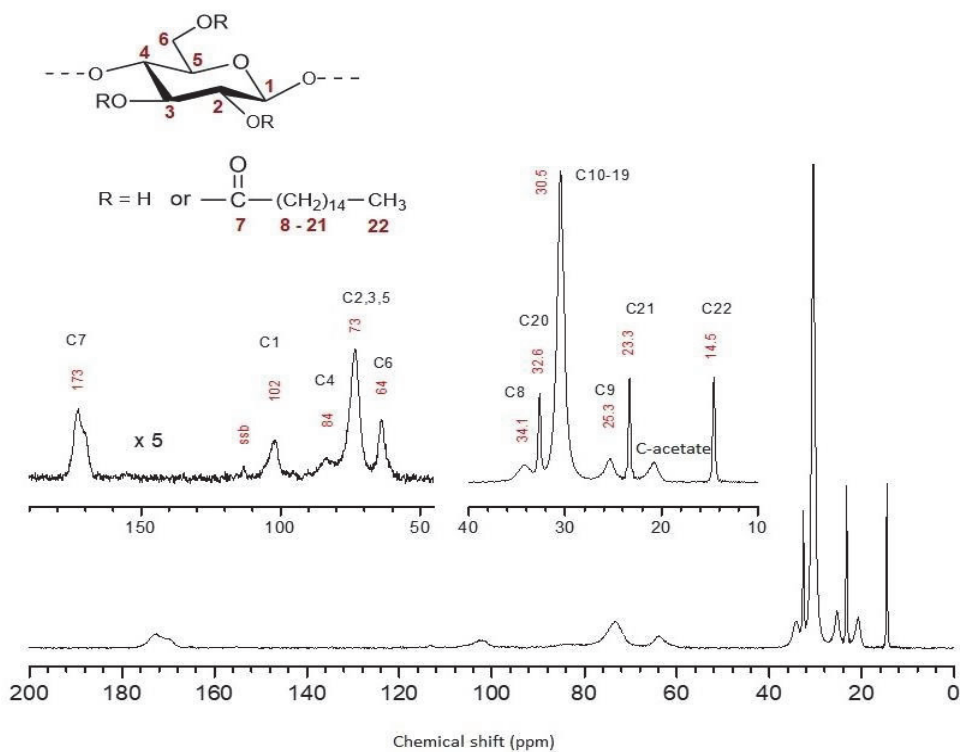
Figure S2. ^{13}C MAS NMR spectrum of CP-5 ((DS= 2.3, 4000 scans, relaxation delay 30 s). The chemical shifts of the peaks are given in red.
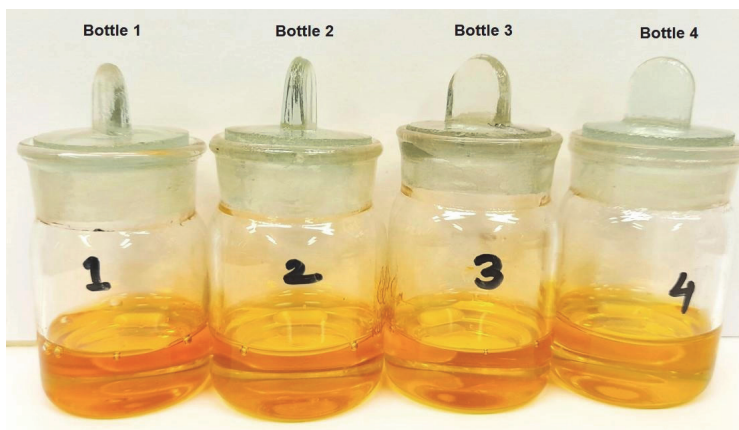
Figure S3. A comparative study of pure IL (Bottle 1) and IL+DMSO (Bottle 2) heated at 100°C for 5 hours with pure IL (Bottle 3) and IL+DMSO (Bottle 4) stored at RT.
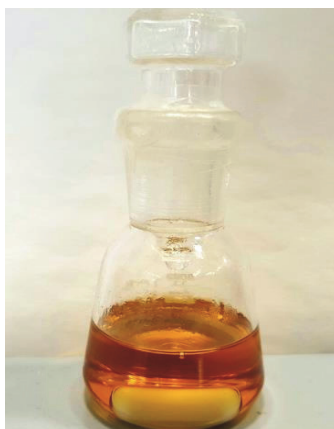
Figure S4. The mixture of cellulose and IL+DMSO after heating for 5 hours at 100°C under an inert atmosphere.

Publication III

Tarasova, E., Savale, N., Ausmaa, P. M., Krasnou, I., & Krumme, A. (2024). Rheology and dissolution capacity of cellulose in novel [mTBNH][OAc] ionic liquid mixed with green co-solvents. Rheologica Acta, 63(2), 167–178.

ORIGINAL CONTRIBUTION

Rheology and dissolution capacity of cellulose in novel [mTBNH][OAc] ionic liquid mixed with green co-solvents

Elvira Tarasova[1] · Nutan Savale[1] · Peeter-Mihkel Ausmaa[1] · Illia Krasnou[1] · Andres Krumme[1]

Abstract

Dissolution of cellulose is crucial for its regeneration and chemical modification, such as homogeneous transesterification, for example. The cellulose dissolution in ionic liquid (IL) media is suggested as a prospective environmentally friendly alternative to conventional solvents. In this study, novel distillable ionic liquid 5-methyl-1,5,7-triaza-bicyclo-[4.3.0]non-6-enium acetate, [mTBNH][OAc] was used for cellulose dissolution. This IL has high dissolving power towards cellulose and durability for recycling. However, the disadvantage of ILs is their high viscosity, which limits the supreme cellulose concentration in IL solutions, and their high cost, hindering their commercialization. The addition of low-viscous, low-cost, and naturally derived co-solvents can reduce the overall viscosity and cost. In this study, rheology experiments were conducted to investigate the flow behavior of cellulose in [mTBNH][OAc] ionic liquid mixed with the green co-solvents such as γ-Valerolactone (GVL), dimethyl isosorbide (DMI), and N,N′-dimethylpropyleneurea (DMPU). A study of the rheology showed that the viscosity reduces at low doses of co-solvent ($\leq$ 50 wt%) but causes the structuring of the cellulose solution and its gelation (or phase separation) at high doses ($\geq$ 50 wt%). The rheological study also indicated that the flow activation energy of cellulose in IL/co-solvent systems is lower than that in pure IL and decays in the order of DMPU > DMI > GVL > DMSO.

Keywords Green solvents · Dissolution capacity · Cellulose solutions · Rheology · [mTBNH][OAc] ionic liquid

Introduction

Cellulose is the most important biopolymer from renewable resources to produce polymeric materials and composites. However, cellulose contains many strong intra- and intermolecular hydrogen bonds. Its semi-rigid chain structure creates the obstacles in its dissolution using traditional organic and inorganic solvents that is a major hindrance to its processing and applications (Qiu and Hu 2013) (Lv et al. 2012). Although the process of the cellulose dissolution varies from solvent to solvent, it is believed that to dissolve cellulose, the inter- and intramolecular hydrogen bonds inside cellulose structure should be destroyed (Liebert 2010). Hence, as a key problem for the cellulose chemical processing and modification, its dissolution in proper solvents has fascinated researchers to find more novel effective solvents or

their combinations (McCormick and Lichatowich 1979) (Fink et al. 2001).

During past decades, a large number of solvent systems were developed to dissolve cellulose, for example, *N*-methylmorpholine *N*-oxide (Fink et al. 2001), *N,N*-dimethylacetamide–lithium chloride (McCormick and Dawsey 1990), and dimethylsulfoxide (DMSO)–tetrabutylammonium fluoride (Heinze et al. 2000), DMSO/KOH (Cao et al. 2013). Used organic solvents are hard to recover, and it reduces the economic feasibility of production and has harmful effects on the environment.

Fortunately, a relatively "green" group of solvents for cellulose—ionic liquids (ILs)—has been invented, and their development continues (Mäki-Arvela et al. 2010). Nowadays, the number of different ILs is nearly unlimited due to the high number of anions and cations that can be combined. Although the first mention of IL has been done in 1914 by Walden (Walden 1914), the possibility of some ILs of imidazolium type to dissolve cellulose was confirmed only in 2002 (Swatloski et al. 2002). Currently, the cellulose can be efficiently dissolved in many ILs. ILs are not volatile; they do not evaporate into the atmosphere causing humans

✉ Elvira Tarasova
    elvira.tarasova@taltech.ee

1   School of Engineering, Department of Materials
    and Environmental Technology, Tallinn University
    of Technology, Ehitajate tee 5, 19086 Tallinn, Estonia

and animals inhalation, ozone depletion, or any climate change (Han et al. 2009) (Flieger and Flieger 2020) (Isik et al. 2014). ILs are the best candidates for upscaling and commercialization in areas regarding environmental and economic aspects.

Up to now, 1-ethyl-3-metyl-imidazolium acetate ([Emim] [OAc]) ionic liquid was considered one of the best ILs for laboratory research which has sufficient solubility to cellulose (Köhler et al. 2007). However, the first generations of imidazolium-based IL-s are complicated products regarding recycling. Their stability is questionable (Xu and Cheng 2021; Kostag et al. 2019), and they cannot be easily distilled due to very low vapor pressure.

Superbases (mostly di- or triazabicyclo compounds) originating from protonic ILs are the most novel and promising solvents both for cellulose dissolution/modification and upscaling due to several reasons. They can dissolve cellulose to a high extent (up to 25 wt%, for the cellulose with degree of polymerization (DP) around 200–300), have low moisture sensitivity, and low toxicity, and can be recycled repeatedly without degradation (King et al. 2011) (Elsayed et al. 2020) (Ostonen et al. 2016).

More recently, 5-methyl-1,5,7-triaza-bicyclo[4.3.0]non-6-enium acetate, [mTBNH][OAc], was offered as a good candidate for cellulose dissolution and regeneration (Martins et al. 2022) (Parviainen et al. 2015). The superbase mTBN shows better stability in water than 7-methyl-1,5,7-triazabi-cyclo[4.4.0]dec-5-enium (mTBD) (Martins et al. 2022) and DBN (Ostonen et al. 2016). Furthermore, [mTBNH][OAc] is a liquid at room temperature (Elsayed et al. 2020) contrary to highly crystalline [mTBDH][OAc] which makes processing with this IL less labor intensive. All those factors make this newly developed IL perspective for industrial application.

It should be stressed here that ILs, especially having halide anions, are highly viscous liquids with the viscosity of two to three orders of magnitude higher than those of commercial organic solvents (Zhang et al. 2006). As a consequence, cellulose solutions in IL frequently have rather high viscosity, even at high temperatures (Kuang et al. 2008) (Sammons et al. 2008) (Chen et al. 2011). The high viscosity of IL is a substantial drawback from a practical point of view, since it will cause trouble in mass transfer and lead to a high consumption of a power for mixing with cellulose in solution.

One of the ways to overcome these drawbacks is the addition of low-viscosity solvents to ILs, thus forming binary solvents for cellulose dissolution (Yuan et al. 2019) (Lv et al. 2012) (Zheng et al. 2019). Minnick et al. (Minnick et al. 2016) stated that the cellulose solubility reduces in the presence of protic solvents such as water, methanol, and ethanol while the addition of aprotic dipolar solvents including dimethyl sulfoxide (DMSO), dimethylformamide, and 1,3-dimethyl-2-imidazolidinone to ILs improves the solubility of

cellulose which was affected both by the composition of co-solvents and temperature (Minnick et al. 2017).

It was established that cellulose solubility in ILs was mostly defined by the ability of anions from ILs to accept the hydrogen bond. Co-solvents may be a factor by supporting cellulose dissolution without the direct interaction with cellulose or causing cation–anion dissociation in IL (Lv et al. 2012). Co-solvents can accelerate mass transfer between molecules of cellulose and solvents and also lower the monomer friction coefficient of cellulose by decreasing the viscosity of the cellulose solution (Lv et al. 2012) (Andanson et al. 2014). DMSO is supposed to enhance the solvation capacities of ILs by expediting mass transport through decreasing the viscosity of the system (Andanson et al. 2014). Others have proposed that DMSO is, however, capable to play a role in dissociation of anions and cations of ILs thus improving the interaction of anions with cellulose (Xu et al. 2013), (Zhao et al. 2013), (Lindman et al. 2010).

Furthermore, the addition of low-cost co-solvents can considerably lower the use of high-cost ILs and hence reduce the processing cost. Although some of the developed mix-solvents have attained sufficient success in cellulose dissolution and modification, the essential weaknesses in some cases such as toxicity, or high cost, or volatility and instability etc. of widely used co-solvents are still large problems in their practical applications.

γ-Valerolactone (GVL), dimethyl isosorbide (DMI), and N,N′-Dimethylpropyleneurea (DMPU) are natural chemicals derived from lignocellulosic biomass, which are considered as green solvents in chemical processes (Horváth 2008), (Byrne et al. 2016), (Dalla Torre et al. 2023). These solvents also belong to the class of dipolar aprotic solvents which are not solvents for the cellulose but can potentially replace DMSO, DMF, and other currently used co-solvents in mixtures with ILs. However, there are limited studies on the viscoelastic and solution behavior of cellulose in ILs mixed with mentioned green co-solvents. By our best knowledge, mixtures of green solvents with novel [mTBNH][OAc] as dissolution/modification media for cellulose are not studied at all. In this sense, such study can help to develop a greener and economically more feasible and efficient method for cellulose dissolution and preparation of cellulose derivatives.

Rheological properties of dilute to concentrated cellulose/IL solutions have attracted much attention owing to their pragmatic usefulness for successful processing and chemical derivatization of cellulose.

The rheological behavior of cellulose dissolved in various ionic liquids as [Amim][Cl], [Bmim][Cl], and [Emim] [Ac] has been studied in details from low to high solution concentrations (Kuang et al. 2008), (Chen et al. 2011), (Gericke et al. 2009), (Lu et al. 2012), (Sammons et al. 2008). Furthermore, a comprehensive study of the effect of co-solvent DMSO on viscoelastic properties, sol–gel

transition (Wittmar et al. 2020), and conformations (Owens et al. 2022) of cellulose chains in cellulose/ILs solutions was implemented at several DMSO and cellulose concentrations (Lv et al. 2012), (Ilyin et al. 2023). It is found that all the solutions showed a shear thinning behavior at high shear rates (Chen et al. 2009), (Kuang et al. 2008) for semidilute and concentrated solutions; for dilute solutions, there existed another shear thinning region at low shear rates. They suggested that cellulose chains perhaps slightly aggregate, even in dilute solutions, due to strong hydrogen bonding interactions (Saalwächter et al. 2000).

The understanding of the rheological properties of cellulose/IL/co-solvent solutions as well as the molecular organization of cellulose in binary solvents is a crucial requirement for a successful processing and for cellulose derivatization as well. It should be taken under consideration that the polymer configuration and solution microstructure in the binary solvent mixture may be affected both by the affinity of polymer and solvents and by the proportion of "good" to "poor" solvent (Porfirio et al. 2021). Therefore, the purpose of the present work was to study the rheological behavior of the concentrated cellulose/[mTBNH][OAc]/co-solvent solutions, which is the basis for further transesterification of cellulose in these IL/co-solvents. Herein, the effect of green co-solvent type and contents on the rheological properties of cellulose/[mTBNH][OAc]/co-solvent mixtures was evaluated under both the steady and oscillatory shear conditions. The dissolution behavior of cellulose and its activation energies in GVL, DMPU, and DMI promoted by [mTBNH][OAc] was investigated in comparison to DMSO.

Experimental section

Materials

Cellulose with 0.02-0.1 mm fiber length used in this work was produced by Carl Roth GMBH (Germany). Ionic liquid 5-methyl-1,5,7-triaza-bicyclo-[4.3.0]non-6-enium acetate, [mTBNH][OAc], was not commercially available and was synthesized by Liuotin Group Oy (Finland). The melting point of IL is 15 °C; flash point is more than 220 °C; viscosity is 205 mPa s (25 °C); and density is 1.16 g/cm³. Dimethyl sulfoxide, DMSO, with purity 99.9% was purchased from Fisher Chemical (US) and has a viscosity 1.99 mPa s (25 °C). γ-Valerolactone, GVL, with purity ≥ 99%, having viscosity 2.18 mPa s (25 °C), and dimethyl isosorbide, DMI, (purity ≥ 99%) with viscosity 6.8 mPa s (25 °C) were purchased from Sigma Aldrich (St. Louis, MO, USA). N,N′-dimethylpropyleneurea, DMPU, with purity 97% and viscosity 3.32 mPa s (20 °C) was purchased from Acros Organics (Geel, Belgium).

Cellulose dissolution and esterification procedure

Cellulose was dried under vacuum at 105 °C for 24 h before use. Cellulose concentration in all studied solutions was 2 wt%. Cellulose was dissolved in pure [mTBNH][OAc] and its mixtures with co-solvents (DMI, DMPU, GVL, DMSO) and stirred at 60 °C for 24 h until the cellulose was completely dissolved (if possible). In the case of the use of co-solvents, IL and co-solvents have been first mixed and then cellulose has been added to the binary solvent. Different weight ratios of IL/co-solvent have been prepared and studied, namely, 2:1, 1:1, and 1:2.

Characterization

To study the rheological properties of the samples, an Anton Paar Physica MCR501 rheometer, with cone-plate measuring geometry, was used (plate diameter 25 mm, cone angle 2°). Flow curves were obtained at a shear rate $\dot{\gamma}$ range from 0.01 to 100–500 s⁻¹. Complex viscosity was determined in the range of angular frequencies $\omega = 0.01$ to 500 rad/s. A constant strain of $\dot{\gamma} = 5\%$ was used defining the linear viscoelastic region (LVR). An amplitude sweep test to determine the LVR was done at a frequency of 1 Hz. The solutions were examined at 25 °C, except temperature dependence of zero-shear viscosity where 25–100 °C temperature range was tested. Ordinary equations were applied to calculate rheological characteristics (Malkin 1994). Each rheological curve has been obtained 2–4 times to ensure the data reproducibility and get average results (if needed).

Optical micrographs of solutions were pictured at Carl Zeiss Axioskop 2 with magnification × 100 in polarized light mode.

Molar mass (MM) of cellulose was determined at 25 °C from the intrinsic viscosity [η] (= 5 dl/g) of cellulose solution in cupriethylenediamine hydroxide solution, Cuene, according to a standard procedure ASTM D1795−13. The MM was then calculated by the Mark-Houwink equation with parameters $K = 1.01 \times 10^{-4}$ dL/g and $a = 0.9$ (Brandrup et al. 2005). The obtained MM is 163,000 g/mol (DP = 1000). The overlap concentration (= 1/[η]) for cellulose in solutions in this case is 0.2%. It means that cellulose solutions used in this study having 2 wt% concentrations are already in concentrated regime. This concentration has been chosen due to the reason that it was used by authors for the synthesis of cellulose derivatives in [mTBNH][OAc]/DMSO solutions in a recently published paper (Tarasova et al. 2023).

Results and discussion

Rheological behavior of cellulose/IL/co-solvent solutions

The major disadvantage of ILs is their high viscosity, which in turn leads to a high viscosity of

cellulose-containing solutions, limiting the mass fraction of cellulose in these solutions. In the current work, for example, it was only possible to dissolve cellulose in pure IL at a concentration of 2 wt%—higher concentrated solutions could not be stirred effectively due to the high viscosity. This disadvantage can be overcome by using mixtures of IL with less viscous co-solvents. A dipolar aprotic solvent such as DMSO is known to be an effective co-solvent for the dissolution of cellulose (Tarasova et al. 2023). When the content of DMSO is increased, the viscosity of the cellulose solution in the binary IL/DMSO solvent decreases significantly. However, DMSO is not considered a "green" solvent anywhere. So, if to follow a greener strategy in cellulose dissolution and modification, DMSO should be replaced with the green dipolar aprotic co-solvents. GVL, DMPU, and DMI can be used as greener alternatives to DMSO.

However, it is not yet clear which of these green co-solvents best preserves the dissolution capacity of GVL for cellulose, how much the viscosity of the cellulose solution is reduced, and how much green co-solvent can be added without loss of cellulose solubility.

For the tests, we used [mTBNH][OAc] mixed with green co-solvents in the ratios 2:1, 1:1, and 1:2. The mass fraction of cellulose in all solutions tested was 2 wt.% without exception. The solutions were tested at 25 °C. To evaluate the quality of the cellulose solutions, we investigated the dependence of their viscosity (η) on the shear rates ($\dot{\gamma}$) and that of their storage (G') and loss (G'') moduli on the angular frequency (ω), which offers the possibility of determining the gel formation due to a decrease in the solubility of a polymer (Heinze et al. 2000).

It was detected that the viscosities of [mTBNH][OAc] (no cellulose added) decreased with addition of any co-solvent, and all studied IL/co-solvent mixtures can be considered as Newtonian fluids; see Fig. 1.

However, the solution of cellulose in pure [mTBNH][OAc] is a non-Newtonian fluid with shear-thinning behavior: Its viscosity is stable at low shear rates but decreases

at high ones as can be seen from Fig. 2a. The high molar mass cellulose with DP = 1000 used in this study forms an entangled solution in IL at the of 2 wt.% concentration used. At high shear rates, the stretching, alignment, and disentanglement of macromolecular chains lead to a decrease in viscosity (Ilyin et al. 2023).

As a reference, the effect of DMSO content on rheological properties of cellulose/IL/DMSO solutions was evaluated.

Fig. 2 shows the angular frequency dependence of the complex viscosity of cellulose solutions with different DMSO contents in the form of a double logarithmic representation. Double logarithmic scales are used for all rheological plots. All solutions show a shear-thinning behavior, indicating that cellulose solutions are in the entanglement region. The addition of DMSO to the cellulose solution in [mTBNH][OAc] (while keeping the cellulose concentration constant) decreases its viscosity, as can be clearly seen in Fig. 2a. This decrease in viscosity may be caused by the lower viscosity of DMSO (2 mPa s) compared to IL (200 mPa s). These results are consistent with data previously shown in literature (Lv et al. 2012), (Seddon et al. 2000) where a decrease in the viscosity of the cellulose solution was observed after dilution of the ionic liquid. In addition, the critical angular frequency, which corresponds to the transition from Newtonian to shear-thinning behavior, shifts to higher values with the increase of DMSO in the binary solvent. However, when a binary solvent of 1:2 IL/DMSO is used, the viscosity of the cellulose solution shows stronger shear thinning behavior than with 2:1 and 1:1 mixtures, which can be explained by the fact that the cellulose solution enters a weakly structured pre-gel state. Such a gelation process was observed in [Emim][OAc]/DMSO and [Emim][Cl]/DMSO at higher DMSO content (75%) in binary solvent (Ilyin et al. 2023), (Wang et al. 2014).

The systems with DMSO as co-solvent are typical polymer solutions: At low frequencies, their loss modulus G'' exceeds the storage modulus G', as shown in Fig. 2b. Note that the data in Fig. 2b have been shifted along the vertical axis by multiplying by 10^n, where $n = 0, 1, 2$, and 2.5 for 1:2,

Fig. 1 **a** Shear rate dependences of η of pure [mTBNH][OAc] and 2:1 [mTBNH][OAc]/co-solvent mixtures; **b** Shear rate dependences of η of [mTBNH][OAc]/DMPU mixtures, as example. The ratio of [mTBNH][OAc]/DMPU is given in the legend
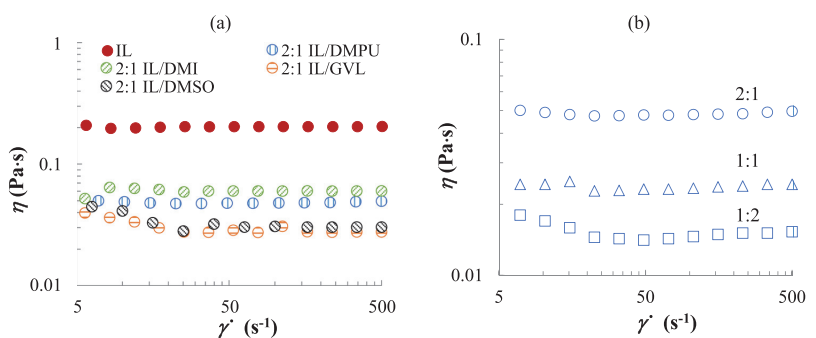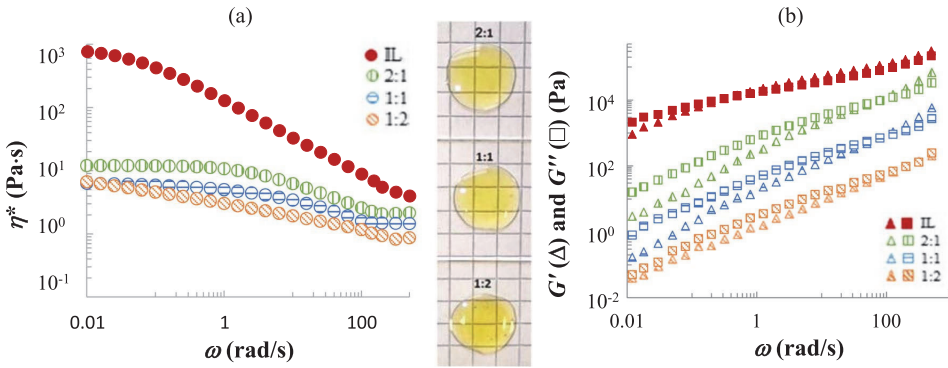
Fig. 2 Dependences of **a** complex viscosity η^* and **b** storage G' (triangle) and loss G'' (square) moduli on angular frequency ω for cellulose so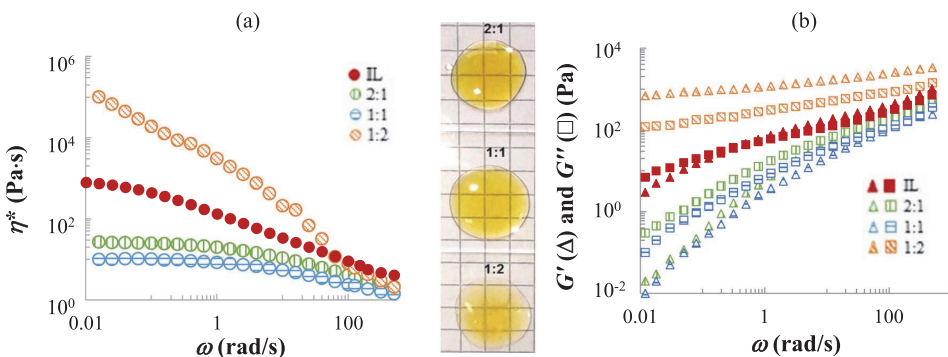lutions in pure [mTBNH][OAc] and in [mTBNH][OAc]/ DMSO binary solvent. The ratio of [mTBNH][OAc]/DMSO is given in the legend. The central part demonstrates the appearance of cellulose solutions in [mTBNH][OAc]/DMSO mixtures

1:1, 2:1 IL/DMSO and pure IL cellulose solutions, respectively, to avoid overlap. The general trend that the moduli decrease with increasing DMSO content was maintained at the figure. At higher frequencies, the G' becomes larger than G''. The crossover frequency ω_c, where $G' = G''$, is characteristic of the viscoelastic behavior of the material and indicates that the system becomes elastic rather than viscous (Zhao et al. 2013), (Xia et al. 2021), (Ilyin et al. 2023). From crossover points of the curves, the useful information about relaxation time via $\tau = \frac{1}{\omega_c}$ can be extracted.

Crossover points of cellulose/IL/DMSO solutions shift to higher ω with an increase in DMSO content, which indicates a faster relaxation of the cellulose chains due to fewer constraints (entanglements) from its neighbor chains.

It can be concluded that although DMSO is not a solvent for cellulose, unlike [mTBNH][OAc], miscibility of the compounds is still quite high for all studied compositions. This is evident from the photographs in Fig. 2, which show that cellulose solutions are transparent in all IL/DMSO mixtures studied, with no phase separation visible.

The behavior of the cellulose solution after addition of GVL to the IL is almost the same as for DMSO-based solutions. Figure 3 represents the angular dependences of η^*, G', and G'' for cellulose in different compositions of [mTBNH][OAc] with GVL as co-solvent. When the ratio of added GVL to IL is 2:1 and 1:1, the viscosities of the cellulose solution decrease as a non-Newtonian fluid with increasing shear rates. In addition, 1:1 IL/GVL solution has a lower viscosity than 2:1 solution, which can

Fig. 3 Dependences of **a** complex viscosity η^* and **b** storage G' (triangle) and loss G'' (square) moduli on angular frequency ω for cellulose solutions in pure [mTBNH][OAc] and in [mTBNH][OAc]/GVL binary solvent. The ratio of [mTBNH][OAc]/GVL is given in the legend. The central part demonstrates the appearance of cellulose solutions in [mTBNH][OAc]/GVL mixtures

be explained similarly to DMSO by the dilution of the cellulose solution with a solvent of lower viscosity (GVL has a viscosity of 1.9 mPa s) compared to IL. A similar behavior was reported for the cellulose in [Emim][OAc]/ GVL mixtures of various compositions (Yuan et al. 2019).

However, at an IL/GVL solvent composition of 1:2, the viscosity of the cellulose solution increases sharply, and the solution starts to exhibit sufficient shear-thinning behavior (Fig. 3a). The viscosity curves are consistent with the results for frequency sweeps. Both storage G' and loss G'' moduli are only slightly dependent on the frequency, and G' is greater than G'' over the measurable frequency range, as can be seen in Fig. 3b. This behavior is characteristic of a gel in which the rheological response of the material is dominated by an elastic or solid-like response. The data presented in literature (Gandhi and Williams 1972) have shown that thermodynamically poor solvents lead to much higher viscosities at high concentrations than good solvents. This behavior is opposite to the results of dilute solutions, where poor solvents lead to lower viscosities due to coil shrinkage.

In poor solvents, the entangled chains cling to each other more tightly and can even form multimolecular aggregates before entanglements in the classical sense occur. Therefore, it can be suggested that a high content of added GVL deteriorates the thermodynamic solvent quality, leading to the formation of an entangled network by an association of cellulose macromolecules. In contrast, the systems with lower GVL content (2:1 and 1:1) are typical polymer solutions: At low frequencies, their loss modulus exceeds the storage modulus, crossover points of cellulose/IL/GVL solutions shift to lower ω with decreasing GVL content.

Considering the interdependencies of storage and loss moduli in Cole–Cole plots presented in Fig. 4, it appears that the experimental points for all DMSO-based solutions fit approximately the same straight line (Fig. 4a) and are superimposed on the data for the cellulose solution in pure IL. The invariant Cole–Cole plots mean that DMSO does not change the microstructure of the cellulose solution (Ilyin

et al. 2020). The pre-gel state of the cellulose solution in 1:2 IL/DMSO can only be recognized as a low-frequency anomaly in the Cole–Cole plots.

Fig. 4b shows the Cole–Cole plots for cellulose solutions in IL/GVL solvents. It can be observed that the data for cellulose solutions in 2:1 and 1:1 IL/GVL lie at the same straight line. However, the microstructure of the system changes with the addition of 66% GVL (1:2 IL/GVL system) as the Cole–Cole plots no longer overlap with others (Fig. 4b). GVL is not a solvent for cellulose and leads to gelation of the solution due to the stronger macromolecular association which can further lead to phase separation, as it is clearly seen in the photos of the cellulose solution in the middle part of Fig. 3. Therefore, dilution of [mTBNH][OAc] with GVL at compositions greater than 1:1 is not a way to reduce the viscosity of the cellulose solution, unlike DMSO.

The behavior of the cellulose solutions in IL when DMI and DMPU are added is almost identical; therefore, only the angular frequency dependencies of η^*, G', and G'' for cellulose solutions in IL/DMI binary solvents of different compositions are presented in Fig. 5.

When cellulose is dissolved in 2:1 IL/DMI and 2:1 IL/ DMPU, the viscosity of such cellulose solutions is lower than that of cellulose in pure IL due to the dilution effect. The absence of gelation is confirmed by frequency dependencies of G' and G'' moduli (Fig. 5b), which are typical for an ordinary concentrated polymer solution, as its storage modulus is lower than the loss modulus at low frequencies and becomes dominant at high frequencies.

However, with increasing content of these green co-solvents in binary mixtures up to 1:1 IL/co-solvent, the viscosity of the cellulose solutions increases by a decimal order of magnitude, as obvious from Fig. 5a. The addition of more DMI or DMPU, up to a ratio 1:2, further increases the cellulose viscosity. An increase in viscosity indicates a greater probability of strong aggregation of macromolecules. The appearance of the solution changes from transparent to opaque, as can be seen from Figure 5. Both G' and G'' depend slightly on the angular frequency and $G'>$
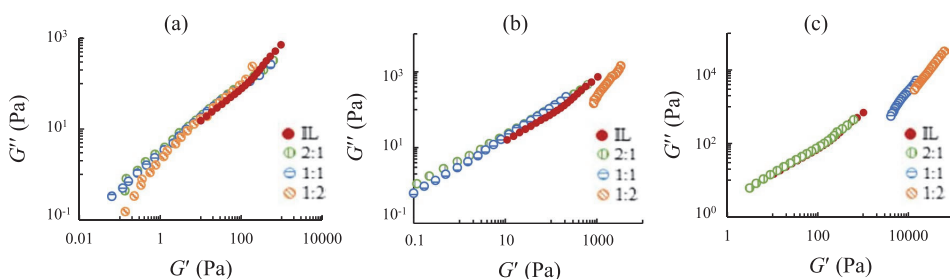
Fig. 4 Cole–Cole plots for cellulose solution in **a** [mTBNH][OAc]/DMSO, **b** [mTBNH][OAc]/GVL, and **c** [mTBNH][OAc]/DMI binary solvents. The ratio of IL/co-solvent is given in the legend
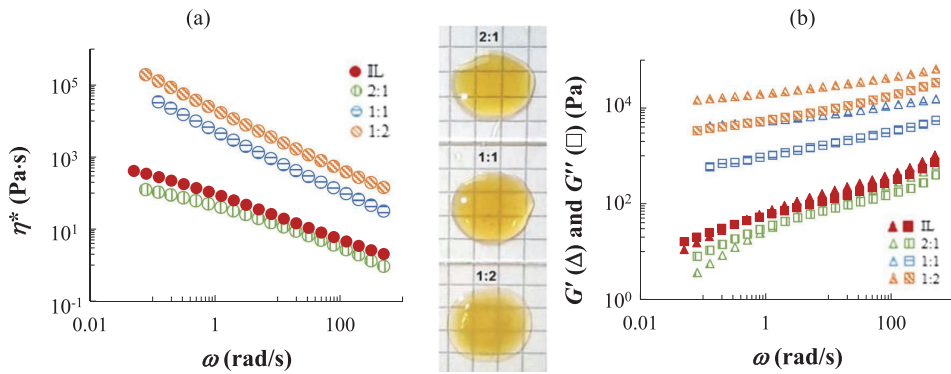
Fig. 5 Dependences of **a** complex viscosity η^* and **b** storage G' (triangle) and loss G'' (square) moduli on angular frequency ω for cellulose solutions in pure IL and in [mTBNH][OAc]/DMI binary solvent.

The ratio of [mTBNH][OAc]/DMI is given in the legend. The central part demonstrates the appearance of cellulose solutions in [mTBNH][OAc]/DMI mixtures

G'' over the entire measurable range, which is characteristic of a gel or a viscoelastic solid. In addition, the values of G' and G'' for cellulose in 1:1 and 1:2 IL/DMI (and IL/DMPU) are 1 and 2 orders of magnitude higher, respectively, than the values for cellulose in pure IL.

The similarity of the curves of 2:1 IL/DMI (as well as 2:1 IL/DMPU) with pure IL in the Cole–Cole plots (see Fig. 4c) indicates that the addition of DMI does not cause new interactions between the cellulose macromolecules until they lose their solubility and gel formation occurs. The experimental points overlay for pure IL and 2:1 solution, indicating the invariance of the microstructure. The addition of a higher content of co-solvent (1:1) triggers gel formation through the microphase separation, as shown by the shift in Cole–Cole dependencies in Fig. 4c.
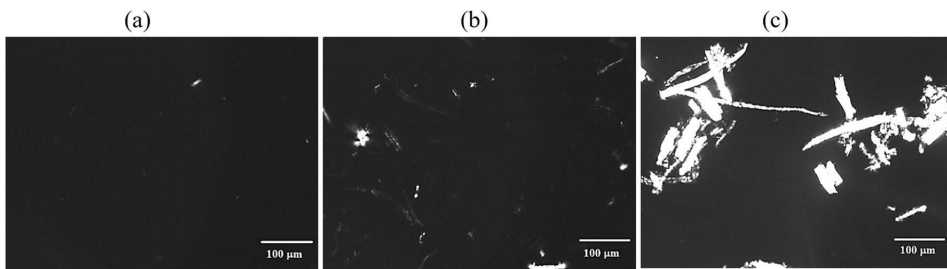
Fig. 6 where optical micrographs for cellulose solution in 2:1, 1:1, and 1:2 IL/DMI taken in polarized light mode are shown additionally proves the gelation and phase separation process in studied systems.

As can be seen from Fig. 6a, 2:1 cellulose solution is completely homogeneous and contains no undissolved or aggregated cellulose crystals, which would be seen as white areas in polarized light due to the crystalline nature of the native cellulose (only a negligible number of crystallites can be seen). Meanwhile, at a ratio of 1:1, the crystallites can already be observed (see Fig. 6b), and their number rises further, leading to the formation of large aggregates of poorly dissolved cellulose at IL/DMI ratio of 1:2 (Fig. 6c), revealing phase separation in this case. Similar behavior was also observed in IL/DMPU systems.

The Cox-Merz rule is usually applied to correlate the dynamic and steady-state shear properties of the solutions (Barnes et al. 1989). In this method, the values of complex viscosity η^* and shear viscosity η are compared at equal values of shear rate $\dot{\gamma}$ and angular frequency ω, and stated that $|\eta^*(\varpi)| \cong |\eta(\dot{\gamma})|_{\dot{\gamma}=\varpi}$. The validity of this rule has been confirmed for many polymer melts and solutions (Marrucci 1996).

Fig. 7 presents as example the η and $\eta*$ of cellulose in 2:1 and 1:2 IL/DMI solutions plotted against $\dot{\gamma}$ and ω, respectively. The applied strain for frequency sweep was selected 1% to ensure the experiments were within linear

Fig. 6 Optical micrographs taken in polarized light mode for cellulose in 2:1 (**a**), 1:1 (**b**), and 1:2 (**c**) IL/DMI at room temperature

viscoelastic range. Similar behavior was observed in all IL/green co-solvent cellulose solutions.

As can be seen, the shear viscosity η for 2:1 IL/green co-solvent cellulose solutions overlaps the complex viscosityη^*, indicating that all these solutions obey the Cox-Merz rule well.

However, a significant deviation from this rule can be observed for 1:2 solutions. A similar deviation was detected for various biopolymer systems and pulps (Quintana et al. 2018) (Bistany and Kokini 1983).

The Cox-Merz rule does not work for materials that exhibit physical and/or chemical interactions, such as gels and colloidal cellulose suspensions (Gleissle and Hochstein 2003). Therefore, in the case of 1:2 solutions, this deviation is most likely due to the formation of structural and intermolecular aggregates of poorly dissolved cellulose, which correlate with the optical microscopy results. Under shear flow, these structures can be ruined, resulting in lower viscosity values than in oscillatory tests.

It can be concluded that DMSO can be used as a nominal co-solvent for [mTBNH][OAc] in a wide range of compositions, at least up to a ratio of 1:2. GVL can be used up to a composition 1:1, while DMI and DMPU provide homogeneous cellulose solutions only at a composition of 2:1 IL/co-solvent.

Since the 2:1 IL/co-solvent composition is the only common composition for all co-solvents investigated that leads to the formation of typical polymer solutions, this composition was chosen for the comparative analysis between the co-solvents. Figure 8 represents the shear rate ($\dot{\gamma}$) dependence of shear viscosity η for cellulose solutions prepared in 2:1 IL/co-solvent mixtures.
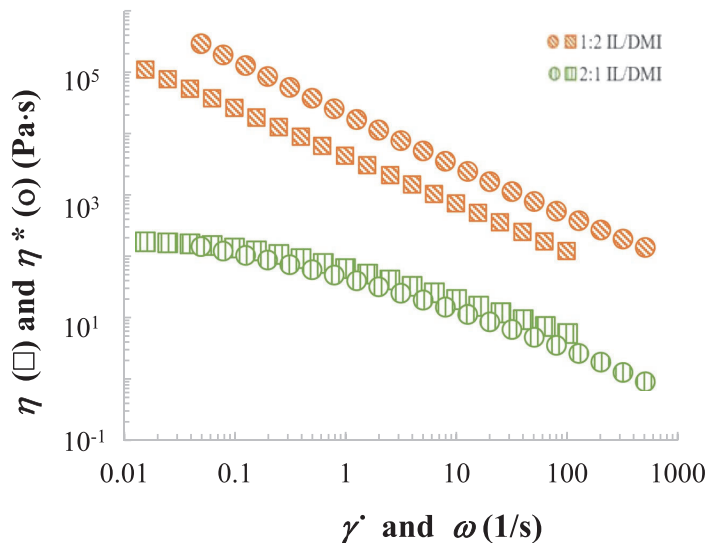
As can be seen from Fig. 8, the DMSO demonstrates the best dilution capacity, which is probably due to the lowest viscosity of 2:1 IL/DMSO solvent (30 mPa s) among all other binary solvents. The viscosity data of the cellulose solution with DMI added to IL are almost identical to those of DMPU, being five and 10 times higher than those for GVL and DMSO, respectively. However, viscosity of DMPU- and DMI-based cellulose solutions is five times lower than that in pure IL. It should be noted that the viscosities of 2:1 IL/DMI and IL/DMPU binary solvents are also rather close to each other (58 and 60 mPa s, respectively) and higher than IL/DMSO (30 mPa s) and IL/GVL (50 mPa s). To eliminate the influence of the viscosity of the binary solvents (IL/co-solvent) on cellulose/IL/co-solvent solutions, the relative viscosity can be considered. The relative viscosity, defined as the ratio between the viscosity of the solution (η of cellulose/IL/co-solvent solution) and the viscosity of the pure solvent (η_s of IL/co-solvent), indicates how much the viscosity of the solution increases in relation to the solvent.

Inset to Fig. 8 shows the relative viscosity for all 2:1 solutions studied. It is obvious that the curves for cellulose in IL/DMPU and IL/DMI are almost superimposed with those in pure IL. It can therefore be assumed that DMPU and DMI simply dilute the IL, thereby reducing the viscosity of cellulose solution. However, relative viscosity at zero shear for GVL- and DMSO-based solutions is still two and five times lower, respectively, than that of the solutions in pure IL. Thus, it is probable that GVL, like DMSO, improves the solvation of the IL ions by dissociating anions and cations of ILs. Such a solvation effect of [Bmim][OAc] by DMSO was discovered by several authors, for example Zhao et al. (2013) and Xu et al. (2013).

Fig. 7 Validity of Cox-Merz rule by comparison of complex viscosityη^* (circles) and shear viscosityη (squares) taken at 190 °C as a function of angular frequency ω and shear rate $\dot{\gamma}$ for cellulose solutions in 2:1 and 1:2 IL/DMI

Fig. 8 Shear rate dependence of shear viscosity for cellulose solutions in 2:1 [mTBNH] [OAc]/co-solvents; inset demonstrates the shear rate dependence of relative viscosity of cellulose solutions. The co-solvent type is given in the legend
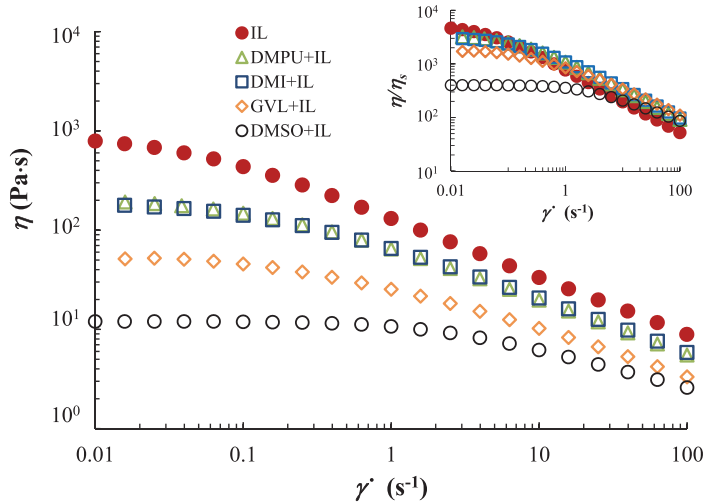
Table 1 Relaxation time τ and activation energy E_a for cellulose solutions in 2:1 [mTBNH][OAc]/Co-solvent mixtures

Cellulose in…	τ, sec	E_a, kJ/mol
IL pure	3.17	45.3
2:1 IL/DMPU	0.53	41.3
2:1 IL/DMI	0.50	40.7
2:1 IL/GVL	0.020	36.9
2:1 IL/DMSO	0.017	33.7

A clear difference in the relaxation time τ was observed when the solvent changed. The relaxation times determined from the crossing points for all 2:1 solutions are listed in Table 1.

The highest τ is observed for cellulose solution in pure IL and decreases in the direction IL/DMPU > IL/DMI > IL/GVL > IL/DMSO. It is known (Tager 1974) that concentrated polymer solutions comprise more or less broken structures of the polymers themselves. Cellulose in concentrated solutions can form such structures due to the high capability of intra- and intermolecular hydrogen bonding and high degree of entanglements. Whether these structures can be ruined depends on the ratio of the structural energy to that of the polymer-solvent interaction. Poor solvents cannot destroy the strong structures, but the molecules of a good solvent can penetrate a structure and destroy it. As a result, the structure should be looser in good solvents and larger and less mobile in solutions with poor solvents. And therefore τ of a polymer solution in a poor solvent is longer than τ of a solution in a good solvent (Cravotto et al. 2008). Considering the values of τ for the studied systems (Table 1), it can be assumed that IL/

DMPU and IL/DMI behave as "poorer" solvents for cellulose than IL/GVL and IL/DMSO. It is obvious that DMPU and DMI have an almost similar dissolving capacity for cellulose. A similar effect was observed for tetraalkylphosphonium IL mixed with DMPU and DMI (Xia et al. 2021).

Thermodynamic quality of the solvent can be effectively analyzed via the viscosity–temperature dependence of fluids.

Therefore, the effect of temperature (T) on the viscosity properties of 2:1 cellulose/IL/co-solvent solutions was also studied. A common way to analyze the viscosity–temperature dependence is to use the Arrhenius equation (Lefroy et al. 2021), (Yuan et al. 2019):

$$\eta_0 = A e^{E_a/RT} \tag{1}$$

where E_a is the activation energy, η_0 is zero shear rate viscosity obtained at low shear rates, A is a constant, R is gas law constant, and T is absolute temperature. Figure 9 demonstrates the dependence of $\ln\eta_0$ as a function of $1/T$ for all 2:1 solutions. To avoid data overlapping, the curves were translated vertically on + 1 for IL/DMPU, IL/DMI, and IL-based solutions.

Figure 9 shows that the viscosity of all solutions decreases with increasing temperature as expected for classical polymer solutions.

The activation energy (E_a) can be calculated from the slope of $\ln \eta_0$ versus $1/T$. As shown in Fig. 9, $\ln\eta_0$ *vs.* $1/T$ is linear ($R^2 \geq 0.998$), which is similar to cellulose/[Bmim] [OAc] (Lefroy et al. 2021) and cellulose/[Emim][OAc]/ GVL (Yuan et al. 2019) but differs from that obtained for the cellulose/[Emim][OAc] solution (Gericke et al. 2009), (Budtova and Navard 2015) where the relationship had a concave form.

Fig. 9 Arrhenius equation plots for cellulose in 2:1 [mTBNH][OAc]/co-solvent. Used co-solvents are listed in the legend
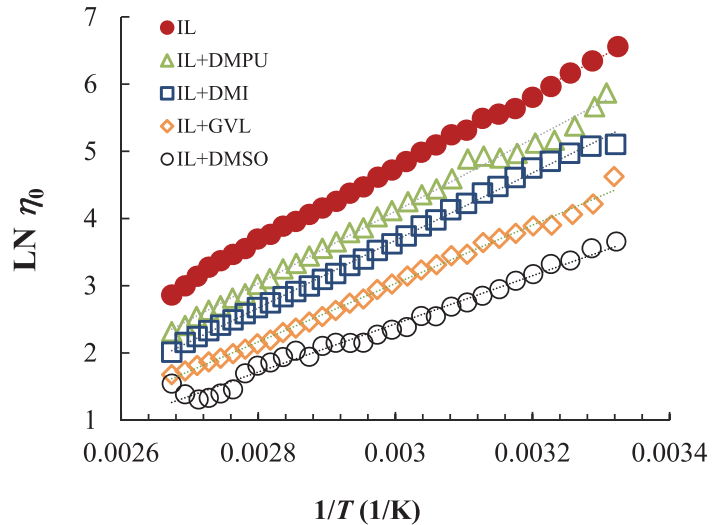
The activation energy values obtained from Fig. 9 are listed in Table 1.

In polymer solutions, E_a is related to the difficulty of moving the polymer chain from one position/state to another (Budtova and Navard 2015), (Hawkins et al. 2021) and to the intensity of interactions between the chains when the same polymer is considered (molar mass, chemical composition and microstructure are the same). The value of E_a is strongly affected by the thermodynamic quality of the solvent and specific behavior of the solvent, as it has been shown for cellulose dissolved in ILs (Budtova and Navard 2015).

As shown in Table 1, the cellulose solution in pure [mTBNH][OAc] has an activation energy 45.3 kJ/mol, which is comparable to $E_a = 46$ and 49 kJ/mol for MCC (with DP 300) and spruce sulfite pulp (DP 1000) in [Emim][OAc], respectively, as reported in literature (Gericke et al. 2009). The obtained result of E_a for 2:1 [mTBNH][OAc]/GVL (36.9 kJ/mol) is comparable to $E_a = 35.1$ kJ/mol for 3:2 [Emim][OAc]/GVL presented by Yuan et al. (Yuan et al. 2019). Flow activation energy data, to the best of our knowledge, are not available for cellulose solution in IL/DMPU and IL/DMI and cannot be compared.

The activation energy of cellulose/IL/co-solvent gradually decreases with the type of co-solvent in the following order: DMPU > DMI > GVL > DMSO. The dissimilarities between activation energies indicate that the co-solvent changes the energy barrier for flow: Slightly more energy is required to flow DMPU- and DMI-solutions compared to GVL and DMSO. The lower E_a values are also consistent with the phenomena that the corresponding dissolution rates of the IL/co-solvent samples were faster than those of the

pure IL, so the co-solvents may improve the efficiency for cellulose chemical modification, such as transesterification of cellulose.

Finally, despite the lower viscosity of cellulose in [mTBNH][OAc]/green co-solvents compared to pure [mTBNH][OAc], the range of co-solvent content in which cellulose can form relatively homogeneous solutions in binary solvents is not very wide.

Furthermore, it can be assumed that the green co-solvents investigated can replace DMSO in many applications, but not to a large extent, and the co-solvent content should not exceed 50% by weight.

Conclusions

In this study, we perform for the first time a detailed rheological characterization of cellulose dissolved in a novel [mTBNH][OAc] ionic liquid with different contents of green co-solvents (GVL, DMPU, DMI) representing different thermodynamic qualities of binary solvents.

The type and content of the co-solvent have a strong influence on the magnitude of the rheological properties. The investigated aprotic green solvents with low viscosity, which are not good solvents for cellulose, can nevertheless be used as "nominal" co-solvents at low contents, reducing the overall viscosity of the cellulose solution by up to one to two decades.

Formulations of cellulose in 2:1 IL/Green co-solvents show normal viscoelastic behavior corresponding to the behavior of polymers in thermodynamically good solvent systems. Meanwhile, cellulose in 1:1 and 1:2 IL/DMPU and IL/DMI (and 1:2 IL/GVL) behaves like viscoelastic solids, where both

G' and G'' are almost independent of ω over the measurable range, $G' > G''$, and viscosity values are increased sharply. Formation of gel is related to the inter-polymer aggregation with tighter entanglements in concentrated solutions due to thermodynamic forces, rendering the viscosities of such poor-solvent systems higher than good-solvent ones. The maximum dissolving capacity was observed in the mixtures of IL with DMSO and GVL.

From the dissolution efficiency viewpoint, an Arrhenius approach was employed to attain the activation energy values from rheological analysis, which are related to the energy barriers to flow. Energy barrier in pure IL was found to be greater than in IL/Green co-solvents. Meanwhile, the capacity of co-solvents for dissolving cellulose in binary solvents can be ranked as follows (from the highest to the lowest): DMSO > GVL > DMI > DMPU. This demonstrates that the energy barrier for flow is significantly affected by the co-solvents used. The solubility can be adjusted by changing the content and type of a co-solvent. In this sense, GVL has a stronger influence on cellulose solubility and flow than DMPU.

The dissolution of cellulose in IL/green co-solvent demonstrates the green potential for further cellulose modification as the biobased GVL, DMPU, and DMI reduce the use of expensive ILs in cellulose processing from a practical and sustainable point of view. These findings can be useful in the development of processes to produce cellulose-based materials for various applications.

Declarations

Conflict of interest The authors declare no competing interests.

References

Andanson J-M, Bordes E et al (2014) Understanding the role of co-solvents in the dissolution of cellulose in ionic liquids. Green Chem 16(5):2528–2538

Barnes HA, Hutton JF, Walters K (1989) An introduction to rheology. Elsevier

Bistany KL, Kokini JL (1983) Dynamic viscoelastic properties of foods in texture control. J Rheol 27(6):605–620

Brandrup J, Immergut EH et al (2005) Polymer handbook, 4th edn. John Wiley & Sons

Budtova T, Navard P (2015) Viscosity-temperature dependence and activation energy of cellulose solutions. Nord Pulp Pap Res J 30(1):99–104

Byrne FP, Jin S et al (2016) Tools and techniques for solvent selection: green solvent selection guides. Sustain Chem Process 4(1):7

Cao X, Sun S et al (2013) Rapid synthesis of cellulose esters by trans-esterification of cellulose with vinyl esters under the catalysis of NaOH or KOH in DMSO. J Agric Food Chem 61(10):2489–2495

Chen X, Zhang Y et al (2009) Rheology of concentrated cellulose solutions in 1-butyl-3-methylimidazolium chloride. J Polym Environ 17(4):273–279

Chen X, Zhang Y et al (2011) Solution rheology of cellulose in 1-butyl-3-methyl imidazolium chloride. J Rheol 55(3):485–494

Cravotto G, Gaudino EC et al (2008) Preparation of second generation ionic liquids by efficient solvent-free alkylation of N-heterocycles with chloroalkanes. Molecules 13:149–156

Dalla Torre D, Annatelli M et al (2023) Acid catalyzed synthesis of dimethyl isosorbide via dimethyl carbonate chemistry. Catal Today 423:113892

Elsayed S, Hellsten S et al (2020) Recycling of superbase-based ionic liquid solvents for the production of textile-grade regenerated cellulose fibers in the lyocell process. ACS Sustain Chem Eng 8(37):14217–14227

Fink HP, Weigel P et al (2001) Structure formation of regenerated cellulose materials from NMMO-solutions. Prog Polym Sci 26(9):1473–1524

Flieger J, Flieger M (2020) Ionic liquids toxicity-benefits and threats. Int J Mol Sci 21(17):6267

Gandhi KS, Williams MC (1972) Effect of solvent character on polymer entanglements. J Appl Polym Sci 16(10):2721–2725

Gericke M, Schlufter K et al (2009) Rheological properties of cellulose/ionic liquid solutions: from dilute to concentrated states. Biomacromolecules 10(5):1188–1194

Gleissle W, Hochstein B (2003) Validity of the Cox-Merz rule for concentrated suspensions. J Rheol 47(4):897–910

Han S, Li J et al (2009) Potential applications of ionic liquids in wood related industries. Bioresources 4(2):825–834

Hawkins JE, Liang Y et al (2021) Time temperature superposition of the dissolution of cellulose fibres by the ionic liquid 1-ethyl-3-methylimidazolium acetate with cosolvent dimethyl sulfoxide. Carbohydrate Polym Technol Appl 2:100021

Heinze T, Dicke R et al (2000) Effective preparation of cellulose derivatives in a new simple cellulose solvent. Macromol Chem Phys 201(6):627–631

Horváth IT (2008) Solvents from nature. Green Chem 10(10):1024–1028

Ilyin SO, Kostyuk AV et al (2023) The effect of non-solvent nature on the rheological properties of cellulose solution in diluted ionic liquid and performance of nanofiltration membranes. Int J Mol Sci 24(9):8057

Ilyin SO, Makarova VV et al (2020) Phase behavior and rheology of miscible and immiscible blends of linear and hyperbranched siloxane macromolecules. Mater Today Commun 22:100833

Isik M, Sardon H et al (2014) Ionic liquids and cellulose: dissolution, chemical modification and preparation of new cellulosic materials. Int J Mol Sci 15(7):11922–11940

King AWT, Asikkala J et al (2011) Distillable acid–base conjugate ionic liquids for cellulose dissolution and processing. Angewandte Chem Int Edition 50(28):6301–6305

Köhler S, Liebert T et al (2007) Interactions of ionic liquids with polysaccharides 1. Unexpected Acetylation of Cellulose with 1-Ethyl-3-ethylimidazolium Acetate. Macromol Rapid Commun 28:2311–2317

Kostag M, Gericke M et al (2019) Twenty-five years of cellulose chemistry: innovations in the dissolution of the biopolymer and its transformation into esters and ethers. Cellulose 26(1):139–184

Kuang Q-L, Zhao J-C et al (2008) Celluloses in an ionic liquid: the rheological properties of the solutions spanning the dilute and semidilute regimes. J Phys Chem B 112(33):10234–10240

Lefroy KS, Murray BS et al (2021) Rheological and NMR studies of cellulose dissolution in the ionic liquid BmimAc. J Phys Chem B 125(29):8205–8218

Liebert T (2010) Cellulose solvents – remarkable history, bright future. Cellulose Solvents: For Analysis, Shaping and Chemical

Modification. American Chemical Society, Washington, DC, ACS Symposium Series;

Lindman B, Karlström G et al (2010) On the mechanism of dissolution of cellulose. J Mol Liquids 156:76–81

Lu F, Cheng B et al (2012) Rheological characterization of concentrated cellulose solutions in 1-Allyl-3-methylimidazolium chloride. J Appl Polym Sci 124:3419–3425

Lv Y, Wu J et al (2012) Rheological properties of cellulose/ionic liquid/dimethylsulfoxide (DMSO) solutions. Polymer 53(12):2524–2531

Mäki-Arvela P, Anugwom I et al (2010) Dissolution of lignocellulosic materials and its constituents using ionic liquids—a review. Ind Crops Prod 32(3):175–201

Malkin AY (1994) Rheology fundamentals. ChemTech Publishing, Ontario

Marrucci G (1996) Dynamics of entanglements: a nonlinear model consistent with the Cox-Merz rule. J Nonnewton Fluid Mech 62(2-3):279–289

Martins MAR, Sosa FHB et al (2022) Physico-chemical characterization of aqueous solutions of superbase ionic liquids with cellulose dissolution capability. Fluid Phase Equilibria 556:113414

McCormick CL, Dawsey TR (1990) Preparation of cellulose derivatives via ring-opening reactions with cyclic reagents in lithium chloride/N, N-dimethylacetamide. Macromolecules 23(15):3606–3610

McCormick CL, Lichatowich DK (1979) Homogeneous solution reactions of cellulose, chitin, and other polysaccharides to produce controlled-activity pesticide systems. J Polym Sci: Polym Lett Edition 17(8):479–484

Minnick DL, Flores RA et al (2016) Cellulose solubility in ionic liquid mixtures: temperature, cosolvent, and antisolvent effects. J Phys Chem B 120(32):7906–7919

Minnick DL, Flores RA et al (2017) Viscosity and rheology of ionic liquid mixtures containing cellulose and cosolvents for advanced processing. Ionic Liquids: Curr State Future Directions Am Chem Soc 1250:189–208

Ostonen A, Bervas J et al (2016) Experimental and theoretical thermodynamic study of distillable ionic liquid 1,5-diazabicyclo[4.3.0] non-5-enium acetate. Ind Eng Chem Res 55(39):10445–10454

Owens CE, Du J et al (2022) Understanding the dynamics of cellulose dissolved in an ionic liquid solvent under shear and extensional flows. Biomacromolecules 23(5):1958–1969

Parviainen A, Wahlström R et al (2015) Sustainability of cellulose dissolution and regeneration in 1,5-diazabicyclo[4.3.0]non-5-enium acetate: a batch simulation of the IONCELL-F process. RSC Adv 5(85):69728–69737

Porfirio T, Galindo-Rosales FJ et al (2021) Rheological characterization of polymeric solutions used in spray drying process. Eur J Pharm Sci 158:105650

Qiu X, Hu S (2013) Smart materials based on cellulose: a review of the preparations, properties, and applications. Materials (Basel) 6(3):738–781

Quintana S, Machacon D, Marsiglia RM, Torregroza E, Garcia-Zapateiro L (2018) Steady and shear dynamic rheological properties of squash (Cucurbita moschata) pulp. Contemp Eng Sci 11(21):1013–1024

Saalwächter K, Burchard W et al (2000) Cellulose solutions in water containing metal complexes †. Macromolecules 33:4094–4107

Sammons RJ, Collier JR et al (2008) Rheology of 1-butyl-3-methylimidazolium chloride cellulose solutions. I. Shear rheology. J Appl Polym Sci 110(2):1175–1181

Seddon KR, Stark A et al (2000) Influence of chloride, water, and organic solvents on the physical properties of ionic liquids. Pure Appl Chem 72(12):2275–2287

Swatloski RP, Spear SK, Holbrey JD, Rogers RD (2002) Dissolution of cellluose with ionic liquids. J Am Chem Soc 124(18):4974–4975

Tager AA (1974) Effect of solvent quality on the viscosity of flexible-chain and rigid-chain polymers in a wide range of concentrations. Rheol Acta 13(2):323–332

Tarasova E, Savale N et al (2023) Preparation of thermoplastic cellulose esters in [mTBNH][OAC] ionic liquid by transesterification reaction. Polymers 15(19):3979

Walden PT (1914) Molecular weights and electrical conductivity of several fused salts. Bull Acad Imp Sci St. Petersburg 1800:405–422

Wang L, Gao L et al (2014) Rheological behaviors of cellulose in 1-ethyl-3-methylimidazolium chloride/dimethylsulfoxide. Carbohydrate Polym 110:292–297

Wittmar ASM, Koch D et al (2020) Factors affecting the nonsolvent-induced phase separation of cellulose from ionic liquid-based solutions. ACS Omega 5(42):27314–27322

Xia J, King AWT et al (2021) Phase-separation of cellulose from ionic liquid upon cooling: preparation of microsized particles. Cellulose 28(17):10921–10938

Xu A, Zhang Y et al (2013) Cellulose dissolution at ambient temperature: role of preferential solvation of cations of ionic liquids by a cosolvent. Carbohydrate Polym 92(1):540–544

Xu C, Cheng Z (2021) Thermal stability of ionic liquids: current status and prospects for future development. Processes 9(2):337

Yuan C, Shi W et al (2019) Dissolution and transesterification of cellulose in γ-valerolactone promoted by ionic liquids. N J Chem 43(1):330–337

Zhang S, Sun N et al (2006) Physical properties of ionic liquids: database and evaluation. J Phys Chem Reference Data 35(4):1475–1517

Zhao Y, Liu X et al (2013) Insight into the cosolvent effect of cellulose dissolution in imidazolium-based ionic liquid systems. J Phys Chem B 117(30):9042–9049

Zheng B, Harris C et al (2019) Dissolution capacity and rheology of cellulose in ionic liquids composed of imidazolium cation and phosphate anions. Polym Adv Technol 30(7):1751–1758

Publication IV
Tarasova, E., Savale, N., Trifonova, L., Krasnou, I., Reile, I., Kudrjašova, M., Mere, A., Kaljuvee, T., Mikli, V., Sedrik, R., Krumme, A. (2024). Effect of green co-solvents on properties and synthesis of cellulose esters in superbase ionic liquid. Cellulose, 31(8), 4911–4927.

ORIGINAL RESEARCH

Effect of green co-solvents on properties and synthesis of cellulose esters in superbase ionic liquid

Elvira Tarasova · Nutan Savale · Lada Trifonova · Illia Krasnou · Indrek Reile · Marina Kudrjašova · Arvo Mere · Tiit Kaljuvee · Valdek Mikli · Rauno Sedrik · Andres Krumme

Abstract The study proposes using the distillable ionic liquid 5-methyl-1,5,7-triaza-bicyclo-[4.3.0]non-6-enium acetate, [mTBNH][OAc], for cellulose dissolution, making it an environmentally friendly alternative to conventional solvents in the transesterification of cellulose with vinyl esters. This ionic liquid (IL) has high dissolving power for cellulose and durability for recycling. However, its high viscosity limits cellulose concentration and its expensiveness hinders commercialization. The addition of naturally derived,

low-cost, and low-viscous co-solvents can reduce overall cost and viscosity. In this study, various green co-solvents, including γ-valerolactone (GVL), dimethyl isosorbide (DMI), sulfolane (SLF), and N,N'-dimethylpropyleneurea (DMPU), were mixed with [mTBNH][OAc] to test their ability to enhance cellulose transesterification. Cellulose esters with a degree of substitution (DS) up to 1.6 have been synthesized. The chemical composition of the materials was confirmed by FTIR and NMR. Green co-solvents alter the solubility and flow activation energy of cellulose in binary solvents. The produced cellulose esters become more amorphous, and their viscosity and complex moduli decrease because of the DS changing in the following order: DMPU < SLF < DMI < GVL. The efficiency of internal plasticization of cellulose esters was studied through melt flow rheology, which indicated that it increases with increasing DS. All tested cellulose esters have almost identical degradation temperatures, as detected by TGA.

Keywords Cellulose esters · [mTBNH][OAc] ionic liquid · Physical properties · Green solvents

E. Tarasova (✉) · N. Savale · L. Trifonova · I. Krasnou · A. Mere · T. Kaljuvee · V. Mikli · A. Krumme
School of Engineering, Department of Materials and Environmental Technology, Tallinn University of Technology, Ehitajate Tee 5, 19086 Tallinn, Estonia
e-mail: elvira.tarasova@taltech.ee

I. Reile
National Institute of Chemical Physics and Biophysics, Akadeemia Tee 23, Tallinn, Estonia

M. Kudrjašova
School of Science, Department of Chemistry and Biotechnology, Tallinn University of Technology, Akadeemia Tee 15, 12618 Tallinn, Estonia

R. Sedrik
Faculty of Science and Technology, Institute of Technology, Tartu University, Nooruse 1, 50090 Tartu, Estonia

Introduction

Cellulose, the Earth's most abundant natural polymer found in plants, is renewable and possesses unique qualities: Biodegradability, non-toxicity, biocompatibility, mechanical strength, heat resistance, and

solvent resilience (Feng and Chen 2008). However, its semi-rigid chain structure creates obstacles to its dissolution using traditional organic and inorganic solvents, which is a major hindrance to its processing and applications (Qiu and Hu 2013).

It is commonly believed that the ability of a solvent to break the hydrogen bond network of cellulose is the main factor in its dissolution (Bering et al. 2022). However, since cellulose has an amphiphilic nature, it was suggested that hydrophobic interactions between cellulose and the solvent may also play a significant role in its dissolution (Ghasemi 2018). Former efforts have focused on developing innovative cellulose solvents mix, like dimethyl sulfoxide/tetrabutylammonium fluoride (DMSO/TBAF) (Ciacco 2003), *N,N*-dimethylacetamide/lithium chloride (DMAC/LiCl) (Ass et al. 2006), *N*-methylmorpholine (NMMO) (Fink et al. 2001), and NaOH/urea (Cai and Zhang 2005). Unfortunately, these solvents are either costly or require harsh conditions, posing environmental and economic concerns.

Ionic liquids (ILs) offer sustainable options for cellulose dissolution and derivatization. Their high polarity disrupts hydrogen bonds in cellulose, and they possess characteristics such as non-volatility, and mostly non-toxicity (the latter is still being investigated) (Pinkert et al. 2009), (Han et al. 2009). Historically, 1-ethyl-3-methylimidazolium acetate [Emim][OAc] IL was considered excellent for cellulose solubility in laboratory research (Köhler et al. 2007). However, first-generation imidazolium-based ILs present challenges in recycling and stability, leading to undesired side reactions with cellulose (Xu and Cheng 2021), (Kostag et al. 2019). Recently, the superbase ionic liquid, [mTBNH][OAc] has emerged as a promising choice for cellulose dissolution and regeneration (Martins et al. 2022), (Parviainen et al. 2015). mTBN exhibits superior water stability compared to 7-methyl-1,5,7-triazabicyclo(4.4.0)dec-5-ene (mTBD) and 1,5-diazabicyclo(4.3.0)non-5-ene (Martins et al. 2022), (Ostonen et al. 2016). Additionally, [mTBNH][OAc] is a liquid at room temperature, making it less labor-intensive than highly crystalline 7-methyl-1,5,7-triazabicyclo(4.4.0)dec-5-enium acetate, [mTBDH][OAc], positioning it favorably for industrial use.

Despite their appealing features, ILs have downsides, including slow cellulose dissolution and high solution viscosity, hindering subsequent cellulose modification. Dipolar aprotic solvents (e.g., DMSO, dimethylformamide (DMF), DMAc) are extensively used in organic synthesis due to their polarities and solubilities (Phadagi et al. 2021), (Mohan et al. 2016). IL/DMSO co-solvent system has shown to be more effective in dissolving cellulose than pure ILs (Rinaldi 2011). In our recent work, [mTBNH][OAc]/DMSO-based binary solvent system was employed as a reaction media for the synthesis of thermoplastic long-chain fatty acid esters via catalyst-free cellulose transesterification, and cellulose esters (CEs) with DS = 0.35–2.00 were successfully synthesized (Tarasova et al. 2023). However, the widespread use of the mentioned co-solvents poses environmental and health risks due to inherent toxicity, and high energy inputs, making reducing reliance on such solvents crucial in green chemistry. Replacement of these dipolar aprotic solvents is a significant focus in green chemistry research areas (Constable et al. 2007), (Bryan et al. 2018).

Dipolar aprotic GVL, derived from lignocellulosic biomass, emerges as an excellent bio-sourced alternative due to its renewability, biodegradability, and non-toxicity (Strappaveccia et al. 2015). GVL is a highly suitable and sustainable substitute for typical polar aprotic solvents (Duereh et al. 2015). Additionally, its wide temperature range, with a low melting point of -31 °C and a high boiling point of 207 °C, ensures its safety for larger-scale solvent use. DMI, obtained from glucose via sorbitol, stands out for its chiral structure (Bryan et al. 2018), (Wilson et al. 2018) and high polarity, making it a promising replacement for conventional dipolar solvents. SLF is assessed as a potentially sustainable reaction medium (Tilstam 2012), (Henderson et al. 2011). While sitting lower on the sustainability scale, it proves valuable in various applications, including biomass valorization (Asakawa et al. 2019). Lastly, DMPU deemed a "green solvent" for its favorable properties, adds to the pool of environmentally friendly options with its high boiling point, low melting point, and low toxicity (Gören et al. 2016). In our previous work, we investigated the capacity of [mTBNH][OAc] combined with GVL, DMI, and DMPU to dissolve cellulose (Tarasova et al. 2024). It was shown that cellulose behaves like viscoelastic gels in 1:1 and 1:2 IL/DMPU and IL/DMI (and 1:2 IL/GVL), while it shows normal viscoelastic behavior in 2:1
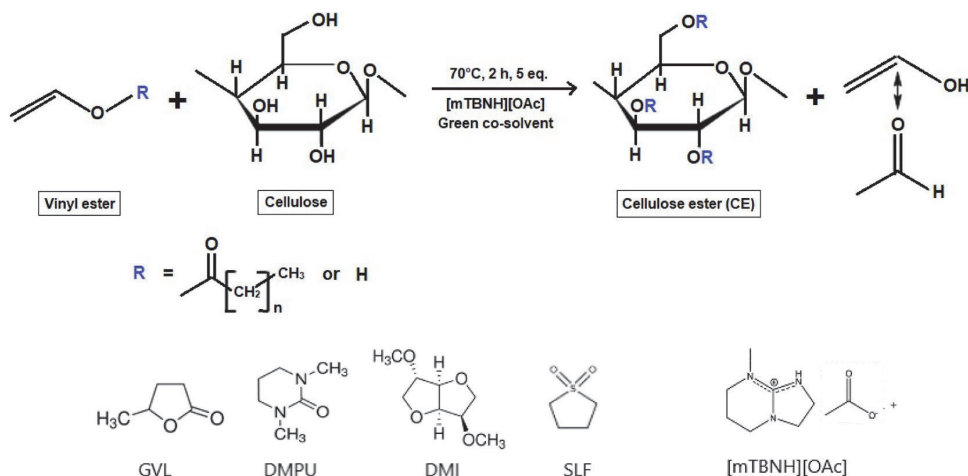
Scheme 1 Transesterification of cellulose with vinyl esters in [mTBNH][OAc] /green co-solvents

IL/green co-solvents, corresponding to the behavior of polymers in thermodynamically good solvent systems.

CEs are commonly synthesized through acylation in either heterogeneous or homogeneous conditions. Homogeneous solutions are preferred for their superior ability to control the DS, ensuring a more consistent product pattern (Heinze and Liebert 2001). In this work, we evaluated for the first time the impact of four bio-based co-solvents such as GVL, DMI, SLF, and DMPU, as a reaction media on the transesterification of cellulose with vinyl esters in the superbase [mTBNH][OAC] IL to produce thermoplastic CEs. The developed process for the functionalization of cellulose might be beneficial for the production, as distillable, low-toxic, and liquid-like IL and (partially) bio-based co-solvents can be used, which is assumed for the future industry by using sustainable, renewable, carbon–neutral, bio-based chemicals instead of fossil-based ones. The co-solvents are also of low toxicity and high boiling point reducing dangers in industrial use. Another goal of this study is to disclose the melt flow behavior, rheology, thermal, and mechanical properties of obtained CEs. Melt properties and thermal behavior are important for understanding the proper processing conditions for blow molding, injection molding, sheet forming, extrusion, fiber spinning, etc.

Experimental Section

Materials

Cellulose used in this work was produced by Carl Roth GMBH (Germany) with fiber length 0.02–0.1 mm. Vinyl laurate, myristate, and palmitate with purity > 98% were purchased from Tokyo Chemical Industry Co (Japan). Ionic liquid 5-methyl-1,5,7-triaza-bicyclo-[4.3.0]non-6-enium acetate, [mTBNH] [OAc], was not commercially available and was synthesized by Liuotin Group Oy (Finland). GVL, SLF, and DMI with purity ≥ 99% were purchased from Sigma Aldrich (St. Louis, MO, USA). DMPU with a purity of 97%, as well as pyridine-d5 (purity = 99.5 atom % D. contains 0.03 v/v% TMS) for NMR, were purchased from Acros Organics (Geel, Belgium). The chemical structure of the co-solvents used is shown in Scheme 1. Trifluoroacetic acid (TFA) with purity ≥ 99.0% was purchased from Sigma Aldrich (St. Louis, MO, USA).

Cellulose dissolution and esterification procedure

Cellulose was dried under vacuum at 105 °C for 24 h before use. Cellulose concentration in all studied solutions was 2 wt%. Cellulose was dissolved in mixtures of [mTBNH][OAc] with co-solvents (DMI, DMPU, GVL, SLF) and stirred at 80 °C for 16 h

until the cellulose was dissolved. Dissolution of cellulose was confirmed by rheology and polarized light microscopy: cellulose solution did not contain undissolved or aggregated cellulose fibers, and the solutions were optically transparent and clear. IL and co-solvents were first mixed in a ratio of 2:1 by weight and then cellulose was added to the binary solvent. Such a ratio has been chosen due to our previous research (Tarasova et al. 2024) where it was found that a 2:1 ratio gives true cellulose solutions for all studied mixtures. The content of green co-solvent higher than 50% can lead to gelation and phase separation of cellulose solutions.

The designed amount of the vinyl ester (5 equivalents to AGU (eq.AGU)) without any external catalyst was added to the 2 wt%-cellulose solution in 2:1 IL:co-solvent in a chemical reactor equipped with a mechanical stirrer and nitrogen flow, and then the reaction was performed at 70 °C during 2 h under nitrogen atmosphere and intensive stirring. When the reaction was completed, the obtained cellulose ester was precipitated into 500 mL of ethanol. To remove solvents, the product was washed several times in 100–200 mL of ethanol, and next in acetone. Finally, it was washed with hexane to remove unreacted vinyl ester. The products were dried under a vacuum at 55 °C overnight.

CEs prepared in a mixture with green co-solvent will be abbreviated as CE-green co-solvent, e.g., cellulose myristate prepared in IL/GVL will be abbreviated as CM-GVL.

Characterization

The ^1H NMR, ^{13}C NMR, and HSQC NMR spectra of the cellulose derivatives were acquired on an Agilent Technologies DD2 500 MHz spectrometer equipped with 5 mm broadband inverse (^1H, HC-HSQC spectra) or broadband observe (^{13}C spectra) probes. A 15-min temperature equilibration delay was allowed between sample insertion and NMR acquisition at 80 °C sample temperature. Typically, for ^1H spectra, 32 scans with 25 s relaxation delay were acquired and for ^{13}C 20000–45000 scans with 2.5 s recycle delay were acquired to achieve the desired signal-to-noise ratio. The NMR samples were prepared in a small glass bottle where 20–25 mg of the sample was dissolved in 0.8 mL of deuterated NMR solvent for 90 min at 40–65 °C until a clear solution

was obtained. 2–3 drops of TFA were added into the dissolved sample during NMR sample preparation to avoid overlapping of signals from unsubstituted OH groups with those of the AGU. The glass bottle containing the mixture was dry and carefully sealed with parafilm. The samples were then subjected to ultrasonic treatment to obtain a transparent solution.

The DS of cellulose myristate was calculated from the ^1H NMR spectrum by taking an integral of the area of terminal methyl groups ($I_{(CH_3)}$) and AGU signals (I_{AGU}) based on the reported method (Lowman 1998):

$$DS = 10 \bullet \frac{I_{(CH_3)}}{(3 \bullet I_{AGU} + I_{(CH_3)})} \qquad (1)$$

The FT-IR spectra of cellulose and cellulose derivatives were recorded on Shimadzu IRAffinity-1S using the Quest ATR accessory purchased from Specac in the range of 500–4000 cm^{-1} with a resolution of 0.5 cm^{-1}. All samples were dried at 80 °C in a vacuum oven overnight before the FTIR measurement to remove the moisture.

To study the rheological properties the CEs were prepared in the form of films by solvent casting on a glass dish. CEs were dissolved in pyridine with 5 wt% concentration and then stirred for 16 h at 40–60 °C until dissolved. After complete dissolution, the ester solution was poured into the glass dish, and the solvent was evaporated at room temperature for 24 h. Samples for rheology were prepared from ~100 μm thick films by cutting 25 mm Ø discs.

The rheology of the samples was tested with an Anton Paar Physica MCR501 rheometer, and cone-plate measuring geometry was used (plate diameter 25 mm, cone angle 2°). Flow curves were obtained at a shear rate $\dot{\gamma}$ range from 0.01 to 100–500 s^{-1}. Complex viscosity was determined in the range of angular frequencies $\omega = 0.1$ to 100–500 rad/s. A constant strain of $\dot{\gamma} = 1\%$ was used to define the linear viscoelastic region (LVR). An amplitude sweep test to determine the LVR was done at a frequency of 1 Hz. The samples were examined at 190 °C. Ordinary equations were applied to calculate rheological characteristics (Malkin 1994). Each rheological curve has been obtained 2–4 times to ensure the data reproducibility and get average results.

The hydrophobicity of the prepared film surface was tested by equilibrium contact angle using

DataPhysics OCA 20 device and the SCA 20 software (Riverside, CA, USA). All experiments were executed on both sides of the films and averages were taken. Distilled water was used as a liquid agent to create a drop on the surface. A total of five measurements were taken and averaged for each variable. All measurements of the contact angle were performed at room temperature and a relative humidity of 40%.

The tensile tests were performed with Instron machine 5866 at a temperature of 22 °C and a humidity of 45% for all the samples. The cast films were cut into ribbons of $20 \times 10 \times$ ca. 0.1 mm. For each sample, 7–10 ribbon specimens were tested and the values of elastic modulus, strain at break, and stress at break were averaged. The pulling rate applied during the measurements was 20 mm/min.

Optical micrographs of cast films were pictured at Carl Zeiss Axioskop 2 with magnification $\times 100$ in polarized light mode.

A Setaram Labsys Evo 1600 thermoanalyzer was exploited for studying the degradation of cellulose myristate (CM) samples. The experiments were carried out under non-isothermal conditions up to 600 °C at the heating rate of 10 °C min^{-1} in the atmosphere of argon. Standard 100 µL alumina crucibles were used, the mass of the samples was 6 ± 1.0 mg, and the gas flow was 20 mL/min. The peak degradation temperatures were determined from the derivative thermograms (DTG).

The structural analysis of the samples in the powder form was assessed from X-ray diffraction (XRD) measurement using the Rigaku Ultima IV diffractometer. The instrument was equipped with a silicon detector and a Cu Kα irradiation source ($\lambda = 1.540$ Å), anode voltage 40 kV, anode current 40 mA, θ-θ regime, step $\theta = 0.02$ deg.

The morphology of the film surface has been analyzed with a scanning electron microscope (SEM) Gemini Zeiss Ultra 55 (Carl Zeiss, Germany).

Molar mass (MM) of pure cellulose was determined at 25 ℃ from the intrinsic viscosity [η] (=5 dl/g) of cellulose solution in cupriethylenediamine hydroxide solution, Cuene, according to a standard procedure ASTM D1795 − 13. The MM was then calculated by the Mark-Houwink equation with parameters K = 1.01×10^{-4} dL/g and a = 0.9 ((Brandrup et al. 1999)). The obtained MM is 163 000 g/mol (DP = 1000).

The size exclusion chromatography (SEC) of CMs in pyridine at 40 °C was done on the Shimadzu Prominence system equipped with a Shodex KF-804 column and a refractive index detector (RID-20A).

Results and discussion

Preparation of cellulose esters in [mTBNH][OAc]/green co-solvents

Following the successful dissolution of cellulose in [mTBNH][OAc] promoted by green co-solvents such as GVL, DMPU, SLF, and DMI, the potential of cellulose modification in the IL/co-solvent systems studied was primarily investigated by transesterification of cellulose with vinyl myristates. The successful synthesis of CEs with vinyl myristate in different mixtures of [mTBNH][OAc] with DMSO was already presented by the authors in a recently published paper (Tarasova et al. 2023). This time, the transesterification of cellulose with vinyl myristate in [mTBNH][OAc] mixed with green co-solvents in a 2:1 ratio was performed under similar reaction conditions, namely a reaction temperature of 70 °C, time of 2 h, and vinyl myristate was added in an amount of 5 eq.AGU. For comparison, several cellulose laurates (CL) and palmitates (CP) were also synthesized in selected IL/Co solvent systems under identical reaction conditions. The mass fraction of cellulose in all solutions considered was 2 wt.% without exception. This concentration is not a limit, it has been chosen for several reasons: first, it gives a high yield (up to 80%) of transesterification reaction with vinyl esters while keeping the stirring ability during the reaction at an appropriate level; second, similar concentrations were also used by us for the synthesis of cellulose derivatives in [mTBNH][OAc]/DMSO solutions in a recently published paper (Tarasova et al. 2023). Additionally, we used this concentration to study the dissolution capacity of green co-solvents towards cellulose (Tarasova et al. 2024). Generally, this concentration can be elevated up to 5–6 wt.%.

Scheme 1 shows the pathway for cellulose transesterification with vinyl esters. CEs were synthesized in one step and low vapor point ethenol (in situ tautomerization to acetaldehyde) as the byproduct can be easily evaporated from the reaction system at elevated temperatures. No external catalyst was added.

After acylation, the FTIR analysis indicated that the long-chain acyl groups were introduced into cellulose for all samples, as can be seen in Figure S1 in Supporting Information, which shows the FTIR spectra of native cellulose and its myristate derivatives.

The appearance of the ester carbonyl (>C=O) group's stretching corresponds to an absorption band at 1746 cm^{-1}, which provides the strongest evidence of successful acylation. In comparison to cellulose, the FTIR spectra of CEs revealed the existence of several new peaks. The peaks at 2950 cm^{-1} and 2847 cm^{-1} indicate the asymmetric and symmetric stretching of the methylene group present in cellulose myristate, respectively. This indicates that the methylene and carbonyl groups were attached to cellulose, thus confirming the successful transesterification of cellulose in the [mTBNH][OAc] IL mixed with a green co-solvent.

All the CEs that have been produced are soluble in several organic solvents, primarily DMSO, THF, and pyridine. This solubility allows for direct measurement of NMR spectra in solution, which is useful for calculating DS. The chemical structure of the CM has been verified by ^{1}H and ^{13}C NMR, and HSQC. Figure 1(a) presents the ^{1}H and ^{13}C NMR spectra of CM-DMI, as an example. Similar spectra have been obtained for all CM samples. In the ^{1}H NMR spectrum of the CMs, the proton signals from approximately 6.00 to 3.50 ppm are assigned to H-1, H-2, H-3, H-4, H-5, H-6, and H-6´ of AGU

in cellulose. The signals at 2.75–2.25, 1.88–1.5, and 1.27 ppm are associated with the methylene protons at H-8, H-9, and H-10–19, respectively. The signals at 0.98–0.79 ppm are attributed to the methyl protons at H-20.

In the ^{13}C NMR spectrum of CM, which is presented in Fig. 1(b), the signals at 35.54, 33.16, 26.37, 23.89, and 15.16 ppm are assigned to carbons of C-8, C-18, C-9, C-19 and C-20 of the aliphatic side chain, respectively. The carbons at C-(10–17) give signals starting from 30.89 to 30.58 ppm. The AGU carbons C-1, C-1′, C-4, C-2,3,5, and C-6 give signals at 105.23, 102.64, 82.75, 77.25–75.08, and 64.66, respectively. The signals from 171.74, 174.22, and 174.59 ppm correspond to the carbonyl carbon at C-7, which provides direct confirmation of the successful attachment of the long-chain fatty acid chain to the cellulose backbone.

To confirm further the assignment of cellulose ester signals, the HSQC spectrum was collected. The example of ^{1}H-^{13}C HSQC for cellulose myristate is presented in Fig. 2, where the cellulose region (Fig. 2a) and aliphatic side chain region (Fig. 2b) are shown. As can be seen, in the aliphatic side chain region, the correlation of C19/H19, C18/H18, C20/H20, and C10-17/H10-17 were located at δH/δC at 1.31/23.83, 1.30/33.21, 0.91/15.19 and 1.29/30.74 respectively. In the cellulose region, the strong correlations were distinguished at δH/δC 5.54/75.11, 5.28/74.96, 4.75/104.01, 4.50/64.76, 4.01/77.37, and
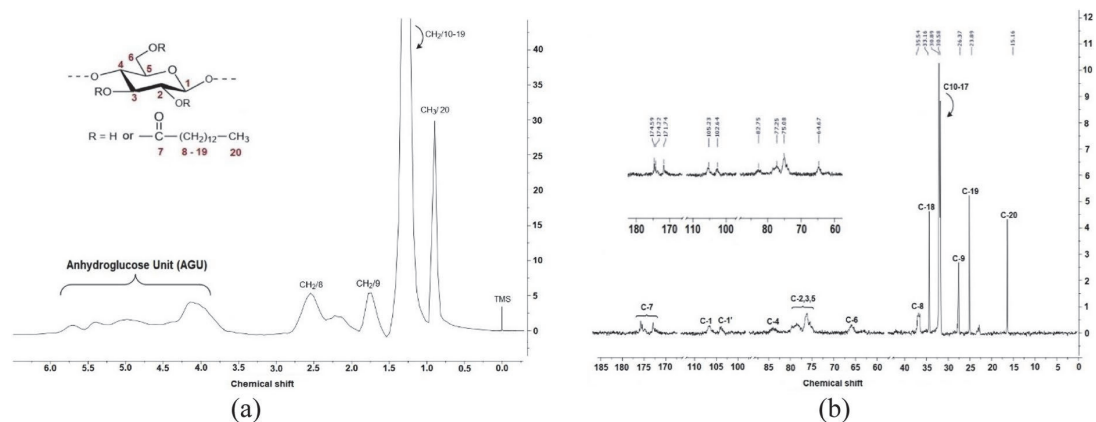
Fig. 1 **a** ^{1}H NMR spectrum of CM-DMI in pyridine-d5; (**b**) ^{13}C NMR spectrum of CM-DMI in pyridine-d5. Empty and solvent regions are left out for clarity
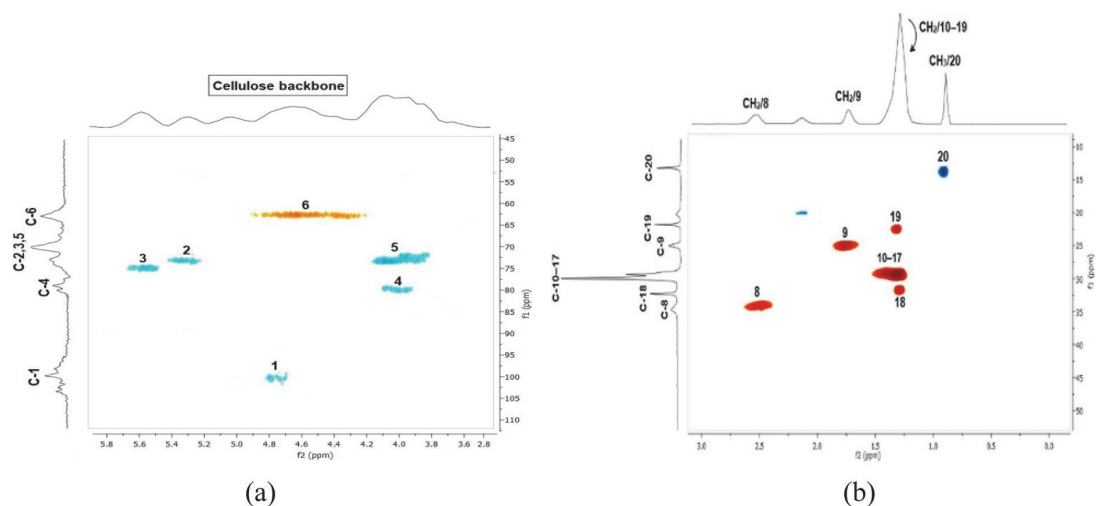
Fig. 2 Cellulose (**a**) and aliphatic side chain (**b**) region of HSQC spectrum of cellulose myristate, CM-DMI, in pyridine-d5. Red indicates methylene protons (-CH$_2$) and blue indicates methyl (-CH$_3$) and methine (-CH-) protons

3.99/82.91 for C3/H3, C2/H2, C1/H1, C6/H6, C5/H5 and C4/H4 respectively. The two decentralized signals of C8/H8 and C9/H9 are represented by δH/δC at 2.50/35.62 and 1.76/26.39, respectively.

Figure 2 indicates the complete acylation of C6-O under optimized conditions, as only a single resonance of the corresponding group is observed in ^{13}C. Additionally, in Fig. 2, the intensity of the characteristic cross-peak of C3-OAcyl (5.6–5.5/75.11 ppm) is slightly higher than that of C2-OAcyl (5.3/74.96 ppm), thus indicating a preferential acylation of the former. Hence, it can be suggested that the order of substitution of the OH group is C6˃C3≥C2. The same order has been observed for all CMs in [mTBNH][OAc]/green co-solvent. In addition, we have previously found a similar substitution pattern for CEs in [mTBNH][OAc]/DMSO solutions in our previous work (Tarasova et al. 2023).

Illustrative NMR spectra for CL and CP samples can be found in Figures S2 and S3, respectively, in Supporting Information.

The transesterification reaction proceeded smoothly, and CEs were obtained in all co-solvent mixtures. The DS obtained from NMR spectra is listed in Table 1.

To examine the structure of obtained CMs, the XRD patterns are obtained (shown in Fig. 3). Cellulose is known to have a crystalline structure with characteristic peaks at $2\theta=14.9°$, 16.7°, 20.7°, 22.8° and 34.8° for (1-10), (110), (102)/(012), (200), and

Table 1 Reaction parameters in 2:1 [mTBNH][OAc]/co-solvent mixtures, and DS of obtained cellulose esters

Sample	Reaction conditions			Green co-solvent	DS
	Time, h	Temperature, °C	eq.AGU		
CM-DMPU	2	70	5	DMPU	1.23
CM-SLF	2	70	5	SLF	1.32
CM-DMI	2	70	5	DMI	1.42
CM-GVL-1	2	70	5	GVL	1.51
CM-GVL-2	2.5	70	3	GVL	1.41
CM-GVL-3	1.5	70	3	GVL	1.27
CL-DMPU	2	70	5	DMPU	1.37
CL-GVL	2	70	5	GVL	1.55
CP-DMPU	2	70	5	DMPU	1.16

(004) diffraction planes, respectively (French 2014). Upon transesterification in the IL/green co-solvent system, the sharp peaks disappeared in the CM patterns, indicating a loss of most, if not all, crystallinity.

Generally, it could be said that all CM patterns are for amorphous cellulose. The peak intensity at $2\theta=20°$ decreases in the following order: CM-DMPU > CM-SLF > CM-DMI > CM-GVL. The observed trend in the amorphization of CMs may be attributed to the
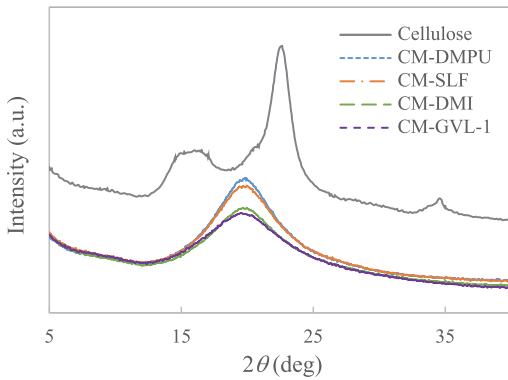
Fig. 3 XRD patterns of CMs obtained in different IL/green co-solvents

DS of the samples: the higher the DS, the stronger the amorphization of CMs.

As can be seen from Table 1, the DS of the CMs obtained in different co-solvents differ from each other, although the reaction conditions are identical (DS of CM-DMPU < CM-SLF < CM-DMI < CM-GVL-1). For example, the highest DS values were obtained for cellulose myristate in GVL, while the DS of CM in DMPU showed the lowest value. Nevertheless, the DS values obtained even for DMPU-containing solvents are still higher than DS = 0.9 of CM obtained in pure IL (without co-solvent). This means that dilution of the cellulose solution in IL with nominal co-solvents improves mass transfer and promotes the transesterification reaction. Note that pure IL has a viscosity of 200 mPa·s, while the viscosity of the green co-solvents is about 2 mPa·s (except SLF with 10 mPa·s).

It is reasonable to believe that the varied solubilizing capacities of the used green co-solvent account for the discrepancies in the DS values of the CMs. From a theoretical point of view, the Hansen solubility parameter model can be used to predict appropriate solvents and non-solvents for polymers. If the Hansen solubility parameters of the liquid and the polymer are close to each other, the liquid is considered a good solvent for the polymer. Hansen solubility values of cellulose (18.03 MPa$^{1/2}$) (Brandrup et al. 1999) with those of GVL, DMI, DMPU, and SLF, which are 17.4 MPa$^{1/2}$ (Rasool and Vankelecom 2021), 20.4 MPa$^{1/2}$ (Russo et al. 2020), 22.2 MPa$^{1/2}$ (Hansen 2007), and 25.8 MPa$^{1/2}$ (Hansen 2007), respectively. It is seen that GVL has the closest affinity to cellulose, in contrast

to DMPU and SLF by comparison. The 3D scatter plot of dispersion δ_d, polar δ_p, and hydrogen bonding δ_h constituents of the Hansen solubility parameter for the green co-solvents used and cellulose is presented in Figure S4 of Supporting Information. We could hypothesize that better cellulose solvation with a co-solvent improves substitution efficiency.

A common way to analyze the solubility of polymers in solutions is to get the values of activation energy E_a. Activation energy E_a of flow can be obtained from the viscosity−temperature dependence via the Arrhenius equation (Lefroy et al. 2021), (Yuan et al. 2019):

$$\eta_0 = A e^{E_a/RT} \qquad (2)$$

where E_a is the activation energy, η_0 is zero shear viscosity obtained at low shear rates, A is a constant, R is the gas law constant, and T is the absolute temperature. The activation energy (E_a) can be calculated from the slope of $\ln \eta_0$ versus $1/T$. A rheological study of cellulose solutions in IL/green co-solvent mixtures has been conducted in our previous work (Tarasova et al. 2024), where the dependence of $\ln \eta_0$ as a function of $1/T$ was obtained for the cellulose solutions in all 2:1 IL/green co-solvents mixtures.

The E_a for polymer solutions is related to the challenge of moving a polymer chain from one state/position to another, as well as to the strength of interchain interactions when considering the same type of polymer (with identical chemical composition, molar mass, and microstructure) (Hawkins et al. 2021), (Budtova and Navard 2015).

Cellulose solution in pure [mTBNH][OAc] had an activation energy 45.3 kJ/mol, which is comparable with E_a = 46 and 49 kJ/mol for cellulose (with DP 300) and spruce sulfite pulp (DP 1000) in [Emim][OAc], respectively, reported in the literature (Gericke et al. 2009). The obtained result of E_a for 2:1 [mTBNH][OAc]/GVL (36.9 kJ/mol) is comparable with E_a = 35.1 kJ/mol for 3:2 [Emim][OAc]/GVL presented by Yuan et al. (Yuan et al. 2019). The obtained E_a value for IL/DMPU was 41.3 kJ/mol, for IL/SLF— 41.1 kJ/mol, and for IL/DMI—40.7 kJ/mol. Flow activation energy data, to the best of our knowledge, are not available for cellulose solutions in IL/DMPU, IL/SLF and IL/DMI and cannot be compared.

The E_a of cellulose in an IL/co-solvent mixture decreases gradually with the type of co-solvent in

the following order: DMPU > SLF > DMI > GVL. The differences in E_a indicate that the co-solvent is modifying the energy barrier to flow. Flowing DMPU and SLF solutions require slightly more energy compared to GVL. It was also shown that DMPU and DMI serve simply as diluents of IL, whereas GVL promotes the solubility of cellulose analogously to DMSO (Tarasova et al. 2024).

Lower E_a values are also consistent with the observation that the corresponding dissolution of IL/green co-solvent towards cellulose is better than that for pure IL. Therefore, co-solvents can enhance the efficiency of cellulose chemical modification, such as transesterification, that is observed in practice.

Physical properties of cellulose esters

To understand the thermoplastic properties of materials, the melt flow behavior was examined. Figure 4 shows the angular frequency dependence of the complex viscosity and moduli of CMs prepared in different green co-solvents. Double-logarithmic scales are used for all rheological plots. As can be seen from Fig. 4(a), all CMs demonstrate shear-thinning behavior in the studied range of angular frequency ω – no linear viscosity range could be observed. Moreover, the viscosity of CM-DMPU is found to be the highest, and that of CM-GVL is the lowest among all others.

The reduction in viscosity for CM samples obtained in various co-solvents cannot be solely attributed to their molar mass. The obtained weight-average M_w

molar mass of CM-DMPU, CM-SLF, CM-DMI and CM-GVL was 202 kg/mol (dispersity Đ 6.2), 302 kg/mol (Đ 4.3), 311 kg/mol (Đ 5.5) and 591 kg/mol (Đ 3.0), respectively. Despite having the highest molar mass among the samples, CM-GVL does not demonstrate the highest viscosity values as expected. In fact, it shows the lowest viscosity among all the samples.

As shown in Fig. 4(b), both storage G' and loss G'' moduli exhibit only slight dependence on frequency. Moreover, G' exceeds G'' over the range of measurable frequency.

It means that the rheological behavior of the material is dominated by an elastic or solid-like response. The dominance of the elastic response could be attributed to the deformation and mobility of the cellulose backbone of the CE macromolecule. Melt elasticity is the main factor that determines how a molten material behaves. This elasticity causes phenomena such as die swell during processing. The behavior of G' relates to the flow behavior in the mold and has a strong influence on the relaxation behavior and, consequently orientation and frozen-in strains. A higher value of G' results in higher die swell and thicker products.

Interestingly, the magnitude of the complex moduli of CMs decreases in the order DMPU > SLF > DMI > GVL which correlates with the viscosity data but is in reverse order to the DS values of the samples.

Similar angular dependencies of complex viscosity and moduli have been detected for CL and CP samples, as can be seen in Fig. 5. Changes in viscosity
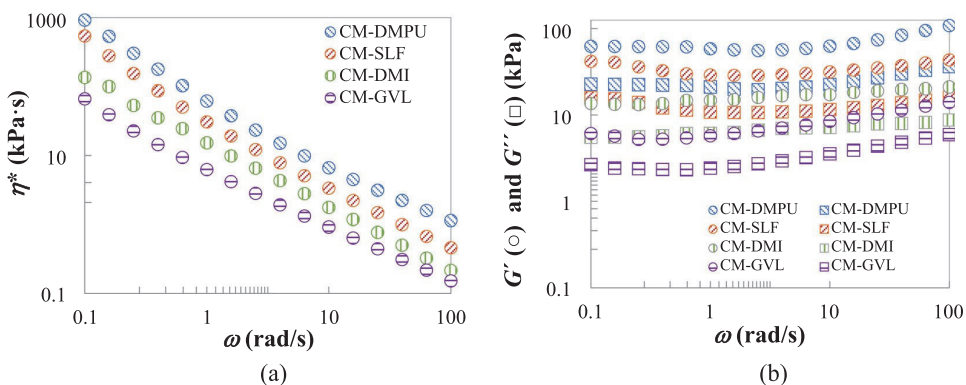
Fig. 4 Dependences of (**a**) complex viscosity η^* and (**b**) storage G' (circle) and loss G'' (square) moduli on angular frequency ω for cellulose myristate films prepared in various green co-solvents, taken at 190 °C

and moduli can be associated either with the nature of the green co-solvent used and its indirect impact on CE properties or with the DS of produced CEs.

Based on the Cole–Cole plots presented in Fig. 6, it appears that the G' and G'' of all CMs (irrespective of their co-solvent nature) are interdependent and fit the same straight line. This suggests that the microstructure of the CM materials remains unchanged (Ilyin et al. 2020).

Surprisingly, the experimental points for CL and CP samples superimpose with the same CM line, as it is obvious from Fig. 6. Cole–Cole plots for these materials seem to be mostly dependent on the degree of substitution of CEs.

To check this idea, additional samples of CMs with lower DS (CM-GVL-2 and CM-GVL-3, as listed in Table 1) have been synthesized. CMs were synthesized using the same IL/GVL systems to eliminate any effects caused by the co-solvent nature. As it is clear from Fig. 7(a), the complex modulus data of the samples CM-GVL-1, -2, and -3 all fall on the same generalized straight line. However, there is a translational shift according to their DS: The higher the DS, the lower the values of the complex moduli.

Complex viscosity magnitudes also decrease with DS, as seen in Fig. 7(b). Thus, it can be concluded that the degree of substitution has a major effect on the viscosities and complex moduli of CEs.

It is well known that the G-moduli reflect the stiffness of the samples, which in turn is affected by the polymer chain structure and interchain interactions. A. Maeda et al. (Maeda, 2014) by
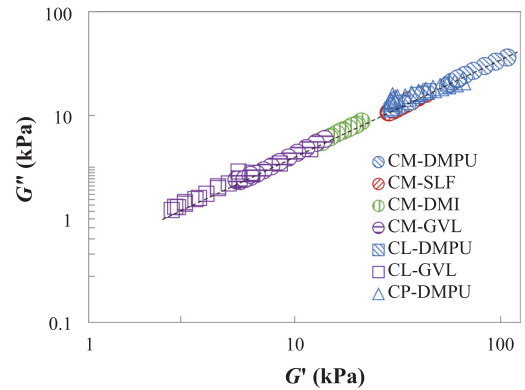

Fig. 6 Cole–Cole plots for CMs, CLs, and CP films obtained in IL/green co-solvent systems

stress-optical analysis stated that esterification does not affect the backbone chain stiffness of cellulose, and side chain fatty acid groups serve as a plasticizer (diluent), reducing the concentration of the contour length. Taking this assumption into account, the decrease in G-moduli for CM films can be explained by the plasticizing effect with increasing DS: The higher the DS, the higher the thermoplasticity of the samples. It correlates with XRD data showing that increasing DS leads to more amorphous and, hence, less rigid CMs.

The rigidity of the samples can also be affected by the dissolution of CMs in the pyridine used for film casting. It is widely known that the dissolution
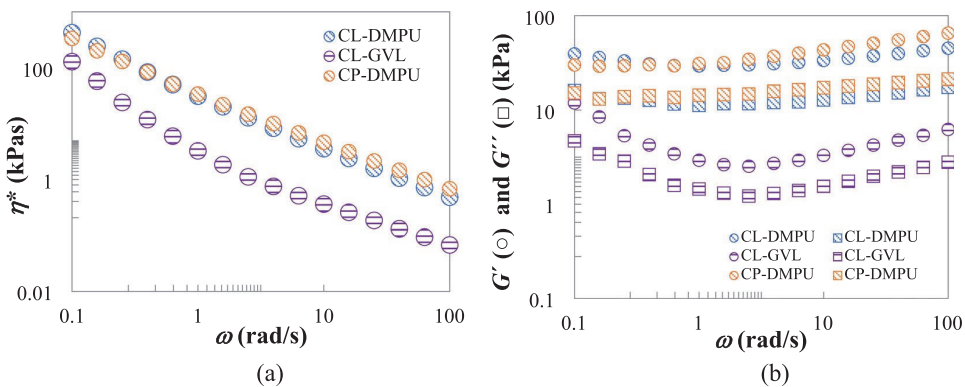
Fig. 5 Dependences of (**a**) complex viscosity η^* and (**b**) storage G' (circle) and loss G'' (square) moduli on angular frequency ω for cellulose laurates and palmitate films prepared in various green co-solvents, taken at 190 °C
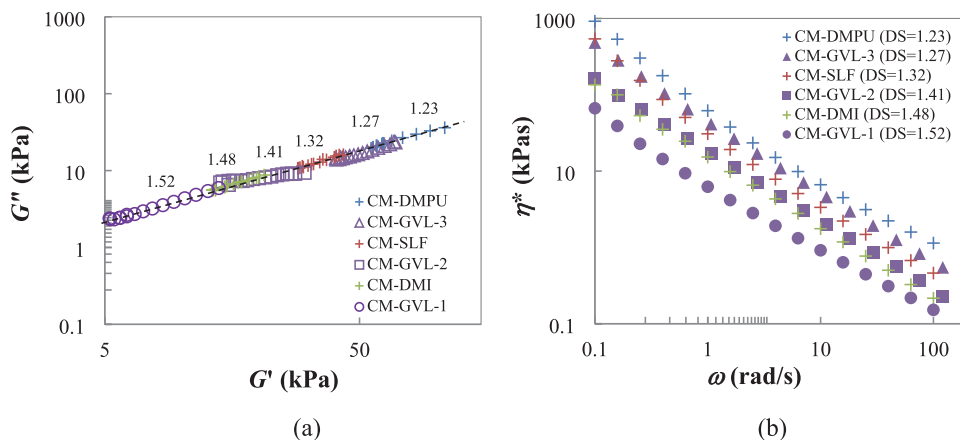
Fig. 7 **a** Cole–Cole plots for CMs with different DS obtained in IL/green co-solvent systems. The values of DS are listed over the line; **b** Dependences of complex viscosity $\eta*$ on angular frequency ω for CMs with various DS

of cellulose esters is strongly affected by their DS. Depending on their DS, cellulose esters can be dissolved in solvents with a wide range of polarity: Highly substituted CEs are soluble in non-polar organic solvents (such as chloroform, for example), while poorly substituted CEs are mostly soluble in polar organic solvents (like DMSO). Hence, CMs with lower DS may have poorer solubility in pyridine compared to CMs with higher DS. IL/DMPU having the lowest solubility capacity of cellulose (its E_a is the highest among all others) leads to the lowest values of DS. Speculatively, one can assume that the lower solubility capacity of IL/DMPU influences the homogeneity of cellulose dissolution, which can lead to inhomogeneity in substitution along the cellulose backbone during the esterification process. Therefore, areas with unsubstituted parts of cellulose having crystalline structure due to intra- and interchain interactions may be present. Such crystalline areas are stiff and not soluble in organic solvents (pyridine) which adds extra rigidity to the CM samples. When cellulose is more homogeneously dissolved in solvents like IL/GVL, it leads to higher DS values, which in turn improves the dissolution of CM samples in pyridine.

Indeed, as can be seen from Fig. 8 where optical micrographs in polarized light mode are shown, the morphology of CM-DMPU films contains a lot of crystallites whereas CM-GVL samples demonstrate few crystallites in their morphology.

Hence, if these crystallites comprise native cellulose structures, they will not completely melt at the studied temperature. This will provide additional rigidity to the samples, which explains the behavior of G-moduli in Figs. 5, 6, 7 and 8.

Unfortunately, it is not possible to evaluate the effect of fatty acid chain length due to the different DS of CLs and CP.

The Cox-Merz rule is usually applied to correlate the dynamic and steady-state shear properties of the solutions (Barnes et al. 1989). In this method, the values of complex viscosity $\eta*$ and shear viscosity η are compared at equal values of shear rate $\dot{\gamma}$ and angular frequency ω. The validity of this rule has been confirmed for many polymer melts and solutions (Mead 2011), (Marrucci 1996).

Figure 9 depicts the η and $\eta*$ of all CM samples plotted against $\dot{\gamma}$ and ω, respectively. For the frequency sweep, we applied a strain of 1% to ensure the experiments were within the linear viscoelastic range.

A significant deviation from this rule can be observed for all CM samples. Similar deviations have been detected for squash pulp (Quintana et al. 2018), for example, and in other biopolymer systems (Bistany and Kokini 1983).

Although the applicability of this principle to polymer melts has been proven (Marrucci 1996), (Mead 2011), the Cox-Merz rule is invalid for materials having any type of physical and/or chemical interactions and thus this principle is not working for such

(a)   (b)
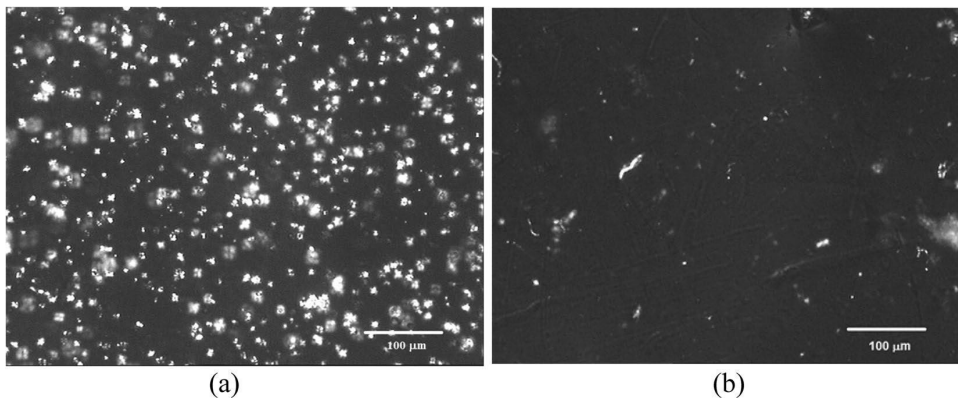
Fig. 8 Optical micrographs taken in the polarized light mode for CM-DMPU (**a**) and CM-GVL (**b**) films at room temperature
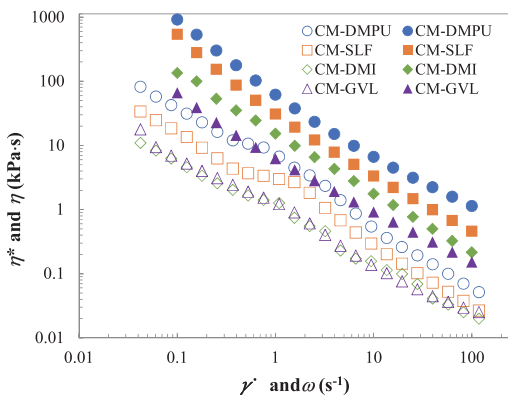
Fig. 9 Comparison of complex viscosity η^* (filled symbols) and shear viscosity η (hollow symbols) taken at 190 °C as a function of angular frequency ω and shear rate $\dot{\gamma}$ for CMs prepared in various 2:1 IL/green co-solvent mixtures

materials as gels, colloidal cellulose suspensions, etc. (Shafiei-Sabet et al. 2012), (Gleissle and Hochstein 2003).

The deviation observed in the case of CMs is likely caused by the formation of structural and intermolecular aggregates, which is consistent with the results obtained from optical microscopy. These structures are prone to being disrupted under shear flow, while low strains applied in oscillatory tests do not have any impact on them.

The mechanical properties of CMs have been evaluated. As DS plays a major role in all studied characteristics, three CM samples with varying degrees

of substitution prepared in the same IL/GVL solvent were also studied by tensile test. Stress–strain curves for studied cellulose myristates at room temperature can be viewed in Figure S5 in Supporting Information.

With an increase in DS, the samples exhibit a thermoplastic behavior, resulting in an increase in strain at break. At the same time, Young's modulus (initial slope of the stress–strain curve) and yield point of CMs decrease. This behavior may be related to the more pronounced plasticizing effect of the myristate chains with increasing DS, as previously shown in the rheological behavior section. In this sense, Young's modulus correlates with the storage modulus: an increase in DS leads to a decrease in the rigidity of the samples. Similar behavior was detected for cellulose laurates (Duchatel-Crépy et al. 2020) and other cellulose esters (Katsuhara et al. 2023), (Crépy et al. 2009).

One important characteristic of films is their hydrophobicity. This property is desired in the food packaging industry as it provides resistance against liquids and water, ensuring a longer shelf life for food products (Asim et al. 2022). Cellulose esters have hydrophobic properties with contact angles over 89°, similar to commercially used polyethylene. (i.e., LDPE, 91°) (Crépy et al. 2009). However, it is dependent on the ester's composition. It is expected that the contact angle will increase with a higher degree of substitution (Willberg-Keyriläinen et al. 2017), (Crépy et al. 2009).

Cellulose myristates prepared in IL/green co-solvents have been evaluated for their surface wettability

using contact angle measurements. Figure 10 (left) shows the average contact angle of different CMs. As can be seen, the contact angles decrease from 104.8° to 84.9° in the order CM-DMPU > CM-SLF > CM-DMI > CM-GVL despite an increase in their DS. Such behavior of the contact angle with DS is unexpected. In general, cellulose esters should be more hydrophobic than cellulose due to acylation (Kramar et al. 2023). Wen et al. (2017) suggest that when cellulose is esterified using a hydrophobic aliphatic chain, the hydrophilic properties of the material are reduced, especially if all the hydrophilic OH groups are substituted. However, research has found that cast films made from cellulose acetate solution are not entirely hydrophobic, and usually exhibit a contact angle of less than 90° (Wu et al. 2014).

The unexpected decrease in the contact angle of CMs can possibly be attributed to the surface roughness of the tested films. Based on the SEM images of the films shown in Fig. 10 (right), it can be assumed that the presence of crystallites (aggregates) affects the surface roughness of the film. As it is obvious, CM-DMPU has a rougher surface than CM-GVL; then CM-SLF and CM-DMI represent intermediate surface roughness between CM-DMPU and CM-GVL. The relationship between roughness and contact angle was defined in 1936 by Wenzel who stated that "adding surface roughness will enhance the wettability caused by the chemistry of the surface" (Wenzel 1936). If a surface is chemically hydrophobic, meaning it has a contact angle greater than 90°, adding surface roughness will increase the contact angle

even more. This suggests that the higher contact angles observed in CM-DMPU and CM-SLF, which both have contact angles greater than 90 degrees, are due to the rougher surfaces.

The thermal stability of CMs (in powder form) was studied using TGA/DTG between 30 °C and 600 °C. The corresponding TGA/DTG curves are shown in Fig. 11. According to the TGA curves, weight loss can be divided into three steps. The initial weight loss observed at around 260 °C can be attributed to the evaporation of moisture or volatile substances from the samples. Interestingly, samples with higher DS, such as CM-GVL exhibit almost no weight loss in this region, probably due to the higher content of the hydrophobic myristate group attached. The next step in the weight loss process was due to the primary sample decomposition. All CM samples show relatively high thermal stability and start to decompose at about 320 °C. At 50% weight loss, the temperature of decomposition was about 355 °C, 355 °C, 361 °C and 367 °C for CM-GVL, CM-DMI, CM-SLF and CM-DMPU, respectively. Similar decomposition temperatures have been observed for cellulose laurates in the work of Wen et al. (Wen et al. 2017). At temperatures higher than 400 °C, the samples undergo pyrolysis in the final step. Differences in pyrolysis residues may be attributed to resistant byproducts of decomposition (Fundador et al. 2012).

DTG curves can provide insight into the decomposition rate of the samples, revealing the details of the process.

As shown by the DTG curves (see inset to Fig. 11), the primary peak for the maximum degradation rate
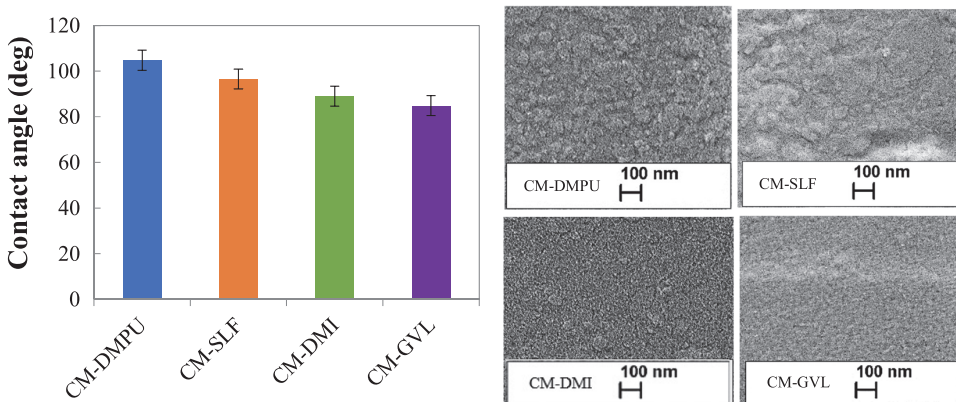
Fig. 10 Average contact angles (left) and SEM images (right) of the films of CMs synthesized in IL/green co-solvent mixtures
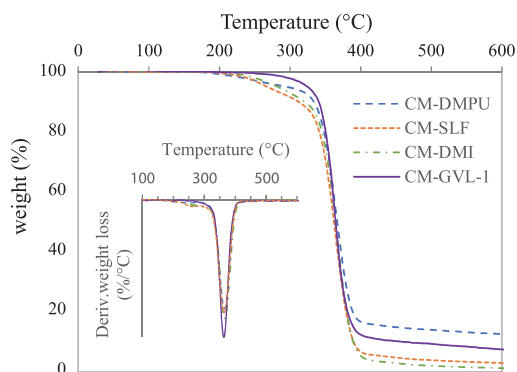
Fig. 11 TGA/DTG curves of CMs prepared in different IL/green co-solvents. Samples are tested in powder form

was observed at 353 °C for CM-GVL and CM-SLF, and 355 °C for CM-DMI and CM-DMPU, indicating almost identical temperatures of decomposition.

Conclusions

In this study, we perform for the first time a transesterification of cellulose in binary mixtures of [mTBNH][OAc] ionic liquid and green co-solvents (GVL, DMPU, DMI) representing different thermodynamic properties of binary solvents. CEs, especially CMs, which are not widely studied in the literature, with different DS have been successfully synthesized. The selection of co-solvent has an evident impact on the microstructure, viscoelasticity, thermal, and mechanical properties of the final product.

The capacity of co-solvents to nominally dissolve cellulose in binary solvents is of crucial importance. Lower solubility (DMPU, SLF) leads to lower values of DS and the formation of aggregates comprised of unsubstituted parts of cellulose chains. Such structures add extra rigidity to the products (CM-DMPU, CM-SLF), and their viscosities, G-moduli, stress level, and Young's modulus are the largest.

One may note that the following order CM-DMPU, CM-SLF, CM-DMI, and CM-GVL is seen leading to a) an increase in DS; b) amorphization of cellulose esters; and c) enhanced mechanical characteristics and processing properties due to better internal plasticization. The degradation temperatures of the CMs made

with different green co-solvents were found to be the same. Additionally, the hydrophobic character of the films was demonstrated by the contact angle measurements. These films are potential materials for use in environmentally friendly packaging because of their hydrophobicity, thermal stability, and ductile nature.

By exiting laboratory practice, we can estimate, that the bio-based co-solvents are cheaper than the IL-s and their higher ratio in the dissolution system will decrease the overall cost. Durability, sustainability, (partly) bio-based nature, low toxicity, high dissolution power, and suitability for conducting the described reactions prove the high potential of the solvent systems. One of the challenges will be further development toward reaction environments, where cellulose concentrations are higher. This can be done by implementing reactive extrusion, for example, which allows for the processing of much more concentrated mixtures, therefore reducing the need for solvents. Another challenge is the efficient separation and recycling of the solvents. This is not so much a fundamental research issue as a task for technology development. To recycle IL, first, it should be filtered from solid residues, then ethanol should be removed by rotary evaporation or thin-film distillation. If recovered IL is contaminated with non-volatile substances, it could be processed by vacuum fractional distillation. These aspects are the focus of our future study toward higher TRL (technology readiness level).

References

Asakawa M, Shrotri A, Kobayashi H, Fukuoka A (2019) Solvent basicity controlled deformylation for the formation of furfural from glucose and fructose. Green Chem 21(22):6146–6153. https://doi.org/10.1039/C9GC02600B

Asim N, Badiei M, Mohammad M (2022) Recent advances in cellulose-based hydrophobic food packaging. Emergent Mater 5(3):703–718. https://doi.org/10.1007/s42247-021-00314-2

Ass BAP, Ciacco GT, Frollini E (2006) Cellulose acetates from linters and sisal: Correlation between synthesis conditions in DMAc/LiCl and product properties. Biores Technol 97(14):1696–1702. https://doi.org/10.1016/j.biortech.2005.10.009

Barnes HA, Hutton JF, Walters K (1989) An Introduction to Rheology. Elsevier

Bering E, Torstensen JØ, Lervik A, de Wijn AS (2022) Computational study of the dissolution of cellulose into single chains: the role of the solvent and agitation. Cellulose 29(3):1365–1380. https://doi.org/10.1007/s10570-021-04382-9

Bistany KL, Kokini JL (1983) Dynamic Viscoelastic Properties of Foods in Texture Control. J Rheol 27(6):605–620. https://doi.org/10.1122/1.549732

Brandrup J, Immergut EH, Grulke EA (1999) Polymer handbook, 4th edn. Wiley

Bryan MC, Dunn PJ, Entwistle D, Gallou F, Koenig SG, Hayler JD, Hickey MR, Hughes S, Kopach ME, Moine G, Richardson P, Roschangar F, Steven A, Weiberth FJ (2018) Key Green Chemistry research areas from a pharmaceutical manufacturers' perspective revisited. Green Chem 20(22):5082–5103. https://doi.org/10.1039/C8GC01276H

Budtova T, Navard P (2015) Viscosity-temperature dependence and activation energy of cellulose solutions. Nord Pulp Paper Res J 30(1):99–104. https://doi.org/10.3183/npprj-2015-30-01-p099-104

Cai J, Zhang L (2005) Rapid Dissolution of Cellulose in LiOH/Urea and NaOH/Urea Aqueous Solutions. Macromol Biosci 5(6):539–548. https://doi.org/10.1002/mabi.200400222

Ciacco GT (2003) Application of the solvent dimethyl sulfoxide/tetrabutyl-ammonium fluoride trihydrate as reaction medium for the homogeneous acylation of Sisal cellulose. Cellulose 10(2):125–132. https://doi.org/10.1023/A:1024064018664

Constable DJC, Dunn PJ, Hayler JD, Humphrey GR, Leazer JL Jr, Linderman RJ, Lorenz K, Manley J, Pearlman BA, Wells A, Zaks A, Zhang TY (2007) Key green chemistry research areas—a perspective from pharmaceutical manufacturers. Green Chem 9(5):411–420. https://doi.org/10.1039/B703488C

Crépy L, Chaveriat L, Banoub J, Martin P, Joly N (2009) Synthesis of cellulose fatty esters as plastics-influence of the degree of substitution and the fatty chain length on mechanical properties. ChemSusChem 2(2):165–170. https://doi.org/10.1002/cssc.200800171

Duchatel-Crépy L, Joly N, Martin P, Marin A, Tahon JF, Lefebvre JM, Gaucher V (2020) Substitution degree and fatty chain length influence on structure and properties of fatty acid cellulose esters. Carbohydr Polym 234:1. https://doi.org/10.1016/j.carbpol.2020.115912

Duereh A, Sato Y, Smith RL, Inomata H (2015) Replacement of Hazardous Chemicals Used in Engineering Plastics with Safe and Renewable Hydrogen-Bond Donor and Acceptor Solvent-Pair Mixtures. ACS Sustain Chem Eng 3(8):1881–1889. https://doi.org/10.1021/acssuschemeng.5b00474

Feng L, Chen Z (2008) Research progress on dissolution and functional modification of cellulose in ionic liquids. J Mol Liq 142(1–3):1–5. https://doi.org/10.1016/j.molliq.2008.06.007

Fink H-P, Weigel P, Purz HJ, Ganster J (2001) Structure formation of regenerated cellulose materials from NMMO-solutions. Prog Polym Sci 26(9):1473–1524. https://doi.org/10.1016/S0079-6700(01)00025-9

French AD (2014) Idealized powder diffraction patterns for cellulose polymorphs. Cellulose 21(2):885–896. https://doi.org/10.1007/s10570-013-0030-4

Fundador NGV, Enomoto-Rogers Y, Takemura A, Iwata T (2012) Syntheses and characterization of xylan esters. Polymer 53(18):3885–3893. https://doi.org/10.1016/J.POLYMER.2012.06.038

Gericke M, Schlufter K, Liebert T, Heinze T, Budtova T (2009) Rheological properties of cellulose/ionic liquid solutions: From dilute to concentrated states. Biomacromolecules 10(5):1188–1194. https://doi.org/10.1021/bm801430x

Ghasemi M (2018) Fundamental Understanding of Cellulose Dissolution Can Improve the Efficiency of Biomass Processing. Agric Res Technol: Open Access J 16(2):1–5. https://doi.org/10.19080/artoaj.2018.15.555985

Gleissle W, Hochstein B (2003) Validity of the Cox–Merz rule for concentrated suspensions. J Rheol 47(4):897–910. https://doi.org/10.1122/1.1574020

Gören A, Mendes J, Rodrigues HM, Sousa RE, Oliveira J, Hilliou L, Costa CM, Silva MM, Lanceros-Méndez S (2016) High performance screen-printed electrodes prepared by a green solvent approach for lithium-ion batteries. J Power Sources 334:65–77. https://doi.org/10.1016/j.jpowsour.2016.10.019

Han S, Li J, Zhu S, Chen R, Wu Y, Zhang X, Yu Z (2009) Potential applications of ionic liquids in wood related industries. BioResources 4(2):825–834. https://doi.org/10.15376/biores.4.2.825-834

Hansen CM (2007) Hansen Solubility Parameters. CRC Press. https://doi.org/10.1201/9781420006834

Hawkins JE, Liang Y, Ries ME, Hine PJ (2021) Time temperature superposition of the dissolution of cellulose fibres by the ionic liquid 1-ethyl-3-methylimidazolium acetate with cosolvent dimethyl sulfoxide. Carbohydr Polym Technol Appl 2:100021. https://doi.org/10.1016/j.carpta.2020.100021

Heinze T, Liebert T (2001) Unconventional methods in cellulose functionalization. Prog Polym Sci 26:1689–1762. https://doi.org/10.1016/S0079-6700(01)00022-3

Henderson RK, Jiménez-González C, Constable DJC, Alston SR, Inglis GGA, Fisher G, Sherwood J, Binks SP, Curzons AD (2011) Expanding GSK's solvent selection guide – embedding sustainability into solvent selection starting at medicinal chemistry. Green Chem 13(4):854. https://doi.org/10.1039/c0gc00918k

Ilyin SO, Makarova VV, Polyakova MY, Kulichikhin VG (2020) Phase behavior and rheology of miscible and immiscible blends of linear and hyperbranched siloxane

macromolecules. Mater Today Commun 22:100833. https://doi.org/10.1016/j.mtcomm.2019.100833

Katsuhara S, Sunagawa N, Igarashi K, Takeuchi Y, Takahashi K, Yamamoto T, Li F, Tajima K, Isono T, Satoh T (2023) Effect of degree of substitution on the microphase separation and mechanical properties of cellooligosaccharide acetate-based elastomers. Carbohydr Polym 316:120976. https://doi.org/10.1016/j.carbpol.2023.120976

Köhler S, Liebert T, Schöbitz M, Schaller J, Meister F, Günther W, Heinze T (2007) Interactions of Ionic Liquids with Polysaccharides 1. Unexpected Acetylation of Cellulose with 1-Ethyl-3-methylimidazolium Acetate. Macromol Rapid Commun 28(24):2311–2317. https://doi.org/10.1002/marc.200700529

Kostag M, Gericke M, Heinze T, El Seoud OA (2019) Twenty-five years of cellulose chemistry: innovations in the dissolution of the biopolymer and its transformation into esters and ethers. Cellulose 26(1):139–184. https://doi.org/10.1007/s10570-018-2198-0

Kramar A, Rodríguez Ortega I, González-Gaitano G, González-Benito J (2023) Solution casting of cellulose acetate films: influence of surface substrate and humidity on wettability, morphology and optical properties. Cellulose 30(4):2037–2052. https://doi.org/10.1007/s10570-022-05026-2

Lefroy KS, Murray BS, Ries ME (2021) Rheological and NMR Studies of Cellulose Dissolution in the Ionic Liquid Bmi-mAc. J Phys Chem B 125(29):8205–8218. https://doi.org/10.1021/acs.jpcb.1c02848

Lowman DW (1998) Characterization of cellulose esters by solution-state and solid-state NMR spectroscopy. ACS Symp Ser 688(10):131–162. https://doi.org/10.1021/bk-1998-0688.ch010

Malkin A (1994) Rheology Fundamentals. In Fundamental Topics in Rheology. ChemTec Publishing 153–165

Marrucci G (1996) Dynamics of entanglements: A nonlinear model consistent with the Cox-Merz rule. J Non-Newtonian Fluid Mech 62(2–3):279–289. https://doi.org/10.1016/0377-0257(95)01407-1

Martins MAR, Sosa FHB, Kilpeläinen I, Coutinho JAP (2022) Physico-chemical characterization of aqueous solutions of superbase ionic liquids with cellulose dissolution capability. Fluid Phase Equilib 556:113414. https://doi.org/10.1016/j.fluid.2022.113414

Mead DW (2011) Analytic derivation of the Cox-Merz rule using the MLD "toy" model for polydisperse linear polymers. Rheol Acta 50(9–10):837–866. https://doi.org/10.1007/s00397-011-0550-5

Mohan M, Banerjee T, Goud VV (2016) Effect of Protic and Aprotic Solvents on the Mechanism of Cellulose Dissolution in Ionic Liquids: A Combined Molecular Dynamics and Experimental Insight. ChemistrySelect 1(15):4823–4832. https://doi.org/10.1002/slct.201601094

Ostonen A, Bervas J, Uusi-Kyyny P, Alopaeus V, Zaitsau DH, Emelyanenko VN, Schick C, King AWT, Helminen J, Kilpeläinen I, Khachatrian AA, Varfolomeev MA, Verevkin SP (2016) Experimental and Theoretical Thermodynamic Study of Distillable Ionic Liquid 1,5-Diazabicyclo[4.3.0]non-5-enium Acetate. Ind Eng Chem Res 55(39):10445–10454. https://doi.org/10.1021/acs.iecr.6b02417

Parviainen A, Wahlström R, Liimatainen U, Liitiä T, Rovio S, Helminen JKJ, Hyväkkö U, King AWT, Suurnäkki A, Kilpeläinen I (2015) Sustainability of cellulose dissolution and regeneration in 1,5-diazabicyclo[4.3.0]non-5-enium acetate: a batch simulation of the IONCELL-F process. RSC Adv 5(85):69728–69737. https://doi.org/10.1039/C5RA12386K

Phadagi R, Singh S, Hashemi H, Kaya S, Venkatesu P, Ramjugernath D, Ebenso EE, Bahadur I (2021) Understanding the role of Dimethylformamide as co-solvents in the dissolution of cellulose in ionic liquids: Experimental and theoretical approach. J Mol Liq 328:115392. https://doi.org/10.1016/j.molliq.2021.115392

Pinkert A, Marsh KN, Pang S, Staiger MP (2009) Ionic liquids and their interaction with cellulose. Chem Rev 109(12):6712–6728. https://doi.org/10.1021/cr9001947

Qiu X, Hu S (2013) "Smart" materials based on cellulose: A review of the preparations, properties, and applications. Materials 6(3):738–781. https://doi.org/10.3390/ma6030738

Quintana SE, Machacon D, Marsiglia RM, Torregroza E, Garcia-Zapateiro LA (2018) Steady and shear dynamic rheological properties of squash (Cucurbita moschata) pulp. Contemp Eng Sci 11(21):1013–1024. https://doi.org/10.12988/ces.2018.8386

Rasool MA, Vankelecom IFJ (2021) γ-Valerolactone as Bio-Based Solvent for Nanofiltration Membrane Preparation. Membranes 11(6):418. https://doi.org/10.3390/membranes11060418

Rinaldi R (2011) Instantaneous dissolution of cellulose in organic electrolyte solutions. Chem Commun 47(1):511–513. https://doi.org/10.1039/C0CC02421J

Russo F, Galiano F, Pedace F, Aricò F, Figoli A (2020) Dimethyl Isosorbide As a Green Solvent for Sustainable Ultrafiltration and Microfiltration Membrane Preparation. ACS Sustain Chem Eng 8(1):659–668. https://doi.org/10.1021/acssuschemeng.9b06496

Shafiei-Sabet S, Hamad WY, Hatzikiriakos SG (2012) Rheology of nanocrystalline cellulose aqueous suspensions. Langmuir 28(49):17124–17133. https://doi.org/10.1021/la303380v

Strappaveccia G, Luciani L, Bartollini E, Marrocchi A, Pizzo F, Vaccaro L (2015) γ-Valerolactone as an alternative biomass-derived medium for the Sonogashira reaction. Green Chem 17(2):1071–1076. https://doi.org/10.1039/C4GC01728E

Tarasova E, Savale N, Krasnou I, Kudrjašova M, Rjabovs V, Reile I, Vares L, Kallakas H, Kers J, Krumme A (2023) Preparation of Thermoplastic Cellulose Esters in [mTBNH][OAC] Ionic Liquid by Transesterification Reaction. Polymers 15(19):3979. https://doi.org/10.3390/polym15193979

Tarasova E, Savale N, Ausmaa P-M, Krasnou I, Krumme A (2024) Rheology and dissolution capacity of cellulose in novel [mTBNH][OAc] ionic liquid mixed with green co-solvents. Rheol Acta. https://doi.org/10.1007/s00397-024-01433-3

Tilstam U (2012) Sulfolane: A Versatile Dipolar Aprotic Solvent. Org Process Res Dev 16(7):1273–1278. https://doi.org/10.1021/op300108w

Wen X, Wang H, Wei Y, Wang X, Liu C (2017) Preparation and characterization of cellulose laurate ester by catalyzed

transesterification. Carbohydr Polym 168:247–254. https://doi.org/10.1016/j.carbpol.2017.03.074

Wenzel RN (1936) Resistance of solid surfaces to wetting by water. Ind Eng Chem 28(8):988–994. https://doi.org/10.1021/ie50320a024

Willberg-Keyriläinen P, Vartiainen J, Harlin A, Ropponen J (2017) The effect of side-chain length of cellulose fatty acid esters on their thermal, barrier and mechanical properties. Cellulose 24(2):505–517. https://doi.org/10.1007/s10570-016-1165-x

Wilson K, Murray J, Sneddon H, Jamieson C, Watson A (2018) Dimethylisosorbide (DMI) as a Bio-Derived Solvent for Pd-Catalyzed Cross-Coupling Reactions. Synlett 29(17):2293–2297. https://doi.org/10.1055/s-0037-1611054

Wu S, Qin X, Li M (2014) The structure and properties of cellulose acetate materials: A comparative study on electrospun membranes and casted films. J Ind Text 44(1):85–98. https://doi.org/10.1177/1528083713477443

Xu C, Cheng Z (2021) Thermal Stability of Ionic Liquids: Current Status and Prospects for Future Development. Processes 9(2):337. https://doi.org/10.3390/pr9020337

Yuan C, Shi W, Chen P, Chen H, Zhang L, Hu G, Jin L, Xie H, Zheng Q, Lu S (2019) Dissolution and transesterification of cellulose in γ-valerolactone promoted by ionic liquids. New J Chem 43(1):330–337. https://doi.org/10.1039/c8nj03505a

Curriculum vitae

Personal data

Name: Nutan Bharat Savale
Date of birth: 14/11/1993
Place of birth: Mumbai, India
Citizenship: India

Contact data

E-mail: nutan.savale@taltech.ee

Professional employment

16.07.2024–01.11.2024   Imperial College London, Visiting Researcher
01.10.2022–31.08.2024   Tallinn University of Technology, School of Engineering, Department of Materials and Environmental Technology, Junior Research Fellow
01.02.2021–31.01.2025   Tallinn University of Technology, PhD student

Education

2021–2025   Doctor of Philosophy (Ph.D.) Engineering Sciences (Chemical and Materials Technology), Tallinn University of Technology, Estonia
2017–2020   Master of Science (M.Sc.) Advanced Synthesis and Catalysis, University of Regensburg, Germany
2011–2014   Bachelor of Science (B.Sc.) Chemistry (Major), University of Mumbai (Ramnarain Ruia College), India

Language competence

English   Fluent
Hindi   Native
Marathi   Native

Publications

Tarasova, Elvira, **Nutan Savale**, Illia Krasnou, Marina Kudrjašova, Vitalijs Rjabovs, Indrek Reile, Lauri Vares, Heikko Kallakas, Jaan Kers, and Andres Krumme. "Preparation of thermoplastic cellulose esters in [mTBNH][OAC] ionic liquid by transesterification reaction." *Polymers* 15, no. 19 (2023): 3979.

Savale, Nutan, Elvira Tarasova, Illia Krasnou, Marina Kudrjašova, Vitālijs Rjabovs, Indrek Reile, Ivo Heinmaa, and Andres Krumme. "Optimization and degradation studies of cellulose transesterification to palmitate esters in superbase ionic liquid." *Carbohydrate Research* 537 (2024): 109047.

Tarasova, Elvira, **Nutan Savale**, Peeter-Mihkel Ausmaa, Illia Krasnou, and Andres Krumme. "Rheology and dissolution capacity of cellulose in novel [mTBNH][OAc] ionic liquid mixed with green co-solvents." *Rheologica Acta* 63, no. 2 (2024): 167-178.

Tarasova, Elvira, **Nutan Savale**, Lada Trifonova, Illia Krasnou, Indrek Reile, Marina Kudrjašova, Arvo Mere, Tiit Kaljuvee, Valdek Mikli, Rauno Sedrik, and Andres Krumme "Effect of green co-solvents on properties and synthesis of cellulose esters in superbase ionic liquid." *Cellulose* 31, no. 8 (2024): 4911-4927.

Tarasova, Elvira, Illia Krasnou, Giiguulen Enkhsaikhan, Ibrahim Abousharabia, Caio César Zandonadi Nunes, Darshni Karthegesu, **Nutan Savale**, Eero Kontturi, and Andres Krumme. "Reactive extrusion of cellulose esters in ionic liquid: exploring properties and performance across different cellulose types and degrees of polymerization." *Cellulose* (2024): 1-18.

Savale, Nutan, Elvira Tarasova, Atanas Katerski, Arvo Mere, Ivo Heinmaa, Tiit Kaljuvee, Valdek Mikli, and Andres Krumme. "Structural and Thermal Properties of Cellulose Regenerated from Superbase Ionic Liquid: Effect of Green Co-Solvents." *Cellulose*. (Submitted).

Elulookirjeldus

Isikuandmed

Nimi:	Nutan Bharat Savale
Sünniaeg:	14/11/1993
Sünnikoht:	Mumbai, India
Kodakondsus:	India

Kontaktandmed

E-post:	nutan.savale@taltech.ee

Hariduskäik

2021–2025	Doctor of Philosophy (Ph.D.) Engineering Sciences (Chemical and Materials Technology), Tallinn University of Technology, Estonia
2017–2020	Master of Science (M.Sc.) Advanced Synthesis and Catalysis, University of Regensburg, Germany
2011–2014	Bachelor of Science (B.Sc.) Chemistry (Major), University of Mumbai (Ramnarain Ruia College), India

Keelteoskus

Inglise keel	Kõrgtase
Hindi keel	Emakeel
Marathi keel	Emakeel

Teenistuskäik

16.07.2024–01.11.2024	Imperial College London, Külalisuurija
01.10.2022–31.08.2024	Tallinna Tehnikaülikool, Inseneriteaduskond, Materjali- ja keskkonnatehnoloogia instituut, doktorant-nooremteadur
01.02.2021–31.01.2025	Tallinna Tehnikaülikool, doktorant

Publikatsioonid

Tarasova, Elvira, **Nutan Savale**, Illia Krasnou, Marina Kudrjašova, Vitalijs Rjabovs, Indrek Reile, Lauri Vares, Heikko Kallakas, Jaan Kers, and Andres Krumme. "Preparation of thermoplastic cellulose esters in [mTBNH][OAC] ionic liquid by transesterification reaction." *Polymers* 15, no. 19 (2023): 3979.

Savale, Nutan, Elvira Tarasova, Illia Krasnou, Marina Kudrjašova, Vitālijs Rjabovs, Indrek Reile, Ivo Heinmaa, and Andres Krumme. "Optimization and degradation studies of cellulose transesterification to palmitate esters in superbase ionic liquid." *Carbohydrate Research* 537 (2024): 109047.

Tarasova, Elvira, **Nutan Savale**, Peeter-Mihkel Ausmaa, Illia Krasnou, and Andres Krumme. "Rheology and dissolution capacity of cellulose in novel [mTBNH][OAc] ionic liquid mixed with green co-solvents." *Rheologica Acta* 63, no. 2 (2024): 167-178.

Tarasova, Elvira, **Nutan Savale**, Lada Trifonova, Illia Krasnou, Indrek Reile, Marina Kudrjašova, Arvo Mere, Tiit Kaljuvee, Valdek Mikli, Rauno Sedrik, and Andres Krumme "Effect of green co-solvents on properties and synthesis of cellulose esters in superbase ionic liquid." *Cellulose* 31, no. 8 (2024): 4911-4927.

Tarasova, Elvira, Illia Krasnou, Giiguulen Enkhsaikhan, Ibrahim Abousharabia, Caio César Zandonadi Nunes, Darshni Karthegesu, **Nutan Savale**, Eero Kontturi, and Andres Krumme. "Reactive extrusion of cellulose esters in ionic liquid: exploring properties and performance across different cellulose types and degrees of polymerization." *Cellulose* (2024): 1-18.

Savale, Nutan, Elvira Tarasova, Atanas Katerski, Arvo Mere, Ivo Heinmaa, Tiit Kaljuvee, Valdek Mikli, and Andres Krumme. "Structural and Thermal Properties of Cellulose Regenerated from Superbase Ionic Liquid: Effect of Green Co-Solvents." *Cellulose*. (Submitted).